THE
PHYSICAL REVIEW
A journal of experimental and theoretical physics established by E. L. Nichols in 1893

VOL. 62, NOS. 9 AND 10 NOVEMBER 1 AND 15, 1942 SECOND SERIES

Calculations of the Scattering of Mesons by the Matrix Method

S. T. MA
Department of Physics, National University of Peking, Kunming, China
(Received September 2, 1942)

The β-matrices in the vector meson theory can be reduced to the simpler ξ-matrices and S matrices (spin matrices). Certain relations concerning the ξ- and S matrices are deduced. These are applied to the calculation of the scattering of mesons by the Coulomb field and the scattering of mesons by the nuclear interaction. Results independent of any particular initial state of polarization of the meson are obtained.

1. INTRODUCTION

MOST of the calculations of the scattering of mesons in recent years have been carried out on the basis of the wave formulation of the meson theory. In calculating the transition probabilities, we have to treat separately the different initial states of polarization of the meson. In the case of multiple scattering this procedure is extremely complicated. In the relativistic electron theory, calculations of this type are very much simplified by the orthogonality relations, the annihilation operators, and the method of spurs.[1] Though similar treatments are possible in a wave theory, they are less easy to carry through. For example, in the wave theory of the meson we have to construct annihilation operators not only for mesons of a certain charge (positive or negative), but also for mesons of a certain polarization (longitudinal or transverse).[2]

The matrix formulation of the meson theory developed by Kemmer,[3] which emphasizes the particle aspect rather than the wave aspect of the meson, provides a basis for carrying out calculations on the lines of those in the electron theory. This formulation has later been extended by Wilson[4] to include the nuclear interaction. The application of this theory to scattering problems has been developed by Booth and Wilson.[5] The authors have shown that, in most cases, the β-matrix method is simpler to manipulate than the wave method.

The treatment of these authors is based largely on the method of spurs. This method is very convenient when we are concerned with the properties of the meson averaged over all initial states of polarization rather than the behavior of one particular state. For the latter, the spur method is no longer applicable. It is my object to show that in such cases the matrix method can still be used with advantage, just as in the electron theory. This is of some interest, because the behavior of mesons of different polarizations is known to be quite different in many phenomena.

As a first application we apply this method to

[1] For an account of such methods in the electron theory, see W. Heitler, *Quantum Theory of Radiation* (Oxford, 1936).
[2] O. Laporte, Phys. Rev. **54**, 905 (1938).
[3] N. Kemmer, Proc. Roy. Soc. **A173**, 91 (1939).
[4] A. H. Wilson, Proc. Camb. Phil. Soc. **36**, 363 (1940).
[5] F. Booth and A. H. Wilson, Proc. Roy. Soc. **A175**, 483 (1940). Editorial note: Compare for further applications R. F. Christy and S. Kusaka, Phys. Rev. **59**, 405 (1941).

the scattering of a meson by an electrostatic field. This has been calculated by Laporte in the first Born approximation on the wave theory.[2] The calculation of higher approximations in the wave theory is very complicated. In the relativistic electron theory, Sauter[6] deduced results for both the first and the second Born approximations, which are applicable to all initial states of the electron. The scattering probabilities for each particular state can then be immediately deduced from the general formulae. Our results obtained by the matrix method for the first and second approximations are similar to those of Sauter's. Recently Sakata and Taketani[7] have calculated the cross section for the elastic scattering of mesons by the β-matrix method, but their result is not so general as Laporte's.

As a second application we apply the method to the scattering of mesons by the nuclear interaction. It is also possible to obtain a general result which includes the results for the special cases calculated by Heitler[8] on the basis of the wave theory.

In the following we first deduce from the results of Kemmer, Wilson, and Booth certain relations concerning the matrices of the meson. We then apply these relations to the scattering of mesons.

2. THE MATRIX METHOD

The meson is described by the wave equation

$$\partial_\nu\beta_\nu\psi+\kappa\psi=0 \quad (\nu=1, 2, 3, 4), \tag{1}$$

where $\kappa=mc/\hbar$. The β-operators satisfy the commutation rules

$$\beta_\lambda\beta_\nu\beta_\rho+\beta_\rho\beta_\nu\beta_\lambda=\beta_\lambda\delta_{\nu\rho}+\beta_\rho\delta_{\nu\lambda}. \tag{2}$$

From (2) it follows that the eigenvalues of the β's are ±1, 0. In this theory the charge density and energy density of the meson are given by

$$e\psi^\dagger\beta_4\psi, \quad \mu\psi^\dagger\psi \quad (\mu=mc^2), \tag{3}$$

respectively, $\psi^\dagger$ being the Hermitian conjugate of ψ.

[6] F. Sauter, Zeits. f. Physik **18**, 61 (1933).
[7] S. Sakata and M. Taketani, Sci. Papers Inst. Phys. Chem. Research **38**, 1 (1940); Proc. Phys. Math. Soc. Japan **22**, 757 (1940).
[8] W. Heitler, Proc. Roy. Soc. **A166**, 529 (1938).

The plane wave solution of (1) is

$$\psi=u^\pm\exp\left[\mp iEt/\hbar+i\mathbf{p}\cdot\mathbf{r}/c\hbar\right], \tag{4}$$

where $\mathbf{p}$ is c times the momentum and $E=(\mu^2+p^2)^{\frac{1}{2}}$ is the energy of the meson. Substituting (4) into (1), we have

$$(\mp E\beta_4+i\mathbf{p}\cdot\boldsymbol{\beta}+\mu)u^\pm=0. \tag{5}$$

In the vector meson theory, the β's have ten rows and ten columns and the u's are column matrices of ten elements. There are six linearly independent solutions of the form (4). We denote the corresponding u's by $u_j(\mathbf{p})$, $j=1, 2, \cdots, 6$. If we take the representation in which β_4 is diagonal, 1, 2, 3 are related to the eigenvalue $+1$ (positive charge) and 4, 5, 6 are related to the eigenvalue -1 (negative charge). In order to reduce the charge and energy densities (3) to the diagonal form, the u's are assumed to satisfy the orthogonality relations

$$\mu u_i^\dagger u_j=E\delta_{ij}, \quad u_i^\dagger\beta_4u_j=\rho_{ij}, \tag{6}$$

where $\rho_{ij}=\pm\delta_{ij}$ for $i, j=1, 2, 3$ and $4, 5, 6$, respectively.

The annihilation operators are defined by the following equations:

$$\frac{1}{2E}\left[E\beta_4+\mu+\frac{1}{\mu}(\mathbf{p}\cdot\boldsymbol{\beta})^2\right]\beta_4{}^2\begin{cases}u^+(\mathbf{p})=\beta_4u^+(\mathbf{p})\\ u^-(\mathbf{p})=0,\end{cases} \tag{7}$$

with a similar operator corresponding to the opposite charge.

For our later calculations the following completeness relations are of importance:

$$\begin{aligned}\sum_{j=1}^{6}\beta_4u_j(\mathbf{p})u_j^\dagger(\mathbf{p})\beta_4&=\frac{1}{E\mu}[\mu^2+(\mathbf{p}\cdot\boldsymbol{\beta})^2]\beta_4{}^2,\\ \sum_{j=1}^{3}\beta_4u_j(\mathbf{p})u_j^\dagger(\mathbf{p})\beta_4&=\frac{1}{2E}\left[E\beta_4+\mu+\frac{1}{\mu}(\mathbf{p}\cdot\boldsymbol{\beta})^2\right]\beta_4{}^2.\end{aligned} \tag{8}$$

The 10 row-10 column β-matrices can be transformed into the following form:

$$\beta_4=\begin{pmatrix}I&0&0\\0&0&0\\0&0&-I\end{pmatrix}, \quad \beta_j=\begin{pmatrix}0&\zeta_j&0\\\zeta_j^\dagger&0&\tilde{\zeta}_j\\0&\zeta_j^*&0\end{pmatrix}, \quad (j=1, 2, 3), \tag{9}$$

in which I is a 3 row-3 column unit matrix, ζ is a 3 row-4 column rectangular matrix, $\zeta^\dagger$, ζ^*, $\bar{\zeta}$ are the Hermitian conjugate, the complex conjugate, and the transposed matrix of ζ, respectively, $\zeta^\dagger$ and $\bar{\zeta}$ having thus four rows and three columns. Corresponding to (9) the 10 elements of ψ can be divided into three components $\psi^{(1)}$, $\psi^{(2)}$, $\psi^{(3)}$ of 3, 4, 3 elements, respectively. In the absence of external fields the components $\psi^{(2)}$ and $\psi^{(3)}$ are small and can be expressed in terms of the large component $\psi^{(1)}$. For the wave functions corresponding to the positive charge, we have

$$\psi^{(2)}=\frac{-2i}{E+\mu}(\boldsymbol{\zeta}^\dagger\cdot\mathbf{p})\psi^{(1)},$$
$$\psi^{(3)}=\frac{-2}{(E+\mu)^2}(\boldsymbol{\zeta}^*\cdot\mathbf{p})(\boldsymbol{\zeta}^\dagger\cdot\mathbf{p})\psi^{(1)}. \tag{10}$$

We need only $\psi^{(3)}$ below. Its Hermitian conjugate is

$$\psi^{(3)\dagger}=\frac{-2}{(E+\mu)^2}\psi^{(1)\dagger}(\boldsymbol{\zeta}\cdot\mathbf{p})(\bar{\boldsymbol{\zeta}}\cdot\mathbf{p}). \tag{10'}$$

A special representation of the ζ's can be easily obtained as follows:

$$\zeta_1=\frac{1}{\sqrt{2}}\begin{pmatrix}\cdot&\cdot&\cdot&-1\\ \cdot&\cdot&-i&\cdot\\ \cdot&i&\cdot&\cdot\end{pmatrix},$$
$$\zeta_2=\frac{1}{\sqrt{2}}\begin{pmatrix}\cdot&\cdot&i&\cdot\\ \cdot&\cdot&\cdot&-1\\ -i&\cdot&\cdot&\cdot\end{pmatrix}, \tag{11}$$
$$\zeta_3=\frac{1}{\sqrt{2}}\begin{pmatrix}\cdot&-i&\cdot&\cdot\\ i&\cdot&\cdot&\cdot\\ \cdot&\cdot&\cdot&-1\end{pmatrix}.$$

We denote the square matrices formed by the first three columns of the ζ's by S_1, S_2, S_3. These are the spin matrices of the meson, which have been discussed by several authors.[9]

From (11) we obtain the following relations:

$$S_iS_kS_j+S_jS_kS_i=S_i\delta_{kj}+S_j\delta_{ik} \qquad (i,k=1,2,3), \tag{12}$$
$$S_iS_j-S_jS_i=iS_{(ij)}, \tag{13}$$

where (ij) denotes the number following i and j in the cyclic order. We have also $S_{(ij)}=-S_{(ji)}$. The relation (12) is the commutation rule satisfied by the β's. The β's do not satisfy (13), which are the general commutation relations for an angular momentum. The relations (13) make the handling of the S's a simpler affair than that of the β's. Relations (12) and (13) can also be deduced directly from (2) (see reference 7).

It can be easily shown that the S's transform like vectors in the 3-dimensional space.[10] They describe the dipole moment of the meson. The symmetrical tensors $S_iS_j+S_jS_i$ which do not vanish for $i\neq j$ as in the case of the electron, correspond to the quadripole moment of the meson.[11] An arbitrary matrix of three rows and three columns can be expressed in terms of the unit matrix I, the three spin matrices S_1, S_2, S_3, and the six matrices of the form $S_iS_j+S_jS_i$.

From (12) and (13) the following relations can be deduced.

$$(\mathbf{S}\cdot\mathbf{a}_1)(\mathbf{S}\cdot\mathbf{a}_2)-(\mathbf{S}\cdot\mathbf{a}_2)(\mathbf{S}\cdot\mathbf{a}_1)=i\mathbf{S}\cdot(\mathbf{a}_1\times\mathbf{a}_2), \tag{14}$$
$$(\mathbf{S}\cdot\mathbf{a}_1)(\mathbf{S}\cdot\mathbf{a}_2)(\mathbf{S}\cdot\mathbf{a}_3)+(\mathbf{S}\cdot\mathbf{a}_3)(\mathbf{S}\cdot\mathbf{a}_2)(\mathbf{S}\cdot\mathbf{a}_1)=(\mathbf{a}_1\cdot\mathbf{a}_2)(\mathbf{S}\cdot\mathbf{a}_3)+(\mathbf{a}_2\cdot\mathbf{a}_3)(\mathbf{S}\cdot\mathbf{a}_1), \tag{15}$$
$$(\mathbf{S}\cdot\mathbf{a}_1)(\mathbf{S}\cdot\mathbf{a}_2)(\mathbf{S}\cdot\mathbf{a}_3)-(\mathbf{S}\cdot\mathbf{a}_3)(\mathbf{S}\cdot\mathbf{a}_2)(\mathbf{S}\cdot\mathbf{a}_1)=2i(\mathbf{a}_1\times\mathbf{a}_2)\cdot\mathbf{a}_3+i[(\mathbf{S}\cdot\mathbf{a}_2),\mathbf{S}\cdot(\mathbf{a}_1\times\mathbf{a}_3)]_+, \tag{16}$$
$$(\mathbf{S}\cdot\mathbf{a}_1)^2(\mathbf{S}\cdot\mathbf{a}_2)^2+(\mathbf{S}\cdot\mathbf{a}_2)^2(\mathbf{S}\cdot\mathbf{a}_1)^2=a_1^2(\mathbf{S}\cdot\mathbf{a}_2)^2+a_2^2(\mathbf{S}\cdot\mathbf{a}_1)^2-[\mathbf{S}\cdot(\mathbf{a}_1\times\mathbf{a}_2)]^2, \tag{17}$$
$$(\mathbf{S}\cdot\mathbf{a}_1)^2(\mathbf{S}\cdot\mathbf{a}_2)^2-(\mathbf{S}\cdot\mathbf{a}_2)^2(\mathbf{S}\cdot\mathbf{a}_1)^2=i(\mathbf{a}_1\cdot\mathbf{a}_2)\mathbf{S}\cdot(\mathbf{a}_1\times\mathbf{a}_2). \tag{18}$$

In these formulae $\mathbf{a}_1$, $\mathbf{a}_2$, $\mathbf{a}_3$ denote arbitrary vectors and

$$[A,B]_+\equiv AB+BA.$$

[9] See, for example, A. Proca, J. de phys. et rad. **9**, 61 (1938).

[10] For an analogous treatment of the Pauli spin matrices see P. A. M. Dirac, *Quantum Mechanics* (Oxford, 1936), Section 19.

[11] W. Heitler and S. T. Ma, Proc. Roy. Soc. **176**, 368 (1940).

From the four rectangular matrices we obtain the following 3 row-3 column matrices:

$$2(\boldsymbol{\zeta}\cdot\mathbf{a}_1)(\boldsymbol{\zeta}^\dagger\cdot\mathbf{a}_2)=2(\boldsymbol{\zeta}^*\cdot\mathbf{a}_1)(\tilde{\boldsymbol{\zeta}}\cdot\mathbf{a}_2)$$
$$=\mathbf{a}_1\cdot\mathbf{a}_2+i\mathbf{S}\cdot(\mathbf{a}_1\times\mathbf{a}_2), \quad (19)$$
$$2(\boldsymbol{\zeta}\cdot\mathbf{a}_1)(\tilde{\boldsymbol{\zeta}}\cdot\mathbf{a}_2)=2(\boldsymbol{\zeta}^*\cdot\mathbf{a}_1)(\boldsymbol{\zeta}^\dagger\cdot\mathbf{a}_2)$$
$$=\mathbf{a}_1\cdot\mathbf{a}_2-[(\mathbf{S}\cdot\mathbf{a}_1),(\mathbf{S}\cdot\mathbf{a}_2)]_+. \quad (20)$$

Any product of the ζ's and the S's can be expressed in terms of I, S_j and $S_iS_j+S_jS_i$. For example,

$$4(\boldsymbol{\zeta}\cdot\mathbf{a}_1)(\tilde{\boldsymbol{\zeta}}\cdot\mathbf{a}_1)\mathbf{S}\cdot(\mathbf{a}_2\times\mathbf{a}_3)(\boldsymbol{\zeta}^*\cdot\mathbf{a}_1)(\boldsymbol{\zeta}^\dagger\cdot\mathbf{a}_1)$$
$$=-a_1^4\mathbf{S}\cdot(\mathbf{a}_2\times\mathbf{a}_3)+2a_1^2\mathbf{a}_1\cdot(\mathbf{a}_2\times\mathbf{a}_3)(\mathbf{S}\cdot\mathbf{a}_1). \quad (21)$$

Sometimes it is convenient to introduce 3 row-3 column matrices Λ_1, Λ_2, Λ_3 defined in terms of the spin matrices S_k by the relation $-i\Lambda_k=S_k$. (This was suggested by Dr. Kemmer.) We also denote the column matrices in the last columns of (11) by $i\iota_k$ $(k=1, 2, 3)$. The ζ-matrices can then be written as follows:

$$\zeta_k=(i/\sqrt{2})(-\Lambda_k, \iota_k). \quad (22)$$

As suggested by their notations the matrices Λ's and ι's satisfy the following simple relations. If w, w_1, and w_2 are column matrices of three elements and $\mathbf{w}$, $\mathbf{w}_1$, $\mathbf{w}_2$ are the vectors whose three components are equal, respectively, to the three elements of the corresponding matrices, we have

$$w_1^\dagger\boldsymbol{\Lambda}w_2=\mathbf{w}_1^*\times\mathbf{w}_2, \quad w^\dagger\boldsymbol{\iota}=i\mathbf{w}^*, \quad \boldsymbol{\iota}^\dagger w=-i\mathbf{w}. \quad (23)$$

In the above equations $\boldsymbol{\Lambda}$ denotes a vector whose three components are equal to the three matrices Λ_1, Λ_2, Λ_3. $\boldsymbol{\iota}$ and $\boldsymbol{\iota}^\dagger$ have similar meanings. From (23) we can deduce the following useful relations.

$$(\boldsymbol{\Lambda}\cdot\mathbf{a})w=-\begin{pmatrix}(\mathbf{a}\times\mathbf{w})_1\\(\mathbf{a}\times\mathbf{w})_2\\(\mathbf{a}\times\mathbf{w})_3\end{pmatrix},$$

$$(\boldsymbol{\Lambda}\cdot\mathbf{a})(\boldsymbol{\Lambda}\cdot\mathbf{b})w=\begin{pmatrix}[\mathbf{a}\times(\mathbf{b}\times\mathbf{w})]_1\\[\mathbf{a}\times(\mathbf{b}\times\mathbf{w})]_2\\[\mathbf{a}\times(\mathbf{b}\times\mathbf{w})]_3\end{pmatrix}, \quad (24)$$

$$w_1^\dagger(\boldsymbol{\Lambda}\cdot\mathbf{a})(\boldsymbol{\Lambda}\cdot\mathbf{b})w_2=(\mathbf{w}_1^*\cdot\mathbf{b})(\mathbf{w}_2\cdot\mathbf{a})$$
$$-(\mathbf{w}_1^*\cdot\mathbf{w}_2)(\mathbf{a}\cdot\mathbf{b})=(\mathbf{w}_1^*\times\mathbf{a})\cdot(\mathbf{b}\times\mathbf{w}_2), \quad (25)$$

$$w_1^\dagger(\mathbf{a}\cdot\boldsymbol{\zeta})\begin{pmatrix}w_2\\\chi_2\end{pmatrix}=\frac{i}{\sqrt{2}}[-\mathbf{a}\cdot(\mathbf{w}_1^*\times\mathbf{w}_2)$$
$$+i(\mathbf{a}\cdot\mathbf{w}_1^*)\chi_2],$$
$$(w_1^\dagger, \chi_1^*)(\mathbf{a}\cdot\boldsymbol{\zeta}^\dagger)w_2=\frac{i}{\sqrt{2}}[-\mathbf{a}\cdot(\mathbf{w}_1^*\times\mathbf{w}_2)$$
$$-i\chi_1^*(\mathbf{a}\cdot\mathbf{w}_2)], \quad (26)$$

$$w_1^\dagger(\mathbf{c}\cdot\boldsymbol{\Lambda})(\mathbf{b}\cdot\boldsymbol{\Lambda})(\mathbf{a}\cdot\boldsymbol{\zeta})\begin{pmatrix}w_2\\\chi_2\end{pmatrix}$$
$$=\frac{i}{\sqrt{2}}[(\mathbf{w}_1^*\cdot\mathbf{b})\mathbf{c}-(\mathbf{b}\cdot\mathbf{c})\mathbf{w}_1^*]$$
$$\cdot[-(\mathbf{w}_2\times\mathbf{a})+i\chi_2\mathbf{a}],$$
$$(w_1^\dagger, \chi_1^*)(\mathbf{a}\cdot\boldsymbol{\zeta}^\dagger)(\mathbf{b}\cdot\boldsymbol{\Lambda})(\mathbf{c}\cdot\boldsymbol{\Lambda})w_2 \quad (27)$$
$$=\frac{i}{\sqrt{2}}[-(\mathbf{a}\times\mathbf{w}_1^*)-i\chi_1^*\mathbf{a}]$$
$$\cdot[\mathbf{c}(\mathbf{b}\cdot\mathbf{w}_2)-\mathbf{w}_2(\mathbf{b}\cdot\mathbf{c})].$$

In these equations $\mathbf{a}$, $\mathbf{b}$, $\mathbf{c}$ denote arbitrary vectors, the w's denote column matrices of three elements, and χ denotes an ordinary number, $\begin{pmatrix}w\\\chi\end{pmatrix}$ being a column matrix of 4 elements.

If we take the representation (9) the second orthogonality condition in (6) becomes

$$u_k^{(1)\dagger}u_l^{(1)}-u_k^{(3)\dagger}u_l^{(3)}=\rho_{kl}.$$

Substituting (10) and (10′) into this equation, we can eliminate the small components $u^{(3)}$ and $u^{(3)\dagger}$. The result is

$$u_k^{(1)\dagger}u_l^{(1)}=\frac{(E+\mu)^2}{4\mu E}\rho_{kl}. \quad (28)$$

The first components of the orthogonal and normalized u's are therefore of the following form:

$$u^{(1)}=\frac{E+\mu}{2(\mu E)^{\frac{1}{2}}}(a_1v_1+a_2v_2+a_3v_3), \quad (29)$$

where

$$v_1=\begin{pmatrix}1\\\cdot\\\cdot\end{pmatrix}, \quad v_2=\begin{pmatrix}\cdot\\1\\\cdot\end{pmatrix}, \quad v_3=\begin{pmatrix}\cdot\\\cdot\\1\end{pmatrix}, \quad (30)$$

and

$$|a_1|^2+|a_2|^2+|a_3|^2=1.$$

If we take the z axis along the direction of motion of the meson, v_3 represents the longitudinal polarization, v_1 and v_2 represent the transverse

polarizations. It is sometimes convenient to work with the right and left circular polarizations instead of the transverse polarizations. For this purpose we introduce

$$\begin{aligned} &v_0=v_3, \quad v_\pm=(v_1\pm iv_2)/\sqrt{2}, \\ &S_0=S_3, \quad S_\pm=(S_1\pm iS_2)/\sqrt{2}. \end{aligned} \tag{31}$$

Then we have

$$\begin{aligned} &S_+v_+=0, \quad S_+v_-=v_0, \quad S_+v_0=-v_+, \\ &S_-v_+=-v_0, \quad S_-v_-=0, \quad S_-v_0=v_-, \\ &S_0v_+=v_+, \quad S_0v_-=-v_-, \quad S_0v_0=0. \end{aligned} \tag{32}$$

The only non-zero matrix elements of a product of two S's are

$$\begin{aligned} v_+^\dagger S_+S_-v_+&=v_-^\dagger S_-S_+v_-=v_0^\dagger S_+S_-v_0 \\ &=v_0^\dagger S_-S_+v_0=v_+^\dagger S_0{}^2v_+ \\ &=v_-^\dagger S_0{}^2v_-=1, \\ v_0^\dagger S_+S_0v_-&=v_0^\dagger S_-S_0v_+=v_+^\dagger S_0S_+v_0 \\ &=v_-^\dagger S_0S_-v_0=v_+^\dagger S_+{}^2v_- \\ &=v_-^\dagger S_-{}^2v_+=-1. \end{aligned} \tag{33}$$

Equation (29) can be written in terms of v_0, v_+, v_- as follows:

$$u^{(1)}=\frac{E+\mu}{2(\mu E)^{\frac{1}{2}}}(a_0v_0+a_+v_++a_-v_-), \tag{34}$$

$$|a_0|^2+|a_+|^2+|a_-|^2=1.$$

3. TRANSITION PROBABILITIES IN AN ELECTROSTATIC FIELD

We calculate the transition probabilities of the meson in an electrostatic field by using the Born approximations. In treating the second approximation, our calculation follows that of Distel[12] for the non-relativistic electron scattering.

Let the energy and momentum of the incident meson be E_0 and $\mathbf{p}_0$. We assume the charge of the incident meson to be positive. The initial wave function is then

$$\psi_0=\frac{1}{(2\pi)^{\frac{3}{2}}}u_0(\mathbf{p}_0)\exp\left[-iE_0t/\hbar+i\mathbf{k}_0\cdot\mathbf{r}\right], \tag{35}$$

where

$$u_0(\mathbf{p}_0)=\sum_{j_0=1}^{3}a_{j_0}(\mathbf{p}_0)u_{j_0}(\mathbf{p}_0), \quad \mathbf{p}_0=c\hbar\mathbf{k}_0.$$

An arbitrary wave function can be expressed in the form

$$\psi=\frac{1}{(2\pi)^{\frac{3}{2}}}\sum_{j=1}^{3}\int\{a_j(\mathbf{p},t)\exp\left[-iEt/\hbar\right]u_j^+(\mathbf{p}) +b_j(\mathbf{p},t)\exp\left[iEt/\hbar\right]u_j^-(\mathbf{p})\}\exp\left[i\mathbf{k}\cdot\mathbf{r}\right]d\mathbf{k}. \tag{36}$$

In an electrostatic field, the meson satisfies the equation

$$i\hbar\beta_4(\partial\psi/\partial t)=(i\mathbf{p}\cdot\boldsymbol{\beta}+\mu+V\beta_4)\psi, \tag{37}$$

V being the electrostatic potential multiplied by $+e$. From (37) we obtain the general formula for the transition from the state $(E, \mathbf{p})$ to the state $(E', \mathbf{p}')$

$$\begin{aligned} i\frac{d}{dt}a_{j'}(\mathbf{p}',t)&=\sum_{j=1}^{3}\int a_j(\mathbf{p},t) \\ &\times\exp\left[i(E'-E)t/\hbar\right]u_{j'}^\dagger(\mathbf{p}') \\ &\times\beta_4u_j(\mathbf{p})\,V(\mathbf{k},\mathbf{k}')d\mathbf{k}', \end{aligned} \tag{38}$$

where

$$V(\mathbf{k},\mathbf{k}')=\frac{1}{(2\pi)^3\hbar}\int V\exp\left[i(\mathbf{k}-\mathbf{k}')\cdot\mathbf{r}\right]d\mathbf{r} \tag{39}$$

is a quantity which is real for a central field.

In the first Born approximation, the initial state is characterized by $(E_0, \mathbf{p}_0)$, the final state by $(E, \mathbf{p})$. On account of the conservation of energy, we have

$$E_0=E. \tag{40}$$

In the second approximation, we take into account the intermediate states $(E', \mathbf{p}')$. The equations for the coefficients $a_j(\mathbf{p}, t)$ for the final states can be solved by the method of successive approximations. In the first approximation we have

$$\begin{aligned} i\frac{d}{dt}a_j^{(1)}(\mathbf{p},t)&=\sum_{j_0=1}^{3}a_{j_0}(\mathbf{p}_0)\exp\left[i(\omega-\omega_0)t\right] \\ &\times V(\mathbf{k}_0,\mathbf{k})u_j^\dagger(\mathbf{p})\beta_4u_{j_0}(\mathbf{p}_0) \\ &=\exp\left[i(\omega-\omega_0)t\right] \\ &\times V(\mathbf{k}_0,\mathbf{k})u_j^\dagger(\mathbf{p})\beta_4u_0(\mathbf{p}_0), \end{aligned} \tag{41}$$

[12] F. Distel, Zeits. f. Physik **74**, 785 (1932).

where $\omega = E/\hbar$. In the second approximation,

$$i\frac{d}{dt}a_j^{(2)}(\mathbf{p},t) = \sum_{j'=1}^{3}\int V(\mathbf{k}_0,\mathbf{k}')\,V(\mathbf{k}',\mathbf{k}) \times (u_j^{\dagger}(\mathbf{p})\beta_4 u_{j'}(\mathbf{p}'))(u_{j'}^{\dagger}(\mathbf{p}')\beta_4 u_0(\mathbf{p}_0)) \times \frac{\exp[i(\omega-\omega_0)t]-\exp[i(\omega-\omega')t]}{\omega_0-\omega'}d\mathbf{k}'. \quad (42)$$

The solutions of (41) and (42) are

$$a_j^{(1)}(\mathbf{p},t) = V(\mathbf{k}_0,\mathbf{k})(u_j^{\dagger}(\mathbf{p})\beta_4 u_0(\mathbf{p}_0)) \times \frac{\exp[i(\omega-\omega_0)t]-1}{\omega_0-\omega}, \quad (43)$$

$$a_j^{(2)}(\mathbf{p},t) = \int\int d\Omega' d\omega' f(\mathbf{k}') \times\left[\frac{\exp[i(\omega-\omega_0)t]-1}{(\omega_0-\omega')(\omega_0-\omega)} - \frac{\exp[i(\omega-\omega')t]-1}{(\omega_0-\omega')(\omega'-\omega)}\right]$$

$$= \int\int d\Omega' d\omega' f(\mathbf{k}') \times\left[\frac{\exp[i(\omega-\omega_0)t]}{\omega_0-\omega} \times\frac{\exp[i(\omega_0-\omega')t]-1}{\omega'-\omega_0} - \frac{\exp[i(\omega-\omega')t]-1}{(\omega_0-\omega)(\omega'-\omega)}\right], \quad (44)$$

where

$$f(\mathbf{k}') = \sum_{j'=1}^{3} V(\mathbf{k}_0,\mathbf{k}')\,V(\mathbf{k}',\mathbf{k})(u_j^{\dagger}(\mathbf{p})\beta_4 u_{j'}(\mathbf{p}')) \times (u_{j'}^{\dagger}(\mathbf{p}')\beta_4 u_0(\mathbf{p}_0))k'^2\frac{dk'}{d\omega'}, \quad (45)$$

and $d\Omega'$ represents the element of solid angle of $\mathbf{p}'$. Integrating over $d\omega'$, we have

$$a_j^{(2)}(\mathbf{p},t) = -i\pi\int d\Omega'\left[\tilde{f}_0\frac{\exp[i(\omega-\omega_0)t]}{\omega_0-\omega} - \tilde{f}\frac{1}{\omega_0-\omega}\right], \quad (46)$$

where $\tilde{f}_0$, $\tilde{f}$ denote the values of $f(\mathbf{k}')$ when $|\mathbf{k}'| = |\mathbf{k}_0|$, $|\mathbf{k}|$, respectively. On account of (40) we have

$$a_j^{(2)}(\mathbf{p},t) = -i\pi\int d\Omega'\tilde{f}_0\frac{\exp[i(\omega-\omega_0)t]-1}{\omega_0-\omega}. \quad (47)$$

The total number of scattered mesons is given by

$$\int\psi^{\dagger}\beta_4\psi d\mathbf{r} = \sum_{j=1}^{3}\int|a_j(\mathbf{p},t)|^2 d\mathbf{k} = \sum_{j=1}^{3}\int\int|a_j(\mathbf{p},t)|^2 k^2 dk d\Omega. \quad (48)$$

The intensity of the scattered mesons at a distance R from the scatterer is therefore

$$J = \frac{1}{R^2}\frac{d}{dt}\sum_{j=1}^{3}\int|a_j(\mathbf{p},t)|^2 k^2 dk. \quad (49)$$

Since

$$|a_j|^2 = |a_j^{(1)}+a_j^{(2)}+\cdots|^2 = |a_j^{(1)}|^2 + (a_j^{(2)*}a_j^{(1)}+a_j^{*(1)}a_j^{(2)})+\cdots, \quad (50)$$

the intensities of the scattered mesons in the first and second Born approximations are given, respectively, by

$$J^{(1)} = \frac{1}{R^2}\frac{d}{dt}\sum_{j=1}^{3}\int|a_j^{(1)}(\mathbf{p},t)|^2 k^2\frac{dk}{d\omega}d\omega, \quad (51)$$

$$J^{(2)} = \frac{1}{R^2}\frac{d}{dt}\sum_{j=1}^{3}\int[a_j^{(2)*}(\mathbf{p},t)a_j^{(1)}(\mathbf{p},t) + a_j^{(1)*}(\mathbf{p},t)a_j^{(2)}(\mathbf{p},t)]k^2\frac{dk}{d\omega}d\omega. \quad (52)$$

Substituting (43) and (47) into (51) and (52) we obtain

$$J^{(1)} = \frac{\pi}{R^2}\sum_{j=1}^{3}V(\mathbf{k}_0,\mathbf{k})^2|u_j^{\dagger}(\mathbf{p})\beta_4 u_0(\mathbf{p}_0)|^2 k^2\frac{dk}{d\omega}, \quad (53)$$

$$J^{(2)} = \frac{i\pi^2}{R^2}\sum_{j,j'=1}^{3}\int d\Omega' V(\mathbf{k}_0,\mathbf{k})\,V(\mathbf{k},\mathbf{k}') \times V(\mathbf{k}',\mathbf{k})\left(k^2\frac{dk}{d\omega}\right)^2 \times[(u_0^{\dagger}\beta_4 u_{j'})(u_{j'}^{\dagger}\beta_4 u_j)(u_j^{\dagger}\beta_4 u_0) - (u_0^{\dagger}\beta_4 u_j)(u_j^{\dagger}\beta_4 u_{j'})(u_{j'}^{\dagger}\beta_4 u_0)]. \quad (54)$$

The factors $V(\mathbf{k}_0, \mathbf{k})$, etc., have been treated in detail by Sauter for a central field, of which the Coulomb field is a special case. For our purpose it is necessary only to evaluate the summations occurring in (53) and (54).

The summation in (53) is

$$S^{(1)} \equiv \sum_{j=1}^{3} (u_0^\dagger \beta_4 u_j)(u_j^\dagger \beta_4 u_0).$$

Making use of (7) and the second formula of (8) we obtain

$$S^{(1)} = (u_0^\dagger \beta_4 u_0) + \frac{1}{2E\mu} u_0^\dagger \beta_4 {}^2[(\mathbf{p}\cdot\boldsymbol{\beta})^2 - (\mathbf{p}_0\cdot\boldsymbol{\beta})^2] u_0. \quad (55)$$

By (9), (10), (10′), we obtain

$$S^{(1)} = u_0{}^{(1)\dagger} s^{(1)} u_0{}^{(1)} \quad (56)$$

with

$$s^{(1)} = 1 - \frac{4}{(E+\mu)^4}(\boldsymbol{\zeta}\cdot\mathbf{p}_0)(\tilde{\boldsymbol{\zeta}}\cdot\mathbf{p}_0)(\boldsymbol{\zeta}^*\cdot\mathbf{p}_0)(\boldsymbol{\zeta}^\dagger\cdot\mathbf{p}_0) - \frac{1}{E\mu(E+\mu)^2}[(\boldsymbol{\zeta}\cdot\mathbf{p}_0)(\tilde{\boldsymbol{\zeta}}\cdot\mathbf{p}_0)(\boldsymbol{\zeta}^*\cdot\mathbf{p})(\boldsymbol{\zeta}^\dagger\cdot\mathbf{p}) + (\boldsymbol{\zeta}\cdot\mathbf{p})(\tilde{\boldsymbol{\zeta}}\cdot\mathbf{p})(\boldsymbol{\zeta}^*\cdot\mathbf{p}_0)(\boldsymbol{\zeta}^\dagger\cdot\mathbf{p}_0) - 2(\boldsymbol{\zeta}\cdot\mathbf{p}_0)(\tilde{\boldsymbol{\zeta}}\cdot\mathbf{p}_0)(\boldsymbol{\zeta}^*\cdot\mathbf{p}_0)(\boldsymbol{\zeta}^\dagger\cdot\mathbf{p}_0)]. \quad (57)$$

With the help of (19), (20), (17) we obtain

$$(\boldsymbol{\zeta}\cdot\mathbf{p}_0)(\tilde{\boldsymbol{\zeta}}\cdot\mathbf{p}_0)(\boldsymbol{\zeta}^*\cdot\mathbf{p})(\boldsymbol{\zeta}^\dagger\cdot\mathbf{p}) + (\boldsymbol{\zeta}\cdot\mathbf{p})(\tilde{\boldsymbol{\zeta}}\cdot\mathbf{p})(\boldsymbol{\zeta}^*\cdot\mathbf{p}_0)(\boldsymbol{\zeta}^\dagger\cdot\mathbf{p}_0) = (p^4/2) - [\mathbf{S}\cdot(\mathbf{p}_0\times\mathbf{p})]^2,$$

$$(\boldsymbol{\zeta}\cdot\mathbf{p}_0)(\tilde{\boldsymbol{\zeta}}\cdot\mathbf{p}_0)(\boldsymbol{\zeta}^*\cdot\mathbf{p}_0)(\boldsymbol{\zeta}^\dagger\cdot\mathbf{p}_0) = (p^4/4).$$

Hence

$$s^{(1)} = \frac{4\mu E}{(E+\mu)^2}\left\{1 + \frac{1}{4E^2\mu^2}[\mathbf{S}\cdot(\mathbf{p}_0\times\mathbf{p})]^2\right\}. \quad (58)$$

Substituting (58) and (34) into (56), we obtain

$$S^{(1)} = \sum_{j_0,\, j_0'=1}^{3} a_{j_0}{}^* a_{j_0'} v_{j_0}{}^\dagger \times\left\{1 + \frac{1}{4E^2\mu^2}[\mathbf{S}\cdot(\mathbf{p}_0\times\mathbf{p})]^2\right\} v_{j_0'}. \quad (59)$$

If we introduce polar coordinates and take the polar axis along $\mathbf{p}_0$, then

$$\mathbf{p}_0 = p(0, 0, 1),$$

$$\mathbf{p} = p(\sin\vartheta\cos\varphi, \sin\vartheta\sin\varphi, \cos\vartheta). \quad (60)$$

Denoting $\mathbf{p}_0\times\mathbf{p}$ by $p^2\mathbf{n}$, we have

$$\mathbf{S}\cdot(\mathbf{p}_0\times\mathbf{p}) = p^2(S_+ n_- + S_- n_+ + S_0 n_0), \quad (61)$$

where

$$n_0 = n_3, \quad n_\pm = (n_1 \pm i n_2)/\sqrt{2}. \quad (62)$$

With the help of (33) we then obtain

$$S^{(1)} = (|a_0{}^0|^2 + |a_+{}^0|^2 + |a_-{}^0|^2) + (p^4/4E^2\mu^2)\sin^2\vartheta[|a_0{}^0|^2 + \tfrac{1}{2}|a_+{}^0 e^{i\varphi} + a_-{}^0 e^{-i\varphi}|^2]. \quad (63)$$

This is the result previously obtained by Laporte. Our result (59) is valid for all initial states.

The summation occurring in (54) can be similarly evaluated. The result is

$$S^{(2)} \equiv \sum_{j,\, j'=1}^{3} [(u_0^\dagger \beta_4 u_{j'})(u_{j'}{}^\dagger \beta_4 u_j)(u_j^\dagger \beta_4 u_0) - (\mu_0^\dagger \beta_4 u_j)(u_j^\dagger \beta_4 u_{j'})(u_{j'}{}^\dagger \beta_4 u_0)] = \frac{i(E^2+\mu^2)}{2E^2\mu^2(E+\mu)^2} u_0{}^{(1)\dagger} s^{(2)} u_0{}^{(1)}, \quad (64)$$

with

$$s^{(2)} = -(\mathbf{p}'\cdot\mathbf{p})\mathbf{S}\cdot(\mathbf{p}\times\mathbf{p}') + (\mathbf{p}'\cdot\mathbf{p}_0)\mathbf{S}\cdot(\mathbf{p}'\times\mathbf{p}_0) - (\mathbf{p}\cdot\mathbf{p}_0)\mathbf{S}\cdot(\mathbf{p}\times\mathbf{p}_0) + \frac{p^2(\mathbf{p}'\cdot\mathbf{p})}{(E+\mu)^2(E^2+\mu^2)}\mathbf{p}_0\cdot(\mathbf{p}'\times\mathbf{p})(\mathbf{S}\cdot\mathbf{p}_0). \quad (65)$$

This is very similar to the second approximation obtained by Sauter for the electron. It would be a rather complicated task to deduce (65) on the basis of the wave theory.

The intensity of the scattered mesons can be evaluated by substituting (59) and (64) into (53) and (54) and evaluating the quantities $V(\mathbf{k}_0, \mathbf{k})$, etc., by assuming a special form for the electrostatic potential. The dependence of the intensity on the energy and the polarization of the incident meson and the direction of the scattered meson can then be calculated. This has been carried out by Laporte for the first Born approximation. The second approximation can be similarly treated. We shall not give the details here.

It has recently been pointed out by several authors that eigenfunctions of the meson in a Coulomb field do not exist; therefore the scattering problem has strictly no solution. Such a divergency depends on the special form of the

electrostatic field. In the above calculation we made no assumption concerning the field except its being spherically symmetrical. Our results will therefore still be applicable for an electrostatic field which does not obey the Coulomb law at small distances. At present our result is purely of mathematical interest.

4. SCATTERING OF MESONS BY THE NUCLEAR INTERACTION

The scattering of a meson by the nuclear interaction takes place in two stages in succession. For example, in the case of the scattering of a positive meson by a neutron,

$$N+M_+{}^0\rightarrow N+M_+,$$

the first stage is the absorption of the incident meson by the neutron and the second stage is the subsequent emission of the scattered meson by the proton in the intermediate state, namely,

$$N+M_+{}^0\rightarrow P, \quad P\rightarrow N+M_+.$$

In the following we shall make the same approximations as in reference 9, namely, we confine ourselves to the non-relativistic approximation and neglect the recoil of the nuclear particle. The matrix element for the scattering is given by

$$V=\frac{H_{fn}H_{ni}}{E_i-E_n}. \tag{66}$$

Here H_{ni} is the matrix element between the initial state and the intermediate state and H_{fn} is the matrix element between the intermediate state and the final state. In our approximations,

$$E_i-E_n=E_0=(p_0{}^2+\mu^2)^{\frac{1}{2}}=c\hbar(k_0{}^2+\kappa^2)^{\frac{1}{2}}, \tag{67}$$

where $\mathbf{p}_0=c\hbar\mathbf{k}_0$ is the momentum of $M_+{}^0$. On account of the conservation of energy, the energy of the scattered meson $E=(p^2+\mu^2)^{\frac{1}{2}}$ is equal to E_0 and hence $|\mathbf{p}_0|=|\mathbf{p}|$. The matrix elements H_{ni} and H_{fn} have been given by Wilson (see reference 4) as follows:

$$\begin{aligned} H_{ni}&=\xi^\dagger\left(1-\frac{i}{\mu}\mathbf{p}_0\cdot\boldsymbol{\beta}\right)\beta_4{}^2\psi_0, \\ H_{fn}&=\psi^\dagger\beta_4{}^2\left(1+\frac{i}{\mu}\mathbf{p}\cdot\boldsymbol{\beta}\right)\xi. \end{aligned} \tag{68}$$

Here ξ is the column matrix describing the nuclear interaction. In the notation of reference 9,

$$\xi=4\sqrt{2}\pi^2c\hbar\eta/\sqrt{\mu}, \tag{69}$$

where η, like ψ, can be divided into three components as in (10). In the non-relativistic approximation,

$$\eta^{(1)}=0, \quad \eta^{(2)}=\begin{pmatrix} -f\sigma_1 \\ -f\sigma_2 \\ -f\sigma_3 \\ g \end{pmatrix}, \quad \eta^{(3)}=0. \tag{70}$$

In (70), f and g are constants and the σ's are Pauli spin matrices for the nuclear particle. From (9) and (70) it follows that

$$\beta_4\eta=0, \quad \eta^\dagger\beta_4=0. \tag{71}$$

Substituting (67), (68), (69), (70), and

$$\begin{aligned} \psi_0&=\frac{1}{(2\pi)^{\frac{3}{2}}}u_0(\mathbf{p}_0)\exp\left[i\mathbf{k}_0\cdot\mathbf{r}-iE_0t/\hbar\right], \\ \psi&=\frac{1}{(2\pi)^{\frac{3}{2}}}u(\mathbf{p})\exp\left[i\mathbf{k}\cdot\mathbf{r}-iEt/\hbar\right], \\ u_0(\mathbf{p}_0)&=\sum_{j_0=1}^{3}a_{j0}u_{j0}(\mathbf{p}_0), \\ u(\mathbf{p})&=\sum_{j=1}^{3}a_ju_j(\mathbf{p}), \end{aligned} \tag{72}$$

into (66), we obtain, apart from an exponential factor,

$$\begin{aligned} V=\frac{4\pi}{\kappa}\frac{1}{(k_0{}^2+\kappa^2)^{\frac{1}{2}}}u^\dagger\beta_4{}^2 \\ \times\left(1+\frac{i}{\mu}\mathbf{p}\cdot\boldsymbol{\beta}\right)\eta\eta^\dagger\left(1-\frac{i}{\mu}\mathbf{p}_0\cdot\boldsymbol{\beta}\right)\beta_4{}^2u_0. \end{aligned} \tag{73}$$

The transition probability is proportional to $\sum_{j=1}^{3}|V|^2$, which can be written in the form

$$\sum_{j=1}^{3}|V|^2=\frac{16\pi^2}{\kappa^2}\frac{1}{k_0{}^2+\kappa^2}ABC,$$

with

$$A=u_0^\dagger\beta_4^2\left(1+\frac{i}{\mu}\mathbf{p}_0\cdot\boldsymbol{\beta}\right)\eta,$$

$$B=\sum_{j=1}^{3}\eta^\dagger\left(1-\frac{i}{\mu}\mathbf{p}\cdot\boldsymbol{\beta}\right)\beta_4^2uu^\dagger\beta_4^2\left(1+\frac{i}{\mu}\mathbf{p}\cdot\boldsymbol{\beta}\right)\eta, \quad (74)$$

$$C=\eta^\dagger\left(1-\frac{i}{\mu}\mathbf{p}_0\cdot\boldsymbol{\beta}\right)\beta_4^2u_0.$$

The expressions can be easily evaluated with the help of (71) and the formulae given in Section 2. For B we have

$$B=\frac{1}{2E}\eta^\dagger\left(1-\frac{i}{\mu}\mathbf{p}\cdot\boldsymbol{\beta}\right)\beta_4\left[E\beta_4+\mu+\frac{1}{\mu}(\mathbf{p}\cdot\boldsymbol{\beta})^2\right]\times\beta_4\left(1+\frac{i}{\mu}\mathbf{p}\cdot\boldsymbol{\beta}\right)\eta$$

$$=\frac{1}{2E\mu}\eta^\dagger(\mathbf{p}\cdot\boldsymbol{\beta})\beta_4^2(\mathbf{p}\cdot\boldsymbol{\beta})\eta$$

$$=\frac{1}{2E\mu}\eta^\dagger[(\mathbf{p}\cdot\boldsymbol{\zeta}^\dagger)(\mathbf{p}\cdot\boldsymbol{\zeta})+(\mathbf{p}\cdot\bar{\boldsymbol{\zeta}})(\mathbf{p}\cdot\boldsymbol{\zeta}^*)]\eta$$

$$=\frac{1}{2E\mu}[f^2(\boldsymbol{\sigma}\times\mathbf{p})\cdot(\boldsymbol{\sigma}\times\mathbf{p})+g^2p^2]$$

$$=\frac{p^2}{2E\mu}(g^2+2f^2). \quad (75)$$

For A we have

$$A=\frac{i}{\mu}u_0^\dagger(\mathbf{p}_0\cdot\boldsymbol{\beta})\eta$$

$$=\frac{i}{\mu}[u_0^{(1)\dagger}(\mathbf{p}_0\cdot\boldsymbol{\zeta})\eta^{(2)}+u_0^{(3)\dagger}(\mathbf{p}_0\cdot\boldsymbol{\zeta}^*)\eta^{(2)}]$$

$$=\frac{i}{u}\left\{u_0^{(1)\dagger}(\mathbf{p}_0\cdot\boldsymbol{\zeta})u_0^{(1)}-\frac{1}{(E+\mu)^2}u_0^{(1)\dagger}\times[p^2-2(\mathbf{S}\cdot\mathbf{p}_0)^2](\mathbf{p}_0\cdot\boldsymbol{\zeta}^*)\eta^{(2)}\right\}$$

$$=\frac{-\sqrt{2}}{E+\mu}[f\mathbf{u}_0^{(1)*}\cdot(\boldsymbol{\sigma}\times\mathbf{p}_0)+ig\mathbf{u}_0^{(1)*}\cdot\mathbf{p}_0]$$

$$=\frac{-1}{(2\mu E)^{\frac{1}{2}}}[f\mathbf{a}_0^*\cdot(\boldsymbol{\sigma}\times\mathbf{p}_0)+ig\mathbf{a}_0^*\cdot\mathbf{p}_0], \quad (76)$$

where $\mathbf{a}_0$ is the vector whose 3 components are equal to the a_{j0}'s in (72). Similarly,

$$C=\frac{-1}{(2\mu E)^{\frac{1}{2}}}[f\mathbf{a}_0\cdot(\boldsymbol{\sigma}\times\mathbf{p}_0)-ig\mathbf{a}_0\cdot\mathbf{p}_0]. \quad (77)$$

Substituting (75), (76), and (77) into (74), we obtain

$$\sum_{j=1}^{3}|V|^2=\frac{4\pi^2}{\kappa^4}\frac{p^2}{E^4}(g^2+2f^2)[f^2(\mathbf{a}_0^*\times\mathbf{p}_0)\cdot\boldsymbol{\sigma}(\mathbf{a}_0\times\mathbf{p}_0)\cdot\boldsymbol{\sigma}+g^2(\mathbf{a}_0^*\cdot\mathbf{p}_0)(\mathbf{a}_0\cdot\mathbf{p}_0)+igf(\mathbf{a}_0\cdot\mathbf{p}_0)\mathbf{a}_0\cdot(\boldsymbol{\sigma}\times\mathbf{p}_0)-igf\mathbf{a}_0^*\cdot(\boldsymbol{\sigma}\times\mathbf{p}_0)(\mathbf{a}\cdot\mathbf{p}_0)]. \quad (78)$$

The result (78) includes all initial states of polarization of the meson. For the scattering of a longitudinal meson, $\mathbf{a}_0=(0,0,1)$ and hence

$$\sum_{j=1}^{3}|V|^2=\frac{4\pi^2}{\kappa^4}\frac{p^4}{E^4}g^2(g^2+2f^2). \quad (79)$$

For the scattering of a transverse meson, $\mathbf{a}_0=(1,0,0)$ or $(0,1,0)$, and hence

$$\sum_{j=1}^{3}|V|^2=\frac{4\pi^2}{\kappa^4}\frac{p^4}{E^4}f^2(g^2+2f^2). \quad (80)$$

The scattering cross section Φ is given by

$$\Phi=\frac{8\pi^2}{\hbar c}\frac{E_0}{p_0}\rho\sum_{j=1}^{3}|V|^2,$$

where

$$\rho=pE/(2\pi\hbar c)^3$$

is the density of energy levels in the final state. Substituting the expressions for ρ and $\sum|V|^2$ into the expression for Φ we obtain, for the scattering of longitudinal and transverse mesons, respectively,

$$\Phi_l=\frac{4\pi}{\kappa^2}\frac{g^2}{\hbar c}\frac{g^2+2f^2}{\hbar c}\frac{p^4}{\mu^2E^2},$$

$$\Phi_t=\frac{4\pi}{\kappa^2}\frac{f^2}{\hbar c}\frac{g^2+2f^2}{\hbar c}\frac{p^4}{\mu^2E^2},$$

in agreement with reference 9.

In conclusion the writer would like to thank Drs. W. Heitler, N. Kemmer, A. H. Wilson, Y. T. Yao, and Ta-You Wu for valuable discussions and their interest in this work.

Radiations from Radioactive Co^{56}

C. SHARP COOK AND PAUL W. MCDANIEL
Department of Physics, Indiana University, Bloomington, Indiana
(Received August 12, 1942)

LIVINGOOD and Seaborg[1] have reported a new cobalt isotope of about 72-days half-life. This isotope emits positrons and gamma-radiation of considerably higher energy than does the previously reported 72-day cobalt activity. It has also been found to be independent of the first-known 72-day activity and has been subsequently assigned to Co^{56}, the lower energy activity being assigned to Co^{58}.

A nickel wire was bombarded by deuterons in the Indiana University cyclotron and was allowed to age for nearly two months before measurements were taken. The shorter-lived isotopes of nickel, cobalt, and copper which would appear normally from such a bombardment thus had time to decay to a point at which they would no longer be of sufficient intensity to cause trouble. The only isotopes of these three elements which would remain active after such a time would be the long-lived isotopes of cobalt (72-day, 270-day, and 5.5-year) which could not be separated chemically. According to Livingood and Seaborg's[1] isotope assignments the 270-day cobalt could not be produced by deuteron bombardment of nickel. Of the other two the probability of producing the 72-day activity is much greater than that of producing the 5.5-year activity.

Measurements were made with a high speed amplifier and scaling circuit, previously developed in this laboratory.[2] The apparatus was capable of measuring radiations of one type or coincidences between two or more types of radiations.

Over a period of two and a half months the activity was measured on a single counter with and without an aluminum absorber. The half-life obtained for the beta-rays and for the gamma-rays was identical, being 80 ± 5 days, with no apparent change to a longer half-life.

The beta-ray end point was found to be at 0.48 g/cm² of aluminum, which corresponds to a particle whose maximum energy is 1.2 Mev. A part of the sample was put in the cloud chamber by Mr. Franklin E. Waterfall. The activity was found to be of positive charge.

The energy of the gamma-rays was investigated by allowing the gamma-rays to eject Compton electrons from an aluminum radiator and measuring the range of these electrons. The electrons produced in the radiator pass through two counters, arranged in a coincidence circuit, and the number of coincidences is studied as a function of the thickness of aluminum placed between the two counters. The range is given by that thickness of aluminum at which the number of coincidences reaches a constant value. At this point all electrons produced in the radiator have been absorbed by the aluminum and the appropriate counter wall thickness (0.18 g/cm²). The range of the Compton electrons from the cobalt sample was 1.34 g/cm², corresponding to an energy (for the highest energy gamma-ray) of 2.9 Mev.[3] By use of the method described by Mitchell and Langer,[4] the average energy of the gamma-rays was found to be 1.74 Mev. An ordinary absorption curve in lead gave an absorption coefficient of 0.536 cm^{-1}, corresponding to an energy of 1.7 Mev.[5]

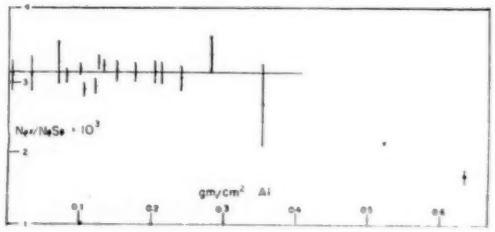

FIG. 1. Beta-gamma-coincidences as a function of the beta-ray energy. Solid circle shows $N_{\gamma\gamma}/N_\gamma S_\gamma$.

[1] J. J. Livingood and G. T. Seaborg, Phys. Rev. **60**, 913 (1941).
[2] A. C. G. Mitchell, L. M. Langer, and P. W. McDaniel, Phys. Rev. **56**, 422 (1939); Phys. Rev. **57**, 1107 (1940); A. F. Clark, Phys. Rev. **61**, 242 (1942).
[3] S. C. Curran, P. I. Dee, and V. Petrzilka, Proc. Roy. Soc. **169**, 269 (1938).
[4] A. C. G. Mitchell and L. M. Langer, Phys. Rev. **52**, 137 (1937).
[5] W. Gentner, J. de phys. et rad. **6**, 274 (1935).

Measurements of the number of beta-gamma-coincidences as a function of the energy of the beta-rays is shown in Fig. 1. Since the number of beta-gamma-coincidences per disintegration does not change with energy, it can be concluded that the beta-ray spectrum is simple. The average number of beta-gamma-coincidences per recorded beta-particle is 3.1×10^{-3}. Gamma-gamma-coincidences were also found, the number per recorded gamma-ray being 1.7×10^{-3}. Gamma-gamma-coincidence measurements were made over a period of about one month and were found to decay with essentially the same half-life as do the singles. The above evidence leads one to believe that positron emission leaves the resulting nucleus in an excited state from which one or more gamma-rays follow. Whether more than one gamma-ray follows the positron cannot be definitely stated at the present time. The fact that the number of recorded gamma-rays is so large in comparison to the number of recorded positive particles (a ratio of about one to three) leads one to suspect a process competing with the positron decay. Thus we are led to the conclusion that perhaps the *K*-capture process is also present.

The authors wish to express their thanks to Professor Allan C. G. Mitchell for his advice and interest during the progress of the work, Mr. Edward der Mateosian for help with certain parts of the chemical separation, and Dr. Hugh Hunter and other members of the cyclotron crew who helped run the cyclotron.

NOVEMBER 1 AND 15, 1942 PHYSICAL REVIEW VOLUME 62

Artificial Radioactivity of Cr^{49}

J. J. O'Connor, M. L. Pool, and J. D. Kurbatov
The Ohio State University, Columbus, Ohio

(Received July 24, 1942)

A radioactive isotope of half-life 41.9 ± 0.3 minutes has been produced by alpha-particle bombardment of titanium and by fast neutron bombardment of chromium. Evidence presented shows that the activity should be assigned to Cr^{49}. Absorption measurements indicate the presence of gamma-rays of energies 0.19 and 1.55 Mev. The end point of the positron spectrum is 1.45 Mev. The 33-minute activity in vanadium is assigned to V^{47}.

INTRODUCTION

MANY radioactive isotopes have been reported in the region of chromium and vanadium. Of particular interest in the present discussion are the 600-day,[1] 16-day,[2] 33-minute,[2] and 3.7-hour[2] periods of vanadium and the 26.5-day[3] period of chromium. In Fig. 1 are shown these and other adjoining isotopes exactly as they have been reported with the exception of the 33-minute period which has been changed from V^{49} to V^{47}. The data necessitating this change will be discussed later.

The present study of this region was begun in an effort to determine the position and characteristics of a newly observed 41.9-minute positron emitter which was obtained after activation of titanium with alpha-particles. Bombardments were made with the cyclotron at The Ohio State University which furnishes approximately 20-Mev alpha-particles, 10-Mev deuterons, and 5-Mev protons. Fast neutrons were obtained from deuteron bombardment of lithium. Decay and absorption measurements were made by means of a Wulf quartz fiber electrometer connected to a Freon filled ionization chamber. The length of bombardment was always adjusted to discriminate against a long period. The substances bombarded include chemically pure TiO_2, Sc_2O_3, Cr_2O_3, and V_2O_5.

[1] H. Walke, E. J. Williams, and G. R. Evans, Proc. Roy. Soc. **A171**, 360 (1939).
[2] H. Walke, Phys. Rev. **51**, 1011 (1937) and **52**, 777 (1937).
[3] H. Walke, F. C. Thompson, and J. Holt, Phys. Rev. **57**, 171 (1940).

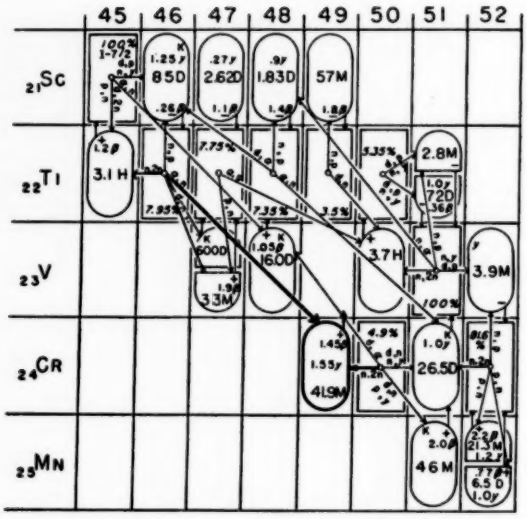

FIG. 1. Chart of region investigated. Abscissas represent mass numbers. Ordinates represent atomic numbers. Oblongs represent stable nuclei. Ovals represent artificial radioactive nuclei. Arrows represent nuclear reactions leading to radioactive nuclei.

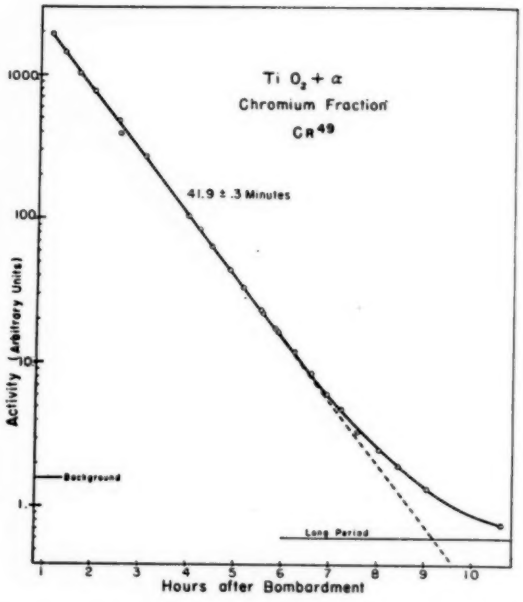

FIG. 2. Decay curve of Cr^{49} obtained from alpha-particle bombardment of titanium.

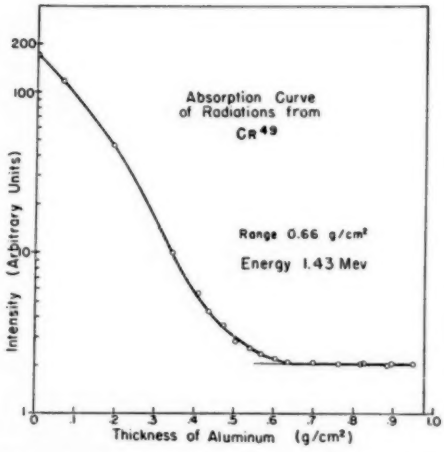

FIG. 3. Aluminum absorption curve for Cr^{49} gives an end point of the positron spectrum at 1.43 Mev.

ACTIVATION OF TITANIUM WITH ALPHA-PARTICLES

The bombardment of titanium with alpha-particles produces a strong activity which decays by positron emission and with a period of 41.9 ± 0.3 minutes. Possible products of the bombardment include $V^{49,50}$ by the (α, p) reaction, $Cr^{49,51}$ by the (α, n) reaction, and Cr^{48} by the $(\alpha, 2n)$ reaction. V^{49} may also be formed as a decay product of Cr^{49}.

Since the accepted methods for the chemical separation of chromium and vanadium require several hours, a short and accurate procedure was worked out after several activations of titanium dioxide with alpha-particles.

In the (α, n) and (α, p) reactions the radioactive isotopes of vanadium and chromium are present in minute concentrations, undiluted by the bulk of the corresponding stable elements. Therefore inactive vanadium and chromium may be added in optimum quantities for precision separation. The method described below can be accomplished in about forty minutes.

Vanadium pentoxide and chromium trioxide were added as carrier to the activated titanium dioxide, and the mixture was fused with sodium carbonate-nitrate. The melt was extracted with water and filtered. Any undissolved titanium dioxide was rejected, and the solution containing all the sodium vanadate and chromate was made acid and reduced. Vanadium was precipitated with cupferron and filtered off. The chromium in solution was neutralized, oxidized to chromate, and precipitated as barium chromate.

This method has been tested with two different relative quantities of chromium and vanadium carrier. In one case 10 milligrams of chromium and 200 milligrams of vanadium were used. In another, 200 milligrams of chromium and 10 milligrams of vanadium were added. In both

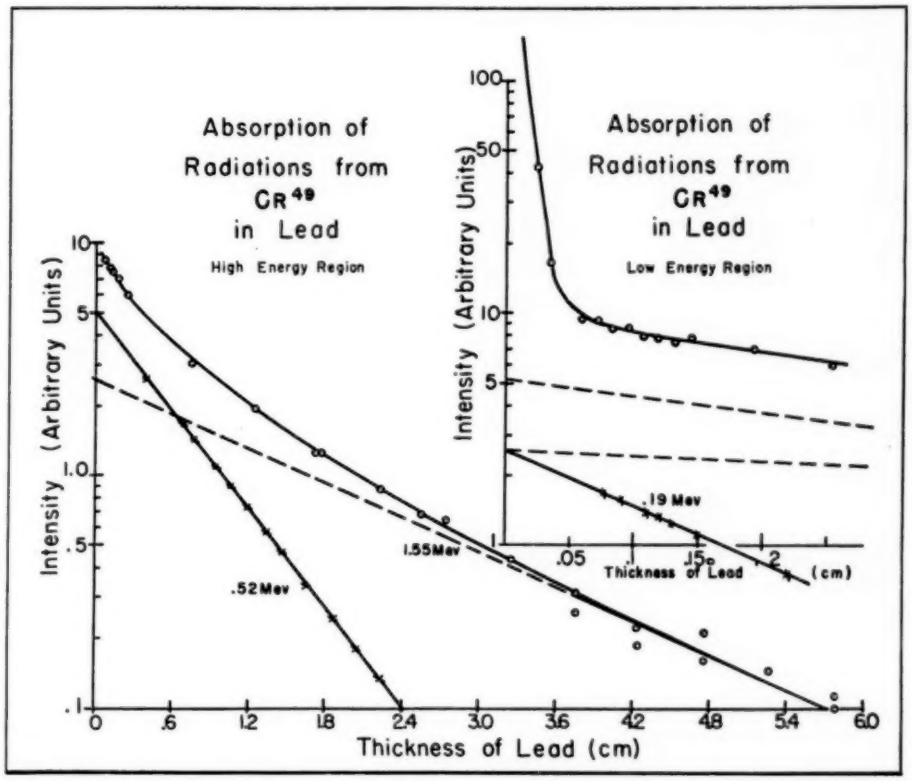

FIG. 4. Lead absorption curve for Cr^{49}. Three gamma-ray energies are evident, 0.19, 0.52, and 1.55 Mev.

cases it was found that the activity of 41.9 minutes was present in the chromium precipitate. The intensity of the activity of the vanadium precipitate was about one-thousandth that of the chromium activity and also decreased with longer half-life. Thus it was established that the 41.9-minute period belonged to chromium. The decay of the activity in the chromium fraction is shown in Fig. 2.

ASSIGNMENT TO Cr^{49}

Only three possibilities remain in the assignment of the activity produced in chromium by alpha-particle bombardment of titanium. These are $Cr^{49,51}$ by (α, n) and Cr^{48} by $(\alpha, 2n)$. Fast neutron bombardment of chromium has been found to produce the 41.9-minute period in chromium by the $(n, 2n)$ reaction. This limits the possibilities to $Cr^{49,51}$.

If the period belongs to Cr^{51}, it should be producible by a (p, n) reaction from V^{51}. Vanadium was bombarded with protons and no 41.9-minute activity was detected.

As an additional check, chromium was bombarded with deuterons. Cr^{51} should be produced by (d, p) reaction; and isotopes of manganese should also be expected by (d, n) or $(d, 2n)$ reactions. A strong 46-minute activity was found in the manganese fraction, but no period of the order of 41.9 minutes was observed in the chromium fraction. The 46-minute manganese period has previously been reported.[4]

Since chemical separation shows that the 41.9-minute activity, produced by alpha-particle bombardment of titanium and by fast neutron bombardment of chromium is an isotope of chromium and since this period has not been found by proton bombardment of vanadium or deuteron bombardment of chromium, the activity must evidently be due to Cr^{49}.

It is interesting to note that on a Konopinski plot[5] (log period *vs.* atomic number), 3.1-hour

[4] J. J. Livingood and G. T. Seaborg, Phys. Rev. **54**, 391 (1938).
[5] G. R. Dickson and E. J. Konopinski, Phys. Rev. **58**, 949 (1940).

Ti^{45}, 41.9-minute Cr^{49}, and 8.9-minute Fe^{53} fall almost on a straight line.

RADIATIONS EMITTED BY Cr^{49}

Since even without chemical separation, the 41.9-minute activity produced by alpha-particle bombardment was found to go through six or more half-lives before any appearance of other activity was noticeable in the decay curve, absorption determinations were made on the activated titanium oxide without chemical separation.

Aluminum absorption measurements, shown in Fig. 3, give an end point at 0.66 g/cm². According to the Sargent equation,[6] this corresponds to a positron energy of 1.43 Mev. A value of 1.48 Mev was obtained by cloud-chamber measurements. The weighted average is 1.45 Mev. On a Sargent diagram this energy together with the value of the period indicates that Cr^{49} decays by an allowed transition.

As shown in Fig. 4 absorption measurements in lead give gamma-rays of three distinct energies. One of these gamma-rays has an energy of 0.5 Mev, probably due to the annihilation radiation. The other two are of about equal intensity and have energies of 1.55 and 0.18 Mev. By measuring the decay through various thicknesses of lead, it has been shown that all three gamma-energies belong to the 41.9-minute period.

33-MINUTE VANADIUM

A 33-minute vanadium period, produced by deuteron and alpha-particle bombardment of titanium has been previously reported.[2] Since the activity could not be produced by fast neutrons on vanadium, the assignment was made to V^{49}. Aluminum absorption measurements gave a value of 0.82 g/cm², which corresponds to 1.8 Mev by the Sargent equation.

A 33-minute activity assigned to V^{49} is inconsistent with the assignment of the 41.9-minute activity to Cr^{49}. In addition several bombardments of titanium with alpha-particles have failed to reveal the 33-minute period.

However, deuteron bombardment of titanium and proton bombardment of titanium produce the 33-minute vanadium period with strong activity. The range of positrons from this isotope was measured and found to be approximately 0.82 g/cm², which agrees sufficiently well with the reported value of 0.86 g/cm². If positrons of such energy and activity existed at V^{49}, the aluminum absorption taken on the 41.9-minute Cr^{49} should have given an end point of 0.86 g/cm² instead of the 0.66 g/cm² which was found.

If the 33-minute period belonged to V^{48}, it should be produced by bombardment of scandium with alpha-particles. This reaction has been tried, but no 33-minute activity was observed. This period therefore seems to belong to V^{47} or V^{46}. If it belongs to V^{47}, then it is produced from titanium by (p, n) and (d, n) reactions and possibly by (p, y) and $(d, 2n)$ reactions. The 33-minute activity has been tentatively assigned to V^{47}.

The period of V^{49} is now undetermined. It is either very short (less than a minute) or else very long. Arguments[7] have been recently presented for placing the 600-day period at V^{49} instead of at V^{47}. Such a change of position would not be inconsistent with the results discussed in this article.

It is a pleasure to acknowledge the support received from the University Development Fund and from Mr. Julius F. Stone. Valuable assistance through the WPA cyclotron project 265–1–42–65 is acknowledged. Appreciation is also due Mr. Richard Forgrave for his interest and technical assistance.

[6] B. W. Sargent, Can. J. Research **A17**, 82 (1939).

[7] L. A. Turner, Phys. Rev. **58**, 679 (1940).

Experimental Determination of the Disintegration Curve of Mesotrons

BRUNO ROSSI AND NORRIS NERESON
Cornell University, Ithaca, New York

(Received September 17, 1942)

The disintegration curve of mesotrons has been experimentally determined by investigating the delayed emission of disintegration electrons which takes place after the absorption of mesotrons by matter. Within the experimental errors, the disintegration curve is exponential and corresponds to a mean lifetime of 2.3 ± 0.2 microseconds.

1. INTRODUCTION

THE purpose of the experiment described in the present paper was to determine the disintegration curve of mesotrons at rest. The experiment was performed by investigating the delayed emission of the disintegration electrons, which takes place after the absorption of mesotrons by matter.

Experiments more or less closely related to the present one have been reported previously by Montgomery, Ramsey, Cowie, and Montgomery,[1] by Rasetti,[2] and by de Souza Santos.[3] The experiment by Montgomery and his collaborators failed to give any significant result. The experiment by Rasetti consists essentially of the determination of two points of the disintegration curve and gives a mean life of (1.5 ± 0.3) μsec. under the assumption of an exponential decay. De Souza Santos reports some very surprising results which seem to indicate that the disintegration processes are not distributed according to an exponential but rather according to a Gaussian law with center at 5 μsec.

The previous experiments were performed by means of special coincidence circuits designed in such a way as to record only those electrons which were emitted from the absorber within preselected time intervals after the arrival of the mesotrons. We have succeeded in increasing the selectivity and the statistical accuracy of the method considerably by recording all decay electrons and measuring the time interval between the arrival of each mesotron and the emission of the corresponding electron. The circuit used for this measurement will be referred to as the *time circuit*. In its simpler form, the time circuit measures the delay τ between the pulses of two Geiger-Müller counter tubes A and B. The two pulses are fed to two separate inputs a and b. At the output a signal is obtained, the amplitude of which is a function of τ. This signal can be recorded either with a cathode-ray oscilloscope and a photographic camera or with a pen-writing instrument. If only counter A is discharged, a large output pulse is recorded (corresponding to $\tau = \infty$). No pulse is recorded if only counter B is discharged. While the circuit is primarily designed for the measurement of *positive* delays (counter B discharged *after* counter A), the "zero line" can be shifted by introducing an artificial delay in the branch b so that small *negative* delays (counter B discharged *before* counter A) may be also measured.

A slight modification of the time circuit makes it possible to measure the delay between a coincidence of two counters A_1 and A_2 and the pulse of a third counter B. In the modified circuit a signal is recorded whenever A_1 and A_2 are discharged within 15 μsec. of each other and the amplitude of the signal is a function of the delay between the pulse of either counter A_1 or A_2, whichever is discharged later, and the pulse of counter B.

The time circuit was calibrated by means of artificially produced double pulses with known time separations. To generate such pulses we used two different circuits, in which the time scale was supplied by the rate of charge of a known condenser through a known resistor and by the period of a crystal-controlled quartz oscillator, respectively. The calibration curves obtained with the two circuits differ by about 10 percent. The circuit involving the quartz oscil-

[1] C. G. Montgomery, W. E. Ramsey, D. B. Cowie, and D. D. Montgomery, Phys. Rev. **56**, 635 (1939).
[2] F. Rasetti, Phys. Rev. **60**, 198 (1941).
[3] M. D. de Souza Santos, Phys. Rev. **62**, 178 (1942).

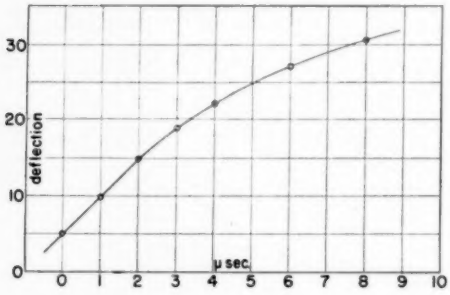

FIG. 1. Calibration curve of the time circuit.

lator appears to be more reliable and has been adopted in the final measurements. Figure 1 gives a sample of a calibration curve obtained with this circuit.

A detailed description of the construction, the operation, and the calibration of the time circuit will be given elsewhere.

2. TIME LAGS OF GEIGER-MÜLLER COUNTERS

The discharges of Geiger-Müller counters are known to be affected by variable time lags.[1,4] Since the data published so far on this phenomenon did not appear sufficiently definite and complete, a preliminary test was made to determine whether or not the natural time lags of the counters could seriously affect our main measurements.

Figure 2 represents schematically the arrangement used for this test. The Geiger-Müller counters L, A, and B are of the all-metal type, filled with a mixture of argon (10 cm Hg) and alcohol (1 cm Hg). A and B are 20 cm long, 2.5 cm in diameter, with a central wire of 7-mil tungsten. They are operated about 120 volts above starting potential. The three counters L are connected in parallel. The pulses of counters L, A, and B are fed to a threefold coincidence circuit C. Counters A and B are also connected to the inputs a and b of the time circuit T. The output pulses of the coincidence circuit are used to turn on the beam of a cathode-ray oscilloscope included in the recording apparatus R, while the output pulses of the time circuit are fed to the deflecting plates of the same oscilloscope. Whenever a particle traverses counters L, A, and B a record is obtained from which the time lag between the discharges of counters A and B can be determined.

Measurements were taken with two different pairs of counters and the distributions of the time lags recorded are represented in Fig. 3. It will be noted that the center of gravity of the delays falls at about 0.1 μsec. rather than at 0. This shift is accounted for by the difference in shape between the pulses of the counters and those of the calibrating circuit. A slight influence of the pulse shape on the output signal of the time circuit may be anticipated from an analysis of this circuit. The existence of such an effect has been experimentally verified by changing the pulse shape of the calibrating circuit with added capacities. It has been verified also that the absolute magnitude of the error involved does not change when the size of the delay is increased.

The observed delays seem to be distributed about 0.1 μsec. according to an approximately Gaussian law with a r.m.s. deviation of about 0.2 μsec. This time is short compared with the lifetime of mesotrons which is known to be of the order of several μsec. We conclude that the natural time lags of alcohol-argon counters are small enough to make their use possible in a direct measurement of the lifetime of mesotrons. This is not necessarily true for other types of counters.

3. THE DETERMINATION OF THE DISINTEGRATION CURVE

The geometrical arrangement of counters and absorbers in our main experiment (Fig. 4) was not essentially different from the arrangements used by Rasetti and by de Souza Santos. The three counters L were connected in parallel and so were the four counters B and the five counters M. Nine cm of lead was placed in P_1 to cut off the electron component of cosmic rays. A brass plate

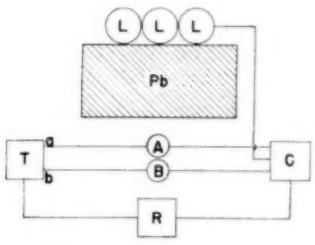

FIG. 2. Experimental arrangement for the measurement of natural time lags of Geiger-Müller counters.

[4] C. G. Montgomery and D. D. Montgomery, Phys. Rev. **59**, 1045 (1941).

of dimensions $25.5 \times 8 \times 2.3$ cm was placed in Br and a lead plate 1.4 cm thick in P_2. The number of mesotrons traversing L, A_1, and A_2 was about 600 per hour, and of those 11 ± 2 were absorbed by the brass plate Br. The last figure was determined by recording the number of anticoincidences (L, A_1, A_2, $-M$) with and without the brass plate.

Counters L, A_1, A_2, and B were connected to the coincidence branch of an anticoincidence circuit C while counters M were connected to the anticoincidence branch of the same circuit. Since counters M completely cover the solid angle subtended by L, A_1, A_2, and B, the mesotrons traversing these counters do not produce anticoincidences except for lack of efficiency of the counter group M and for the few mesotrons stopped by the lead plate P_2. Anticoincidences may also be produced by showers coming from the side or by large-angle scattering of mesotrons in the plate Br. Finally, there will be anticoincidences caused by mesotrons which traverse L, A_1, A_2, and which are stopped in Br and then disintegrate into electrons which discharge one of the counters B. The resolving time of the anticoincidence circuit was very large compared with the lifetime of the mesotrons, so that practically no anticoincidences were lost because of the finite life of the mesotrons in the brass plate. The purpose of the lead plate P_2 was to decrease the probability of counters M being discharged by a decay electron and thus prevent the recording of an anticoincidence.

Counters A_1, A_2, and B were also connected to the inputs a_1, a_2, and b of the time circuit T. The output pulses of C and T were fed to the recording device R, which operated in such a way that a pulse from T was recorded only when it was accompanied by a pulse from C within approximately 10^{-2} second. In the first part of the measurements the recording instrument was a cathode-ray oscilloscope, as in the experiments on the time lags of counters (see Section 2). Later it was found more convenient to change to a pen-writing instrument. It may be mentioned that the results obtained in the two sets of measurements were perfectly consistent with each other.

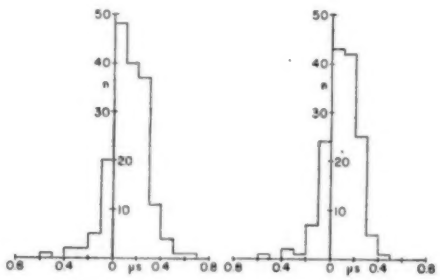

FIG. 3. Distribution of natural time lags for two different pairs of counters. The ordinates n are the numbers of delays recorded per 0.1-μsec. interval.

As we have just seen, a pulse is recorded by R whenever an anticoincidence (L, A_1, A_2, B, $-M$) occurs and the amplitude of this pulse is a measure of the time interval between the coincidence (A_1, A_2) and the pulse of B. Apart from the time lags of the counters, this time is equal to the life of the mesotron in the brass plate Br, when the anticoincidence is caused by a disintegration process. The time is practically zero when the anticoincidence is caused by spurious effects; i.e., lack of efficiency of counters M, absorption of mesotrons in P_2, showers coming from the side, or scattering.

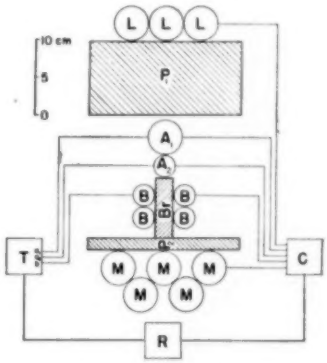

FIG. 4. Experimental arrangement for the determination of the disintegration curve of mesotrons.

The results obtained are summarized in Table I (Exp. A) along with the results of some control runs carried out without the brass plate Br (Exp. B). The last measurements were taken partly with and partly without the lead plate P_2. No difference exceeding the statistical fluctuations was found in the two cases. We consider the delays larger than 0.99 μsec. almost entirely caused by disintegration processes. In the interval $0.55 < \tau < 0.99$ μsec. most of the delays are again due to the same cause, at least in Exp. A, while most of the anticoincidences accompanied by delays smaller than 0.55 μsec. are accounted for

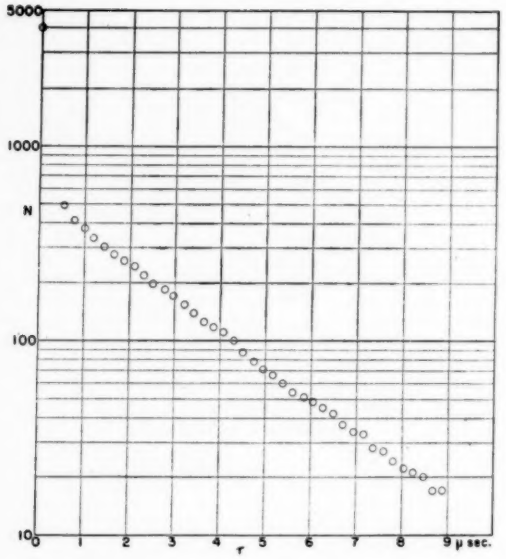

FIG. 5. Experimental disintegration curve of mesotrons. The abscissa τ is the delay recorded by the time circuit, the ordinate is the logarithm of the number N of anticoincidences accompanied by delays larger than the corresponding abscissa (Exp. A).

by spurious effects. The frequency distribution of the delays recorded in Exp. A is represented on a semi-logarithmic scale in Fig. 5. The experimental points lie on a straight line as closely as one can expect considering the statistical fluctuations, with the exception, of course, of the point at $\tau=0$ and possibly the one at 0.55 μsec. Hence the disintegration of mesotrons follows an exponential law as does any ordinary disintegration process.

The above interpretation of our experimental results is substantiated by the following analysis of possible sources of error.

(a) A delay may be recorded if a spurious anticoincidence is accompanied by a spontaneous time lag in counter B. However, direct measurements have shown (Section 2) that the natural time lags of counters hardly ever exceed 1 μsec., while in Exp. A almost 10 percent of the anticoincidences were accompanied by delays larger than this amount.

(b) When counters A_1, A_2 are discharged and none of counters B is, the time circuit T gives a large pulse. This pulse will be recorded by R if it is preceded by an anticoincidence (L, A_1, A_2, B, $-M$) within a time shorter than the recovery time of $C(\sim 10^{-2}$ sec.), or if it is followed by such an anticoincidence within a time shorter than the recovery time of $T(\sim 10^{-2}$ sec.). It can be shown that about 0.3 percent of the anticoincidences recorded should be accompanied by such spurious pulses simulating delays larger than 1 μsec., and that more than half of these delays should be larger than 10 μsec. Hence only the number of very long delays may be affected appreciably by the above chance coincidences.

(c) A delay may be recorded when an anticoincidence (L, A_1, A_2, $-M$) is followed by an independent pulse in one of counters B within a time shorter than the resolving time of the anticoincidence circuit. It may be estimated that this will happen about once every 1500 events recorded under the conditions of Exp. A. Thus the effect is negligible.

That neither natural time lags of counters nor chance coincidences are responsible for any large fraction of the observed delays is most clearly confirmed by Exp. B where the removal of the brass plate Br is seen to reduce the number of delays larger than 0.99 μsec. much more strongly than the total number of anticoincidences recorded. This result is self-evident if the delays are produced by disintegration of mesotrons in Br. It could hardly be understood if the delays were to be accounted for by time lags or by chance coincidences. It seems likely that the most of the delays between 0.99 and 8.91 μsec. in Exp. B are due to disintegration processes taking place mainly in the walls of the counters. This view is supported by the fact that the distribution of these delays seems to be more or less the same as in Exp. A as far as one can tell from the small number of events recorded. In Exp. B more delays between 0.55 and 0.99 μsec. were recorded than are explainable by decay of mesotrons. Some

TABLE I. Summary of the experimental results. t is the time of observation in hours, n the number of anticoincidences recorded for which the delay τ is within the specified interval. Experiments A and B were performed with and without the brass plate Br, respectively.

Interval (microseconds)	Experiment A n	Experiment A n/t	Experiment B n	Experiment B n/t
$\tau<0.55$	3506	6.51	1298	5.57
$0.55<\tau<0.99$	121	0.22	23	0.10
$0.99<\tau<4.95$	307	0.57	21	0.09
$4.95<\tau<8.91$	54	0.10	2	0.01
$\tau>8.91$	17	0.03	5	0.02
Total	4005	7.43	1349	5.79

of these delays must be attributed to time lags of the counters.

4. NUMERICAL VALUE OF THE LIFETIME

For the evaluation of the lifetime τ_0 we shall use the following equation:

$$\rho=[N(\tau_1)-N(\tau_2)]/[N(\tau_2)-N(\tau_3)]$$
$$=[\exp(-\tau_1/\tau_0)-\exp(-\tau_2/\tau_0)]/[\exp(-\tau_2/\tau_0)-\exp(-\tau_3/\tau_0)], \quad (1)$$

where $N(\tau)$ is the number of mesotrons surviving at the time τ after their absorption in the brass plate. If we take $\tau_1=0.99$ μsec., $\tau_2=4.95$ μsec., $\tau_3=8.91$ μsec., then $\tau_2-\tau_1=\tau_3-\tau_2=\Delta\tau=3.96$ μsec. Equation (1) reduces to

$$\rho=\exp(\Delta\tau/\tau_0),$$

and the experimental data set forth in Table I yield

$$\tau_0=2.3\pm0.2 \text{ μsec.},$$

where the error indicated is the standard statistical error.

We have selected the above method of calculation which does not involve delays larger than 8.91 μsec. because an appreciable number of these delays may have been produced by chance coincidences.

It is important to examine whether and to what extent our results may be affected by errors other than purely statistical.

(a) Delays due to chance coincidences have been neglected. An approximate correction for these delays would lower the value of the lifetime by 0.05 μsec. which is negligible compared with the statistical error.

(b) When a disintegration process is recorded, the time measured by the time circuit is not exactly equal to the time interval between the arrival of the mesotron and the emission of the decay electron. This is so because of the time lags of the counters and because of the small error caused by the difference in shape between the pulses of the counters and of the calibration circuit (see Section 2). Both sources of error may be included in an error function $f(\tau')$ such that $f(\tau')d\tau'$ gives the probability of recording a delay between $\tau+\tau'$ and $\tau+\tau'+d\tau'$ when the actual delay is τ. The function $f(\tau')$ is not symmetrical with respect to zero. It is important to note that it is independent of τ. Let $N(\tau)$ be the true disintegration curve of mesotrons. The observed disintegration curve will be, for all $\tau>\tau_1$:

$$N_{\text{obs}}(\tau)=\int_{-\tau_1}^{+\tau_1}N(\tau-\tau')f(\tau')d\tau',$$

where τ_1 is such that $f(\tau')$ is practically zero for $|\tau'|>|\tau_1|$ and we may take $\tau_1=0.99$ μsec. If $N(\tau)$ is an exponential function, $N(\tau)=A\exp(-\tau/\tau_0)$, then

$$N_{\text{obs}}(\tau)=A\exp(-\tau/\tau_0)\times\int_{-\tau_1}^{+\tau_1}f(\tau')\exp(\tau'/\tau_0)d\tau'$$
$$=\text{const.}\times\exp(-\tau/\tau_0).$$

It is seen that the observed and the true disintegration curves have identical shapes for $\tau>\tau_1$. Hence no error will be made by evaluating the lifetime from the observed disintegration curve if delays smaller than τ_1 are disregarded.

(c) Apart from the statistical fluctuations, the only serious source of error may thus lie in the calibration curve of the time circuit. The accuracy of this calibration is difficult to evaluate. As already mentioned in Section 1 two separate methods gave calibration curves different by about 10 percent. It is easy to see how time intervals determined by the rate of charge of a condenser may be in error by as much as 10 percent, mainly on account of the difficulty in the evaluation of stray capacities. It seems, however, that time intervals determined by the period of a quartz oscillator should be considerably more accurate. Since the calibration curve obtained with the quartz oscillator was finally adopted, we feel safe in assuming that the error in the calibration is small compared with the statistical error.

The value of the lifetime given by the present experiment is larger than the one determined by Rasetti. We do not feel, however, that the two experiments are in serious disagreement, because of the statistical errors and also because of the possibility of some error in the calibration of Rasetti's circuit.

Our results are in complete disagreement with those of de Souza Santos with regard to the shape

of the disintegration curve as well as to the average value of the lifetime.

A comparison between the present results and those obtained from the absorption anomaly in air involves knowledge of the mesotron mass μ because the latter method gives essentially the ratio τ_0/μ. According to the most reliable measurements, μ seems to be between 160 and 240 electron masses.[5] The present value of τ_0 together with the value of τ_0/μ determined by Rossi and his collaborators[6] gives $\mu=160$ electron masses which is within the above limits, while the value of τ_0/μ determined by Nielsen and his collaborators[7] would give $\mu=360$ which seems definitely too large.

[5] See T. A. Wheeler and R. Ladenburg, Phys. Rev. **60**, 754 (1941).

[6] B. Rossi and D. B. Hall, Phys. Rev. **59**, 223 (1941). B. Rossi, K. Greisen, J. C. Stearns, D. K. Froman, and P. G. Koontz, Phys. Rev. **61**, 675 (1942).

[7] W. M. Nielsen, C. M. Ryerson, L. W. Nordheim, and K. Z. Morgan, Phys. Rev. **59**, 547 (1941).

NOVEMBER 1 AND 15, 1942 PHYSICAL REVIEW VOLUME 62

The Near Infra-Red Spectrum of Water Vapor

Part II. The Parallel Bands ν_3, $\nu_1+\nu_3$, $\nu_2+\nu_3$ and the Perpendicular Band ν_1

HARALD H. NIELSEN
Mendenhall Laboratory of Physics, Ohio State University, Columbus, Ohio

(Received August 31, 1942)

An analysis of the rotational structure of the three "parallel" type bands, ν_3, $\nu_1+\nu_3$, and $\nu_2+\nu_3$ and the "perpendicular" type band ν_1 has been carried out. The data lead to the following effective values of A, B, and C: ($A=h/8\pi^2I_a$, $B=h/8\pi^2I_b$, $C=h/8\pi^2I_c$); $A(\nu_1)=27.26$ cm^{-1}, $B(\nu_1)=14.28$ cm^{-1}, $C(\nu_1)=9.17$ cm^{-1}; $A(\nu_3)=26.50$ cm^{-1}, $B(\nu_3)=14.40$ cm^{-1}, $C(\nu_3)=9.10$ cm^{-1}; $A(\nu_1+\nu_3)=26.04$ cm^{-1}, $B(\nu_1+\nu_3)=14.16$ cm^{-1}, $C(\nu_1+\nu_3)=8.95$ cm^{-1}; $A(\nu_2+\nu_3)=29.32$ cm^{-1}, $B(\nu_2+\nu_3)=14.56$ cm^{-1}, $C(\nu_2+\nu_3)=9.06$ cm^{-1}. These data permit a redetermination of the vibrational constants ω_i, x_i, x_{ik}, and γ. The new values obtained for the ω_i are the following: $\omega_1=3829.4$, $\omega_2=1654.5$, and $\omega_3=3940.1$.

INTRODUCTION

IN a relatively recent article[1] the author has reported new and much improved data on the vibration-rotation bands ν_2 and $2\nu_2$ which arise out of variations of the electric moment parallel to the axis of the intermediate moment of inertia. From an analysis of these data certain of the vibration-rotation constants, already evaluated by Darling and Dennison,[2] have been verified. In this communication a set of improved data is presented on the bands ν_3, $\nu_1+\nu_3$, and $\nu_2+\nu_3$ which originate with variations of the electric moment parallel to the axis of the smallest moment of inertia and the band ν_1 which is of the perpendicular type. The former oscillations are sometimes spoken of as parallel oscillations because they are parallel to the axis of the smallest moment of inertia which in a limiting case may be thought of as an approximate symmetry axis. The band ν_1 is of the type discussed in Part I. The analysis of these bands permits one to make somewhat improved determinations of a considerable number of the vibration-rotation constants of the water vapor molecule.

EXPERIMENTAL

The experimental procedure was here entirely the same as for the work reported in Part I, the water vapor in the optical path of the spectrometer acting as the absorbing layer. In order to obtain any resolution whatever in the region of intense absorption near 2.7μ it was necessary

[1] H. H. Nielsen, Phys. Rev. **59**, 565 (1941).

[2] B. T. Darling and D. M. Dennison, Phys. Rev. **57**, 128 (1940). Cited as D and D later.

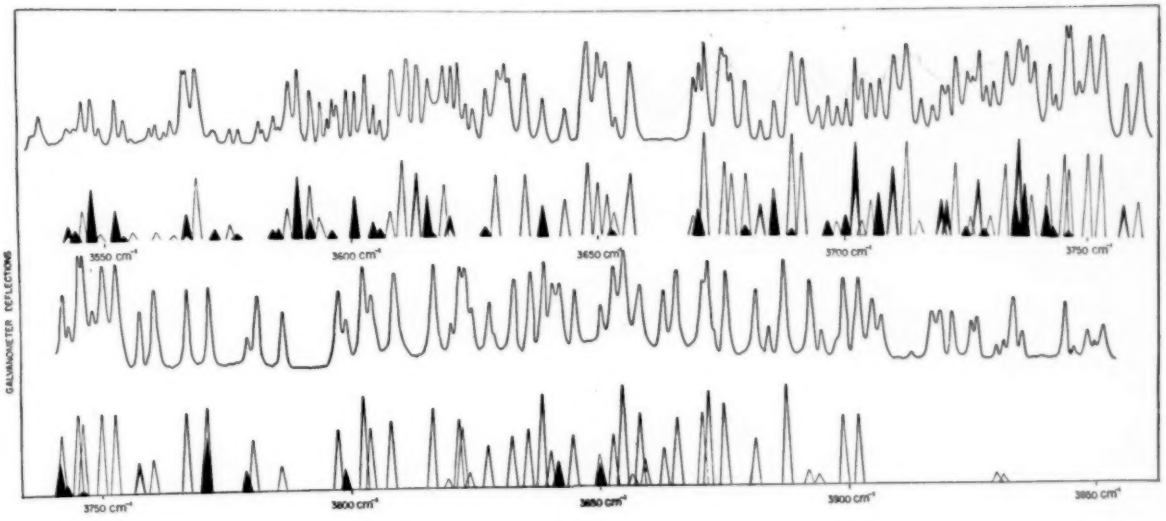

FIG. 1.

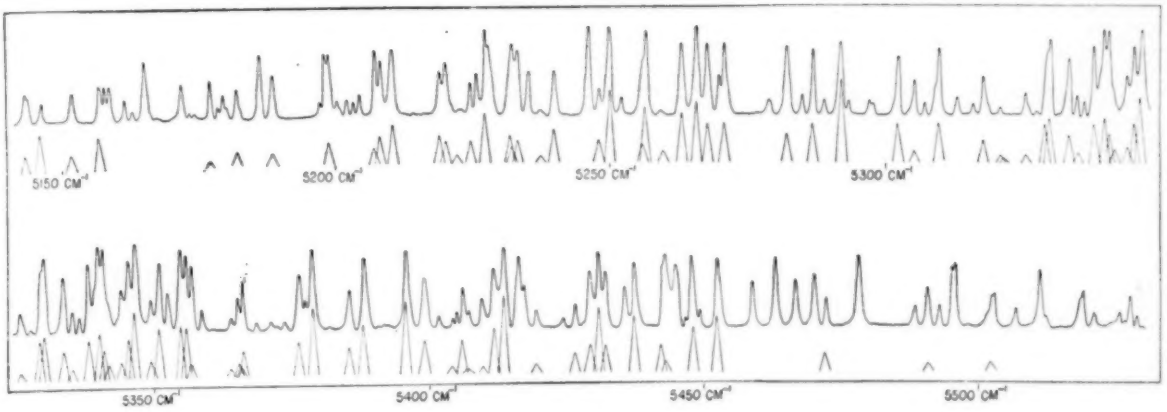

FIG. 2.

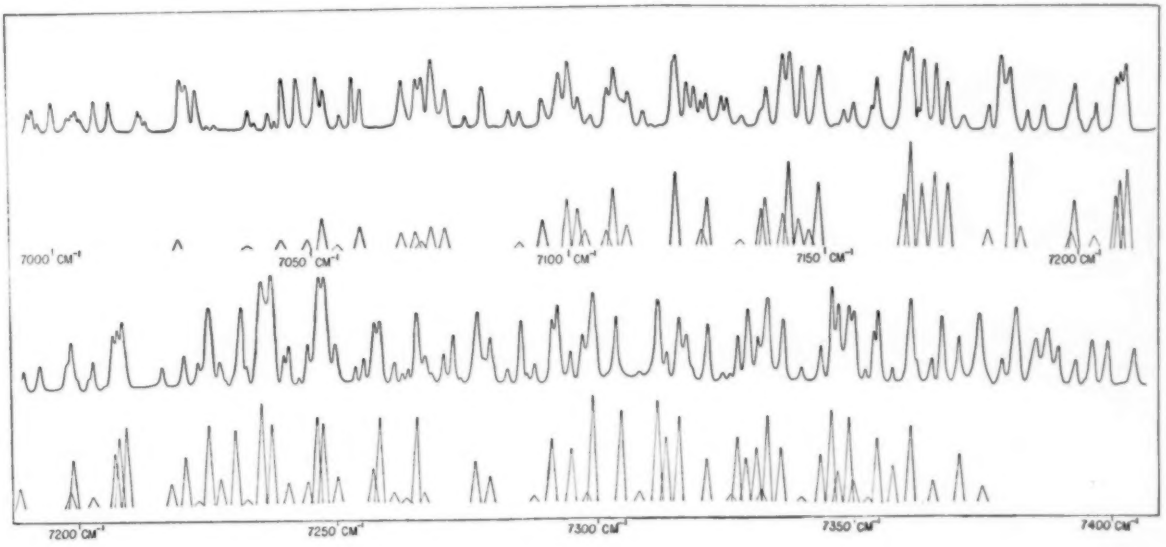

FIG. 3.

TABLE I. Frequency positions and identifications of water vapor lines near 2.7μ.

ν obs.	ν calc.	Transition
3525.3		
3528.3		
3529.6	3529.3	$5_0 - 6_{-2}^*$
3531.4	3531.2	$5_1 - 5_3^*$
3537.6		
3543.2	3543.5	$6_{-5} - 6_{-3}^*$
	3543.5	$3_{-1} - 4_2$
3544.6	3544.6	$4_{-4} - 5_{-4}^*$
	3544.4	$6_4 - 7_3$
	3544.6	$6_3 - 7_2$
3548.4	3548.5	$2_{-1} - 3_2$
	3548.0	$4_{-3} - 5_{-5}^*$
	3548.0	$6_1 - 7_{-1}^*$
3549.3	3549.0	
3552.5	3552.5	$6_0 - 7_{-1}$
	3552.7	$6_{-3} - 6_{-1}^*$
	3552.6	$4_{-1} - 5_3^*$
	3552.2	$5_{-4} - 5_{-2}^*$
	3552.6	$6_1 - 7_0$
3554.0	3553.7	$6_{-6} - 6_{-4}^*$
3556.0	3556.1	$6_{-2} - 7_{-3}$
3560.7	3560.7	$6_2 - 7_1$
3564.5	3564.7	$2_0 - 3_3$
3566.2		
3566.8	3566.9	$3_0 - 3_2^*$
	3567.0	$5_{-5} - 5_{-3}^*$
	3566.6	$5_{-1} - 5_1^*$
3568.7	3568.0	$3_{-2} - 4_{-4}^*$
	3568.9	$6_{-1} - 7_{-2}$
3575.7	3575.3	$2_{-2} - 3_{-2}^*$
	3576.0	$3_{-3} - 4_0$
	3576.2	$5_{-1} - 5_2$
	3574.5(?)	$5_4 - 6_3$
	3574.5(?)	$5_5 - 6_4$
3577.2	3577.1	$3_0 - 4_{-2}^*$
	3577.3	$4_0 - 4_2^*$
3581.3		
3584.1	3584.0	$5_{-5} - 4_1^*$
3585.6	3585.8	$4_{-4} - 3_2^*$
3587.7	3588.1	$5_2 - 6_2$
	3588.1	$5_1 - 6_0$
3589.3	3588.7	$5_{-3} - 5_{-1}^*$
	3589.0	$5_2 - 6_1$
	3589.6	$2_{-1} - 3_{-3}^*$
	3589.3	$6_{-4} - 6_{-2}^*$
3591.8	3591.5	$2_{-1} - 2_1^*$
	3591.9	$6_{-3} - 7_{-4}$
	3592.0	$6_3 - 7_1^*$
3593.7	3594.1	$4_{-3} - 4_2$
	3593.0	$6_{-4} - 7_{-5}$
3596.5	3596.9	$4_{-4} - 4_{-2}^*$
	3596.4	$6_4 - 7_0^*$
3597.3	3597.6	$1_{-1} - 2_{-1}^*$
3599.2		
3600.8		
3602.9		
3604.8	3605.0	$4_4 - 5_3$
	3604.3	$4_2 - 5_1$
	3604.8	$4_3 - 5_2$
3606.0	3606.2	$4_{-2} - 4_0^*$
3608.1	3607.9	$5_{-3} - 6_{-4}$
	3608.1	$3_{-1} - 3_1^*$
3610.4	3610.6	$3_{-2} - 3_3$
	3610.3	$6_{-5} - 7_{-6}$
	3610.3	$6_{-6} - 7_{-5}$
3613.3	3614.1	$2_{-2} - 3_1$
	3612.9	$5_{-2} - 6_{-3}$
	3613.2	$3_{-3} - 3_{-1}^*$
3615.6	3615.6	$0_0 - 1_0^*$
	3616.1	$3_2 - 4_0^*$
3618.5	3618.2	$4_3 - 5_1^*$
3620.1	3620.3	$4_0 - 5_{-1}$
	3619.8	$1_0 - 2_{-2}^*$
3622.4	3622.5	$2_{-2} - 2_0^*$
3623.3	3623.2	$4_4 - 5_0^*$
3624.6		
3627.2		
3629.2	3628.7	$4_2 - 5_{-2}^*$
3630.8		
3631.8		
3635.1	3635.2	$4_{-1} - 5_{-2}$
	3635.2	$5_{-4} - 6_{-5}$
	3634.2	$5_{-5} - 6_{-6}$
	3634.7	$4_0 - 5_{-4}^*$
	3634.7	$1_{-1} - 1_1^*$
3638.6	3638.4	$2_2 - 3_{-2}^*$
3643.5	3643.7	$1_{-1} - 2_2$
	3643.2	$3_3 - 4_2$
	3643.9	$5_0 - 4_4^*$
3648.2	3643.2	$6_{-6} - 6_{-3}$
	3648.1	$3_1 - 4_0$
	3648.3	$6_{-4} - 6_{-1}$
3650.1	3650.3	$4_{-4} - 5_{-5}$
	3650.0	$6_{-5} - 5_{-1}^*$
3652.1	3652.2	$3_{-1} - 4_{-2}$
	3651.5	$4_{-3} - 5_{-4}$
	3652.9	$6_0 - 5_5$
	3652.2	$6_2 - 5_4^*$
3653.8	3653.8	$3_{-2} - 2_2^*$
	3653.4	$5_1 - 4_3^*$
	3654.0	$6_{-5} - 6_{-4}$
	3653.0	$6_{-2} - 7_{-6}^*$
3656.8	3656.9	$3_0 - 4_{-1}$
	3656.8	$4_1 - 5_0$
3669.6	3669.8	$3_{-3} - 4_{-4}$
3670.7	3670.7	$1_1 - 1_{-1}^*$
	3670.3	$5_{-2} - 4_2^*$
3671.7	3671.4	$3_{-2} - 4_{-3}$
3675.2	3675.1	$2_2 - 3_1$
	3675.2	$4_{-4} - 4_{-1}$
	3675.9	$4_0 - 3_2^*$
3677.2	3676.9	$2_0 - 3_{-1}$
	3677.7	$5_{-2} - 4_3$
	3676.0(?)	$5_{-1} - 5_{-3}^*$
3680.1	3679.9	$2_1 - 3_0$
	3680.4	$2_{-2} - 1_0^*$
	3682.9	$5_{-4} - 5_{-3}$
3683.4	3683.5	$3_{-1} - 3_{-2}^*$
	3683.6	$6_0 - 5_2^*$
	3685.4	$3_{-3} - 3_0$
	3685.6	$2_2 - 2_0^*$
3685.8	3685.0	$3_1 - 3_{-1}^*$
	3685.4	$3_{-1} - 2_1^*$
	3685.4	$5_0 - 6_{-6}^*$
	3686.0	$4_0 - 4_{-2}^*$
3689.5	3689.5	$2_{-2} - 3_{-3}$
	3689.8	$1_0 - 0_0^*$
3691.5	3691.6	$2_{-1} - 3_{-2}$
	3691.4	$2_{-2} - 2_1$
	3692.7(?)	$4_{-3} - 3_2$
	3691.0	$6_0 - 6_{-2}^*$
3694.9	3695.1	$5_1 - 5_{-1}^*$
3696.9	3696.7	$6_{-2} - 6_{-4}^*$
3698.6	3698.2	$5_{-1} - 4_4$
	3697.9	$4_1 - 5_{-5}^*$
	3698.6	$6_{-3} - 6_{-2}$
3700.0	3699.9	$5_{-4} - 4_1$
	3700.0	$2_1 - 2_{-1}^*$
	3700.0	$4_{-2} - 4_{-4}^*$
3702.3	3702.3	$1_1 - 2_0$
	3702.8	$4_{-3} - 4_{-2}$
	3702.5	$2_{-1} - 1_{-1}^*$
	3702.4	$6_{-1} - 7_{-7}^*$
3705.5	3705.6	$6_6 - 6_5$
	3705.6	$6_5 - 6_6$
3707.1	3706.9	$5_1 - 6_{-4}$
	3707.1	$3_{-3} - 2_{-1}^*$
3709.9	3709.8	$1_{-1} - 2_{-2}$
	3709.9	$3_2 - 4_{-4}^*$
	3710.1	$3_0 - 3_{-2}^*$
	3710.0	$5_{-3} - 5_{-5}^*$
3712.7	3712.7	$1_0 - 2_{-1}$
	3712.5	$4_2 - 4_0^*$
3715.6	3715.6	$4_{-2} - 3_0^*$
	3716.1	$5_0 - 5_{-2}^*$
	3715.6	$6_4 - 6_3$
	3715.6	$6_3 - 6_4$
3718.0		
3719.9	3719.4	$5_{-2} - 5_{-1}$
	3719.9	$3_{-2} - 2_{-2}^*$
3721.1	3721.1	$5_5 - 5_4$
	3721.1	$5_4 - 5_5$
	3721.3	$3_3 - 3_1^*$
3722.8	3722.8	$3_{-2} - 3_{-1}$
	3722.8	$4_1 - 4_{-1}^*$
	3722.7	$6_1 - 6_2$
3725.3	3725.5	$3_2 - 3_0^*$
3726.2	3726.2	$5_0 - 5_1$
3727.3	3727.2	$4_4 - 4_3$
	3726.8	$4_3 - 4_4$
	3727.6	$4_3 - 5_{-3}^*$
	3727.4	$4_{-1} - 4_{-3}^*$
3729.0	3728.9	$4_{-4} - 3_{-2}^*$
3730.6	3730.6	$4_2 - 4_1$
3733.0	3733.0	$0_0 - 1_{-1}$
	3732.9	$6_2 - 6_0^*$
3735.7	3735.5	$4_{-1} - 4_0$
	3735.7	$5_3 - 5_2$
	3735.5	$5_2 - 5_3$
	3734.9(?)	$5_{-3} - 4_{-1}^*$
	3735.5	$4_{-1} - 4_0$
	3735.3	$6_2 - 6_1$
	3735.7	$6_{-1} - 6_{-3}^*$
3737.1	3737.1	$2_1 - 1_1^*$
	3736.5	$4_{-3} - 3_{-3}^*$
3738.8	3738.8	$2_{-1} - 2_0$
3741.8	3741.8	$3_3 - 3_2$
	3741.6	$3_2 - 3_3$
	3741.9	$3_1 - 4_{-4}$
	3741.6	$4_0 - 5_{-5}$
	3741.8	$5_{-5} - 4_{-3}^*$
	3741.6	$6_1 - 6_{-1}^*$
3743.0	3742.9	$4_{-2} - 3_3$
	3743.1	$5_3 - 6_{-2}$
	3743.5	$2_2 - 1_0^*$
	3743.2	$4_4 - 4_2^*$
3745.1	3745.1	$3_0 - 3_1$
	3744.6	$4_3 - 4_1^*$
3745.9	3745.8	$5_1 - 5_0$
	3746.3	$5_{-4} - 4_{-4}^*$
	3746.1	$6_0 - 6_{-1}$
	3745.4	$6_{-4} - 6_{-6}^*$
3747.9		
3749.8	3750.1	$2_1 - 2_2$
	3749.8	$1_0 - 1_1$
	3750.5	$2_2 - 3_{-3}$
	3750.1	$2_1 - 2_2$
	3749.7	$6_{-6} - 5_{-1}$

TABLE I. Frequency positions and identifications of water vapor lines near 2.7μ.—*Continued.*

ν obs.	ν calc.	Transition	ν obs.	ν calc.	Transition	ν obs.	ν calc.	Transition
	3752.4	$2_2 - 2_1$		3819.4	$6_6 - 7_1$		3870.7	$5_{-1} - 4_0$
3752.5	3751.9(?)	$3_3 - 4_{-2}$	3819.6	3820.5	$3_0 - 3_{-3}$	3870.5	3870.3	$6_{-5} - 5_{-4}$
	3752.3	$6_{-2} - 7_{-7}$		3819.0	$4_0 - 3_{-2}^*$		3871.0	$6_{-6} - 5_{-5}$
	3757.5	$3_1 - 3_0$	3821.8	3821.9	$4_2 - 3_0^*$	3872.0		
3757.3	3757.3	$3_0 - 2_0^*$		3821.7	$3_{-3} - 2_{-2}$	3872.8		
3760.2	3760.2	$1_1 - 1_0$	3822.5	3822.4	$3_0 - 2_1$	3875.3	3875.5	$5_{-3} - 4_{-2}$
	3766.5	$4_0 - 4_{-1}$		3823.0	$6_5 - 7_0$		3881.8	$6_2 - 5_3$
3766.8	3766.8	$5_{-3} - 4_2$	3824.0	3824.2	$5_{-2} - 5_{-4}$	3881.6	3881.8	$6_{-1} - 5_0$
	3766.5	$6_4 - 6_2^*$	3827.6	3826.7(?)	$4_1 - 3_2$		3881.8	$6_1 - 5_1^*$
	3766.6	$6_3 - 6_1^*$		3827.7	$3_1 - 2_2$	3883.7		
	3770.8	$2_0 - 2_{-1}$	3832.4	3832.4	$3_{-1} - 2_0$	3886.8	3886.4	$4_1 - 3_{-2}^*$
	3770.4	$5_{-1} - 5_{-2}$		3832.2	$6_5 - 7_{-1}^*$	3892.2	3892.1	$6_{-2} - 5_{-1}$
3770.9	3771.0	$6_1 - 7_{-4}$	3835.7	3835.8	$4_{-2} - 3_{-2}$	3894.6		
	3770.0(?)	$6_{-6} - 5_{-4}^*$		3835.6	$5_0 - 5_{-3}$	3899.5	3899.2	$5_3 - 6_{-6}$
	3771.3	$6_{-5} - 5_{-5}^*$	3838.5	3838.8	$4_{-4} - 3_{-3}$		3899.4	$5_2 - 5_{-1}$
	3778.9	$3_1 - 2_{-1}^*$	3840.8	3840.7	$5_{-2} - 5_{-5}$	3902.5	3902.4	$4_3 - 4_{-3}^*$
3778.9	3779.0	$5_{-2} - 4_{-2}^*$		3841.3	$5_1 - 4_{-1}^*$	3905.1		
	3778.8	$4_{-1} - 3_{-1}^*$	3841.9	3841.6	$4_3 - 3_3^*$	3906.7		
3780.1	3779.8	$1_{-1} - 0_0$		3841.8	$4_4 - 3_3^*$	3912.9	3913.0	$6_{-2} - 5_{-4}^*$
	3785.2	$3_{-1} - 3_{-2}$		3842.2	$6_{-1} - 5_{-1}^*$	3917.0		
	3785.6	$6_{-2} - 6_{-3}$	3844.7	3844.9	$4_{-1} - 3_0$	3918.8		
3785.6	3785.5	$4_1 - 5_{-4}$	3849.0			3921.1	3920.6	$5_5 - 6_{-4}$
	3786.0	$6_6 - 6_4^*$	3850.2	3850.8	$5_{-1} - 4_{-3}^*$		3921.5	$6_4 - 6_{-2}^*$
	3786.0	$6_5 - 6_3^*$		3850.2	$6_{-4} - 6_{-5}$	3925.0		
3797.0	3796.7	$2_{-1} - 1_0$	3852.8	3852.6	$5_0 - 4_1$	3926.2		
	3796.7	$3_3 - 3_{-3}^*$		3853.8	$3_2 - 3_{-1}$	3930.0	3930.1	$4_0 - 3_{-2}$
	3799.0	$4_3 - 5_{-2}$	3854.6	3854.7	$4_0 - 3_1$		3929.9	$5_3 - 5_{-2}$
3798.7	3798.6	$3_3 - 2_1^*$		3855.1	$4_{-2} - 3_{-1}$	3932.0	3932.1	$3_3 - 2_0$
	3799.2	$6_{-1} - 7_{-6}$		3854.7	$6_{-3} - 6_{-6}$	3933.1		
	3802.4	$2_{-2} - 1_{-1}$		3857.7	$5_3 - 4_4$	3935.3		
3802.4	3802.4	$3_2 - 4_{-3}$		3857.7	$5_2 - 4_3$	3944.1		
	3801.8	$5_5 - 6_0$	3858.0	3857.7	$5_{-4} - 4_{-3}$	3945.8		
3803.8	3803.7	$4_{-2} - 4_{-3}$		3859.0(?)	$5_{-5} - 4_{-4}$	3948.3	3947.7(?)	$3_2 - 2_{-1}$
3807.9	3807.9	$2_0 - 1_1$		3858.1	$6_6 - 7_{-2}^*$	3949.9		
	3816.2	$2_1 - 2_{-2}$	3863.0	3863.4	$2_2 - 1_{-1}$	3951.6		
3816.4	3816.7	$3_{-2} - 2_{-1}$	3865.5	3865.6	$5_{-2} - 4_{-1}$			
	3816.4	$5_0 - 4_0^*$		3865.8	$5_1 - 4_2$			
	3816.4	$5_1 - 5_{-5}^*$						

to dry the air in the spectrometer thoroughly. This was accomplished by placing large glass trays containing P_2O_5 in the bottom of the airtight box which surrounds the optical parts of the spectrometer. It was found profitable to allow the spectrometer to stand for a period of from 15 to 20 hours before beginning observations. In the case of the regions $\nu_1+\nu_3(1.4\mu)$ and $\nu_2+\nu_3(1.9\mu)$ it was unnecessary to dry the air in the spectrometer.

For the measurements on the regions ν_1 and ν_3, $\nu_1+\nu_3$ and $\nu_2+\nu_3$, an echelette diffraction grating ruled with 4800 lines to the inch by R. W. Wood was used, respectively, in the first, second, and third orders. The sensitivity was sufficient to permit operation of the spectrometer with slits subtending arcs of from 0.2 cm^{-1} to 0.5 cm^{-1}. The data were recorded in terms of galvanometer deflections, the foreprism being set before observing was begun so that the deflections between the peaks near the beginning and the end of the band were the same. It was believed that a fairly accurate representation of the relative intensities could be obtained in this manner. Composite pictures of the data obtained are shown in the upper curves shown in Figs. 1, 2, and 3, and the frequency positions of the lines and their identifications are shown in Tables I, II, and III.

In each case far better resolution of the lines has been achieved and much more detail has been observed than in the earlier measurements made on these regions by Plyler and Sleator[3] and by Plyler.[4]

IDENTIFICATION OF THE OBSERVED LINES

In an effort to identify as many as possible of the lines in the bands herein referred to we have

[3] E. K. Plyler and W. W. Sleator, Phys. Rev. **37**, 1433 (1931).

[4] E. K. Plyler, Phys. Rev. **39**, 77 (1932).

TABLE II. Frequency positions and identifications of water vapor absorption lines near 1.87μ.

ν obs.	ν calc.	Transition	ν obs.	ν calc.	Transition	ν obs.	ν calc.	Transition
5143.5	5143.8	$6_{-6}-7_{-7}$	5282.1	5282.0	1_1-2_0	5388.0	5387.9	2_0-1_1
5146.3	5145.6	$6_{-5}-7_{-6}$	5286.8	5286.7	$1_{-1}-2_{-2}$	5395.8	5395.8	$3_{-2}-2_{-1}$
	5146.7	$5_{-4}-5_1$	5288.9				5397.9(?)	$5_{-3}-5_{-4}$
5152.0	5152.2	$6_{-4}-7_{-5}$	5292.0	5292.0	1_0-2_{-1}	5399.6	5399.5	2_1-2_{-2}
5157.1	5156.8	$6_{-3}-7_{-4}$	5297.0				5399.6	$3_{-3}-2_{-2}$
5158.0			5302.0	5301.9	$3_{-2}-3_{-1}$		5400.0	5_0-6_{-5}
5159.0			5305.4	5305.7	$5_{-2}-5_{-1}$		5405.9	3_2-4_{-3}
5161.5			5309.7	5309.7	0_0-1_{-1}	5406.0	5405.9	3_0-2_1
5165.5	5165.7	$5_{-5}-4_4$	5313.1				5406.8(?)	5_2-6_{-3}
5172.0				5318.1	$2_{-1}-2_0$	5409.6	5409.4	$6_{-1}-6_{-5}$
5177.3	5177.1	$6_{-6}-6_{-3}$	5318.0	5318.3	6_2-7_{-3}	5411.9	5411.8	3_1-2_2
	5177.2	$5_{-1}-6_{-2}$	5325.8	5326.0	3_1-4_{-4}		5412.2	$3_{-1}-2_0$
5180.0				5328.4	4_2-5_{-3}	5413.7	5413.5	$4_{-4}-3_{-3}$
5181.9	5181.6	$5_{-3}-6_{-4}$	5329.0	5328.6	3_0-3_1		5414.2	$4_{-1}-4_{-4}$
5186.4				5329.1	1_0-1_1	5416.7		
5189.0	5188.8	5_1-6_0		5329.5	6_0-6_{-1}	5419.6	5419.6	$6_{-3}-6_{-6}$
	5189.3	$6_{-5}-6_{-4}$	5333.4	5333.3	$5_{-1}-6_{-6}$	5424.8	5424.6	$6_{-1}-5_0$
5198.1	5198.1	5_0-6_{-1}		5337.0	2_2-2_1	5426.8	5427.0	$5_{-2}-5_{-5}$
5199.0	5199.2	$5_{-2}-6_{-3}$	5338.0	5338.1	$4_{-1}-3_1$	5429.6	5429.8	$4_{-1}-3_0$
5204.4				5338.2	$5_{-5}-4_0$	5431.0	5430.9	$5_{-4}-4_{-3}$
5207.3	5207.2	$5_{-5}-6_{-6}$		5338.3	5_0-5_1	5432.2	5432.0	$5_{-5}-4_{-4}$
5208.5	5208.4	$5_{-4}-6_{-5}$	5339.9	5339.9	1_1-1_0	5435.7		
	5208.7	4_0-5_{-1}	5340.8	5340.8	6_1-6_2	5437.3	5436.8	$4_{-2}-3_{-1}$
5210.6	5210.6	$4_{-2}-5_{-3}$	5341.7	5341.6	3_1-3_0	5443.2	5443.1	4_0-3_1
5219.0	5219.0	4_2-5_1	5344.0	5343.9	6_2-6_1	5445.1		
	5219.7	5_4-6_3		5344.0	4_1-4_2	5448.0	5447.7	5_0-5_{-3}
	5219.8	5_5-6_4	5345.2	5345.1	3_2-3_3		5448.0	2_2-1_{-1}
5220.3	5220.1	$4_{-1}-5_{-2}$		5345.4	4_2-4_1	5452.6	5451.9(?)	$5_{-2}-4_{-1}$
	5220.5	$5_{-3}-5_0$		5345.3	3_3-3_2		5452.7	4_1-4_{-2}
	5220.6	$1_{-1}-2_2$	5346.4	5346.5	5_1-5_0	5459.3	5459.5	5_4-6_{-1}
5223.9			5349.5	5349.4	5_2-5_3	5464.1	5464.3	$5_{-1}-4_0$
5224.8	5224.0	4_1-5_0		5349.7	5_3-5_2	5466.7		
	5225.0	$4_{-4}-5_{-5}$	5350.8	5350.8	2_0-2_{-1}	5470.0	5469.7	6_0-5_1
5227.5	5227.6	$4_{-2}-4_1$	5352.5				5471.6	5_2-4_3
5232.2	5232.2	3_1-4_0	5354.9	5354.9	4_0-4_{-1}	5472.0	5471.7	5_3-4_4
	5232.0	$3_{-1}-4_{-2}$		5355.4	3_3-4_{-2}		5472.3	$6_{-2}-5_{-1}$
5233.6	5233.5	4_4-5_3	5355.7	5355.6	4_3-4_4	5488.4	5488.4	3_3-3_{-2}
	5233.7	4_3-5_2		5355.7	4_4-4_3		5488.4	6_1-5_2
5235.3				5355.7	6_4-6_3	5490.6	5490.4	6_2-5_3
5239.9	5240.4	3_0-4_{-1}		5355.7	6_3-6_4	5492.9		
5246.6	5246.7	3_3-4_2	5356.7	5356.7	$1_{-1}-0_0$	5495.1		
5248.0	5247.7	$3_{-3}-4_{-4}$		5357.1	5_3-6_{-2}	5495.8	5495.8	6_1-6_{-2}
	5248.1	3_2-4_1	5364.0	5364.0	$5_{-1}-5_{-2}$	5502.3	5502.3	6_3-5_4
5250.1	5249.9	$4_{-4}-4_{-1}$	5365.2	5365.0	$3_{-1}-3_{-2}$		5502.3	6_4-5_5
	5250.5	$3_{-2}-4_{-3}$		5365.9	$6_{-2}-6_{-3}$		5502.9	6_5-7_0
5252.4			5366.1	5366.3	5_4-5_5	5510.7		
5256.6	5256.1	$5_{-4}-5_{-3}$		5366.4	5_5-5_4	5519.9		
	5256.9	2_0-3_{-1}	5376.3	5376.0	$2_{-1}-1_0$	5525.4		
	5263.2	2_1-3_0	5378.7	5378.7	$2_{-2}-1_{-1}$	5527.2		
5263.3	5263.3	$3_{-3}-3_0$		5385.4	$4_{-2}-4_{-3}$			
	5264.0	$5_{-2}-4_3$	5385.5	5385.5	6_6-6_5			
5265.9	5265.9	$2_{-2}-3_{-3}$		5385.5	6_5-6_6			
5267.9	5267.8	$2_{-2}-2_1$		5385.7	$6_{-1}-6_{-4}$			
5270.9	5270.9	$2_{-1}-3_{-2}$						

proceeded after the manner discussed in Part I, where also was given a summary of the theory of the non-linear triatomic molecule as developed by Shaffer and Nielsen.[5] Each line in one of the bands ν_i is due to the molecules making a transition from a rotation level in the normal vibration state to a rotation level in the vibration state ν_i and the frequency of such a line will be the difference between a term value in ν_i and one in the normal state. The selection rules governing what transitions may take place have been stated very conveniently by Dennison[6] and we shall not repeat them here. By trial and error enough lines are identified so that the

[5] W. H. Shaffer and H. H. Nielsen, Phys. Rev. **56**, 188 (1939).

[6] D. M. Dennison, Rev. Mod. Phys. **3**, 280 (1931).

TABLE III. Frequency positions and identifications of water vapor absorption lines near 1.39μ.

ν obs.	ν calc.	Transition
6995.8		
6999.6		
7004.2		
7007.7		
	7010.7	$6_5 - 7_4$
7010.7	7010.7	$6_5 - 7_5$
	7010.9	$4_{-2} - 5_1$
7016.1		
7023.7	7023.5	$4_{-4} - 5_{-1}$
7025.4		
7027.3		
7037.3	7038.3(?)	$3_{-1} - 4_2$
	7037.0	$6_0 - 7_{-1}$
7040.4		
7042.7		
7043.5	7043.3	$2_{-1} - 3_2$
7045.8		
7049.5	7049.1	$6_2 - 7_1$
7052.0	7052.2	$6_{-1} - 7_{-2}$
7054.6	7054.5	$4_{-1} - 4_4$
7056.6		
	7059.1	$2_0 - 3_3$
7059.0	7060.7(?)	$5_5 - 6_4$
	7060.7(?)	$5_4 - 6_3$
7067.0	7066.8	$5_{-1} - 5_2$
7069.9	7069.8	$4_0 - 4_3$
	7070.1	$6_{-4} - 7_{-5}$
7071.1	7071.0	$3_{-3} - 4_0$
7073.1	7072.9	$5_3 - 6_2$
	7073.6	$5_2 - 6_1$
7075.8	7074.9	$5_1 - 6_0$
	7076.2	$6_{-3} - 7_{-4}$
7079.7		
7082.9		
7088.0		
7089.9	7089.8	$4_{-3} - 4_2$
7094.3	7094.0	$5_{-3} - 6_{-4}$
7097.8		
7099.6	7100.0	$6_{-6} - 7_{-7}$
	7101.5	$5_{-2} - 6_{-3}$
7101.5	7102.6(?)	$4_4 - 5_3$
	7102.8(?)	$4_3 - 5_2$
	7101.5	$6_{-5} - 7_{-6}$
7104.5		
7107.3	7107.2	$4_1 - 5_0$
7108.5	7108.3	$4_2 - 5_1$
7111.2	7111.1	$2_{-2} - 3_1$
	7111.5	$4_0 - 5_{-1}$
7114.4		
7120.5	7120.3	$4_{-2} - 5_{-3}$
7123.1		
7124.3		
7125.7	7125.5	$5_{-5} - 6_{-6}$
7126.7	7126.7	$4_{-1} - 5_{-2}$
	7126.6	$5_{-4} - 6_{-5}$
7129.5		
7131.0		
7133.3	7132.9	$5_{-3} - 5_0$
	7133.3	$6_{-6} - 6_{-3}$
7137.5	7137.3	$4_{-2} - 4_1$
	7137.4	$6_0 - 5_5$
7138.3	7138.4	$3_3 - 4_2$
	7138.0	$3_2 - 4_1$
7141.9	7142.1	$3_1 - 4_0$
7144.0	7144.8	$4_{-4} - 5_{-5}$
7145.4	7145.2	$6_{-5} - 6_{-4}$
7148.6	7148.4	$3_0 - 4_{-1}$
7153.5		
7155.5	7156.2	$5_{-5} - 5_{-2}$
7159.9		
7165.3	7164.8	$3_{-3} - 4_{-4}$
7166.7	7166.7	$3_{-2} - 4_{-2}$
	7166.3	$5_{-2} - 4_3$
7169.5	7169.5	$2_2 - 3_1$
	7169.7	$4_{-4} - 4_{-1}$
7171.4	7171.3	$2_0 - 3_{-1}$
7174.1	7174.0	$2_1 - 3_0$
	7174.3	$5_{-4} - 5_{-3}$
7177.2		
	7182.0	$6_5 - 6_6$
7182.0	7182.0	$6_6 - 6_5$
	7182.9	$6_{-3} - 6_{-2}$
7184.0		
7186.3	7186.4	$2_{-1} - 3_{-2}$
	7186.3	$2_{-2} - 3_{-3}$
7188.3	7188.4	$2_{-2} - 2_1$
	7188.4	$4_{-3} - 3_2$
	7188.8	$5_{-1} - 4_4$
7192.6		
	7198.9	$1_1 - 2_0$
7198.7	7198.5	$4_{-3} - 4_{-2}$
	7198.1	$6_2 - 7_{-3}$
7202.7	7202.6	$6_4 - 6_3$
	7202.6	$6_3 - 6_4$
7206.8	7206.8	$1_{-1} - 2_{-2}$
	7207.3	$5_5 - 5_4$
7207.4	7207.3	$5_4 - 5_5$
	7207.4	$6_{-1} - 6_0$
7209.0	7209.0	$1_0 - 2_{-1}$
7217.7	7218.1	$3_{-2} - 3_{-1}$
	7217.6	$6_1 - 6_2$
7220.3	7220.5	$5_3 - 5_2$
	7220.1	$5_2 - 5_3$
7223.3	7223.7	$6_2 - 6_1$
7224.8	7224.8	$4_4 - 4_3$
	7224.8	$4_3 - 4_4$
7227.2	7227.2	$4_1 - 4_2$
	7227.0	$4_{-1} - 4_0$
	7227.9	$5_3 - 6_{-2}$
7230.3	7229.8	$0_0 - 1_{-1}$
	7230.3	$5_{-1} - 6_{-6}$
	7230.4	$6_{-2} - 7_{-7}$
	7230.6	$6_0 - 6_{-1}$
7235.0	7235.0	$3_2 - 3_3$
	7235.9	$3_1 - 4_{-4}$
	7234.7	$4_2 - 4_1$
	7234.3	$4_{-2} - 3_3$
7237.0	7237.0	$3_3 - 3_2$
	7236.6	$3_0 - 3_1$
7239.0		
7240.4		
7244.4	7244.9	$2_2 - 3_{-3}$
	7244.2	$2_1 - 2_2$
7246.3	7246.1	$1_0 - 1_1$
7247.5	7246.8	$2_2 - 2_1$
	7247.1	$3_3 - 4_{-2}$
7251.7	7251.5	$3_1 - 3_0$
7253.4	7252.9	$5_{-3} - 4_2$
7254.8		
7256.9	7256.8	$1_1 - 1_0$
	7258.1	$5_{-4} - 4_0$
7258.1	7257.7	$4_0 - 4_{-1}$
	7257.9	$4_{-4} - 3_1$
7261.0	7261.0	$5_{-1} - 5_{-2}$
7262.7		
7263.5	7263.7	$6_{-2} - 6_{-3}$
7265.1	7265.2	$2_0 - 2_{-1}$
7266.7	7266.5	$4_4 - 5_{-1}$
7270.6		
7272.2		
7276.8	7276.8	$1_{-1} - 0_0$
7279.7	7280.0	$3_{-1} - 3_{-2}$
	7279.0	$5_0 - 6_{-5}$
7285.0	7284.6	$4_1 - 5_{-4}$
7288.0	7288.0	$5_5 - 6_0$
7291.4	7291.5	$2_{-1} - 1_0$
7292.6		
	7295.8	$3_2 - 4_{-3}$
7295.3	7295.1	$4_{-2} - 4_{-3}$
	7295.8	$6_6 - 7_1$
7297.2	7297.0	$4_3 - 5_{-2}$
	7299.4	$6_5 - 7_0$
7299.3	7299.4	$2_{-2} - 1_{-1}$
	7300.5(?)	$5_4 - 6_{-1}$
7304.8	7302.3(?)	$2_0 - 1_1$
7311.9	7312.0	$3_0 - 3_{-3}$
	7312.0	$3_{-2} - 2_{-1}$
7313.7	7313.9	$3_0 - 2_1$
7316.3	7316.7	$3_{-3} - 2_{-2}$
7317.4		
7321.6	7321.7	$3_1 - 2_2$
	7320.8	$4_{-1} - 4_{-4}$
7324.6		
7326.2	7325.8	$4_1 - 3_2$
	7326.7	$5_0 - 5_{-3}$
7327.4	7327.2	$3_{-1} - 2_0$
	7327.3	$6_{-4} - 6_{-5}$
7329.2	7329.3	$5_{-2} - 5_{-5}$
7331.5	7331.7	$4_2 - 3_3$
	7331.5	$4_{-3} - 3_{-2}$
7333.4	7333.3	$4_{-4} - 3_{-3}$
7336.0	7335.9	$4_1 - 4_{-2}$
	7336.4	$4_{-1} - 3_0$
7339.6	7339.0	$6_{-3} - 6_{-6}$
7343.6	7342.5(?)	$5_3 - 4_4$
	7342.5(?)	$5_2 - 4_3$
	7343.7	$5_0 - 4_1$
7345.7	7345.9	$4_0 - 3_1$
	7346.5	$4_{-2} - 3_{-1}$
7347.0	7347.2	$3_2 - 3_{-1}$
7349.1	7349.2	$6_3 - 5_4$
	7349.2	$6_4 - 5_5$
	7349.1	$5_{-4} - 4_{-3}$
7350.1	7350.3	$5_{-5} - 4_{-4}$
7352.8	7352.6	$5_1 - 4_2$
7354.1	7354.2	$5_{-2} - 4_{-1}$
7357.6	7357.8	$2_2 - 1_{-1}$
	7361.3	$5_{-1} - 4_0$
7361.2	7361.6	$5_{-3} - 4_{-2}$
	7361.5	$6_{-5} - 5_{-4}$
	7361.1	$6_{-6} - 5_{-5}$
7365.3	7365.1	$6_{-1} - 5_0$
	7365.2	$6_1 - 5_2$
7370.4	7370.8	$6_0 - 5_1$
	7370.2	$6_2 - 5_3$
	7370.2	$6_{-2} - 5_{-1}$
	7369.7	$6_{-3} - 5_{-2}$
7374.5	7375.0	$6_{-4} - 5_{-3}$
7379.0		
7381.4		
7385.5		
7387.6	7387.8	$3_1 - 2_{-2}$
	7387.8	$4_4 - 5_{-5}$
7389.7		
7393.0	7392.5	$4_2 - 4_{-3}$
7396.2		
7399.2		
7404.4		
7411.3		

term values for the quantum numbers $J=0$, $J=1$, and $J=2$ can be established. In evaluating these term values it has been assumed that the energy levels of the water vapor molecule inferred from the data on the pure rotation spectrum reported by Randall, Dennison, Ginsburg, and Weber[7] can be relied upon with considerable certainty. As a verification that the lines have been correctly identified, combination relations are employed. For example, take two lines from the band $\nu_1+\nu_3$ which have been identified in the following manner: $1_{-1}-0_0=7276.8$ cm^{-1} and $1_{-1}-2_{-2}=7206.8$ cm^{-1}. Adding to these the term values 0_0, which is zero, and 2_{-2}, which is 70.0 cm^{-1}, respectively (taken from the data of RDGW), we obtain for the term value 1_{-1} in the state $\nu_1+\nu_3$, 7276.8 cm^{-1}. By identifying the experimentally determined values for $J=0$, $J=1$, and $J=2$ with the corresponding ones of Eq. (1) of Part I,[8] and by using for the coefficients of centrifugal stretching the values determined in that work, we may obtain values for R_1, R_2, and R_4, with the notation of Shaffer and Nielsen, which will be effective for the state ν_i. With the values $R_s(\nu_i)$ so determined, values for the rotational energies for a higher value of J, say $J=5$, are computed and from these additional lines are predicted. These lines are then hunted for in the spectrum and when they are located their experimental values can be used to improve upon the values of the $R_s(\nu_i)$. One may then proceed to predict more lines in the spectrum and perhaps further improve the values of the $R_s(\nu_i)$. To guard against incorrect assignment of lines combination relations have been used consistently and in most cases the agreement has been satisfactory. The lines in the spectrum have been identified for levels up to and including $J=6$ and it is found that most of the important lines on either side of the center of the bands to a distance of about 100 cm^{-1} have been accounted for. The identification of the lines is set down in the third column of Tables I, II, and III. In Table IV are set down the energy levels deduced from the identification of the lines and for comparison the positions of the lines in the bands as computed from these deduced energies are set down in the second column of Tables I, II, and III.

As a further test that the correct identification

TABLE IV. Vibration-rotation term values for the frequencies, ν_1, ν_3, $\nu_1+\nu_3$, $\nu_2+\nu_3$.

J	ν_1	ν_3	$\nu_1+\nu_3$	$\nu_2+\nu_3$
0_0	3652.7 cm^{-1}	3756.8 cm^{-1}	7253.6 cm^{-1}	5333.5 cm^{-1}
1_1	3694.5	3797.3	7293.9	5377.0
1_0	3689.8	3792.1	7288.4	5371.4
1_{-1}	3677.0	3779.8	7276.8	5356.7
2_2	3780.6	3887.2	7381.6	5471.8
2_1	3779.4	3886.2	7380.3	5469.5
2_0	3740.7	3850.2	7344.6	5430.2
2_{-1}	3726.3	3833.8	7328.6	5413.1
2_{-2}	3717.5	3826.2	7323.2	5402.6
3_3	3933.4	4027.1	7522.3	5630.6
3_2	3931.8	4027.1	7520.5	5630.6
3_1	3858.3	3963.8	7457.8	5547.9
3_0	3852.3	3957.2	7448.7	5540.7
3_{-1}	3820.2	3927.4	7422.2	5507.2
3_{-2}	3789.9	3896.1	7391.4	5475.2
3_{-3}	3786.5	3891.7	7386.7	5469.6
4_4	4127.1	4215.4	7713.0	5843.9
4_3	4127.1	4215.0	7713.0	5843.8
4_2	4028.2	4113.2	7617.2	5727.9
4_1	4023.1	4112.0	7611.1	5727.9
4_0	3961.2	4066.8	7558.0	5655.2
4_{-1}	3952.1	4051.2	7542.7	5636.1
4_{-2}	3921.9	4028.4	7519.8	5610.1
4_{-3}	3873.2	3978.0	7473.7	—
4_{-4}	3871.1	3975.5	7470.0	5550.2
5_5	—	4463.4	7949.6	6108.7
5_4	—	4463.4	7949.6	6108.6
5_3	—	4345.9	7830.7	5959.9
5_2	4242.4	4345.9	7830.5	5959.8
5_1	4141.6	4249.7	7736.5	5850.4
5_0	4132.1	4235.1	7726.2	5847.2
5_{-1}	4075.5	4186.4	7677.0	5780.0
5_{-2}	4054.2	4165.9	7654.5	5752.2
5_{-3}	4035.2	4150.7	7636.8	5724.4
5_{-4}	3968.2	4082.4	7573.8	5655.6
5_{-5}	3966.5	4080.9	7572.2	5653.9
6_6	4674.9	4750.9	8227.3	6430.8
6_5	4674.9	4750.9	8227.3	6430.8
6_4	4524.3	4604.5	8091.5	6244.6
6_3	4523.5	4604.5	8091.5	6244.6
6_2	4394.5	4492.2	7980.6	6100.8
6_1	4390.7	4480.5	7975.4	6098.6
6_0	4293.8	4395.2	7879.7	5978.6
6_{-1}	4288.7	4385.7	7869.0	5928.5
6_{-2}	4239.5	4338.6	7816.7	5918.8
6_{-3}	4201.8	4301.4	7785.7	5866.3
6_{-4}	4192.1	4297.4	7774.5	5856.6
6_{-5}	4096.5	4196.8	7688.0	5732.1
6_{-6}	4096.5	4196.2	7686.3	5730.1

[7] H. M. Randall, D. M. Dennison, N. Ginsburg, and L. R. Weber, Phys. Rev. **52**, 160 (1937). Cited as RDGW later.

[8] In Eq. (5) of Part I which determines what the values ϵ to be used in the relation I are, it has been noted that in the case of $J=5$ the second member of the term linear in ϵ should be $(34R_2+706R_3)(R_2+R_3\mp(R_4+2R_5)f)$ and that the term (R_2+25R_3) occurring as a factor in the first and second members of the constant term should be (R_2+35R_3).

of the lines has been made the intensities of the lines were computed for comparison with the observed values. As was pointed out in Part I, to calculate the intensities rigorously becomes a prohibitive task and some approximation method must be resorted to. The argument for the method used here is analogous to the one of RDGW[7] and is somewhat as follows. In the classical theory of the asymmetric rotator, rotation about the axis of the largest moment of inertia and rotation about the axis of the smallest moment of inertia represent stable types of motion. In the quantum theory the energies are, of course, discrete and each discrete energy level has associated with it two symbols J and τ. The symbol J is the quantum number of total angular momentum and is always a positive integer. The symbol τ is not a quantum number but is merely an index taking all integral values from $\tau=+J$ to $\tau=-J$. For a given J value the largest rotation term value is associated with $\tau=+J$ and the lowest rotation term value with $\tau=-J$.

For a given value of J the rotational energies associated with a value of $\tau\approx -J$ correspond to the classical case of the rotator, rotating about the axis of the largest moment of inertia. If we take this axis as the approximately unique axis of the rotator the energies are found to be fairly accurately represented by the relation

$$E=J(J+1)\frac{h^2}{8\pi^2}\left[\frac{1}{2}\left(\frac{1}{I_A}+\frac{1}{I_B}\right)\right]+\frac{K^2h^2}{8\pi^2}\left[\frac{1}{I_C}-\frac{1}{2}\left(\frac{1}{I_A}+\frac{1}{I_B}\right)\right],\quad \text{where } K\approx J. \quad (1)$$

For a given J value, however, those rotational energies identified with $\tau\approx +J$ correspond to the limiting case where the molecule rotates almost entirely about the axis of the smallest moment of inertia. If we take this axis as the approximately unique axis of the rotator we find the energies are fairly well approximated by the equation:

$$E=J(J+1)\frac{h^2}{8\pi^2}\left[\frac{1}{2}\left(\frac{1}{I_B}+\frac{1}{I_C}\right)\right]+\frac{K^2h^2}{8\pi^2}\left[\frac{1}{I_A}-\frac{1}{2}\left(\frac{1}{I_B}+\frac{1}{I_C}\right)\right],\quad \text{where } K\approx J. \quad (2)$$

Levels which are associated with values of τ quite different from $|\tau|=J$ correspond in a very rough manner to the classical motion of the asymmetric rotator about its third axis of inertia and the energies in these cases will be badly represented by either Eqs. (1) or (2).

The pure rotation bands and the type of vibration-rotation band discussed in Part I arise when the electric moment lies along the axis of the intermediate moment of inertia. In such cases the electric moment is therefore normal to both the axis of the smallest and the axis of the largest moment of inertia about which rotation is a stable type of motion in the classical treatment of the asymmetric rotator. Such oscillations must therefore in both of the limiting cases represented by Eqs. (1) and (2) behave as those vibrations termed "perpendicular" in the theory of the symmetric rotator. RDGW have indicated how the intensities may be approximated by using the intensity relations valid for the perpendicular bands in symmetric molecules.

In the case we wish to consider here the oscillation induces a variation of the electric moment in a direction parallel to the axis of the smallest moment of inertia. Hence the electric moment is parallel to one of the axes (the smallest) but normal to the other axis (the largest) about which rotation represents a stable type of motion in the classical theory of the asymmetric rotator.

In the case where the rotator is spinning almost entirely about the axis of the largest moment of inertia; i.e., where $\tau\approx -J$, the energy levels are approximated by Eq. (1). When this condition prevails the oscillations must again behave very much like a perpendicular vibration and again we may expect the intensities to be approximated by the relations set down by RDGW, namely:

$$(J-1, K-1\,|\,I\,|\,J, K)=F\exp\left(-(W_{J-1,K-1})/kT\right)\times\frac{(J+K)(J+K-1)}{J}; \quad (3a)$$

$$(J-1, K+1\,|\,I\,|\,J, K)=F\exp\left(-(W_{J-1,K+1})/kT\right)\times\frac{(J-K)(J-K-1)}{J}; \quad (3b)$$

$$(J, K-1|I|J, K) = F\exp(-(W_{J,K-1})/kT) \times \frac{(2J+1)(J+K)(J-K+1)}{J(J+1)}. \quad (3c)$$

The quantity F takes the values $\frac{1}{4}$ and $\frac{3}{4}$, respectively, as the value of τ in the initial state is even or odd. The two values of F come about because of the division into a symmetric and an antisymmetric classification of the levels arising out of the presence of the two identical hydrogen atoms in the molecule.

When, however, the rotator is spinning mainly about the axis of the smallest moment of inertia, i.e., $\tau \approx +J$, the energy levels are given approximately by Eq. (2). Under these conditions the oscillation must behave very much like that which in the theory of the symmetric molecule is called a parallel vibration. We should therefore expect the intensities this time to be approximately those given by the intensity relations valid for the parallel band in symmetric molecules, namely:

$$(J-1, K|I|J, K) = F\frac{2(J^2-K^2)}{J}\exp(-(W_{J-1,K})/kT); \quad (4a)$$

$$(J, K|I|J, K) = F\frac{2K^2(2J+1)}{J(J+1)}\exp(-(W_{J,K})/kT); \quad (4b)$$

$$(J, K|I|J-1, K) = (J-1, K|I|J, K)\exp(Jh^2/4\pi^2IkT); \quad (4c)$$

where F takes the values $\frac{1}{4}$ and $\frac{3}{4}$, respectively, depending upon whether τ in the initial state is even or odd.

For example, we take the transition $5_{-4}-5_{-3}$. The τ values are both of the order -5. The levels 5_{-5} and 5_{-4} are nearly coincident and are approximately given by Eq. (1) by setting $J=5$ and $K=5$. The levels 5_{-3} and 5_{-2} are also fairly nearly coincident and are approximately given by the same equation with $K=4$. When the above levels are regarded in this manner the transition $5_{-4}-5_{-3}$ is of the type $\Delta J=0$, $\Delta K=1$, and its intensity will be given by Eq. (3b) in which $J=5$ and $K=5$. These same two levels might also be thought of as fitting into the scheme of levels given by (2) (although numerically there will be no agreement whatever), where $J=5$ and $K=1$. In this light the transition is of the type $\Delta J=0$, $\Delta K=0$ and its intensity would accordingly be given by Eq. (4b). The actual intensity of the transition $5_{-4}-5_{-3}$ should therefore be some value interpolated between the two values given by (3b) and (4b); in this case the transition is between levels so nearly approximated by Eq. (1) that the intensity may be computed from (3b) alone. Consider now also the transition 5_5-5_4. The levels 5_5 and 5_4 are very nearly coincident and their values are given very nearly by the relation (2) by setting $J=K=5$. The transition is clearly, from this point of view, of the kind $\Delta J=\Delta K=0$ and its intensity will be given by the relation (4b). Again we may here regard these two levels as fitting into the scheme of Eq. (1) where $J=5$, $K=0$, and $K=1$. In this sense the transition is of the type $\Delta J=0$, $\Delta K=1$ and the intensity of the transition must accordingly be obtained from (3b). Actually, as before, the intensity will be some value intermediate between these two; in this case the value given by (4b) is probably good enough.

For values of τ not at all nearly equal to J the energy levels are badly approximated by both (1) and (2). So also one may expect the intensities of the transitions between such levels to be badly estimated by both (3) and (4). In such cases one must interpolate between the values given for the transition by Eqs. (3) and Eqs. (4), but just how this interpolation is to be effected is not very clear. RDGW have suggested how one might proceed in making such interpolations and here we have followed somewhat their scheme. The validity of the intensities calculated in this manner is open to considerable speculation. It seems quite evident, however, that they will be at least qualitatively right and will serve to aid materially in the analysis of the bands, i.e., if a certain transition should in the actual case occur with a very small intensity our

TABLE V. Values of the reciprocals of inertia, A, B, and C for ν_1, ν_3, $\nu_1+\nu_3$, and $\nu_2+\nu_3$.

	ν_1	ν_3	$\nu_1+\nu_3$	$\nu_2+\nu_3$
A	27.26 cm^{-1}	26.50 cm^{-1}	26.04 cm^{-1}	29.32 cm^{-1}
B	14.28 cm^{-1}	14.40 cm^{-1}	14.16 cm^{-1}	14.56 cm^{-1}
C	9.17 cm^{-1}	9.10 cm^{-1}	8.95 cm^{-1}	9.06 cm^{-1}

calculated value will not be very large; similarly, if the actual intensity is great our calculated value will also be large. For the sake of comparison the lines have been plotted below the experimental curves in Figs. 1, 2, and 3 with their intensities computed on the above basis. In several instances where several lines have fallen at the same place the composite line has been drawn in. In a few cases the most intense lines have not been drawn quite as intense as their computed value because an awkward scale would have been required. As we have suggested, no great accuracy for the computed line intensities is claimed, but it is of interest to note that in most cases the agreement between the computed and the experimentally observed lines is surprisingly good. Not all of the lines have been identified, but it is believed that those remaining must be due to quantum transitions involving quantum numbers greater than $J=6$.

In the region near 2.7μ, especially on the low frequency side, a considerable number of lines of some intensity could not be accounted for on the basis that this region was due to ν_3 alone. It seemed not unreasonable to suppose that many of these lines were due to the third fundamental vibration ν_1 of the water vapor molecule, particularly since the concentration of these unidentified lines seems to center more or less about the frequency position observed in the Raman spectrum of H_2O for ν_1. It has been possible on this basis to identify a great many more of the remaining lines and these are indicated in the figure as "black" lines. The frequency positions of the lines will be found in the first column and their identifications occur in the third column of Table I. To the identifications of the transitions attributed to ν_1 are affixed asterisks, in order at once to distinguish them from the identifications of lines attributed to ν_3. The energy levels deduced from the identification of the lines attributed to ν_1 are also given in Table IV.

The vibration ν_1 is one where the induced electric moment lies along the axis of the intermediate moment of inertia and the intensities must be computed by the method employed by RDGW and by us in Part I. Best agreement seems to prevail if the intensities computed in this manner are multiplied by a factor of about $\frac{3}{4}$, which is equivalent to saying that the vibration ν_1 occurs with an intensity of about $\frac{3}{4}$ of that of ν_3. This value must, however, be regarded as very rough.

DISCUSSION OF THE RESULTS

From the energy level values obtained from the analysis of the preceding bands the values of the quantities R_i which occur in Eq. (2), Part I, and which are defined in the earlier paper by Shaffer and Nielsen are evaluated. From these the values of the moments of inertia are computed by making use of the theoretically computed centrifugal stretching coefficients. Most weight is given to the levels where $J=0$, $J=1$, $J=2$, and $J=3$ because of the fact that in these the centrifugal stretching will be small. As the value of J increases it has been shown by RDGW that the centrifugal stretching cannot be adequately corrected for in the above manner.

In Table V are gathered the reciprocals of the moment of inertia A, B, and C, defined as $h/(8\pi^2 I_A)$, $h/(8\pi^2 I_B)$, and $h/(8\pi^2 I_C)$, respectively, for the vibration states ν_1, ν_3, $\nu_1+\nu_3$, and $\nu_2+\nu_3$. In Table VI are given the observed values of I_A, I_B, and I_C effective in these vibration states. In addition the values of these, calculated from the semi-theoretical relations of D and D, are set down as well as the observed and theoretical values of the quantity Δ defined by them. It will be seen that the agreement between the observed and the predicted values is uniformly better than in the paper by D and D.

The rotation level 0_0 in any vibration state is identical with the value of the vibration term value itself. From Table IV we may then obtain the vibration term values of the vibration ν_1, ν_3, $\nu_1+\nu_3$, and $\nu_2+\nu_3$. These are set down in Table VII.

The vibration term values for the triatomic molecule may be written:

$$W(v_1, v_2, v_3)/hc = \sum_{i=1}^{3} (v_i+\tfrac{1}{2})\omega_i + \sum_{i\geq k=1}^{3} (v_i+\tfrac{1}{2})(v_k+\tfrac{1}{2})x_{ik}, \quad (5)$$

where the ω_i are the normal frequencies ($\omega_i = x_i - x_{ii} - \frac{1}{2}(x_{ij}+x_{ik})$) and the x_{ik} are the anharmonic constants which depend in an involved manner on the potential energy constants. The constants ω_i, x_i, and x_{ik} were evaluated by D and D on the basis of the data available to them. They have pointed out, moreover, that many of the combination bands in the very near infra-red occur in pairs and actually even in multiplets. The positions of these combination bands are badly reproduced by Eq. (5); in fact the levels which occur in pairs or multiplets are predicted to be almost degenerate. This fact is attributed by D and D in an ingenious way to a term $q_1^2q_3^2$ which occurs in the second-order transformed[9] Hamiltonian. This term will have the following matrix components $(v_1, v_2, v_3|q_1^2q_3^2|v_1, v_2, v_3)$ and $(v_1, v_2, v_3|q_1^2q_3^2|v_1\pm2, v_2, v_3\pm2)$. In arriving at Eq. (5) only the diagonal components have been taken into account, the second kind contributing in general only in higher orders of approximation. Since ω_1 and ω_3 are so nearly degenerate, however, frequencies of the kind $\nu(v_1, v_2, v_3)$ and $\nu(v_1\pm2, v_2, v_3\mp2)$ will also be nearly degenerate. In such cases the off diagonal components $(v_1, v_2, v_3|q_1^2q_3^2|v_1\pm2, v_2, v_3\mp2)$ may yield contributions which are significant to the energy and for the frequency positions of the doublet components D and D obtain:

$$\nu = \left(\frac{\nu_a+\nu_b}{2}\right) \pm \left[\left(\frac{\nu_a-\nu_b}{2}\right)^2 + a\gamma^2\right]^{\frac{1}{2}}, \quad (6)$$

where $a = \frac{1}{2}\gamma[v_1(v_1-1)(v_3+1)(v_3+2)]^{\frac{1}{2}}$ and γ is a constant depending only on the potential energy constants. ν_a and ν_b are the values of the two component frequencies when evaluated by Eq. (5). With the aid of ten of the observed vibration frequencies, some of them single levels, some of the doublet levels and in one case the average value of a doublet level D and D have evaluated the ω_i, x_i, x_{ik}, and γ.

Having now available the new data discussed in this paper it becomes of interest to reinvestigate the values of these constants. To do this we have proceeded in a manner slightly different from that of D and D. As our data for evaluating x_i and x_{ik} we have used ν_1, ν_2, ν_3, $2\nu_2$, $\nu_2+\nu_3$, $\nu_1+\nu_3$, and the average value of all the doublet levels, i.e., $(\nu_a+\nu_b)/2$. This is more than enough to evaluate the x_i and the x_{ik} and the values taken to be the best are values which when put back into (5) will reproduce these data again to within 1 cm^{-1}. By proceeding in this manner the determination of the x_i and x_{ik} is independent of the value of γ. The constant γ is then evaluated from the separations between the doublet levels, i.e., $\Delta\nu = 2\{[(\nu_a-\nu_b)/2]^2+a\gamma^2\}^{\frac{1}{2}}$ and the value of γ which seems most satisfactory for the doublet levels on the whole is actually just that obtained by D and D.

TABLE VI. Theoretical and observed values of I_A, I_B, I_C, and Δ.

v_1, v_2, v_3	I_A (obs.)	I_A (calc.)	I_B (obs.)	I_B (calc.)	I_C (obs.)	I_C (calc.)	Δ (obs.)	Δ (calc.)
(1, 0, 0)	1.028	1.029	1.959	1.972	3.050	3.076	.063	.076
(0, 0, 1)	1.055	1.056	1.942	1.939	3.073	3.059	.076	.064
(1, 0, 1)	1.074	1.076	1.975	1.979	3.125	3.120	.076	.064
(0, 1, 1)	.954	.955	1.920	1.915	3.086	3.099	.212	.228

TABLE VII. Vibrational term values.

$\nu_1 = 3652.7$ cm^{-1},	$\nu_1+\nu_3 = 7253.6$ cm^{-1},
$\nu_3 = 3756.8$ cm^{-1},	$\nu_2+\nu_3 = 5333.5$ cm^{-1}

Whether our scheme for the determination of these constants is better than the method used by D and D may certainly be brought into question. The opinion is, however, here advanced that the positions of the centers of gravity of the doublet levels are probably more significant than the values of the component levels themselves. This opinion is based on the fact that $(\nu_a+\nu_b)/2$ can be determined directly experimentally. No direct experimental method is, however, avail-

[9] The first-order Hamiltonian H_1 will contribute nothing in first order of approximation. It is therefore possible to carry out a contact transformation on the Hamiltonian H so that $H_0 = H_0'$, $H_1' = 0$, and $H_2' = H_2 - (i/2)[SH_1 - H_1S]$, S being the transformation function. [See Shaffer, Nielsen, and Thomas, Phys. Rev. **56**, 895 (1939).] While H_1 does contain terms which contribute to the above-mentioned perturbation, after the contact transformation they are of the form $q_1^2q_3^2$.

able to determine how much of the separation $\Delta\nu$ is actually due to the interaction. The theory of D and D affords, to be sure, a method of calculating this theoretically, and it is indeed found that the γ's computed in this manner from the several doublet levels agree among themselves to within one or two percent, but it is not inconceivable that the splitting is further influenced to a small extent by still higher order terms.

The values of ω_i, x_i, x_{ik}, and γ obtained from our data are the following:

$$x_1=3696.5 \quad x_{11}=-43.8 \quad x_{12}=-\ 22.2$$
$$x_2=1614.7 \quad x_{22}=-19.3 \quad x_{13}=-155.9$$
$$x_3=3804.8 \quad x_{33}=-48.0 \quad x_{23}=-\ 18.7$$

$\omega_1=3829.4$, $\omega_2=1654.5$, $\omega_3=3940.1$, $|\gamma|=74.46$.

In the first column of Table VIII are given the known vibrational term values for the water vapor spectrum. In the second column are given the computed values with the above values of ω_i, x_i, x_{ik}, and γ. In the third column will be found the actual data used to make our determinations of ω_i, x_i, and x_{ik}, i.e., the frequency positions of the single levels and the average values of the doublet levels $(\nu_a+\nu_b)/2$. In the fourth column are set down the values of these data recomputed from Eq. (5). As a final check the two observed component levels of the triplet set of levels (4, 0, 1), (2, 0, 3), and (0, 0, 5) have been computed theoretically for comparison with the experimental values. The fact that the calculated values of these levels agree almost exactly with the measured values is no doubt somewhat accidental, but it serves as another verification that the values ω_i, x_i, x_{ik}, and γ given above are quite good. As a matter of fact the new values of ω_i, x_i, x_{ik}, and γ given here are in general in very good agreement with those given by D and D.

TABLE VIII. Observed and calculated values of W/hc.

v_1, v_2, v_3	W/hc (obs.)	W/hc (calc.)	$\frac{1}{2}(W_a+W_b)/hc$ (obs.)	$\frac{1}{2}(W_a+W_b)/hc$ (calc.)
(0, 1, 0)	1595.4	1595.4		
(0, 2, 0)	3152.3	3152.3		
(1, 0, 0)	3652.7	3652.7		
(0, 0, 1)	3756.8	3756.8		
(0, 1, 1)	5333.5	5333.5		
(1, 0, 1)	7253.6	7253.6		
(1, 1, 1)	8807.1	8808.1		
(2, 0, 1)	10613.1	10617.1	10822.7	10822.6
(0, 0, 3)	11032.4	11028.0		
(2, 1, 1)	12151.2	12150.3	12358.1	12358.4
(0, 1, 3)	12565.0	12566.5		
(3, 0, 1)	13830.9	13834.4	14074.8	14075.8
(1, 0, 3)	14318.8	14317.2		
(3, 1, 1)	15347.9	15346.8	15590.2	15589.5
(1, 1, 3)	15832.5	15832.2		
(3, 2, 1)	16821.6	16820.4	—	17064.5
(1, 2, 3)	—	17308.6		
(4, 0, 1)	16899.0	16899.0		
(2, 0, 3)	17495.8	17495.6		
(0, 0, 5)	—			

On $s^2p^4\ {}^1S$ and $sp^5\ {}^1P$ in the S I Isoelectronic Sequence

BENGT EDLÉN
Physics Institute, University of Upsala, Sweden
(Received September 8, 1942)

A STRONG unidentified line in the extreme ultraviolet has been recognized for some time as strictly following the "irregular doublet" law through the five elements from chlorine to scandium. For various reasons it was suspected to be $s^2p^4\ {}^1D-sp^5\ {}^1P$, and this explanation has recently been confirmed through the identifications in Cl II by Kiess and de Bruin.[1] The data for the transition including those of Kiess and de Bruin for Cl II are collected in Table I, where the last column gives the value for $sp^5\ {}^1P$ relative to the ground level $s^2p^4\ {}^3P_2$. The observations for K IV, Ca V, and Sc VI are taken from Ekefors[2] and Beckman.[3] The A III line is contained in Boyce's paper on argon[4] with the classification $s^2p^4\ {}^1S-sp^5\ {}^1P$. In consequence of the new identification the previous values for both terms involved are shown to be in error. The term ^1S of the ground configuration s^2p^4 has been fixed for the higher members in the S I sequence[5] but—in spite of many efforts—a considerable uncertainty has remained about its position in S I, Cl II, A III, and K IV. It was expected that the newly-found term $sp^5\ {}^1P$ would aid effectively in the search for ^1S, but unfortunately the combination $s^2p^4\ {}^1S-sp^5\ {}^1P$ seems to be quite faint, judging from the absence of the corresponding line in the tables for Sc and Ca. Nevertheless, it has been possible to find the arrangement discussed below, which probably solves the problem of locating $s^2p^4\ {}^1S$ in the first four spectra of the S I sequence.

TABLE I. $3s^23p^4\ {}^1D_2-3s3p^5\ {}^1P_1$.

	Int.	λ	ν	Diff.	$3s3p^5\ {}^1P_1$
Cl II	10	961.49	104005	26008	115657
A III	12	769.152	130013	24741	144023
K IV	15	646.188	154754	24264	171140
Ca V	10	558.602	179018	24059	197849
Sc VI	6	492.423	203077	.	224474

The level values of the ground configuration must show a quite smooth change in their relative position through the sequence. Specially suitable for the comparison in the actual case are the quantities $^1D-{}^3P_c$, $^1S-{}^1D$ and the Slater ratio $(^1S-{}^1D):(^1D-{}^3P_c)$, which are collected in Table II, including the new values suggested in the present note. As usual, ^3P_c denotes the mean of the ^3P levels, weighted according to $2J+1$. The last column gives the value for ^1S with reference to the ground-level $^3P_2$. For all the spectra tabulated[6,1,4,5] the term ^1D has been found and connected with the triplets. The trend of the ^1S position through the series Ti VII, Sc VI, and Ca V is definitely in favor of changing Ruedy's classification[6] in S I in the way suggested by Bowen,[7] to which the figures in the first row of Table II correspond. On this basis the difference $^1S-{}^1D$ can be accurately interpolated for A III. At the corresponding wave-length one finds the strongest unidentified nebular line as observed by Bowen and Wyse[8] in the three nebulae: *NGC* 6572 λ5190.8 (2), *NGC* 7027 λ5192.0 (5), and *NGC* 7662 λ5192? (3). If we accept the identification [A III] $^1S-{}^1D$ for this

TABLE II. Configuration $3s^23p^4$.

	$^1D-{}^3P_c$		$^1S-{}^1D$		$\frac{^1S-{}^1D}{^1D-{}^3P_c}$	^1S
S I	9044	2265	12942	3308	1.4310	22182
Cl II	11309	2156	[16250]	3007	[1.437]	[27900]
A III	13465	2105	19257	2905	1.4302	33267
K IV	15570	2096	22162	2854	1.4234	38548
Ca V	17666	2119	25016	2825	1.4161	43847
Sc VI	19785	2162	27841	2803	1.4072	49238
Ti VII	21947		30644		1.3963	54757

[1] C. C. Kiess and T. L. de Bruin, J. Research Nat. Bur. Stand. **23**, 443 (1939).
[2] E. Ekefors, Zeits. f. Physik **71**, 53 (1931).
[3] A. Beckman, Thesis, Upsala, 1937.
[4] J. C. Boyce, Phys. Rev. **48**, 400 (1935); ibid. **49**, 351 (1936).
[5] I. S. Bowen, Phys. Rev. **46**, 791 (1934), (Ca V); P. G. Kruger and H. S. Pattin, Phys. Rev. **52**, 621 (1937), (Sc VI); and B. Edlén, Zeits. f. Physik **104**, 188 (1937), (Ti VII, V VIII, Cr IX, Mn X).
[6] J. E. Ruedy, Phys. Rev. **44**, 757 (1933).
[7] I. S. Bowen, Rev. Mod. Phys. **8**, 78 (1936).
[8] I. S. Bowen and A. B. Wyse, Lick Obs. Bull. **19**, No. 495 (1939).

line and use as mean λ5191.4, the figures for A III in the Table II are obtained. It should be possible to check the new identification of ^1S in A III through combinations in the extreme ultraviolet.

The A III identification permits a reliable interpolation for K IV. Through the identification of two lines in Ekefors' list as shown in Table III a value for $s^2p^4\,{}^1S$ is found, which agrees perfectly with the isoelectronic comparison.[9] For $^1S-{}^1D$ follows λ_{air}4511.0, which might explain the faint line in the nebulae *NGC* 7027 λ4511.8? (1) and *NGC* 7662 λ4510.8 (0.5).[8]

Figure 1 shows the variation in the observed Slater ratio for $3s^23p^4$ and $3s^23p^2$. In order to allow a direct comparison with the theoretical formulae for intermediate coupling, we follow Robinson and Shortley's very useful methods[10] and plot the ratio against the parameter χ as determined from the coupling ratios $(^3P_2-{}^3P_0):(^1D-{}^3P_c)$ and $(^3P_1-{}^3P_2):(^1D-{}^3P_c)$ for p^2 and p^4, respectively. It should be noticed that the

TABLE III. K IV.

Combination	ν calc.	ν obs.	λ obs.
$s^2p^4\,{}^1S_0-sp^5\,{}^1P_1$	132592	132591.9	754.194 (3?)
$-(^2P)4s\,{}^3P_1$	254925	254923.9	392.274 (2)
$-3d\,{}^1P_1$	222897	—	masked
$-(^2P)4s\,{}^1P_1$	259586	—	absent

[9] A previous tentative location of ^1S in K IV by H. A. Robinson and G. H. Shortley [Phys. Rev. **52**, 725 (1937)] repeated by Wei-Zang Tsien [Chinese J. Phys. **3**, 117 (1939)] admits too large errors for Ekefors' measurements and involves an impermissible deviation in the isoelectronic comparison.

[10] H. A. Robinson and G. H. Shortley, Phys. Rev. **52**, 713 (1937). Two minor errors in Tables I and II of this reference were corrected while constructing the theoretical curves in Fig. 1.

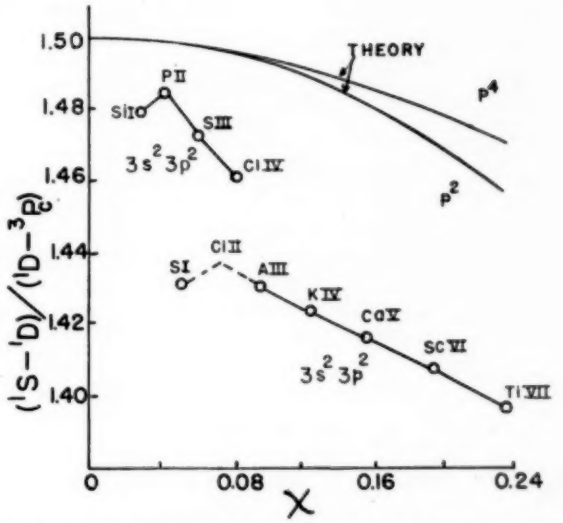

FIG. 1. The Slater ratio $(^1S-{}^1D):(^1D-{}^3P_c)$ as a function of the coupling parameter $\chi=\zeta_p/5F_2$.

scale used for Fig. 1 is such that an error in the position of ^1S of less than 50 cm^{-1} would cause an easily recognized discontinuity in the smooth curve from Ti VII to A III. By assuming now a drop in the Slater ratio from Cl II to S I, similar to that observed from P II to Si I, the ratio 1.437 for Cl II may be obtained from the diagram, corresponding to 27900 cm^{-1} as predicted position for ^1S. The published tables of the chlorine spectrum are, however, insufficient for a further confirmation. Kiess and de Bruin[1] were also unable to find the term in spite of careful examination of various unpublished lists. It seems inevitable to assume that $3s^23p^4\,{}^1S$ has only quite few and comparatively faint combinations, at least for the first elements in the S I sequence.

COMMENTS

I am indebted to the author of this article for the opportunity to comment upon it. It is clear from his data that my earlier identification of λ769.152 was incorrect, as were my values of the $s^2p^4\,{}^1S_0$ and $sp^5\,{}^1P_1{}^0$ terms based upon it. A re-examination of unpublished argon lists in the vacuum ultraviolet gives no evidence of the $s^2p^4\,{}^1S_0-sp^5\,{}^1P_1{}^0$ line in A III or of other lines which might serve to locate the $^1S_0$ term of the ground configuration. A similar re-examination by C. C. Kiess of unpublished lists of chlorine gives the same negative result for Cl II and confirms the conclusion that lines to the $^1S_0$ state must be relatively faint.

Line lists and term values in A III already published* must now be revised. In addition to the change indicated above, previous identifications of the lines λ1205.95, λ676.241, and λ623.767 must now be withdrawn, as well as the tentative ones for λ604.152 and λ536.745. The four intersystem combinations locating the $s^2p^4\,{}^1D_2$ term relative to the triplet system are in no way affected by this revision.

J. C. BOYCE
Massachusetts Institute of Technology

* J. C. Boyce, Phys. Rev. **48**, 396 (1935); **49**, 351 (1936).

Calculations on Classical Field Theory

A. C. MENIUS, JR.* AND N. ROSEN
Department of Physics, University of North Carolina, Chapel Hill, North Carolina

(Received August 22, 1942)

The equations of the classical field theory of elementary particles proposed by one of the authors were integrated numerically for the static, spherically-symmetric case. A solution was obtained corresponding essentially to minimum energy, and hence describing a classical electron according to the theory. It was found that the frequency associated with the solution was zero, to within the accuracy of the calculations, for the case of minimum energy. Hence the theory, in its present form, is not capable of accounting for the Sommerfeld fine-structure constant, as had seemed possible.

1. CALCULATIONS

SOME time ago one of the authors[1] proposed a classical field theory of elementary particles. This theory was based on a Lagrangian involving the electromagnetic field components $F_{\mu\nu}$, the electromagnetic potentials φ_u, and also a scalar "matter function" ψ, which bore a formal resemblance to the relativistic Schrödinger function. The field equations obtained were applied to the case of a static, spherically-symmetric charge distribution which was to be interpreted as a classical electron. It was found that, in spite of the fact that the charge density was static, the function ψ could have a periodic dependence on the time. The frequency associated with ψ was determined by the solution of the field equations. As there was a whole family of solutions satisfying the equations and the boundary conditions, that solution was to be chosen which made the total energy of the system a minimum. In this way one would obtain a classical particle which had associated with it both an energy and a frequency. If the latter turned out to be different from zero, there would exist the possibility of accounting for the Sommerfeld fine-structure constant on a purely classical basis.

The present paper has for its purpose to report on the results of calculations carried out to obtain solutions of these equations.

The field equations were taken in the form of Eqs. (44) and (45) of reference 1,[2] together with the boundary conditions of Eq. (46a). The solutions of the equations depended on the choice of the parameters a and b of Eq. (51). For each value of a taken, a number of values of b were tried until the one had been found which gave a solution satisfying the boundary conditions. The total energy (49) was calculated from this solution, and that value of a was sought which made this energy a minimum.

The equations were integrated numerically, by starting with a power series solution near the origin. Preliminary calculations showed that the desired solution corresponded to a value of a not far from 1.63. Hence first a solution was obtained for $a=1.63$, in which intervals of 0.05 were used for the independent variable x, in the range 0 to 2, and intervals of 0.1 for $x>2$. The correct value of b (2.21493) was determined by trial. The solution was determined to 7 figures, of which 6 were reliable in the important range of $x(0<x<2)$. Then solutions were obtained for values of a near 1.63 by working, not with the unknown functions themselves, but with the differences from their values for $a=1.63$. These differences were small and varied slowly with x, so that intervals of 0.1

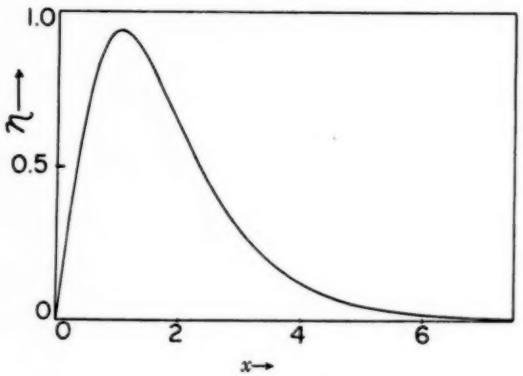

FIG. 1. Plot of η as a function of x.

* Now in the Department of Physics, Clemson College.
[1] N. Rosen, Phys. Rev. 55, 94 (1939).
[2] All equations referred to are in the paper of reference (1).

in the latter gave sufficient accuracy. From the solutions obtained in this way, the energy was calculated for $a=1.61$, 1.62, 1.63, 1.64. A cubic curve was passed through the calculated points, and the value of a at the energy minimum determined; it was found to be 1.629.

By interpolation, the constant β of Eq. (46b) was calculated for this value of a. This constant, according to the paper referred to, should be related to the Sommerfeld fine-structure constant by the equation

$$\alpha' = |2\alpha^2\beta/(\alpha\beta+\gamma)|,$$

where α' is the fine-structure constant, and α, β, and γ are quantities given in terms of the solution by Eqs. (48), (46b), and (50b), respectively. If one considers the values of the other quantities involved, in order to get the correct value for the fine-structure constant, the value β should have come out to be about ± 0.00283. The calculations gave $\beta = -0.00012$, too small in absolute value by a factor of about 24. One can say that, to within the accuracy of the calculations, β and therefore

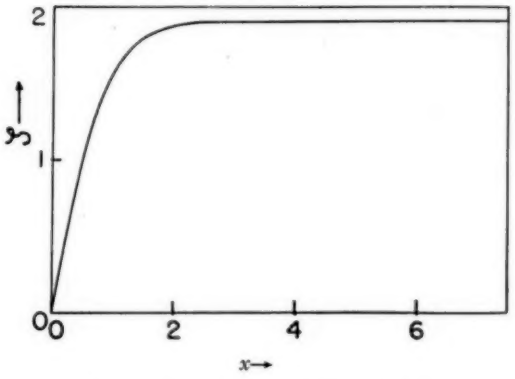

FIG. 2. Plot of ζ as a function of x.

the fine-structure constant are zero. Hence for the case of minimum energy, not only the charge density, but also the function ψ turns out to be static.

Figures 1 and 2 give graphs of the functions $\eta(x)$ and $\zeta(x)$ as defined by Eqs. (41a) for the case $a=1.63$. Figure 3 gives the corresponding charge distribution for the electron according to the field equations. These graphs can be taken to represent the functions for $a=1.629$, since the small change in a will not alter them to any noticeable degree.

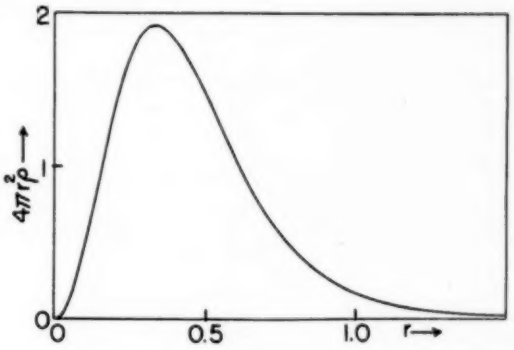

FIG. 3. Plot of $4\pi r^2\rho$ as a function of r, where ρ is the charge density, e being the unit of charge and e^2/mc^2 the unit of length.

2. DISCUSSION

The results of the calculation indicate that the present classical electron theory cannot account for the Sommerfeld fine-structure constant (or for Planck's constant). This means that, in the quantization of the field equations, h must be introduced from the outside. Naturally this is less satisfying than if the theory had turned out to be self-contained.

As was pointed out in the earlier paper, there exist Lagrangians, other than the one adopted, which satisfy the same conditions as this one and which could be chosen instead. It is possible that some one of these Lagrangians might lead to a satisfactory explanation of the fine-structure constant.

On the other hand, the Lagrangian used is outstanding in its simplicity. If one takes it seriously, then one is led to say that a classical theory is incapable of providing a basis for an explanation of quantum phenomena. From this point of view the success of the present classical theory could only be judged by the extent to which, after the usual quantization, it could remove the difficulties in the quantum theory believed to be associated with the point electron. This is a question for investigation.

Theory of Complex Spectra. II

GIULIO RACAH
The Hebrew University, Jerusalem, Palestine

(Received August 5, 1942)

The spectra of two-electron configurations in (jj) and (jl) coupling and of the configurations d^n, f^3, d^2p, and d^3p in (LS) coupling are calculated with tensor operators. The agreement with the odd terms of Ti II and Ni II is satisfactory. It is also proved that $G^k/(2k+1)$ is a positive decreasing function of k.

§1. INTRODUCTION

IN a first paper on this matter[1] a general formula was given for the coefficients of Slater's integrals for the two-electron configurations in (LS) coupling. It was also shown that this formula gives the possibility of calculating the terms of more complex configurations, and some simple examples were given. But the method used for the configurations p^2l still necessitates for d^3 very long calculations, because we must calculate the fourth power of the matrix of the scalar product of two angular momenta. It appeared therefore more convenient to develop a new method, based on tensor operators.

The algebra of tensor operators is developed in analogy to the treatment of Chapter III of TAS[2] for the vector operators. With this method some group-theoretical results of Wigner and of Kramers are obtained by a direct algebraical way, and in some cases also in a more simple and general form.

Expressing the coefficients of Slater's integrals as scalar products of tensors, we give a direct demonstration of Eq. (12′) I, and obtain also its extension to (jj) and (jl) coupling. This new method is more suitable for calculations of many-electron spectra, and applications are made to the configurations d^n, f^3, d^2p, and d^3p.

Since the whole method is based on Wigner's[3] transformation formula for vector addition (TAS 14[3]5), we shall begin with a direct algebraical derivation of this formula, without the use of the theory of groups.

§2. THE ALGEBRAIC CALCULATION OF $(j_1j_2m_1m_2|j_1j_2jm)$

It is shown in §14[3] of TAS that the transformation coefficients $(m_1m_2|jm)$ for the addition of two angular momenta are defined by the relation

$$\psi(\gamma j_1 j_2 jm)=\sum_{m_1m_2}\phi(\gamma j_1 j_2 m_1 m_2)(m_1m_2|jm) \tag{1}$$

and are completely determined by the initial condition

$$(j_1j_2|j_1+j_2\,j_1+j_2)=1 \tag{2}$$

and by the two recursion formulas

$$[(j+m)(j-m+1)]^{\frac{1}{2}}(m_1m_2|jm-1)=[(j_1+m_1+1)(j_1-m_1)]^{\frac{1}{2}}(m_1+1\,m_2|jm)$$
$$+[(j_2+m_2+1)(j_2-m_2)]^{\frac{1}{2}}(m_1m_2+1|jm) \tag{3}$$

and

$$[(j-m)(j+m)]^{\frac{1}{2}}(j-1\vdots J_1\vdots j)(m_1m_2|j-1m)$$
$$=[m_1-m(j\vdots J_1\vdots j)](m_1m_2|jm)-[(j-m+1)(j+m+1)]^{\frac{1}{2}}(j+1\vdots J_1\vdots j)(m_1m_2|j+1m). \tag{4}$$

[1] G. Racah, Phys. Rev. **61**, 186 (1942), which will be referred to as I.
[2] E. U. Condon and G. H. Shortley, *Theory of Atomic Spectra* (Cambridge, 1935). We refer to this book (TAS) and to I for definitions, notations, and bibliographical indications.
[3] E. Wigner, *Gruppentheorie* (Vieweg, 1931), Chapter 17, Eq. (27).

But it is also pointed out there that a general formula for such coefficients is very difficult to obtain from these relations.

The calculation is however much simplified if we add a third recursion formula, which follows also, as (3), from TAS $3^3 3$ if we take the upper sign instead of the lower:

$$[(j-m)(j+m+1)]^{\frac{1}{2}}(m_1m_2|jm+1)$$
$$=[(j_1-m_1+1)(j_1+m_1)]^{\frac{1}{2}}(m_1-1m_2|jm)+[(j_2-m_2+1)(j_2+m_2)]^{\frac{1}{2}}(m_1m_2-1|jm). \quad (5)$$

In order to avoid the irrational factors we put

$$(m_1m_2|jm)=(-1)^{j_1-m_1}f(m_1m_2;\,jm)[(j_1+m_1)!(j_2+m_2)!(j+m)!]^{\frac{1}{2}}/[(j_1-m_1)!(j_2-m_2)!(j-m)!]^{\frac{1}{2}}, \quad (6)$$

and obtain from (3) and (5)

$$f(m_1m_2;\,jm-1)=(j_2+m_2+1)(j_2-m_2)f(m_1m_2+1;\,jm)-(j_1+m_1+1)(j_1-m_1)f(m_1+1m_2;\,jm) \quad (3')$$

and

$$(j-m)(j+m+1)f(m_1m_2;\,jm+1)=f(m_1m_2-1;\,jm)-f(m_1-1m_2;\,jm). \quad (5')$$

Putting $m=j$ in (5′), we see that $f(m_1m_2;\,jj)$ is independent of m_1 and m_2 and we may write

$$f(m_1m_2;\,jj)=A_j. \quad (7)$$

From (7) and (3′) we get

$$f(m_1m_2;\,jj-1)=[(j_2+m_2+1)(j_2-m_2)-(j_1+m_1+1)(j_1-m_1)]A_j; \quad (7')$$

from (7′) and (3′) we get

$$f(m_1m_2;\,jj-2)=[(j_2+m_2+1)(j_2+m_2+2)(j_2-m_2)(j_2-m_2-1)$$
$$-2(j_2+m_2+1)(j_2-m_2)(j_1+m_1+1)(j_1-m_1)+(j_1+m_1+1)(j_1+m_1+2)(j_1-m_1)(j_1-m_1-1)]A_j \quad (7'')$$

and we see that the general formula will be

$$f(m_1m_2;\,jj-u)=A_j\sum_t(-1)^t\binom{u}{t}\frac{(j_1+m_1+t)!(j_1-m_1)!(j_2+m_2+u-t)!(j_2-m_2)!}{(j_1+m_1)!(j_1-m_1-t)!(j_2+m_2)!(j_2-m_2-u+t)!}, \quad (8)$$

where, as in all formulas of this paper, the summation parameter takes on all integral values consistent with the factorial notation, the factorial of a negative number being meaningless. To demonstrate (8) it suffices to verify that it satisfies (3′); this verification is very simple and will be omitted for brevity.

Introducing (8) in (6) and remembering that

$$m=m_1+m_2, \quad (9)$$

we obtain the dependence of $(m_1m_2|jm)$ on m_1, m_2, and m:

$$(m_1m_2|jm)=\delta(m_1+m_2,\,m)A_j\left[\frac{(j_1-m_1)!(j_2-m_2)!(j-m)!(j+m)!}{(j_1+m_1)!(j_2+m_2)!}\right]^{\frac{1}{2}}\sum_t(-1)^{j_1-m_1+t}$$
$$\times\frac{(j_1+m_1+t)!(j+j_2-m_1-t)!}{t!(j-m-t)!(j_1-m_1-t)(j_2-j+m_1+t)!}. \quad (10)$$

In order to obtain from (4) the dependence of A_j on j, we calculate at first from (10) the expression of $(m_1m_2|j+1j)$: owing to the δ factor and to the expression of $(j_1'J_1'j)$ (TAS $10^3 2a$), we have

$$(m_1m_2|j+1j)=\delta(m_1+m_2,\,)(-1)^{j_1-m_1}A_{j+1}\left[\frac{(j_1+m_1)!(j_2+m_2)!(2j+1)!}{(j_1-m_1)!(j_2-m_2)!}\right]^{\frac{1}{2}}2(j+1)[m_1-j(j_1'J_1'j)]. \quad (11)$$

The left side of (4) vanishes for $m=j$; introducing (7) and (11) and eliminating the common factors, we get

$$0=A_j-2(j+1)(2j+1)(j+1\,|\,J_1\,|\,j)A_{j+1},$$

and owing to the expression of $(j+1\,|\,J_1\,|\,j)$ (TAS 10^3 2b), this becomes

$$A_j=[(j_1+j_2+j+2)(j_1+j_2-j)(j+j_1-j_2+1)(j+j_2-j_1+1)(2j+1)/(2j+3)]^{\frac{1}{2}}A_{j+1} \tag{12}$$

and is satisfied by

$$A_j=B[(2j+1)(j_1+j_2-j)!]^{\frac{1}{2}}/[(j_1+j_2+j+1)!(j+j_1-j_2)!(j+j_2-j_1)!]^{\frac{1}{2}}, \tag{13}$$

where B is also independent of j.

It follows from (2) that

$$B=1; \tag{14}$$

and collecting (10), (13), and (14) we have at last

$$(m_1m_2|jm)=\delta(m_1+m_2,\,m)\left[\frac{(2j+1)(j_1+j_2-j)!(j_1-m_1)!(j_2-m_2)!(j-m)!(j+m)!}{(j_1+j_2+j+1)!(j+j_1-j_2)!(j+j_2-j_1)!(j_1+m_1)!(j_2+m_2)!}\right]^{\frac{1}{2}}$$
$$\times\sum_t(-1)^{j_1-m_1+t}\frac{(j_1+m_1+t)!(j+j_2-m_1-t)!}{t!(j-m-t)!(j_1-m_1-t)!(j_2-j+m_1+t)!}. \tag{15}$$

This formula is similar to Wigner's formula (TAS $14^3$5), and is, also, unsymmetrical and unpractical for the use; it is, however, possible to obtain a more symmetrical and useful form, by transforming it with the methods shown in the appendix of I: using (52) I and (55′) I we have

$$\sum_t(-1)^{j_1-m_1+t}\frac{(j_1+m_1+t)!(j+j_2-m_1-t)!}{t!(j-m-t)!(j_1-m_1-t)!(j_2-j+m_1+t)!}$$
$$=\sum_{tu}(-1)^{j_1-m_1+t}\frac{(j_1+m_1+t)!}{t!(j_2-j+m_1+t)!}\cdot\frac{(j_2+m_2)!(j+j_2-j_1)!}{(j_2+m_2-u)!(j+j_2-j_1-u)!(j_1-j_2-m-t+u)!u!}$$
$$=\sum_u(-1)^{j_2+m_2-u}\frac{(j_1+m_1)!(j+j_1-j_2)!(j_2+m_2)!(j+j_2-j_1)!}{(j_1-j_2-m+u)!(j_1-j-m_2+u)!(j+m-u)!(j_2+m_2-u)!(j+j_2-j_1-u)!u!},$$

and putting $z=j_2+m_2-u$ we get

$$(j_1j_2m_1m_2|j_1j_2jm)=\delta(m_1+m_2,\,m)[(2j+1)(j_1+j_2-j)!(j+j_1-j_2)!(j+j_2-j_1)!/(j_1+j_2+j+1)!]^{\frac{1}{2}}$$
$$\cdot\sum_z(-1)^z\frac{[(j_1+m_1)!(j_1-m_1)!(j_2+m_2)!(j_2-m_2)!(j+m)!(j-m)!]^{\frac{1}{2}}}{z!(j_1+j_2-j-z)!(j_1-m_1-z)!(j_2+m_2-z)!(j-j_2+m_1+z)!(j-j_1-m_2+z)!}. \tag{16}$$

We might also transform TAS $14^3$5 in the same way, and the result would of course be the same.

For further use it is convenient to introduce the abbreviations

$$v(abc;\,\alpha\beta\gamma)=\delta(\alpha+\beta+\gamma,\,0)\sum_z(-1)^{c-\gamma+z}$$
$$\times\frac{[(a+\alpha)!(a-\alpha)!(b+\beta)!(b-\beta)!(c+\gamma)!(c-\gamma)!]^{\frac{1}{2}}}{z!(a+b-c-z)!(a-\alpha-z)!(b+\beta-z)!(c-b+\alpha+z)!(c-a-\beta+z)!} \tag{17}$$

and

$$V(abc;\,\alpha\beta\gamma)=[(a+b-c)!(a+c-b)!(b+c-a)!/(a+b+c+1)!]^{\frac{1}{2}}v(abc;\,\alpha\beta\gamma) \tag{17′}$$

and to write

$$(j_1j_2m_1m_2|j_1j_2jm)=(-1)^{j+m}(2j+1)^{\frac{1}{2}}V(j_1j_2j;\,m_1m_2-m). \tag{16′}$$

The functions v and V are defined for integral and half-integral values of the arguments, with the limitation that $a-\alpha$, $b-\beta$, $c-\gamma$ must be integers; it follows from this limitation and from the factor $\delta(\alpha+\beta+\gamma, 0)$ that all the nine numbers

$$a+\alpha, \quad a-\alpha, \quad b+\beta, \quad b-\beta, \quad c+\gamma, \quad c-\gamma, \quad a+b-c, \quad a+c-b, \quad b+c-a \tag{18}$$

must be integers.

Since in (17) z takes on only such integral values for which the argument of every factorial is not negative, the number of terms in this sum is one more than the *smallest* of the nine numbers (18) (and not only of four of them, as in (15) or in TAS 14[3]5); therefore V vanishes if one of the numbers (18) is negative, and the summation reduces to one term if one of these numbers vanishes.

Assuming the argument of one of the five other factorials instead of z as summation parameter in (17), we obtain some symmetry properties for v and V:

$$V(abc;\alpha\beta\gamma)=(-1)^{a+b-c}V(bac;\beta\alpha\gamma)=(-1)^{a+b+c}V(acb;\alpha\gamma\beta)=(-1)^{a-b+c}V(cba;\gamma\beta\alpha)$$
$$=(-1)^{2b}V(cab;\gamma\alpha\beta)=(-1)^{2c}V(bca;\beta\gamma\alpha). \tag{19a}$$

Interchanging in (17) a with b and α with $-\beta$, we have

$$V(abc;\alpha\beta\gamma)=(-1)^{2\gamma}V(bac;-\beta-\alpha-\gamma);$$

and owing to the first of (19a) and to the fact that $2(c-\gamma)$ is even, we get also

$$V(abc;\alpha\beta\gamma)=(-1)^{a+b+c}V(abc;-\alpha-\beta-\gamma). \tag{19b}$$

Since the transformation matrix $(j_1j_2m_1m_2|j_1j_2jm)$ is a unitary one, it follows from (16′) that the real function V must satisfy the orthogonality relations

$$\sum_{\alpha\beta} V(abc;\alpha\beta\gamma)\,V(abc';\alpha\beta\gamma')=\delta(c,c')\delta(\gamma,\gamma')/(2c+1) \quad (a+b\geqslant c\geqslant|a-b|,\ c\geqslant|\gamma|), \tag{20a}$$

and

$$\sum_{c\gamma}(2c+1)\,V(abc;\alpha\beta\gamma)\,V(abc;\alpha'\beta'\gamma)=\delta(\alpha,\alpha')\delta(\beta,\beta') \quad (a\geqslant|\alpha|,\ b\geqslant|\beta|); \tag{20b}$$

if the inequalities in parentheses are not satisfied, the left side vanishes.

The sum in (17) cannot generally be transformed into a closed form; it is, however, possible to do so for the particular case $\alpha=\beta=\gamma=0$ (a, b, c integers!): if $a+b+c$ is odd, it follows from (19b) that $V(abc;000)$ vanishes; if

$$a+b+c=2g \tag{21}$$

with g integer, it is shown in Appendix A that

$$v(abc;000)=(-1)^g g!/[(g-a)!(g-b)!(g-c)!] \tag{22}$$

and therefore

$$\begin{cases} V(abc;000)=(-1)^g\left[\dfrac{(a+b-c)!(a+c-b)!(b+c-a)!}{(a+b+c+1)!}\right]^{\frac{1}{2}}\dfrac{g!}{(g-a)!(g-b)!(g-c)!}, & (a+b+c \text{ even}) \\ V(abc;000)=0, & (a+b+c \text{ odd}). \end{cases} \tag{22′}$$

§3. THE ALGEBRA OF TENSOR OPERATORS

(1) Definition of Tensor Operator

It is shown in §8[6] of TAS that the matrix components of the electrostatic interaction between two electrons depend on the matrix elements of the spherical harmonics $\Theta(km)\Phi(m)$; in this case the spherical harmonics play the role of operators and not of eigenfunctions, and it appears convenient to consider in a general way the algebra of such operators.

In Chapter III of TAS the algebra of vector operators was developed from the sole assumption that their components satisfy the commutation rule 8³2 with respect to **J**; this assumption is indeed equivalent to the definition of a vector, because the operators J_x, J_y, and J_z are proportional to the rotation operators,[4] and therefore the commutation law with respect to **J** determines completely the transformation law of each quantity considered for a rotation of the axes; since 8³2 holds for x, y, and z, each group of three quantities which satisfies 8³2 has the same transformation law as x, y, and z, and is therefore a vector.

It is shown in the theory of tensors that by means of symmetrizations and contractions each tensor may be decomposed in parts which transform themselves independently for a rotation of the axes, the transformation law of each irreducible part being the same as that of the spherical harmonics of a determinate degree. We may therefore define as "irreducible tensor operator of the degree k" each operator $\mathbf{T}^{(k)}$ whose $2k+1$ components $T_q^{(k)}$ $(q=-k, -k+1, \cdots, k-1, k)$ satisfy the same commutation rule with respect to **J** as the spherical-harmonic operators $\Theta(kq)\Phi(q)$; this commutation rule is easily derived from §§3³ and 4³ of TAS, and is

$$[(J_x \pm iJ_y), T_q^{(k)}] = [(k \mp q)(k \pm q + 1)]^{\frac{1}{2}} T_{q\pm 1}^{(k)}, \tag{23a}$$

$$[J_z, T_q^{(k)}] = qT_q^{(k)}. \tag{23b}$$

It is easily seen that for $k=1$ (23) reduce to TAS 8³2, if we put

$$T_1^{(1)} = -(T_x + iT_y)/(2)^{\frac{1}{2}}, \quad T_0^{(1)} = T_z, \quad T_{-1}^{(1)} = (T_x - iT_y)/(2)^{\frac{1}{2}}. \tag{24}$$

In view of TAS 4³18 we shall say that an irreducible tensor operator is Hermitian, if

$$T_q^{(k)\dagger} = (-1)^q T_{-q}^{(k)}. \tag{25}$$

(2) Dependence of the Matrix of $T^{(k)}$ on m

The dependence on m of the matrix elements of $T_q^{(k)}$ in the jm scheme will readily be derived from (23). The relation (23b) gives us in the usual manner the selection rule: the only non-vanishing elements of $(\alpha jm|T_q^{(k)}|\alpha' j'm')$ are those for which

$$m' = m - q. \tag{26}$$

The two relations (23a), written for a general non-vanishing element, give

$$\begin{aligned}
[(j+m)(j-m+1)]^{\frac{1}{2}}(\alpha jm-1|T_q^{(k)}|\alpha' j'm-q-1) &= [(j'+m-q)(j'-m+q+1)]^{\frac{1}{2}}(\alpha jm|T_q^{(k)}|\alpha' j'm-q) \\
&\quad + [(k-q)(k+q+1)]^{\frac{1}{2}}(\alpha jm|T_{q+1}^{(k)}|\alpha' j'm-q-1), \\
[(j-m)(j+m+1)]^{\frac{1}{2}}(\alpha jm+1|T_q^{(k)}|\alpha' j'm-q+1) &= [(j'-m+q)(j'+m-q+1)]^{\frac{1}{2}} \\
&\quad \times (\alpha jm|T_q^{(k)}|\alpha' j'm-q) + [(k+q)(k-q+1)]^{\frac{1}{2}}(\alpha jm|T_{q-1}^{(k)}|\alpha' j'm-q+1).
\end{aligned} \tag{27}$$

We observe now that if we replace $(\alpha jm|T_q^{(k)}|\alpha' j'm')$ by $(j'km'q|j'kjm)$, (27), we reduce exactly to (3) and (5); since we saw that these equations were sufficient to determine the dependence of $(j_1j_2m_1m_2|j_1j_2jm)$ on m_1, m_2, and m, it follows that

$$(\alpha jm|T_q^{(k)}|\alpha' j'm') = A(j'km'q|j'kjm), \tag{28}$$

where A is independent of m, m', and q.[5] Owing to (16′) and (19), we write

$$(\alpha jm|T_q^{(k)}|\alpha' j'm') = (-1)^{j+m}(\alpha j\|T^{(k)}\|\alpha' j')\, V(jj'k\,; -mm'q). \tag{29}$$

[4] P. A. M. Dirac, *Quantum Mechanics* (Oxford, 1935), §29.

[5] This relation was already given by Wigner, Reference 3, Chapter 21, Eq. (19), with group-theoretical methods.

This formula is the tensorial extension of TAS 9^3H; in order to avoid mistakes we wrote the quantities which are independent of m, m', and q with $\|$ instead of $\vdots$, since for $k=1$ these quantities differ from the analogous quantities defined in §9^3 of TAS; it is easy to see that they are related by the following relations:

$$\begin{aligned}(\alpha j\|T^{(1)}\|\alpha' j) &= [j(j+1)(2j+1)]^{\frac{1}{2}}(\alpha j\vdots T\vdots\alpha' j),\\ (\alpha j\|T^{(1)}\|\alpha' j-1) &= [j(2j-1)(2j+1)]^{\frac{1}{2}}(\alpha j\vdots T\vdots\alpha' j-1),\\ (\alpha j\|T^{(1)}\|\alpha' j+1) &= -[(j+1)(2j+1)(2j+3)]^{\frac{1}{2}}(\alpha j\vdots T\vdots\alpha' j+1).\end{aligned} \tag{30}$$

It must also be observed that for a Hermitian tensor $\mathbf{T}^{(k)}$ the matrix $(\alpha j\|T^{(k)}\|\alpha' j')$ is not Hermitian, but satisfies the relation

$$(\alpha j\|T^{(k)}\|\alpha' j') = (-1)^{j-j'}\overline{(\alpha' j'\|T^{(k)}\|\alpha j)}\,; \tag{31}$$

the general relation for any tensor is

$$(\alpha j\|T^{(k)}\|\alpha' j') = (-1)^{j-j'}\overline{(\alpha' j'\|T^{(k)\dagger}\|\alpha j)}. \tag{31'}$$

The reasons which brought us to this choice of phases are similar to those which fixed the phases in TAS $4^3$17.

(3) Scalar Product of Tensors

If two irreducible tensors of the same degree are given, we consider the quantity

$$Q=\sum_q(-1)^q T_q^{(k)}U_{-q}^{(k)}\,; \tag{32}$$

owing to (29), (19), and (20a), the matrix elements of Q are

$$(\alpha jm|Q|\alpha' j'm') = \sum_{\alpha'' j''}(-1)^{j-j''}(\alpha j\|T^{(k)}\|\alpha'' j'')(\alpha'' j''\|U^{(k)}\|\alpha' j')\delta(j,j')\delta(m,m')/(2j+1). \tag{33}$$

The matrix of Q is then diagonal with respect to j and m, and entirely independent of m; it follows that Q commutes with $\mathbf{J}$, and is therefore a scalar. Since, owing to (24), Q is for $k=1$ the scalar product of the two vectors, we shall in general name Q the scalar product of $\mathbf{T}^{(k)}$ and $\mathbf{U}^{(k)}$, and write

$$Q=(\mathbf{T}^{(k)}\cdot\mathbf{U}^{(k)})=\sum_q(-1)^q T_q^{(k)}U_{-q}^{(k)}. \tag{32'}$$

The most important example of such scalar products is given by the spherical-harmonic addition theorem (TAS $4^3$22).

The tensorial extension of TAS $12^3$2 may be obtained by a direct use of (16′) and (29). If $\mathbf{T}^{(k)}$ and $\mathbf{U}^{(k)}$ are of such a character that, when a resolution of the type TAS $6^3$5 is made of the states in question, $\mathbf{T}^{(k)}$ operates only on ϕ_1 and $\mathbf{U}^{(k)}$ only on ϕ_2, the matrix elements of Q will be

$$\begin{aligned}(\gamma j_1 j_2 jm|(\mathbf{T}^{(k)}\cdot\mathbf{U}^{(k)})|\gamma' j'_1 j'_2 j'm') &= \sum_{\gamma'' q m_1 m_2 m'_1 m'_2}(-1)^q(j_1 j_2 jm|j_1 j_2 m_1 m_2)(\gamma j_1 m_1|T_q^{(k)}|\gamma'' j'_1 m'_1)\\ &\times(\gamma'' j_2 m_2|U_{-q}^{(k)}|\gamma' j'_2 m'_2)(j'_1 j'_2 m'_1 m'_2|j'_1 j'_2 j'm') = (-1)^{j_1+j_2-j-j'-m}[(2j+1)(2j'+1)]^{\frac{1}{2}}\\ &\times\sum_{\gamma''}(\gamma j_1\|T^{(k)}\|\gamma'' j'_1)(\gamma'' j_2\|U^{(k)}\|\gamma' j'_2)\sum(-1)^q V(j_1 j_2 j\,;\,m_1 m_2 -m)\,V(j_1 j'_1 k\,;\,-m_1 m'_1 q)\\ &\qquad\times V(j_2 j'_2 k\,;\,-m_2 m'_2 -q)\,V(j'_1 j'_2 j'\,;\,m'_1 m'_2 -m').\end{aligned} \tag{34}$$

The last sum is very difficult to evaluate for general values of the parameters; but, owing to (33), it suffices to calculate it for the particular case $j=j'=m=m'$. It is shown in Appendix B that

$$\sum_{\alpha\beta\gamma\delta\varphi}(-1)^{f+\varphi}v(abe\,;\,\alpha\beta-e)v(acf\,;\,-\alpha\gamma\varphi)v(bdf\,;\,-\beta\delta-\varphi)v(cde\,;\,\gamma\delta-e)$$

$$=(-1)^{2e+f+d-b}w(abcd\,;\,ef)/(2e+1), \tag{35}$$

where

$$w(abcd\,;ef)=\sum_z (-1)^z \frac{(a+b+c+d+1-z)!}{(a+b-e-z)!(c+d-e-z)!(a+c-f-z)!} \times (b+d-f-z)!z!(e+f-a-d+z)!(e+f-b-c+z)!. \quad (36)$$

Putting also

$$W(abcd\,;ef)=\left[\frac{(a+b-e)!(a+e-b)!(b+e-a)!(c+d-e)!(c+e-d)!(d+e-c)!}{(a+b+e+1)!(c+d+e+1)!(a+c+f+1)!(b+d+f+1)!}\right.$$
$$\left.\cdot(a+c-f)!(a+f-c)!(c+f-a)!(b+d-f)!(b+f-d)!(d+f-b)!\right]^{\frac{1}{2}} w(abcd\,;ef), \quad (36')$$

we have

$$\sum_{\alpha\beta\gamma\delta\varphi}(-1)^{f+\varphi}V(abe\,;\alpha\beta-e)\,V(acf\,;-\alpha\gamma\,\varphi)\,V(bdf\,;-\beta\delta-\varphi)\,V(cde\,;\gamma\delta-e)$$
$$=(-1)^{2e+f+d-b}W(abcd\,;ef)/(2e+1)\,; \quad (35')$$

and owing to (34) and (33) we get

$$\sum_{\alpha\beta\gamma\delta\varphi}(-1)^{f+\varphi}V(abe\,;\alpha\beta-\epsilon)\,V(acf\,;-\alpha\gamma\,\varphi)\,V(bdf\,;-\beta\delta-\varphi)\,V(cdg\,;\gamma\delta-\eta)$$
$$=(-1)^{e+\epsilon+f+d-b}W(abcd\,;ef)\delta(e,g)\delta(\epsilon,\eta)/(2e+1) \quad (37)$$

and

$$(\gamma j_1 j_2 jm|(\mathbf{T}^{(k)}\cdot\mathbf{U}^{(k)})|\gamma' j'_1 j'_2 jm)$$
$$=(-1)^{j_1+j'_2-j}\sum_{\gamma''}(\gamma j_1\|T^{(k)}\|\gamma'' j'_1)(\gamma'' j_2\|U^{(k)}\|\gamma' j'_2)W(j_1 j_2 j'_1 j'_2\,;jk), \quad (38)$$

which is the tensorial extension of TAS 12[3]2.[6]

(4) Properties of W

The functions w and W are defined for integral and half-integral values of the parameters, with the limitation that each of the four triads

$$(a,b,e),\quad (c,d,e),\quad (a,c,f),\quad (b,d,f) \quad (39)$$

has an integral sum. Since in (36) z takes on only such integral values for which the argument of every factorial is not negative, W vanishes unless the elements of each triad (39) satisfy the triangular inequalities; if one of these triangles reduces to a segment, the summation reduces to one term.

It follows from the symmetry of (36) and (36′) that

$$W(abcd\,;ef)=W(badc\,;ef)=W(cdab\,;ef)=W(acbd\,;fe)\,; \quad (40a)$$

assuming the argument of one of the two last factorials instead of z as summation parameter in (36), we obtain other symmetry properties of W:

$$W(abcd\,;ef)=(-1)^{e+f-a-d}W(ebcf\,;ad)=(-1)^{e+f-b-c}W(aefd\,;bc)\,; \quad (40b)$$

combining (40a) and (40b) we obtain 24 different permutations of the parameters of W, which correspond to all possible permutations between the four triads (39).

Since (33) and (34) have a meaning only for integral values of f, our demonstration of (37) holds only for integral values of f; but it follows from the symmetry properties of V and W that (37) holds also for half-integral values of f.

[6] For the diagonal elements of this matrix an equivalent formula was given by H. A. Kramers, Proc. Amst. Akad. Sci. 34, 965 (1931).

If we multiply the two sides of (37) by $(2g+1)\,V(cdg;\gamma'\delta'-\eta)$ and extend a summation over all possible values of g and η, we obtain, owing to (20b),

$$\sum_{\alpha\beta\varphi}(-1)^{f+\varphi}V(abe;\alpha\beta-\epsilon)\,V(acf;-\alpha\gamma'\varphi)\,V(bdf;-\beta\delta'-\varphi)=(-1)^{e+\epsilon+f+d-b}W(abcd;ef)\,V(cde;\gamma'\delta'-\epsilon),$$

or, owing to (19) and (40) and omitting the dashes,

$$\sum_{\alpha\beta\varphi}(-1)^{f+\varphi}V(abe;\alpha\beta-\epsilon)\,V(afc;-\alpha\varphi\gamma)\,V(fbd;\varphi\beta-\delta)$$
$$=(-1)^{b+c-a-d+e+\epsilon}W(aefd;bc)\,V(edc;-\epsilon\delta\gamma). \quad (41)$$

We rewrite (41) with slightly different parameters,

$$\sum_{\alpha'\beta'\eta}(-1)^{g+\eta}V(abe;\alpha'\beta'-\epsilon)\,V(agc;-\alpha'\eta\gamma)\,V(gbd;\eta\beta'-\delta)$$
$$=(-1)^{b+c-a-d+e+\epsilon}W(aegd;bc)\,V(edc;-\epsilon\delta\gamma), \quad (41')$$

and multiply the two sides by the two sides of (41) and by $(2d+1)(2e+1)$; extending a summation over all possible values of γ, ϵ, and e, and owing to (20), we obtain an orthogonality relation between the W:

$$\textstyle\sum_e (2e+1)W(aefd;bc)W(aegd;bc)=\delta(f,g)/(2f+1). \quad (42)$$

Interchanging a with b and α' with β' in (41') and operating as before, we obtain another useful relation between the W:

$$\textstyle\sum_e(-1)^{a+b+c+d+e+f+g}(2e+1)W(acbd;fe)W(abdc;eg)=W(acdb;fg). \quad (43)$$

(5) Matrix of a Tensor $T^{(k)}$ Which Commutes with J_2 or with J_1

From (16'), (29), and (41) we have

$$(\gamma j_1 j_2 jm|T_q^{(k)}|\gamma' j'_1 j'_2 j'm')=\sum_{m_1 m'_1 m_2}(j_1 j_2 jm|j_1 j_2 m_1 m_2)(\gamma j_1 m_1|T_q^{(k)}|\gamma' j'_1 m'_1)(j'_1 j_2 m'_1 m_2|j'_1 j_2 j'm')$$
$$=(-1)^{j_2+k-j'_1+m}[(2j+1)(2j'+1)]^{\frac{1}{2}}(\gamma j_1\|T^{(k)}\|\gamma' j'_1)W(j_1 j j'_1 j';j_2 k)\,V(jj'k;-mm'q),$$

and owing again to (29) we get

$$(\gamma j_1 j_2 j\|T^{(k)}\|\gamma' j'_1 j_2 j')=(-1)^{j_2+k-j'_1-j}(\gamma j_1\|T^{(k)}\|\gamma' j'_1)[(2j+1)(2j'+1)]^{\frac{1}{2}}W(j_1 j j'_1 j';j_2 k), \quad (44a)$$

which is the tensorial extension of TAS 11[3]8. In the same way we obtain also

$$(\gamma j_1 j_2 j\|U^{(k)}\|\gamma' j_1 j'_2 j')=(-1)^{j_1+k-j_2-j'}(\gamma j_2\|U^{(k)}\|\gamma' j'_2)[(2j+1)(2j'+1)]^{\frac{1}{2}}W(j_2 j j'_2 j';j_1 k). \quad (44b)$$

§4. THE ELECTROSTATIC INTERACTION BETWEEN TWO ELECTRONS

It was shown in I that the coefficients of Slater's integrals F^k and G^k in the two-electron configurations are the matrix elements of $P_k(\cos\omega)$, where ω is the angle between the radii vectors of the two electrons. It follows from (32') and from the spherical-harmonic addition theorem (TAS 4[3]22) that

$$P_k(\cos\omega)=(\mathbf{C}_1^{(k)}\cdot\mathbf{C}_2^{(k)}), \quad (45)$$

where $\mathbf{C}^{(k)}$ is the tensor operator defined by

$$C_q^{(k)}=[4\pi/(2k+1)]^{\frac{1}{2}}\Theta(kq)\Phi(q); \quad (46)$$

we see from TAS 8[6]6 that the non-vanishing matrix elements of $C_q^{(k)}$ are the c^k of Condon and Shortley.

Confronting the expressions TAS 9[6]8 and (29) of $(l0\|C_0^{(k)}\|l'0)$, we obtain

$$(-1)^l(l\|C^{(k)}\|l')\,V(ll'k;000)=\tfrac{1}{2}[(2l+1)(2l'+1)]^{\frac{1}{2}}C_{lkl'}, \quad (47)$$

where (TAS 9[6]7)

$$C_{lkl'}=\int_0^\pi P_l(\cos\omega)P_k(\cos\omega)P_{l'}(\cos\omega)\sin\omega d\omega. \tag{48}$$

In order to calculate algebraically $C_{lkl'}$ we express the Legendre polynomials by means of TAS 4[3]22 and 4[3]18,

$$P_l(\cos\omega)=\bar{P}_l(\cos\omega)=[4\pi/(2l+1)]\sum_m(-1)^m\bar{\Theta}(lm)\bar{\Phi}(m)\bar{\Theta}'(l-m)\bar{\Phi}'(-m),$$
$$P_k(\cos\omega)=[4\pi/(2k+1)]\sum_q(-1)^q\Theta(kq)\Phi(q)\Theta'(k-q)\Phi'(-q),$$
$$P_{l'}(\cos\omega)=[4\pi/(2l'+1)]\sum_{m'}(-1)^{m'}\Theta(l'm')\Phi(m')\Theta'(l'-m')\Phi'(-m'),$$

and integrate their product over the spheres $(\theta\varphi)$ and $(\theta'\varphi')$; we obtain

$$8\pi^2\int_0^\pi P_l(\cos\omega)P_k(\cos\omega)P_{l'}(\cos\omega)\sin\omega d\omega=64\pi^3[(2l+1)(2k+1)(2l'+1)]^{-1}$$
$$\sum_{mqm'}\int_0^\pi\int_0^{2\pi}\bar{\Theta}(lm)\bar{\Phi}(m)\Theta(kq)\Phi(q)\Theta(l'm')\Phi(m')\sin\theta d\theta d\varphi$$
$$\cdot\int_0^\pi\int_0^{2\pi}\bar{\Theta}'(l-m)\bar{\Phi}'(-m)\Theta'(k-q)\Phi'(-q)\Theta'(l'-m')\Phi'(-m')\sin\theta' d\theta' d\varphi',$$

or, if we use successively (46), (29), (19b), and (20a),

$$(2l+1)(2l'+1)C_{lkl'}=2\sum_{mqm'}(lm|C_q^{(k)}|l'm')(l-m|C_{-q}^{(k)}|l'-m')$$
$$=2(l\|C^{(k)}\|l')^2\sum_{mqm'}V(ll'k\,;-mm'q)\,V(ll'k\,;m-m'-q)=2(-1)^{l+l'+k}(l\|C^{(k)}\|l')^2. \tag{49}$$

It follows from the comparison of (47) and (49) that

$$C_{lkl'}=2(-1)^{l+l'+k}[V(ll'k\,;000)]^2, \tag{50}$$

and owing to (22′) we obtain

$$\begin{cases} C_{lkl'}=0 & (l+l'+k\ \text{odd}) \\ C_{lkl'}=\dfrac{2(l+l'-k)!(l+k-l')!(l'+k-l)!g!^2}{(l+l'+k+1)!(g-l)!^2(g-l')!^2(g-k)!^2} & (l+l'+k=2g\ \text{even}), \end{cases} \tag{50′}$$

which agrees with TAS 9[6]9. The numerical values of $C_{lkl'}$ are tabulated by Shortley and Fried.[7]

It follows also from (47), (49), and (22′) that

$$(l\|C^{(k)}\|l')=(-1)^{g-l}[\tfrac{1}{2}(2l+1)(2l'+1)C_{lkl'}]^{\frac{1}{2}}, \tag{51}$$

and therefore

$$c^k(lm,\,l'm')=(lm|C^{(k)}_{m-m'}|l'm')=(-1)^{g+m}[\tfrac{1}{2}(2l+1)(2l'+1)C_{lkl'}]^{\frac{1}{2}}V(ll'k\,;-mm'm-m'). \tag{52}$$

We do not know to what extent this derivation is different from Gaunt's derivation, because we had no opportunity of consulting his paper;[8] in every case (52) has the same advantages in comparison to Gaunt's formula (TAS 8[6]11) as (16) in comparison to Wigner's formula.

Introducing (45) and (51) in (38) we have a direct demonstration of Eq. (12′) I, from which we obtained the coefficients of F^k and G^k for two-electron configurations in (LS) coupling.

[7] G. H. Shortley and B. Fried, Phys. Rev. **54**, 739 (1938), Table III.
[8] J. A. Gaunt, Phil. Trans. Roy. Soc. **A228**, 195 (1929).

In order to obtain from (45) and (38) the matrix elements of the electrostatic interaction in (jj) coupling, it suffices to calculate the elements $(\frac{1}{2}lj\|C^{(k)}\|\frac{1}{2}l'j')$; it follows from (44b) and (51) that

$$(\tfrac{1}{2}ll\pm\tfrac{1}{2}\|C^{(k)}\|\tfrac{1}{2}l'l'\pm\tfrac{1}{2})=(-1)^{(j'+k-j)/2}\left[\frac{(j+j'-k)!(j+k-j')!(j'+k-j)!}{(j+j'+k+1)!}\right]^{\frac{1}{2}}$$
$$\times\frac{(j+j'+k+1)!!}{(j+j'-k-1)!!(j+k-j')!!(j'+k-j)!!}, \quad (53a)$$

$$(\tfrac{1}{2}ll\pm\tfrac{1}{2}\|C^{(k)}\|\tfrac{1}{2}l'l'\mp\tfrac{1}{2})=(-1)^{(j'+k-j-1)/2}\left[\frac{(j+j'-k)!(j+k-j')!(j'+k-j)!}{(j+j'+k+1)!}\right]^{\frac{1}{2}}$$
$$\times\frac{(j+j'+k)!!}{(j+j'-k)!!(j+k-j'-1)!!(j'+k-j-1)!!}, \quad (53b)$$

and then

$$f_k(l_1j_1l_2j_2J)=\frac{(k-1)!!^4(2j_1-k)!!(2j_2-k)!!}{(2j_1+k)!!(2j_2+k)!!}$$
$$\cdot\sum_w(-1)^w\binom{j_1+j_2+J+1+w}{w}\binom{j_1+j_2-J}{w}\binom{J+j_1-j_2}{k-w}\binom{J+j_2-j_1}{k-w}. \quad (54)$$

It is remarkable that (54) depends only on the j's and not on the l's of the electrons, and therefore the coefficients of F^k for the interaction between two $p_{1\frac{1}{2}}$ electrons are the same as between two $d_{1\frac{1}{2}}$ or between a $p_{1\frac{1}{2}}$ and a $d_{1\frac{1}{2}}$.

For the coefficients of the G^k the situation is somewhat different, because, although g_k does not depend explicitly on l, in the case that both the electrons have their spins parallel or antiparallel to their orbital momenta the formula is not the same as in the case that one spin is parallel to its orbital momentum and the other is antiparallel. In the first case

$$g_k(l_1l_1\pm\tfrac{1}{2}l_2l_2\pm\tfrac{1}{2}J)=(-1)^{j_1+j_2-J}\frac{(j_1+j_2-k)!!^2(k+j_1-j_2-1)!!^2(k+j_2-j_1-1)!!^2}{(j_1+j_2+k)!!^2}$$
$$\cdot\sum_w(-1)^w\binom{j_1+j_2+J+1+w}{w}\binom{j_1+j_2-J}{w}\binom{J+j_1-j_2}{k+j_1-j_2-w}\binom{J+j_2-j_1}{k+j_2-j_1-w} \quad (55a)$$

and in the second case

$$g_k(l_1l_1\pm\tfrac{1}{2}l_2l_2\mp\tfrac{1}{2}J)=(-1)^{j_1+j_2-J}\frac{(j_1+j_2-k-1)!!^2(k+j_1-j_2)!!^2(k+j_2-j_1)!!^2}{(j_1+j_2+k+1)!!^2}$$
$$\cdot\sum_w(-1)^w\binom{j_1+j_2+J+1+w}{w}\binom{j_1+j_2-J}{w}\binom{J+j_1-j_2}{k+j_1-j_2-w}\binom{J+j_2-j_1}{k+j_2-j_1-w}. \quad (55b)$$

It must also be noted that in (LS) coupling g_k is preceded by different signs, corresponding to the singlet and triplet states; but in (jj) coupling g_k is always preceded by a minus sign, since in (jj) coupling only antisymmetrical eigenfunctions are possible.

By means of these formulas the results of Inglis[9] were checked, and the following mistakes were found: the coefficient of $-G^1$ 225 for the level $p_1d_{1\frac{1}{2}}$ with $J=2$ is not 25, but 75; the denominators of F^2 and F^4 in the configuration dd' are not 25 and 49, but 1225 and 441.

[9] D. R. Inglis, Phys. Rev. **38**, 862 (1931), Table II.

The non-diagonal elements of the electrostatic interaction in (jj) coupling may also easily be calculated in this way.

From our results follows also that the coefficients of F^k in (jl) coupling[10] are

$$f_k(jlK)=\frac{(k-1)!!(2j-k)!!(2l-k-1)!!(2l+1)}{(2j+k)!!(2l+k+1)!!}$$
$$\cdot\sum_w(-1)^w\binom{j+l+K+1+w}{w}\binom{j+l-K}{w}\binom{K+j-l}{k-w}\binom{K+l-j}{k-w}. \quad (56)$$

The particular expression for $k=2$ which we gave already for the rare-gas spectra differs from (56) in the sign, owing to the fact that in the rare-gas configurations there is an almost closed shell (see §6).

§5. MANY-ELECTRON SPECTRA. GENERAL PART

In §4 we expressed the coefficients of the F^k in the interaction between two electrons as scalar products of tensors, each of which operates on a definite electron (type (34)); thus by the general methods of §3 we may calculate for every configuration that part of the energy matrix which depends on the F^k, in a schema in which each state is defined by its "genealogical characterizations" (TAS §2[8]).

The problem is more complex for the coefficients of the G^k, since the g_k are not scalar products of tensors of the type (34); in the particular cases considered in §§5 and 6 of I we gave to g_k the form of a polynomial in λ, but in more general cases it appears convenient to develop g_k in a sum of scalar products of tensors of the type (34).[11] It follows from (6) I and (45) that

$$g_k(l_1l_2L)=(-1)^{l_1+l_2-L}(l_1l_2LM|(\mathbf{C}_1^{(k)}\cdot\mathbf{C}_2^{(k)})|l_2l_1LM), \quad (57)$$

and owing to (38), (31), and (43) we obtain

$$g_k(l_1l_2L)=(l_1\|C^{(k)}\|l_2)^2\sum_r(-1)^{L+k+r}(2r+1)W(l_1l_2l_1l_2;Lr)W(l_1l_1l_2l_2;rk);$$

if we define the tensor $\mathbf{u}^{(r)}$ by

$$(l\|u^{(r)}\|l')=\delta(l,l') \quad (58)$$

and take into account (38) and the fact that l_1+l_2+k is even, we may also write

$$g_k(l_1l_2L)=(l_1\|C^{(k)}\|l_2)^2\sum(-1)^r(2r+1)W(l_1l_1l_2l_2;rk)(l_1l_2LM|(\mathbf{u}_1^{(r)}\cdot\mathbf{u}_2^{(r)})|l_1l_2LM). \quad (59)$$

Following Dirac's vector model we can also substitute the operator (37) I for the double sign which precedes g_k and assume as coefficient of G^k in the exchange interaction between two electrons the expression

$$-[\tfrac{1}{2}+2(\mathbf{s}_1\cdot\mathbf{s}_2)](l_1\|C^{(k)}\|l_2)^2\sum_r(-1)^r(2r+1)W(l_1l_1l_2l_2;rk)(\mathbf{u}_1^{(r)}\cdot\mathbf{u}_2^{(r)}). \quad (60)$$

It will also be convenient to consider the quantities $(\mathbf{s}_1\cdot\mathbf{s}_2)(\mathbf{u}_1\cdot\mathbf{u}_2)$ as scalar products of "double tensors";[12] a double tensor of the degree (κ, k) is defined as a quantity which behaves as an irreducible tensor of the degree κ with respect to **S** and as an irreducible tensor of the degree k with respect to **L**. The algebra of these double tensors is a trivial extension of the tensor algebra developed in §3; it must be noted only that such a double tensor does not satisfy the commutation rule (23) with respect to **J**, because with respect to **J** it is reducible and may be decomposed in a sum of irreducible tensors, the degrees of which lie between $|k-\kappa|$ and $k+\kappa$. From this point of view the scalar product $(\mathbf{l}\cdot\mathbf{s})$ is the scalar part of the decomposition of the double vector $\mathbf{ls}$.

[10] G. Racah, Phys. Rev. **61**, 537 (1942).
[11] These two different possibilities correspond to the developments of a function in series of powers or of Legendre polynomials.
[12] Reference 3, p. 295.

If x electrons of a configuration are equivalent, it has no sense to speak of the tensor (or double tensor) $\mathbf{t}_L^{(ak)}$ which operates on the electron i (TAS §I[8]), but we must be content to consider tensors of the type

$$\mathbf{T}^{(ak)} = \sum_1^x{}_i \, \mathbf{t}_i^{(ak)}, \tag{61}$$

which operate on the whole group of equivalent electrons; it is easily seen that every symmetrical operator may be built up with such tensors. The matrix elements of a tensor (61) must be calculated in the scheme of the allowed states of the group: for $x \geqslant 3$ this calculation is not very simple, as a general method of vector coupling for equivalent electrons is not yet known; however, it is possible at first to couple the vectors and then to antisymmetrize the obtained states, but in this paper we shall not deal with such cases.

§6. CONFIGURATIONS CONTAINING ALMOST CLOSED SHELLS

Let us consider a shell "$\mathfrak{S}$" which is complete except for ϵ missing electrons; if the number of places in the shell is m, this configuration "$\mathfrak{R}$" will contain $m-\epsilon$ electrons. We shall in this paragraph determine a simple relation between the matrix of a tensor of the type (61) which operates on $\mathfrak{R}$ and the matrix of the corresponding tensor for the simpler group "$\mathfrak{L}$" of ϵ equivalent electrons.

Let us denote by $\Phi_{\mathfrak{L}}(aSLM_SM_L)$ the eigenfunctions of the allowed states of $\mathfrak{L}$ and by $\Phi_{\mathfrak{R}}(bSLM_SM_L)$ those of $\mathfrak{R}$, the parameters a and b being introduced in order to distinguish the different multiplets of the same type which may occur in the given configurations. We consider now a fictive configuration $\mathfrak{L}+\mathfrak{R}$ in which the exclusion principle does not hold between the electrons of $\mathfrak{L}$ and those of $\mathfrak{R}$: a complete set of eigenfunctions of such configuration is given by the functions

$$\Phi_{\mathfrak{L}}(aS'L'M'_SM'_L)\Phi_{\mathfrak{R}}(bS''L''M''_SM''_L)$$

or by the functions

$$\Psi(abS'S''L'L''SLM_SM_L) = \sum_{M'_SM''_SM'_LM''_L} \Phi_{\mathfrak{L}}(aS'L'M'_SM'_L)\Phi_{\mathfrak{R}}(bS''L''M''_SM''_L) \times (S'S''M'_SM''_S \mid S'S''SM_S)(L'L''M'_LM''_L \mid L'L''LM_L). \tag{62}$$

If the exclusion principle holds also between the two groups of electrons, only one state will be allowed, a particular ^1S state which we shall denote by $^1S^*$; its eigenfunction will be

$$\Psi(^1S^*) = \sum_{abSL} q(abSL)\Psi(abSSLL0000). \tag{63}$$

In order to establish a correlation between the states of $\mathfrak{L}$ and those of $\mathfrak{R}$ and between the phases of their eigenfunctions, we consider, for S and L given, the Hermitian matrix

$$A_{ac} = \sum_b \bar{q}(ab)q(cb) \tag{64}$$

and the unitary transformation $u_{c\gamma}$ which diagonalizes it: in view of the special form of (64) it will be

$$\sum_{ac} \bar{u}_{a\alpha}u_{c\gamma}A_{ac} = Q^2(\alpha)\delta(\alpha\gamma), \tag{65}$$

where the $Q(\alpha)$ are real numbers, which we may assume are not negative. If we put for each value of β for which $Q(\beta)$ does not vanish

$$v_{b\beta} = \sum_c \bar{u}_{c\beta}q(cb)/Q(\beta) \quad (Q(\beta) \neq 0), \tag{66}$$

it follows from (64) and (65) that

$$\sum_b \bar{v}_{b\beta}v_{b\alpha} = \delta(\alpha\beta). \tag{67}$$

If $Q(\beta)$ vanishes for some values of β, we complete the matrix $v_{b\beta}$ so that it be unitary: owing to (64) and (65) it will be anyway

$$Q(\beta)v_{b\beta}=\sum_c \bar{u}_{c\beta}q(cb). \tag{66'}$$

We change now the schemes of the states of $\mathfrak{L}$ and $\mathfrak{R}$, putting

$$\begin{aligned}\Phi_{\mathfrak{L}}(\alpha SLM_SM_L)&=\sum_a \Phi_{\mathfrak{L}}(aSLM_SM_L)u_{a\alpha}(SL),\\ \Phi_{\mathfrak{R}}(\alpha SLM_SM_L)&=\sum_b \Phi_{\mathfrak{R}}(bSLM_SM_L)v_{b\alpha}(SL)\end{aligned} \tag{68}$$

and shall consider two terms of $\mathfrak{L}$ and $\mathfrak{R}$ as correlated, if they have the same values of α, S, and L. It follows from (62) that

$$\Psi(\alpha'\alpha''S'S''L'L''SLM_SM_L)=\sum_{ab}\Psi(abS'S''L'L''SLM_SM_L)u_{a\alpha'}(S'L')v_{b\alpha''}(S''L''), \tag{68'}$$

and from the unitarity of $u_{a\alpha}$ and $v_{b\beta}$ that

$$\Psi(abS'S''L'L''SLM_SM_L)=\sum_{\alpha'\alpha''}\bar{u}_{a\alpha'}(S'L')\bar{v}_{b\alpha''}(S''L'')\Psi(\alpha'\alpha''S'S''L'L''SLM_SM_L); \tag{68''}$$

introducing this result in (63) and owing to (66') we obtain

$$\Psi(^1S^*)=\sum_{\alpha SL}Q(\alpha SL)\Psi(\alpha\alpha SSLL0000). \tag{63'}$$

Since $\Psi(^1S^*)$ is the only antisymmetrical eigenfunction of the configuration $\mathfrak{L}+\mathfrak{R}$, the matrix elements connecting $^1S^*$ with every state (68') will vanish for every symmetrical operator, unless $S=L=0$. If $\mathbf{T}_{\mathfrak{L}}^{(\kappa k)}$ and $\mathbf{T}_{\mathfrak{R}}^{(\kappa k)}$ are two tensors which operate on the groups $\mathfrak{L}$ and $\mathfrak{R}$ according to (61), $\mathbf{T}_{\mathfrak{L}}^{(\kappa k)}+\mathbf{T}_{\mathfrak{R}}^{(\kappa k)}$ is symmetrical in all the electrons, and then

$$(\alpha'\alpha''S'S''L'L''SL\|T_{\mathfrak{L}}^{(\kappa k)}\|^1S^*)+(\alpha'\alpha''S'S''L'L''SL\|T_{\mathfrak{R}}^{(\kappa k)}\|^1S^*) \tag{69}$$

vanishes, unless $S=L=0$. Owing to the triangular conditions, each term vanishes alone unless $S=\kappa$ and $L=\kappa$; we shall therefore consider only the remaining equations

$$(\alpha'\alpha''S'S''L'L''\kappa k\|T_{\mathfrak{L}}^{(\kappa k)}\|^1S^*)+(\alpha'\alpha''S'S''L'L''\kappa k\|T_{\mathfrak{R}}^{(\kappa k)}\|^1S^*)=0 \tag{70}$$

which hold for every double tensor, excepting the double scalars.

Owing to (63') and to the fact that $\mathbf{T}_{\mathfrak{L}}^{(\kappa k)}$ is diagonal with respect to $\alpha''S''L''$ and $\mathbf{T}_{\mathfrak{R}}^{(\kappa k)}$ with respect to $\alpha'S'L'$, we get

$$\begin{aligned}&(\alpha'\alpha''S'S''L'L''\kappa k\|T_{\mathfrak{L}}^{(\kappa k)}\|\alpha''\alpha''S''S''L''L''00)Q(\alpha''S''L'')\\ &\qquad+(\alpha'\alpha''S'S''L'L''\kappa k\|T_{\mathfrak{R}}^{(\kappa k)}\|\alpha'\alpha'S'S'L'L'00)Q(\alpha'S'L')=0,\end{aligned}$$

and introducing (44) and (36') this becomes

$$\begin{aligned}&(\alpha'S'L'\|T_{\mathfrak{L}}^{(\kappa k)}\|\alpha''S''L'')Q(\alpha''S''L'')/[(2S''+1)(2L''+1)]^{\frac{1}{2}}+(-1)^{S'+L'-S''-L''+\kappa+k}\\ &\qquad\times(\alpha''S''L''\|T_{\mathfrak{R}}^{(\kappa k)}\|\alpha'S'L')Q(\alpha'S'L')/[(2S'+1)(2L'+1)]^{\frac{1}{2}}=0.\end{aligned} \tag{71a}$$

Also, since $\mathbf{T}_{\mathfrak{L}}^{(\kappa k)\dagger}+\mathbf{T}_{\mathfrak{R}}^{(\kappa k)\dagger}$ is a symmetrical operator, and since the $Q(\alpha SL)$ are real, it follows from (71a) that

$$\begin{aligned}&\langle(\alpha''S''L''\|T_{\mathfrak{L}}^{(\kappa k)\dagger}\|\alpha'S'L')\rangle Q(\alpha'S'L')/[(2S'+1)(2L'+1)]^{\frac{1}{2}}+(-1)^{S''+L''-S'-L'+\kappa+k}\\ &\qquad\times\langle(\alpha'S'L'\|T_{\mathfrak{R}}^{(\kappa k)\dagger}\|\alpha''S''L'')\rangle Q(\alpha''S''L'')/[(2S''+1)(2L''+1)]^{\frac{1}{2}}=0,\end{aligned}$$

and owing to (31′) we get

$$(\alpha' S'L' \| T^{\mathfrak{L}(\varkappa k)} \| \alpha'' S''L'') Q(\alpha' S'L') / [(2S'+1)(2L'+1)]^{\frac{1}{2}} + (-1)^{S'+L'-S''-L''+\varkappa+k} \times (\alpha'' S''L'' \| T^{\mathfrak{R}(\varkappa k)} \| \alpha' S'L') Q(\alpha'' S''L'') / [(2S''+1)(2L''+1)]^{\frac{1}{2}} = 0. \quad (71b)$$

It follows from the homogeneous equation system (71) that the matrix elements connecting two terms $\alpha' S'L'$ and $\alpha'' S''L''$ vanish for every tensor (61) operating on $\mathfrak{L}$ or on $\mathfrak{R}$, unless

$$\frac{Q(\alpha' S'L')}{[(2S'+1)(2L'+1)]^{\frac{1}{2}}} = \frac{Q(\alpha'' S''L'')}{[(2S''+1)(2L''+1)]^{\frac{1}{2}}}; \quad (72)$$

since every symmetrical operator may be expressed as a function of tensors (61), and since there exists always at least one symmetrical operator connecting two allowed terms, it follows that (72) must hold for every couple of allowed terms, or that

$$Q(\alpha SL) = C[(2S+1)(2L+1)]^{\frac{1}{2}}.$$

Since $(2S+1)(2L+1)$ is the number of states of the term αSL, it follows from the normalization of $\Psi(^1S^*)$ that $1/C^2$ equals the number of states of the configuration $\mathfrak{L}$, or that

$$C = \binom{m}{\epsilon}^{-\frac{1}{2}}. \quad (73)$$

It follows from (65) and (72′) that the matrix (64) is a multiple of the unit matrix: the unitary matrix $u_{c\gamma}$ is then entirely arbitrary and to every αSL scheme of $\mathfrak{L}$ a scheme of $\mathfrak{R}$ may be correlated.

From (71) and (72) we have also

$$(\alpha' S'L' \| T^{\mathfrak{L}(\varkappa k)} \| \alpha'' S''L'') = -(-1)^{S'+L'-S''-L''+\varkappa+k} (\alpha'' S''L'' \| T^{\mathfrak{R}(\varkappa k)} \| \alpha' S'L'),$$

and owing to (31′)

$$(\alpha'' S''L'' \| T^{\mathfrak{R}(\varkappa k)} \| \alpha' S'L') = -(-1)^{\varkappa+k} \langle (\alpha'' S''L'' \| T^{\mathfrak{L}(\varkappa k)\dagger} \| \alpha' S'L') \rangle, \quad (74)$$

which is the requested relation between the matrices of $T^{\mathfrak{R}(\varkappa k)}$ and $T^{\mathfrak{L}(\varkappa k)}$.

This demonstration, however, does not hold for scalars. In this case $(lm \| \mathbf{t}^{(00)} \| lm')$ is a multiple of the unit matrix; if its value is a, the matrix of $\mathbf{T}^{\mathfrak{L}(00)}$ has the value ϵa and the matrix of $\mathbf{T}^{\mathfrak{R}(00)}$ has the value $ma - \epsilon a$; we may, therefore, say that apart from a constant diagonal term (74) holds also for scalars, and if only differences of energies are considered we may use (74) even in this case.

The coefficients of F^k for the terms of a configuration l^x are, apart from a constant term, the squares of the tensor $\sum_i C_i^{(k)}$; the relative electrostatic energies of correlated terms are then the same.

Since the expression for the coefficients of F^k contains only tensors with $\varkappa = 0$ and k even, we obtain immediately the known rule that the coefficients of F^k in the interaction between the group $l^{m-\epsilon}$ and an electron l' are the negatives of those for l^ϵ and l'.

For the coefficients of G^k the situation is more complex, since in (60) there are tensors of even and of odd degrees. For two-electron-like configurations $l^{m-1}l'$ the result is, however, very simple, since it follows from (60), (74), and (58) that the coefficient of G^k is

$$[\tfrac{1}{2} - 2(\mathbf{s} \cdot \mathbf{s}')] (l \| C^{(k)} \| l')^2 (-1)^{L+k} \sum_r (2r+1) W(ll'll'; Lr) W(lll'l'; rk),$$

and reduces, owing to (40), (42), and (51), to

$$\frac{1 - 4(s \cdot s')}{4} \cdot \frac{(2l+1)(2l'+1)}{(2k+1)} C_{ll'k} \delta(L, k); \quad (75)$$

this formula agrees with the result of Shortley and Fried,[7] since the first coefficient vanishes for triplets and equals unity for singlets.

Some interesting results may be obtained for the configurations with $\epsilon=m/2$, which may be considered as "self-corresponding." Since the electrostatic energies of two corresponding terms are the same, it follows that in (LS) coupling each term is self-corresponding;[13] it is therefore

$$\Phi_{\mathfrak{E}}(\alpha SLM_SM_L)=c\Phi_{\mathfrak{R}}(\alpha SLM_SM_L)$$

with $|c|=1$, and since with our choice of phases all transformation coefficients are real,

$$\Phi_{\mathfrak{E}}(\alpha SLM_SM_L)=\pm\Phi_{\mathfrak{R}}(\alpha SLM_SM_L). \tag{76}$$

According to these two possibilities the terms of a self-corresponding configuration split in two classes, and a remarkable selection rule follows from (74): the elements of $\mathbf{T}^{(\kappa k)}$ connecting two terms of the same class vanish if $k+\kappa$ is even, the elements connecting two terms of different classes vanish if $k+\kappa$ is odd. A particular case of it is the vanishing of the diagonal elements of the double vector $\sum_i \mathbf{s}_i\mathbf{l}_i$, which causes the vanishing of the spin-orbit interaction constants for all terms of $l^{m/2}$.

This splitting in two classes is also the cause of the unexpected number of rational roots found by Laporte[14] in the electrostatic-energy matrix of d^5.

§7. THE CONFIGURATIONS d^n

d^2

The formulas for this configuration are well known (TAS p. 202); we wish only to point out that putting

$$A=F_0-49F_4=F^0-F^4/9,\quad B=F_2-5F_4=(9F^2-5F^4)/441,\quad C=35F_4=5F^4/63, \tag{77}$$

they get the simpler form

$$^1S=A+14B+7C,\quad ^3P=A+7B,\quad ^1D=A-3B+2C,\quad ^3F=A-8B,\quad ^1G=A+4B+2C. \tag{78}$$

d^3

Condon and Shortley calculated the formulas for this configuration, but they could not separate the energies of the two ^2D terms; this separation was performed by Ufford and Shortley by calculating the eigenfunctions of these terms. We shall calculate in detail this configuration with the tensor method, since the same method will be used without greater complication in the cases d^4, d^5, and f^3.

The term energies of d^3 are the eigenvalues of that part of

$$3F^0+[(\mathbf{C}_1^{(2)}\cdot\mathbf{C}_2^{(2)})+(\mathbf{C}_1^{(2)}\cdot\mathbf{C}_3^{(2)})+(\mathbf{C}_2^{(2)}\cdot\mathbf{C}_3^{(2)})]F^2$$
$$+[(\mathbf{C}_1^{(4)}\cdot\mathbf{C}_2^{(4)})+(\mathbf{C}_1^{(4)}\cdot\mathbf{C}_3^{(4)})+(\mathbf{C}_2^{(4)}\cdot\mathbf{C}_3^{(4)})]F^4 \tag{79}$$

which operates in the space of the antisymmetrical states with $l_1=l_2=l_3=2$. Since this operator does not affect the spins, we shall calculate its matrix in a m_SL scheme, and it will be sufficient to consider the elements corresponding to $ms_1=ms_2=\frac{1}{2}$ and $ms_3=-\frac{1}{2}$; in this scheme only the two first electrons are to be considered as equivalent, and we can thus avoid the difficulties arising from the coupling of three equivalent electrons.

It follows from (51) that

$$(2\|C^{(2)}\|2)=-(10/7)^{\frac{1}{2}},\quad (2\|C^{(4)}\|2)=(10/7)^{\frac{1}{2}}, \tag{80}$$

[13] This holds only in (LS) coupling: it is, for instance, evident that in (jj) coupling of the three levels with $J=\frac{3}{2}$ in the p^3 configuration, only the level $p_{\frac{1}{2}}{}^2p_{\frac{3}{2}}$ is self-corresponding.

[14] O. Laporte, Phys. Rev. **61**, 302 (1942).

and hence and from (44) that

$$(22L\|C_1^{(2)}+C_2^{(2)}\|22L')=\begin{array}{c}\\P\\F\end{array}\begin{array}{c}\begin{array}{cc}P & F\end{array}\\\begin{vmatrix}(6/5)^{\frac{1}{2}} & -(48/35)^{\frac{1}{2}}\\ -(48/35)^{\frac{1}{2}} & -(12/35)^{\frac{1}{2}}\end{vmatrix}\end{array} \tag{81}$$

$$(22L\|C_1^{(4)}+C_2^{(4)}\|22L')=\begin{array}{c}\\P\\F\end{array}\begin{array}{c}\begin{array}{cc}P & F\end{array}\\\begin{vmatrix}0 & -(4/7)^{\frac{1}{2}}\\ -(4/7)^{\frac{1}{2}} & -(22/7)^{\frac{1}{2}}\end{vmatrix}\end{array}.$$

From (38) we obtain now easily the interaction matrix between the d^2 group and the third d electron:

$$W(d^2,d)=2F_0+\begin{Vmatrix}(-1)^L\frac{7\Lambda}{30}\binom{7}{3-L} & \frac{2\Lambda}{15}\left[\binom{6+L}{2}\binom{5-L}{2}\right]^{\frac{1}{2}}\\ \frac{2\Lambda}{15}\left[\binom{6+L}{2}\binom{5-L}{2}\right]^{\frac{1}{2}} & \frac{\Lambda^2-35\Lambda+210}{30}\end{Vmatrix}F_2$$

$$+(-1)^L\begin{Vmatrix}0 & \left[\binom{9}{5-L}\binom{9}{3-L}\right]^{\frac{1}{2}}\\ \left[\binom{9}{5-L}\binom{9}{3-L}\right]^{\frac{1}{2}} & \frac{\Lambda}{10}\binom{11}{5-L}\end{Vmatrix}F_4, \tag{82}$$

where

$$\Lambda=L(L+1). \tag{83}$$

It suffices now to add to (82) the diagonal matrix of the internal energy of d^2, and to diagonalize this sum for each possible value of L; with this method we cannot specify to which value of S each eigenvalue belongs, but the quartet terms may be recognized, according to (23) I, as those for which the coefficient of C vanishes. The results are

$$\begin{aligned}&{}^2P=3A-6B+3C, && {}^4F=3A-15B,\\ &{}^4P=3A, && {}^2G=3A-11B+3C,\\ &{}^2D=3A+5B+5C\pm(193B^2+8BC+4C^2)^{\frac{1}{2}}, && {}^2H=3A-6B+3C,\\ &{}^2F=3A+9B+3C,\end{aligned} \tag{84}$$

and agree with those of the above-mentioned authors (TAS pp. 206 and 233).

d^4

This configuration was calculated by Ostrofsky,[15] but Laporte and Platt[16] found some mistakes in his results.

If we assume $ms_1=ms_2=\frac{1}{2}$ and $ms_3=ms_4=-\frac{1}{2}$, the scheme will be an L_1L_2L one, where $\mathbf{L}_1=\mathbf{l}_1+\mathbf{l}_2$ and $\mathbf{L}_2=\mathbf{l}_3+\mathbf{l}_4$; the interaction matrix $W(d^2,d^2)$ between the two d^2 groups is of the fourth degree and was calculated in the same way as for d^3. Adding to it the diagonal matrix of the internal energies of the two d^2 groups, we obtained the complete energy matrix, the eigenvalues of which are the requested energies of the configuration d^4; the singlet and the triplet terms were distinguished by the

[15] M. Ostrofsky, Phys. Rev. **46**, 604 (1934).
[16] O. Laporte and J. R. Platt, Phys. Rev. **62**, 305 (1942).

irrationality of the results in the cases of two expected terms of the same kind. The results are

$$\begin{aligned}
&{}^1S=6A+10B+10C\pm 2(193B^2+8BC+4C^2)^{\frac{1}{2}},\\
&{}^3P=6A-5B+(11/2)C\pm\tfrac{1}{2}(912B^2-24BC+9C^2)^{\frac{1}{2}},\\
&{}^1D=6A+9B+(15/2)C\pm\tfrac{3}{2}(144B^2+8BC+C^2)^{\frac{1}{2}},\\
&{}^3D=6A-5B+4C,\\
&{}^5D=6A-21B,\\
&{}^1F=6A+6C,\\
&{}^3F=6A-5B+(11/2)C\pm\tfrac{3}{2}(68B^2+4BC+C^2)^{\frac{1}{2}},\\
&{}^1G=6A-5B+(15/2)C\pm\tfrac{1}{2}(708B^2-12BC+9C^2)^{\frac{1}{2}},\\
&{}^3G=6A-12B+4C,\\
&{}^3H=6A-17B+4C,\\
&{}^1I=6A-15B+6C,
\end{aligned}\tag{85}$$

and agree with those of Laporte and Platt, with the exception of a misprint for the term ${}^1F$, which must be $6F_0-84F_4$.

d^5

Catalan and Antunes[17] and also Bowman[18] calculated the formulas for this configuration, but they could not separate the energies of the terms of the same kind.

Assuming $ms_1=ms_2=ms_3=\frac{1}{2}$ and $ms_4=ms_5=-\frac{1}{2}$, we need at first the elements of $(222L\|C_1^{(k)}+C_2^{(k)}+C_3^{(k)}\|222L')$ for the antisymmetrical states; but if we consider only electrons with $m_S=\frac{1}{2}$, d^3 is the almost closed shell corresponding to d^2, and according to (74) the needed matrix elements are the same as (81) with inverted signs; it follows that the interaction between the d^3 and the d^2 group is

$$W(d^3,d^2)=10F^0-W(d^2,d^2)\tag{86}$$

and we can proceed as for d^4. It must, however, be noted that the irrationality criterion is not sufficient in this case for the distinction between quartets and doublets, since almost all the eigenvalues are rational; this distinction may be based on the property that the relative positions of the quartets and of the sextet are exactly opposed to those of the terms of d^2 with the same L; this property follows immediately from the possibility of calculating these terms in a scheme in which $ms_1=ms_2=ms_3=ms_4=\frac{1}{2}$ and $ms_5=-\frac{1}{2}$. The results are

$$\begin{aligned}
&{}^2S=10A-3B+8C, && {}^2F'=10A-25B+10C,\\
&{}^6S=10A-35B, && {}^4F=10A-13B+7C,\\
&{}^2P=10A+20B+10C, && {}^2G=10A-13B+8C,\\
&{}^4P=10A-28B+7C, && {}^2G'=10A+3B+10C,\\
&{}^2D=10A-3B+11C\pm 3(57B^2+2BC+C^2)^{\frac{1}{2}}, && {}^4G=10A-25B+5C,\\
&{}^2D'=10A-4B+10C, && {}^2H=10A-22B+10C,\\
&{}^4D=10A-18B+5C, && {}^2I=10A-24B+8C,\\
&{}^2F=10A-9B+8C, &&
\end{aligned}\tag{87}$$

and agree with the recent results of Laporte.[14]

[17] M. A. Catalan and M. T. Antunes, Zeits. f. Physik **102**, 432 (1936).
[18] D. S. Bowman, Phys. Rev. **59**, 386 (1941).

The Coefficients of C

It is pointed out by Laporte and Platt[16] that if B vanishes all the energies of the d^n terms are rational and show high degree degeneracies; this fact may be explained by general considerations similar to those of §3 of I.

It follows from (20)I and (77) that if B vanishes the interaction between two electrons is

$$W_{ij}=A+\frac{\lambda_{ij}^4+5\lambda_{ij}^3-15\lambda_{ij}^2-75\lambda_{ij}}{18}C; \tag{88}$$

owing to the relation

$$(\mathbf{s}_i\cdot\mathbf{s}_j)=-\frac{\lambda_{ij}^4+6\lambda_{ij}^3-13\lambda_{ij}^2-90\lambda_{ij}-18}{72}, \tag{89}$$

which corresponds for equivalent d electrons to Van Vleck's relation for p electrons,[19] we may also write

$$W_{ij}=A+[\tfrac{1}{2}-2(\mathbf{s}_i\cdot\mathbf{s}_j)+q_{ij}]C, \tag{88'}$$

where

$$q_{ij}=\frac{(\lambda_{ij}-4)\lambda_{ij}(\lambda_{ij}+3)(\lambda_{ij}+5)}{36} \tag{90}$$

is an operator which has the eigenvalue 0 in all cases, except if the resultant of the two electrons is a ^1S state. Owing to the relation

$$S(S+1)=\tfrac{3}{4}n+2\sum_{i<j}(\mathbf{s}_i\cdot\mathbf{s}_j), \tag{91}$$

we find that

$$W=\sum_{i<j}W_{ij}=\frac{n(n-1)}{2}A+\left[\frac{n(n+2)}{4}-S(S+1)+Q\right]C, \tag{92}$$

where

$$Q=\sum_{i<j}q_{ij}. \tag{93}$$

If in the configuration d^n a term occurs which does not occur in d^{n-2}, it is impossible that in this state two electrons are connected so as to have a ^1S resultant, and therefore Q vanishes in all such terms.

For the terms which occur also in d^{n-2} the calculation of Q may be made as follows. Each m_sm_l state of d^{n-2} gives rise in d^n to a "family" of states in which the first $n-2$ electrons have the quantum numbers of the "parent" state and the last two electrons have the quantum numbers m^+ and $-m^-$. The number of states of each family equals five minus the number of possibilities forbidden by the exclusion principle: if in the parent state there are no other couples of electrons of the type m'^+ and $-m'^-$ (and this is always the case when the values of M_S and M_L under consideration are not allowed for d^{n-1}), each electron of the parent state excludes a possibility, and the residual number is then $7-n$.

Since the matrix elements of q_{ij} are

$$(m_im_j|q_{ij}|m_i'm_j')=(-1)^{m_i-m_i'}\delta(m_i,-m_j)\delta(m_i',-m_j'), \tag{94}$$

and the exchange term compensates the direct term for electrons of like spins, the only non-vanishing q_{ij} is q_{n-1n} and the only non-vanishing elements of q_{n-1n} are those connecting states of the same family, the values of these elements being $(-1)^{m-m'}$. The eigenvalues of these submatrices, owing to this particular expression of their elements, are all 0 except one, which equals the trace of the submatrix, i.e., $7-n$. We can then say that each term of d^{n-2} gives rise in d^n to a term with $Q=7-n$, and that the other eigenvalues of Q vanish also in d^n.

[19] J. H. Van Vleck, Phys. Rev. **45**, 412 (1934), Eq. (33).

If more than a couple of the type m^+ and $-m^-$ may be simultaneously present in a $m_s m_l$ state, the calculation is more complex, but the result is almost the same: each term which occurs in d^{n-2} has in d^n its Q value increased by $7-n$; each further term has $Q=0$.

Since $F_2 \geqslant 9F_4$ (TAS p. 177) and it is therefore impossible that B could vanish, we omitted in §3 of I this application; but the recent paper of Laporte and Platt induced us to put here these considerations. The high degree degeneracies remarked by these authors for this hypothetical case and the relation between their Table II and an old table of Hund[20] are really based on the simple form of (92) and on the properties of the operator Q.

We take this opportunity for pointing out that Eq. (6) of Laporte and Platt is right only for certain m, since its exact form is

$$\sum_k \frac{2k+1}{2} \frac{c^k(lmlm')c^k(lm_1lm'_1)}{c^k(l0l0)} = \delta(mm_1)\delta(m'm'_1) + (-1)^{m-m_1}\delta(m, -m'_1)\delta(m_1, -m') \frac{2l+1}{4}; \quad (95)$$

its demonstration follows almost immediately from (52), (20b), and (19a).

The ratios between the distances of the ^1S terms in f^2 and g^2 from the other singlets and the distances between these singlets and the triplets are also incorrect by a factor 2.

§8. THE CONFIGURATION f^3

For the configurations f^n it is also convenient to introduce new parameters; if we put

$$A = F_0 - 21F_4 - 468F_6, \quad B = (5F_2 + 6F_4 - 91F_6)/5, \quad C = 7(F_4 - 6F_6)/5, \quad D = 462F_6, \quad (96)$$

the formulas for f^2 assume the simpler form

$$\begin{aligned} &^1S = A + 60B + 105C + 9D, \quad &&^1G = A - 30B + 110C + 2D, \\ &^3P = A + 45B, &&^3H = A - 25B, \\ &^1D = A + 19B - 72C + 2D, &&^1I = A + 25B + 2D. \\ &^3F = A - 10B, \end{aligned} \quad (97)$$

The calculation for f^3 was made exactly in the same way as for d^3, and gave the following results:

$$\begin{aligned} &^4S = 3A - 30B, \\ &^2P = 3A - 25B + 35C + 3D, \\ &^2D = 3A - 7B + (57/2)C + 3D \pm \tfrac{1}{2}(2176B^2 - 18096BC + 74529C^2)^{\frac{1}{2}}, \\ &^4D = 3A + 25B, \\ &^2F = 3A + 55B + (75/2)C + 6D \pm \tfrac{1}{2}[9700B^2 - 180B(45C + 2D) + 9(45C + 2D)^2]^{\frac{1}{2}}, \\ &^4F = 3A - 30B, \\ &^2G = 3A + 7B + (113/2)C + 3D \pm \tfrac{1}{2}(12676B^2 - 31676BC + 36169C^2)^{\frac{1}{2}}, \\ &^4G = 3A - 10B, \\ &^2H = 3A - 23B + (63/2)C + 3D \pm \tfrac{1}{2}(5056B^2 - 18816BC + 29169C^2)^{\frac{1}{2}}, \\ &^2I = 3A - 5B + 45C + 3D, \\ &^4I = 3A - 65B, \\ &^2K = 3A - 40B + 80C + 3D, \\ &^2L = 3A + 3D. \end{aligned} \quad (98)$$

[20] F. Hund, Zeits. f. Physik **33**, 345 (1925), Table IV.

§9. THE CONFIGURATIONS d^2p AND d^3p

The energy matrix of the configuration d^2p will be calculated in a scheme in which each term is characterized by a definite state of the core d^2. In this scheme the interaction between the two d electrons is diagonal and has the values given by (78); the interaction between each d electron and the p electron follows from (60) and is

$$W(d,p)=F_0+10(21)^{\frac{1}{2}}(\mathbf{u}_d^{(2)}\cdot\mathbf{u}_p^{(2)})F_2-[\tfrac{1}{2}+2(\mathbf{s}_d\cdot\mathbf{s}_p)]\{[2+9\sqrt{5}(\mathbf{u}_d^{(1)}\cdot\mathbf{u}_p^{(1)})$$
$$+5(21)^{\frac{1}{2}}(\mathbf{u}_d^{(2)}\cdot\mathbf{u}_p^{(2)})]G_1+[7-21\sqrt{5}(\mathbf{u}_d^{(1)}\cdot\mathbf{u}_p^{(1)})+5(21)^{\frac{1}{2}}(\mathbf{u}_d^{(2)}\cdot\mathbf{u}_p^{(2)})]G_3\}, \quad (99)$$

where[21]

$$F_0=F^0(nd,n'p), \quad F_2=F^2(nd,n'p)/35, \quad G_1=G^1(nd,n'p)/15, \quad G_3=3G^3(nd,n'p)/245. \quad (100)$$

In order to obtain the matrix of

$$W(d^2,p)=W(d_1,p)+W(d_2,p), \quad (101)$$

we calculate at first, by means of (44), the matrices of the tensors

$$\mathbf{U}^{(k)}=\mathbf{u}_1^{(k)}+\mathbf{u}_2^{(k)} \quad (102a)$$

and of the double tensors

$$\mathbf{V}^{(1k)}=\mathbf{s}_1\mathbf{u}_1^{(k)}+\mathbf{s}_2\mathbf{u}_2^{(k)} \quad (102b)$$

for two equivalent d electrons; the results are

$(SL\|U^{(1)}\|S'L')$ (103a)

	^1S	^3P	^1D	^3F	^1G
^1S	0	0	0	0	0
^3P	0	$(1/5)^{\frac{1}{2}}$	0	0	0
^1D	0	0	1	0	0
^3F	0	0	0	$(14/5)^{\frac{1}{2}}$	0
^1G	0	0	0	0	$(6)^{\frac{1}{2}}$

$(SL\|U^{(2)}\|S'L')$ (103b)

	^1S	^3P	^1D	^3F	^1G
^1S	0	0	$(4/5)^{\frac{1}{2}}$	0	0
^3P	0	$-(21/25)^{\frac{1}{2}}$	0	$(24/25)^{\frac{1}{2}}$	0
^1D	$(4/5)^{\frac{1}{2}}$	0	$-3/7$	0	$(144/245)^{\frac{1}{2}}$
^3F	0	$(24/25)^{\frac{1}{2}}$	0	$(6/25)^{\frac{1}{2}}$	0
^1G	0	0	$(144/245)^{\frac{1}{2}}$	0	$(198/49)^{\frac{1}{2}}$

$(SL\|V^{(11)}\|S'L')$ (103c)

	^1S	^3P	^1D	^3F	^1G
^1S	0	$(2/5)^{\frac{1}{2}}$	0	0	0
^3P	$(2/5)^{\frac{1}{2}}$	$(1/5)^{\frac{1}{2}}$	$-(7/10)^{\frac{1}{2}}$	0	0
^1D	0	$-(7/10)^{\frac{1}{2}}$	0	$(4/5)^{\frac{1}{2}}$	0
F^3	0	0	$(4/5)^{\frac{1}{2}}$	$(14/5)^{\frac{1}{2}}$	$-(3/5)^{\frac{1}{2}}$
^1G	0	0	0	$-(3/5)^{\frac{1}{2}}$	0

[21] This definition of G_3 differs by a factor 3 from that of TAS, but agrees with (50) I.

$$(SL\|V^{(12)}\|S'L')=\begin{array}{c|ccccc} & {}^1S & {}^3P & {}^1D & {}^3F & {}^1G \\ \hline {}^1S & 0 & 0 & 0 & 0 & 0 \\ {}^3P & 0 & -(21/25)^{\frac{1}{2}} & -(3/10)^{\frac{1}{2}} & (24/25)^{\frac{1}{2}} & 0 \\ {}^1D & 0 & -(3/10)^{\frac{1}{2}} & 0 & (32/35)^{\frac{1}{2}} & 0 \\ {}^3F & 0 & (24/25)^{\frac{1}{2}} & (32/35)^{\frac{1}{2}} & (6/25)^{\frac{1}{2}} & -(9/7)^{\frac{1}{2}} \\ {}^1G & 0 & 0 & 0 & -(9/7)^{\frac{1}{2}} & 0 \end{array} \qquad (103d)$$

The matrix of (101) follows from (99), (103), and (38); adding to it the energy of the core we obtain the following results for the terms of d^2p [22]

$$^3S=A+7B-14F_2-3G_1+7G_3$$
$$^4S=A+7B-14F_2+6G_1-14G_3$$
$$^4P=A+7B+7F_2-6G_1-21G_3$$
$$^4F=A-8B-3F_2-G_1-16G_3$$
$$^4G=A-8B+F_2-9G_1-4G_3$$
$$^2H=A+4B+2C+4F_2-6G_1-G_3$$

$$^4D=\begin{Vmatrix} A+7B-(7F_2+24G_1+49G_3)/5 & (12F_2-6G_1-6G_3)(14/25)^{\frac{1}{2}} \\ (12F_2-6G_1-6G_3)(14/25)^{\frac{1}{2}} & A-8B+(12F_2+4G_1-146G_3)/5 \end{Vmatrix}$$

$$^2G=\begin{Vmatrix} A-8B+F_2+(9/2)G_1+2G_3 & (-\tfrac{3}{2}G_1+G_3)(15)^{\frac{1}{2}} \\ (-\tfrac{3}{2}G_1+G_3)(15)^{\frac{1}{2}} & A+4B+2C-11F_2+\tfrac{3}{2}G_1-6G_3 \end{Vmatrix}$$

$$^2P=\begin{Vmatrix} A+14B+7C-2G_1-7G_3 & (-3G_1+7G_3)(3)^{\frac{1}{2}} & (4F_2-G_1-G_3)(7)^{\frac{1}{2}} \\ (-3G_1+7G_3)(3)^{\frac{1}{2}} & A+7B+7F_2+3G_1+(21/2)G_3 & (5/2)G_3(21)^{\frac{1}{2}} \\ (4F_2-G_1-G_3)(7)^{\frac{1}{2}} & (5/2)G_3(21)^{\frac{1}{2}} & A-3B+2C-3F_2+G_1-(23/2)G_3 \end{Vmatrix}$$

$$^2D=\begin{Vmatrix} A+7B+(-7F_2+12G_1+(49/2)G_3)/5 & (-6G_1+9G_3)(21/20)^{\frac{1}{2}} & (12F_2+3G_1+3G_3)(14/25)^{\frac{1}{2}} \\ (-6G_1+9G_3)(21/20)^{\frac{1}{2}} & A-3B+2C+3F_2-2G_1-(19/2)G_3 & (G_1+11G_3)(6/5)^{\frac{1}{2}} \\ (12F_2+3G_1+3G)(14/25)^{\frac{1}{2}} & (G_1+11G_3)(6/5)^{\frac{1}{2}} & A-8B+(12F_2-2G_1+73G_3)/5 \end{Vmatrix}$$

$$^2F=\begin{Vmatrix} A-3B+2C-(6F_2+23G_1+23G_3)/7 & (-10G_1+10G_3)(3/7)^{\frac{1}{2}} & (24F_2-6G_1-6G_3)(3/49)^{\frac{1}{2}} \\ (-10G_1+10G_3)(3/7)^{\frac{1}{2}} & A-8B-3F_2+\tfrac{1}{2}G_1+8G_3 & (9G_1+54G_3)/(28)^{\frac{1}{2}} \\ (24F_2-6G_1-6G_3)(3/49)^{\frac{1}{2}} & (9G_1+54G_3)/(28)^{\frac{1}{2}} & A+4B+2C+(55F_2-\tfrac{3}{2}G_1-124G_3)/7 \end{Vmatrix}$$

For calculating the terms of d^8p it suffices to take into account the fact that the constant matrix and the matrices of $\mathbf{U}^{(2)}$ and $\mathbf{V}^{(11)}$ change their signs at passing from the core d^2 to d^8, according to (74). The results are:

$$^2S=\ ^4S=A+7B+14F_2$$
$$^4P=A+7B-7F_2$$
$$^4F=A-8B+3F_2$$
$$^4G=A-8B-F_2$$
$$^2H=A+4B+2C-4F_2+15G_3$$

[22] The parameters have the meaning given in (77) and (100), with the exception of A which contains also $2F^0(nd, n'p)$.

TABLE I. The configuration $3d^3 4p$ of Ti II.

Term	Obs.	Calc. A	Calc. B
$(^3F)\ ^4G$	29936	29748	29823
$(^3F)\ ^4F$	31108	31028	31125
$(^3F)\ ^2F$	31369	31375	31471
$(^3F)\ ^2D$	31918	32132	32251
$(^3F)\ ^4D$	32690	32813	32890
$(^3F)\ ^2G$	34657	33951	34109
$(^3P)\ ^2S$	37431	37623	37628
$(^1D)\ ^2D$	39380	40461	40000
$(^1D)\ ^2P$	39627	40035	39496
$(^1D)\ ^2F$	40011	39983	39507
$(^3P)\ ^4S$	40027	40233	40237
$(^3P)\ ^4D$	40612	40518	40441
$(^3P)\ ^4P$	42127	42213	42100
$(^1G)\ ^2G$	43763	43259	43675
$(^3P)\ ^2D$	44907	44807	44737
$(^3P)\ ^2P$	45524	45672	45673
$(^1G)\ ^2H$	45802	44822	45184
$(^1G)\ ^2F$	47535	47751	48078
$(^1S)\ ^2P$	=	64692	(64465)
Parameters:			
B		669	=
C		2563	=
ϵ		=	0.9484
F_2		290	288
G_1		332	337
G_3		18	20.2

TABLE II. The configuration $3d^4 4p$ of Ni II.

Term	Obs.	Calc.
$(^3F)\ ^4D$	52588	52581
$(^3F)\ ^4G$	53883	53707
$(^3F)\ ^4F$	55394	55163
$(^3F)\ ^2G$	55775	55735
$(^3F)\ ^2F$	57685	57492
$(^3F)\ ^2D$	57933	57892
$(^3P)\ ^4P$	66649	66853
$(^1D)\ ^2F$	67943	68729
$(^1D)\ ^2D$	68442	68929
$(^1D)\ ^2P$	68636	69013
$(^3P)\ ^4D$	70716	70527
$(^3P)\ ^2D$	72011	72159
$(^3P)\ ^2P$	73256	73245
$(^3P)\ ^2S$	74282	74497
$(^3P)\ ^4S$	74299	74497
$(^1G)\ ^2H$	75460	74713
$(^1G)\ ^2F$	75904	75494
$(^1G)\ ^2G$	79878	79505
$(^1S)\ ^2P$	=	109339
Parameters:		
B		1022
C		4509
F_2		364
G_1		303
G_3		54.4

$$^4D=\begin{Vmatrix} A+7B+7F_2/5 & -12F_2(14/25)^{\frac{1}{2}} \\ -12F_2(14/25)^{\frac{1}{2}} & A-8B-12F_2/5 \end{Vmatrix}$$

$$^2G=\begin{Vmatrix} A-8B-F_2+75G_3/2 & -5G_3(15/4)^{\frac{1}{2}} \\ -5G_3(15/4)^{\frac{1}{2}} & A+4B+2C+11F_2+5G_3/2 \end{Vmatrix}$$

$$^2P=\begin{Vmatrix} A+14B+7C+2G_1+7G_3 & (3G_1-7G_3)(3)^{\frac{1}{2}} & (-4F_2+G_1+G_3)(7)^{\frac{1}{2}} \\ (3G_1-7G_3)(3)^{\frac{1}{2}} & A+7B-7F_2+(27/2)G_1+21G_3 & (3G_1-2G_3)(21/4)^{\frac{1}{2}} \\ (-4F_2+G_1+G_3)(7)^{\frac{1}{2}} & (3G_1-2G_3)(21/4)^{\frac{1}{2}} & A-3B+2C+3F_2+(7/2)G_1+G_3 \end{Vmatrix}$$

$$^2D=\begin{Vmatrix} A+7B+(7F_2+(27/2)G_1+126G_3)/5 & (3G_1-12G_3)(21/20)^{\frac{1}{2}} & (-12F_2+9G_1+9G_3)(14/25)^{\frac{1}{2}} \\ (3G_1-12G_3)(21/20)^{\frac{1}{2}} & A-3B+2C-3F_2+(7/2)G_1+6G_3 & (7G_1-3G_3)(6/5)^{\frac{1}{2}} \\ (-12F_2+9G_1+9G_3)(14/25)^{\frac{1}{2}} & (7G_1-3G_3)(6/5)^{\frac{1}{2}} & A-8B+(-12F_2+84G_1+9G_3)/5 \end{Vmatrix}$$

$$^2F=\begin{Vmatrix} A-3B+2C+(6F_2+2G_1+72G_3)/7 & (2G_1-18G_3)(3/7)^{\frac{1}{2}} & (-24F_2+6G_1+6G_3)(3/49)^{\frac{1}{2}} \\ (2G_1-18G_3)(3/7)^{\frac{1}{2}} & A-8B+3F_2+6G_1+(27/2)G_3 & (18G_1-(9/2)G_3)/(7)^{\frac{1}{2}} \\ (-24F_2+6G_1+6G_3)(3/49)^{\frac{1}{2}} & (18G_1-(9/2)G_3)/(7)^{\frac{1}{2}} & A+4B+2C+(-55F_2+54G_1+\tfrac{3}{2}G_3)/7 \end{Vmatrix}$$

We fitted the experimental values[23] of Ti II and Ni II to the theoretical formulas by least squares, and obtained the results given in Table I (column A) and Table II. The mean deviations are ± 430 for Ti II and ± 347 for Ni II, and confirm the known fact that the agreement is better for the elements on the right side of the periodic table.

It must also be observed that these deviations show a certain regularity: in almost all the cases the differences between observed and calculated values are positive for the terms grounded on the

[23] R. F. Bacher and S. Goudsmit, *Atomic Energy States* (McGraw-Hill, 1932).

^3F and ^1G terms of the core, and negative for those grounded on ^3P and ^1D. Since the configurations d^2, d^2s, d^8, d^8s of the whole iron group show the same regularities in the deviations,[24] the main part of these deviations may be attributed to second-order effects in the coupling of the core electrons.

It seems therefore reasonable to substitute in the formulas of d^2p and d^8p for the part depending on the energy of the core (terms with B and C) the experimental values of the corresponding ions d^2 and d^8; these values must, however, be multiplied with a convenient reduction factor ϵ, since with increasing ionization all coupling parameters increase slightly.

The result of fitting the terms of Ti II to such semi-theoretical formulas by least squares is shown in Table I, column B; the mean deviation reduces to ± 332, although the number of free parameters is also reduced (ϵ instead of B and C).

For writing down the matrix of the ^2P terms we needed also the value of the term $3d^2\ ^1S$ of Ti III: since this is still unknown, we calculated it from the other $3d^2$ terms by least squares; this approximated value suffices for calculating the perturbation of $(^1S)\ ^2P$ of Ti II on the other ^2P terms, but cannot be of use for predicting with the same approximation the position of $(^1S)\ ^2P$ himself.

We could not apply this method of calculation to Ni II, since the terms of Ni III are still unknown, as far as known to us.

§10. THE INTEGRALS G^k

It is noted in TAS (p. 177) that F^k is essentially positive and a decreasing function of k, and it is stated as an empirical fact that also G^k shares the same properties, although they do not follow from its definition. Since this fact was sometimes questioned,[25] it seemed worth while to us to seek for a mathematical demonstration: we found that the first property may be proved, but only $G^k/(2k+1)$ is necessarily a decreasing function of k.

According to its definition, G^k has the form

$$G^k=\int_0^\infty\int_0^\infty (r_<{}^k/r_>{}^{k+1})f(r_1)f(r_2)dr_1dr_2, \tag{104}$$

where $r_<$ is the lesser and $r_>$ the greater of r_1 and r_2; we may also write

$$G^k=\int_0^\infty f(x)\,\varphi(x)dx \tag{105}$$

with

$$\varphi(x)=x^{-k-1}\int_0^x y^k f(y)dy+x^k\int_x^\infty y^{-k-1}f(y)dy. \tag{106}$$

It follows from (106) that

$$f(x)=-x^{k+1}[x^{-2k}(x^{k+1}\varphi)']'/(2k+1)\,; \tag{106'}$$

introducing this expression in (105) and integrating by parts we get

$$G^k=\int_0^\infty x^{-2k}[(x^{k+1}\varphi)']^2dx/(2k+1)\geqslant 0. \tag{107}$$

In the same way, putting

$$G^k/(2k+1)-G^{k+1}/(2k+3)=\int_0^\infty f(x)\psi(x)dx \tag{108}$$

[24] TAS, Figs. 3[7] and 4[7]; G. Racah, Phys. Rev. **61**, 538 (1942), Table I.
[25] TAS, p. 366.

with

$$\psi(x)=\left[x^{-k-1}\int_0^x y^k f(y)dy+x^k\int_x^\infty y^{-k-1}f(y)dy\right]/(2k+1)$$
$$+\left[x^{-k-2}\int_0^x y^{k+1}f(y)dy+x^{k+1}\int_x^\infty y^{-k-2}f(y)dy\right]/(2k+3), \quad (109)$$

we have

$$f(x)=x^{k+2}[x^{-2k}(x^{k+2}\psi)'']''/(2k+2), \quad (109')$$

and from (108) we get with a double integration by parts

$$G^k/(2k+1)-G^{k+1}/(2k+3)=\int_0^\infty x^{-2k}[(x^{k+2}\psi)'']^2dx/(2k+2)\geqslant 0. \quad (110)$$

It is also possible to find particular functions $f(x)$ for which the ratio G^{k+1}/G^k tends to the theoretical limit $(2k+3)/(2k+1)$; an example is given by

$$f(x)=\delta(x-a)-\delta(x-a-b) \quad (111)$$

with $b\ll a$.

APPENDIX A

From the definition (17) we have

$$v(abc\,;000)=\frac{a!b!c!}{a+b-c}\Sigma_z(-1)^{c+z}\frac{(a+b-c-z)+z}{z!(a+b-c-z)!(a-z)!(b-z)!(c-a+z)!(c-b+z)!}$$
$$=\frac{a!b!c!}{a+b-c}\Sigma_z(-1)^{c+z}\{[z!(a+b-c-z-1)!(a-z)!(b-z)!(c-a+z)!(c-b+z)!]^{-1}$$
$$+[(z-1)!(a+b-c-z)!(a-z)!(b-z)!(c-a+z)!(c-b+z)!]^{-1}\},$$

and changing the summation parameter in the second term of the brackets,

$$v(abc\,;000)=\frac{a!b!c!}{a+b-c}\Sigma_z(-1)^{c+z}\{[z!(a+b-c-z-1)!(a-z)!(b-z)!(c-a+z)!(c-b+z)!]^{-1}$$
$$-[z!(a+b-c-z-1)!(a-z-1)!(b-z-1)!(c-a+z+1)!(c-b+z+1)!]^{-1}\}$$
$$=\frac{a!b!(c+1)!}{a+b-c}\Sigma_z(-1)^{c+z+1}\frac{a+b-c-2z-1}{z!(a+b-c-z-1)!(a-z)!(b-z)!(c-a+z+1)!(c-b+z+1)!};$$

owing to the identity

$$a(a+b-c-2z-1)=(a-z)(a+b-c-z-1)-z(c-b+z+1),$$

we have also

$$v(abc\,;000)=\frac{(a-1)!b!(c+1)!}{a+b-c}\Sigma_z(-1)^{c+z+1}\{[z!(a+b-c-z-2)!(a-z-1)!(b-z)!(c-a+z+1)!(c-b+z+1)!]^{-1}$$
$$-[(z-1)!(a+b-c-z-1)!(a-z)!(b-z)!(c-a+z+1)!(c-b+z)!]^{-1}\},$$

and changing again the summation parameter in the second term of the brackets,

$$v(abc\,;000)=\frac{(a-1)!b!(c+1)!}{a+b-c}\Sigma_z(-1)^{c+z+1}\{[z!(a+b-c-z-2)!(a-z-1)!(b-z)!(c-a+z+1)!(c-b+z+1)!]^{-1}$$
$$+[z!(a+b-c-z-2)!(a-z-1)!(b-z-1)!(c-a+z+2)!(c-b+z+1)!]^{-1}\}$$
$$=\frac{b+c-a+2}{a+b-c}\Sigma_z(-1)^{c+z+1}\frac{(a-1)!b!(c+1)!}{z!(a+b-c-z-2)!(a-z-1)!(b-z)!(c-a+z+2)!(c-b+z+1)!}$$
$$=[(g-a+1)/(g-c)]v(a-1bc+1\,;000).$$

From this recursion formula we have

$$v(abc\,;000)=(g-a+x)!(g-c-x)!v(a-xbc+x\,;000)/[(g-a)!(g-c)!],$$

and for $x=g-c$,

$$v(abc\,;000)=b!v(g-bbg\,;000)/[(g-a)!(g-c)!];$$

since

$$v(g-bbg\,;000)=(-1)^g g!/[b!(g-b)!],$$

we obtain at last (22).

APPENDIX B

Using repeatedly Eqs. (52), and (55′) of I, and also the relation

$$\Sigma_s \frac{(a+s)!(b-s)!}{(c+s)!(d-s)!}=\frac{(a+b+1)!(a-c)!(b-d)!}{(c+d)!(a+b-c-d+1)!}, \tag{112}$$

which follows from (51) I for x and y negative, we obtain from the definition (17):

$$\sum_{\alpha\beta\gamma\delta\varphi}(-1)^{f+\varphi}v(abe;\alpha\beta-e)v(acf;-\alpha\gamma\varphi)v(bdf;-\beta\delta-\varphi)v(cde;\gamma\delta-e)$$

$$=\sum_{\alpha\gamma}(-1)^{f+a-\gamma}v(abe;\alpha e-\alpha-e)v(acf;-\alpha\gamma\ \alpha-\gamma)v(bdf;\alpha-e\ e-\gamma\ \gamma-\alpha)v(cde;\gamma e-\gamma-e)$$

$$=\sum_{\alpha\gamma tu}\frac{(-1)^{a-c-f+t+u}2e!(a+\alpha)!(b+e-\alpha)!(c+\gamma)!(d+e-\gamma)!(f+\alpha-\gamma)!(f-\alpha+\gamma)!}{(e+a-b)!(e+b-a)!(e+c-d)!(e+d-c)!t!(a+c-f-t)!u!(b+d-f-u)!(a+\alpha-t)!(f-a-\gamma+t)!}$$
$$\cdot(d+e-\gamma-u)!(f-d+\alpha-e+u)!(c+\gamma-t)!(f-c-\alpha+t)!(b+e-\alpha-u)!(f-b+\gamma-e+u)!$$

$$=\sum_{\alpha\gamma tuvw}\frac{(-1)^{a-c-f+t+u}2e!(a+\alpha)!(b+e-\alpha)!(c+\gamma)!(d+e-y)!}{(e+a-b)!(e+b-a)!(e+c-d)!(e+d-c)!t!(a+c-f-t)!u!(b+d-f-u)!}$$
$$\cdot(f-a+c+t-v)!(c+d+e-u-v)!(a-c-d-e+\alpha-t+u+v)!(v-c-\gamma)!$$
$$\cdot(v-t-w)!(f-b-c-e+u+v-w)!(b+e-\alpha+t-u-v+w)!(c+\gamma-v+w)!$$

$$=\sum_{tuvw}\frac{(-1)^{a-c-f+t+u}2e!(a+b+e+1)!(c+d+e+1)!(c+d+e-v)!(v-w)!(u+v-t-w)!(c+d+e+t-u-v)!}{(e+a-b)!(e+b-a)!(e+c-d)!(e+d-c)!w!(a+b-c-d+w)!(c+d+e+1-w)!^2(f-b-c-e+u+v-w)!}$$
$$\cdot u!(v-t-w)!(a+c-f-t)!(f-a+c+t-v)!t!(c+d+e-u-v)!(b+d-f-u)!$$

$$=\sum_{tuvwxz}\frac{(-1)^{a-c-f+t+u}2e!(a+b+e+1)!(c+d+e+1)!(c+d+e-v)!(v-w)!(f-a-c+u+v-w)!(c+e+f-b+t-v)!}{(e+a-b)!(e+b-a)!(e+c-d)!(e+d-c)!w!(a+b-c-d+w)!(c+d+e+1-w)!^2}$$
$$\cdot(f-b-c-e+u+v-w)!(u-x)!(a+c-f-t-x)!(f-a-c+v-w+x)!x!$$
$$\cdot(f-a+c+t-v)!(t-z+x)!(b+d-f-u-z+x)!(c+e+f-b-v+z-x)!(z-x)!$$

$$=\sum_{vwxz}\frac{(-1)^{2e+f+d-b+z}2e!(a+b+e+1)!(c+d+e+1)!(c+d+e-v)!(v-w)!}{(e+c-d)!(e+d-c)!w!(a+b-c-d+w)!(c+d+e+1-w)!^2(2c-v-x)!(d-c-e+v-w+x-z)!}$$
$$\cdot x!(z-x)!(a+c-f-z)!(b+d-f-z)!(e+f-a-d+z)!(e+f-b-c+z)!$$

$$=\sum_{wx}\frac{(-1)^{2e+f+d-b+z}2e!(a+b+e+1)!(c+d+e+1)!(d+e-c+x)!(c+e-d+z-x)!}{(e+c-d)!(e+d-c)!w!(a+b-c-d+w)!(c+d+e+1-w)!(c+d-e-w-z)!(2e+z+1)!}$$
$$\cdot x!(z-x)!(a+c-f-z)!(b+d-f-z)!(e+f-a-d+z)!(e+f-b-c+z)!$$

$$=\frac{(-1)^{2e+f+d-b}}{2e+1}\Sigma_z\frac{(-1)^z(a+b+c+d+1-z)!}{(a+b-e-z)!(c+d-e-z)!z!(a+c-f-z)!(b+d-f-z)!(e+f-a-d+z)!(e+f-b-c+z)!}.$$

ERRATA OF PART I

Last line of the summary: read p^n for p''; element $(^1D|E|^3P)$ of the ^3P matrix on p. 195: read $(\frac{1}{2}G_0+2G_2)\sqrt{5}$ for $(-G_0+2G_2)\sqrt{5}$; second line of §6: read G^{l+1} for G^{l+2}.

A Statistical Theory of Liquids. I

GEORGE JAFFÉ
Louisiana State University, Baton Rouge, Louisiana
(Received August 3, 1942)

A theory is developed which deduces the elastic and thermal properties of a liquid from the expression of the mutual potential between two molecules, these being considered as centers of force. The two-phase system consisting of liquid and vapor is treated as a statistical unit and thus dynamical expressions for the vapor pressure and the surface tension are obtained. The characteristic parameter of the theory is the mean distance between nearest neighbors, σ. Its dependence on molecular density and temperature is determined by combining Boltzmann's theorem with a geometrical formula due to P. Hertz. The agreement with experimental data (after introduction of a specialized form of the potential) is satisfactory and will be further investigated in subsequent papers. The Introduction (Section I) exposes the general scope of the theory. In Section II the expression for the potential energy is established and suitably simplified by integration. In Section III the partition function for the two-phase system is formed without further neglections. In Section IV the co-existence of the two phases is shown to be possible only if surface tension is taken into account. Section V contains the determination of σ as sketched above. In Section VI the general formulae for the liquid state are established. Section VII introduces a special form for the intermolecular forces and in Section VIII comparison with experimental data, covering heat of vaporization, compressibility, expansion, and specific heat, is carried through for ten liquids widely different in character.

I. INTRODUCTION

IMPORTANT progress in the statistical treatment of the liquid state has been made in recent years. Still it can hardly be claimed that an entirely satisfactory kinetic theory of liquids exists. All attempts are based on the method of the partition sum which, in itself, gives rise to no objections. However, the efforts of Mayer, Born, and their co-workers[1] to evaluate the partition sum in a rigorous way lead into a jungle of mathematical complications. On the other hand, the so-called cell method which has been shown by Lennard-Jones, Eyring,[2] and their co-workers to lead to numerically satisfactory results is subject to serious objections. These objections have been formulated in a lucid way in J. E. Mayer and M. G. Mayer's recent book.[3]

It seems to the author that the cell method, apart from the difficulties connected with the arbitrary introduction of a term for the "communal entropy,"[3] gives the liquid too crystal-like a structure. The concept of treating a liquid as a kind of quasi-crystal has been shown by the quoted authors, as well as by previous work by Mott,[4] to yield valuable results. However, this holds principally for the neighborhood of the point of fusion and the author is of the opinion that a random treatment, as modified by the strong forces in the environment of molecules, should be reintroduced, at least for regions sufficiently far from the point of fusion.

Furthermore, no attempt has been made, so far as the author is aware, to introduce the phenomenon of surface tension into the statistical treatment. It is, however, exactly this phenomenon which characterizes a liquid in the most significant way. From the physical point of view a liquid phase can be distinguished from an adjacent vapor phase only as long as a meniscus exists. On the other hand, the influence of the surface tension in determining the shape of liquids distinguishes them in a most marked way from solids. It will be shown in what follows that, even theoretically, a vapor and a liquid can coexist in equilibrium only if surface tension, i.e., a layer of transition between the two phases, is taken into consideration.

The present theory does not attempt the rigor of treatment aimed at by the first group of

[1] J. E. Mayer, J. Chem. Phys. **5**, 68 (1937); J. E. Mayer and P. G. Ackermann, J. Chem. Phys. **5**, 74 (1937), and subsequent papers; M. Born and K. Fuchs, Proc. Roy. Soc. London, **A166**, 391 (1938).

[2] H. Eyring, J. Chem. Phys. **4**, 283 (1936); R. Newton and H. Eyring, Trans. Faraday Soc. **33**, 73 (1936); H. Eyring and J. Hirschfelder, J. Phys. Chem. **41**, 249 (1937), and subsequent papers; J. E. Lennard-Jones and A. F. Devonshire, Proc. Roy. Soc. London, **A163**, 53 (1937); **A165**, 1 (1938), and subsequent papers.

[3] J. E. Mayer and M. G. Mayer, *Statistical Mechanics* (John Wiley and Sons, New York, 1940), cf. Section 141.

[4] N. F. Mott, Proc. Roy. Soc. London **A146**, 465 (1934).

investigations mentioned above. On the other hand, it avoids the arbitrariness of the cell method. The necessary simplifications are introduced into the expression of the potential energy itself. Then the statistical part of the treatment can be carried through without neglect of any term. The potential to which any one molecule is subject owing to the presence of other molecules is decidedly influenced by its immediate environment and by its distance from the surface. The latter influence can be calculated in the classical way. The former influence can be averaged suitably by replacing the sum (in the expression for the potential energy) by an integral which is to be extended from a certain distance σ, to the boundaries of the system. This procedure constitutes in a certain way a return to very much older methods. However, the distance σ is not treated as a constant here but as depending on the density and the temperature of the medium. These dependencies are derived by a second application of statistical principles to the immediate neighborhood of each molecule, somewhat in the line of the well-known treatment of electrolytes by Debye and Hückel. Thus the distance σ becomes the characteristic parameter of the present theory and constitutes, together with the consideration of surface tension, its essential features.

Furthermore, the system consisting of liquid and vapor is treated as a statistical unit. Expressions for the vapor pressure and the surface tension result automatically from this treatment. Upon introduction of a specialized form of the potential between two molecules the expressions for the various physical coefficients can be evaluated. Though this evaluation is carried through by somewhat rough approximations it will be seen that an adequate agreement with empirical data can be obtained for liquids of very different character. It should be emphasized, however, that it is not the aim of the present investigation to obtain a good numerical agreement (which might be done by a more elaborate choice of the potential and by better methods of evaluation). It is rather the object of the paper to derive, in a classical way, the essential features of a liquid from the knowledge of the mutual potential energy of the molecules.

II. THE POTENTIAL

We are going to assume that the molecules are extensionless points, of mass m, and that the total potential energy is the sum of the binary contributions. These two assumptions are necessarily correlated and are known not to be true. However, it seems reasonable to investigate how far one can proceed with this simplest model in which the complicated interactions of deformable molecules are approximated by the idealization of classical central forces.

As to $\varphi(r)$, the mutual potential energy of two molecules separated by the distance r, only its typical form need be known for the general part of the theory. To be explicit we assume: that $\varphi(r)$ becomes $+\infty$ at $r=0$ of a higher order than r^{-3}; that, with increasing r, it has a steep descent and positive curvature until it reaches the value zero at $r=r_1$ and a negative minimum at $r=r_2$; and that, as r increases further, it remains negative with positive slope, approaching the value zero asymptotically. In order to safeguard integrability in the following calculations it must be assumed that, for $r\to\infty$, $\varphi(r)$ becomes zero of higher order than r^{-3}.

If we have a system of N identical molecules occupying a volume V, whether in the liquid phase or in the vapor phase or distributed between the two phases, the total potential energy is assumed to be of the form

$$U=\tfrac{1}{2}\sum_{i=1}^{N}{\sum_{j=1}^{N}}'\,\varphi(r_{ij}), \tag{2.01}$$

where the apostrophe indicates that the terms with $i=j$ have to be excluded. This expression for U can be written in the form

$$U=\sum_{i=1}^{N}u_i,\quad u_i=\tfrac{1}{2}{\sum_{j=1}^{N}}'\,\varphi_{ij}. \tag{2.02}$$

As mentioned in the Introduction, our averaging process will consist in transforming the sum in the expression for u_i into an integral. In order to include "long range forces" this integral is to be extended over the whole volume V with the exception of a little cavity v surrounding the molecule i. Thus we obtain, dropping the index i and using n for the local molecular density,

$$u=\int_{V-v}\tfrac{1}{2}n\varphi(r)\,d\tau. \tag{2.03}$$

Since the integration represents an averaging over all directions as well as over all possible configurations of the environment, the cavity may be assumed to be spherical in an isotropic liquid. The radius of this sphere, σ, is to be defined as the average value of the distance between two nearest neighbors. It will be determined later (Section V). In general σ will depend on the location of the molecule. If there are no external forces such as gravity—and this we are going to assume—σ will be constant in the interior of any phase sufficiently far from its boundary. There, in the interior, it will be a function of the mean molecular density and of the temperature.

We are going to determine now the potential of a molecule which is to be found in the liquid phase at a depth h under a surface. We are going to assume that the radii of curvature of all surfaces are large compared with the radius of molecular action. Then the surface may be treated as plane and the necessary integrations become quite straightforward. The curvature of the surface might be considered in the way which is classical since Laplace. This would lead, ultimately, to the known dependence of the vapor pressure on the curvature but we shall avoid this complication at present.

In the calculation of (2.03) the two cases $h \geq \sigma_1$ and $h \leq \sigma_1$ have to be distinguished. Here σ_1 signifies the value which holds for σ in the interior of the liquid. If we count the angle ϑ from an axis pointing normally to the surface we obtain, for $h \geq \sigma_1$,

$$u = \pi(J_1 - J_2), \quad h \geq \sigma_1, \tag{2.04}$$

with

$$J_1 = \int_0^{\pi} \sin\vartheta d\vartheta \int_{\sigma}^{\infty} n\varphi(r) r^2 dr \tag{2.05}$$

and

$$J_2 = \int_0^{\pi/2} \sin\vartheta d\vartheta \int_{h/\cos\vartheta}^{\infty} n\varphi(r) r^2 dr. \tag{2.06}$$

Correspondingly we have, for $h \leq \sigma_1$,

$$u = \pi(J_3 + J_4), \quad h \leq \sigma_1, \tag{2.07}$$

with

$$J_3 = \int_{\pi/2}^{\pi} \sin\vartheta d\vartheta \int_{\sigma}^{\infty} n\varphi(r) r^2 dr \tag{2.08}$$

and

$$J_4 = \int_{\cos^{-1}(h/\sigma_1)}^{\pi/2} \sin\vartheta d\vartheta \int_{\sigma}^{h/\cos\vartheta} n\varphi(r) r^2 dr. \tag{2.09}$$

In these formulae n signifies the local molecular density which must be distinguished from its average value n_1 as pointed out by Fowler.[5] It depends on the value of h and r, and as a result, σ is also a function of h. When the integrations in (2.04) to (2.09) are performed u remains a function of h and σ_1, i.e., of h, n_1, and the temperature T.

In order to evaluate the integrals, n must be determined as a function of h and r. The dependence on h can be obtained by the solution of an integral equation.[5] The dependence on r will be considered in the determination of σ_1 (Section V). If, *in first approximation*, n is given its average value n_1 we obtain

$$u = \pi n_1\{2\psi(\sigma_1) - \psi(h) + h\chi(h)\}, \quad h \geq \sigma_1, \tag{2.10}$$

and

$$u = \pi n_1\{\psi(\sigma_1) + h\chi(\sigma_1)\}, \quad h \leq \sigma_1. \tag{2.11}$$

The functions newly introduced are defined by

$$\psi(\sigma_1) = \int_{\sigma_1}^{\infty} \varphi(r) r^2 dr \tag{2.12}$$

and

$$\chi(\sigma_1) = \int_{\sigma_1}^{\infty} \varphi(r) r dr. \tag{2.13}$$

They depend, as does σ_1, on n_1 and T.

An important remark regarding the limits of validity of our formulae should be added. In setting up Eqs. (2.04) and (2.07) we have assumed that, at the boundary between liquid and vapor, contributions of the vapor phase to the potential u can be neglected. Thus we have limited ourselves to such conditions under which the mean molecular density in the vapor phase n_2 is small compared with the corresponding density in the liquid phase n_1. As we intend to study in this paper principally the behavior of liquids, the assumption of $n_2 \ll n_1$ is legitimate though it restricts the validity to temperature regions which are sufficiently far from the critical point. If the critical region where n_1 and n_2 become comparable were to be examined the expressions (2.04) and (2.07) would have to be supplemented by the contributions of the adjacent vapor phase.

According to our assumptions regarding $\varphi(r)$ the two functions $\psi(h)$ and $h\chi(h)$ will decrease

[5] R. H. Fowler, Phil. Mag. **43**, 785 (1922).

to zero as h increases. Therefore, at distances from the surface which are large compared with the radius of molecular action, (2.10) will reduce to the constant value

$$u_1 = 2\pi n_1 \psi(\sigma_1). \tag{2.14}$$

In the vapor phase we will have correspondingly

$$u_2 = 2\pi n_2 \psi(\sigma_2), \tag{2.15}$$

holding up to the boundary under our present assumptions. For low vapor densities u_2 approaches the value zero.

The two Eqs. (2.14) and (2.15) are contained in (2.07) which, therefore, together with (2.04), holds for the entire system even if it consists of two phases.

III. THE PARTITION FUNCTION

Since we consider the molecules as devoid of internal degrees of freedom the kinetic factor of the partition function takes the well-known form and the normalized phase integral can be written as[6]

$$Q = (2mkT/h^2)^{3N/2} Q_\tau / N!. \tag{3.01}$$

Here the "configuration integral Q_τ" is defined by

$$Q_\tau = \int\int \cdots \int \exp(-U/kT) d\tau_1 \cdots d\tau_i \cdots d\tau_N \tag{3.02}$$

with

$$d\tau_i = dx_i dy_i dz_i. \tag{3.03}$$

As the potential energy, in virtue of (2.04), (2.07), separates into N terms, each depending on the location of of one molecule only, Q_τ becomes the product of N identical factors:

$$Q_\tau = q_\tau^N, \tag{3.04}$$

where q_τ is defined as

$$q_\tau = \int_V \exp(-u/kT) d\tau. \tag{3.05}$$

The value of u has to be taken, in general, from (2.04), (2.07).

The molecules being assumed as dimensionless the integration has to be extended over the entire disposable volume. This leads to no singularities and represents a great simplification. The "impenetrability" of the molecules is sufficiently taken care of by the strong repulsive forces at close approaches.

As stated in the Introduction the two-phase system is going to be treated as a statistical unit, the two phases being distinguished sufficiently by the difference of potential.[7] Consequently, we are going to assume that of the N molecules contained in the total volume V, N_1 are to be found in the liquid phase of volume V_1 and N_2 in the vapor phase of volume V_2. It will have to be *proved* that such a state of affairs is compatible with the conditions of equilibrium. However, in order to obtain expressions of sufficient generality, the possibility of a two-phase arrangement has to be included.

With our form of the potential the integral (3.05) can be simplified considerably. First of all, in the vapor phase the constant value (2.15) may be inserted and the integration performed. In the liquid phase, in order to separate the influence of the surface layer, we subtract and add $\exp(-u_1/kT)$ to the integrand. In the integral with $\exp(-u_1/kT)$ as integrand the integration is immediate. In the integral where the integrand is $[\exp(-u/kT) - \exp(-u_1/kT)]$ the volume element $d\tau$ may be replaced by $dSdh$, where dS is an element of surface of the liquid phase. Then the integration over dS can be performed (u depending on h only) and the integration over h may be extended from $h=0$ to $h=\infty$.

Thus we obtain finally

$$q_\tau = \Pi = \Pi_1 V_1 + \omega S + \Pi_2 V_2 \tag{3.06}$$

with

$$\Pi_1 = \exp(-u_1/kT), \tag{3.07}$$

$$\Pi_2 = \exp(-u_2/kT), \tag{3.08}$$

and

$$\omega = \int_0^\infty [\exp(-u/kT) - \exp(-u_1/kT)] dh. \tag{3.09}$$

Before we prove the possibility of the coexistence of two phases it will be useful to deduce the equations of state of the two phases, and the

[6] We choose our notation, as far as feasible, in accordance with J. E. and M. G. Mayer, reference 3; for the above formulation compare p. 222 and 263.

[7] Under our present assumptions the potential is discontinuous at $h=0$, jumping there from $(u_1)_0 = \pi I_3$ to a very low value $(u_2)_0$. If the vapor density is taken into account (see above, p. 465) the potential becomes continuous.

expressions for the vapor pressure and the surface tension.

With (3.01), (3.04), and (3.06) the "work function" of the entire system, $A=-kT\ln Q$, becomes:

$$A=-kTN\{(3/2)\ln\Theta+\ln\Pi-\ln N+1\}, \quad (3.10)$$

where Θ depends on T only and is defined as

$$\Theta=2\pi mkT/h^2. \quad (3.11)$$

From (3.10) we obtain the equations of state

$$p_1=-\frac{\partial A}{\partial V_1}=\frac{kTN}{\Pi}\left\{\Pi_1+V_1\frac{\partial\Pi_1}{\partial V_1}+S\frac{\partial\omega}{\partial V_1}\right\}, \quad (3.12)$$

$$p_2=-\frac{\partial A}{\partial V_2}=\frac{kTN}{\Pi}\left\{\Pi_2+V_2\frac{\partial\Pi_2}{\partial V_2}\right\}, \quad (3.13)$$

and the surface tension γ becomes

$$\gamma=\partial A/\partial S=-kTN\omega/\Pi. \quad (3.14)$$

These expressions can still be transformed by introducing the molecular densities n_1 and n_2 for the two phases. According to the fundamental principles of statistical mechanics, the probability of finding the system in an element of phase space $d\tau=d\tau_1\cdots d\tau_i\cdots d\tau_N$ is given by[8]

$$Pd\tau=[\exp(-U/kT)/Q_\tau]d\tau. \quad (3.15)$$

Choosing for any one molecule the disposable volume first as V_1, then as V_2, and finally as V, and integrating for all other molecules over the whole volume we obtain the relation

$$P_1:P_2:1=(\Pi_1V_1+\omega S):\Pi_2V_2:\Pi. \quad (3.16)$$

Since $P_1=N_1/N$ and $P_2=N_2/N$ (3.16) can be written in the form

$$N_1:N_2:N=(\Pi_1V_1+\omega S):\Pi_2V_2:\Pi. \quad (3.17)$$

As a first important application of this we deduce

$$n_2=n_1\Pi_2/(\Pi_1+(S/V_1)\omega), \quad (3.18)$$

which relation contains the dependence of the vapor pressure on temperature and density of the liquid. If the unimportant surface term is neglected (3.18) changes to a form which might have been derived immediately from Boltzmann's theorem.

Furthermore, (3.12) to (3.14) can now be written in expressions which contain terms referring to one phase only, namely:

$$p_1=kTn_1\left\{1+\frac{V_1}{\Pi_1}\left(\frac{\partial\Pi_1}{\partial V_1}+\frac{S}{V_1}\frac{\partial\omega}{\partial V_1}\right)\right\}\Big/\left(1+\frac{\omega S}{\Pi_1V_1}\right), \quad (3.19)$$

$$p_2=kTn_2\left\{1+\frac{V_2}{\Pi_2}\frac{\partial\Pi_2}{\partial V_2}\right\}, \quad (3.20)$$

and

$$\gamma=-kTn_1\frac{\omega}{\Pi_1}\Big/\left(1+\frac{\omega S}{\Pi_1V_1}\right). \quad (3.21)$$

The last of these equations must be regarded as the kinetic generalization of the well-known law of Eötvös (Section X). On the other hand, (3.20) reduces in the limiting case $\sigma_2\to\infty$ to the gas law

$$p_2=kTN_2/V_2. \quad (3.22)$$

IV. CONDITIONS OF EQUILIBRIUM

It remains to be proved that the two-phase system which, so far, we have presupposed to exist, represents a possible form of statistical equilibrium. We proceed in the usual way by making the work function A (3.10) a minimum at constant temperature. The variables are N_1, N_2, V_1, V_2, and S, subject to the restrictions

$$N_1+N_2=N, \quad (4.01)$$

and

$$V_1+V_2=V. \quad (4.02)$$

We first eliminate the variation of S. Since, evidently, the shape of the liquid phase can be changed without changing anything else we must have

$$(\delta S)_{N_1,\,N_2,\,V_1,\,V_2}=0. \quad (4.03)$$

Consequently the shape of the liquid phase must be spherical in the absence of external forces. Therefore, in the further treatment, we retain the spherical shape, and make S dependent on V_1 by

$$\delta S=(2S/3V_1)\delta V_1. \quad (4.04)$$

[8] J. E. and M. G. Mayer, reference 3, p. 231.

Proceeding now by the Lagrangian method we find

$$\frac{NkT}{\Pi}\left\{\Pi_1+V_1\frac{\partial\Pi_1}{\partial V_1}+S\frac{\partial\omega}{\partial V_1}+\frac{2}{3}\frac{S\omega}{V_1}\right\}$$
$$=\frac{NkT}{\Pi}\left\{\Pi_2+V_2\frac{\partial\Pi_2}{\partial V_2}\right\}, \quad (4.05)$$

and

$$-\left(\frac{A}{N}+kT\right)+\frac{NkT}{\Pi}\left\{V_1\frac{\partial\Pi_1}{\partial N_1}+S\frac{\partial\omega}{\partial N_1}\right\}$$
$$=-\left(\frac{A}{N}+kT\right)+\frac{NkT}{\Pi}V_2\frac{\partial\Pi_2}{\partial N_2}. \quad (4.06)$$

These equations represent the conditions of equilibrium which, together with (4.01) and (4.02) determine the four unknowns N_1, N_2, V_1, V_2. The two Eqs. (4.05) and (4.06) suffice to determine the "inner variables" $n_1=N_1/V_1$ and $n_2=N_2/V_2$; (4.05), the first equation, expresses the equality of pressure and the second the equality of the chemical potential. When n_1 and n_2 are determined the external variables follow from (4.01) and (4.02).

To proceed further, we must remember that, at constant temperature, Π_1 and ω depend on V_1 and N_1 exclusively in being functions of n_1. This dependence is as well explicit as implicit via σ. Therefore, in what follows, we shall understand by Π_1', ω' the differential coefficients of these functions with regard to n_1, and correspondingly by Π_2' the differential coefficient of Π_2 with regard to n_2.

Making use of the dependencies just stated we reduce Eq. (4.06) to

$$\Omega_1=\Pi_1'+(S/V_1)\omega'=\Pi_2'. \quad (4.07)$$

Under our assumptions the surface term in (4.07) represents a very small correction. Neglecting higher powers in ω and making use of the relations (3.17) we can bring the conditional Eq. (4.05) into the form

$$(N/\Pi)(\Pi_1-\Pi_2)\{1-n_1(\Omega_1/\Pi_1)\}$$
$$=(N/\Pi)\{n_1(\Omega_1/\Pi_1)(\Pi_2/\Pi_1)$$
$$\times(S\omega/V_1)-2S\omega/3V_1\}. \quad (4.08)$$

As our equations are not sufficiently general for including all values of n_1 and n_2 we shall restrict ourselves to showing that the conditions admit of a solution for which $n_2\ll n_1$. Before doing so we shall investigate whether a solution can be obtained if the terms with ω which involve surface tension are neglected.

Under this assumption (4.07) becomes

$$\Pi_1'=\Pi_2', \quad (4.09)$$

and (4.05) can be brought into one of the two alternate forms

$$n_1(1-(\Pi_2/\Pi_1))(1-n_1\Pi_1'/\Pi_1)=0, \quad (4.10)$$

or

$$n_2((\Pi_1/\Pi_2)-1)(1-n_2\Pi_2'/\Pi_2)=0. \quad (4.11)$$

It is easy to see that these equations admit of no solutions which correspond to a two-phase system with $n_1\gg n_2$. The solution $\Pi_1=\Pi_2$ leads to a one-phase system since it makes the densities equal [by (3.18) with $\omega=0$]. The last factor in (4.11) cannot vanish because in the vapor phase $\Pi_2\sim 1$ and $\Pi_2'\sim 0$. Thus there remains only the possibility that the last factor in (4.10) vanishes. Then [by (3.19) with $\omega=0$] the pressure would have to be zero, with the necessary consequence $n_2=0$.

We see, then, that the statistical treatment does not lead to a solution representing two phases with widely different densities if the surface tension is neglected. However, we shall show that the solution $n_2=0$, $1-n_1\Pi_1'/\Pi_1=0$ represents the limiting case of a solution which gives physical sense. We are going to construct this solution by successive approximations by use of the equations which involve surface tension.

First of all, it is easy to show that with our assumptions regarding the nature of the potential $\varphi(r)$, and with the correlation between σ and n which we are going to establish in the next section, the equation

$$1-n_1\Pi_1'/\Pi_1=1+n_1u_1'/kT=0 \quad (4.12)$$

has, at sufficiently low temperatures, a solution $n_1=n_{10}$.[9] This solution corresponds to a value $\sigma=\sigma_{10}$ where σ_{10} is smaller than r_1, the value of r making $\varphi(r)$ equal to zero. Therefore, n_{10} represents a solution of high density compared with vapor densities characterized by $\sigma\gg r_1$. We take as our zero approximations, $(\Pi_1)_0$ and $(\Pi_2)_0$, the

[9] See Appendix I.

value assumed by Π_1 for $n_1=n_{10}$ and the value $\Pi_2=1$ assumed by Π_2 for $n_2=n_{20}=0$.

The objection to the solution $(\Pi_1)_0$, $(\Pi_2)_0$, in the absence of surface tension, was that it made the pressure vanish. Under our present assumption of a spherical surface S, the pressure in the two phases is given by the two sides of (4.05). It is seen that the zero solutions lead to a pressure different from zero if the terms involving ω are not omitted. Furthermore, if the approximations (2.10), (2.11) are used in the calculation of ω, it is easy to show [from (3.09) and (4.12)] that the pressure becomes positive as it should. Hence the next approximation, $(\Pi_2)_1$, can be calculated from (4.05) by inserting on the left side the zero approximation for $(\Pi_1)_0$.

Solving now (4.08) with regard to $\Pi_1-\Pi_2$, and inserting the zero solutions into the small terms, we obtain

$$(\Pi_1-\Pi_2)_1=\left\{\frac{\Pi_1}{n_1}\frac{\omega}{\omega'}\left(\frac{2}{3}-\frac{\Pi_2}{\Pi_1}\right)\right\}_0. \quad (4.13)$$

From this equation $(\Pi_1)_1$ can be determined.

Continuing in the same way, i.e., by an alternate application of (4.05) and (4.08), the final solutions can be constructed. It is evident that, in a similar way, the solution $\Pi_1=\Pi_2$ which we had to discard as leading to one phase only can be taken as the zero approximation for the neighborhood of the critical point. However, as stated before, the surface term has to be supplemented first.

The preceding argument shows that the consideration of the surface tension is essential, even mathematically, for the existence of a two-phase system. This appears satisfactory from the point of view adopted in the Introduction. However, when the curvature of the surface can be neglected, the *numerical* influence of the surface term is so insignificant that one is led to anticipate the possibility of a procedure which does not make *explicit* use of the surface tension. Such a procedure can be established in the following way: first $(\Pi_1)_0$ and $(\Pi_2)_0$ are taken as zero approximations as above. Then n_{21} is determined from (3.18) with $\omega=0$, and the pressure is determined in the first approximation from the gas law (3.22). Now n_{11} becomes calculable from (3.19), when we set $\omega=0$, and so on.

As we have discussed exclusively a solution for which $n_1 \gg n_2$ we have implicitly assumed that the temperature is sufficiently low and that the external variables N and V are given in such a way that a liquid phase of sufficient bulk (to make the curvature of the surface insignificant) can exist. The discussion of the distribution of the N molecules between the two phases can be carried through by the usual thermodynamical method.[10] However, a general remark must be made in this connection.

Our fundamental expression for the work function (3.10) is *not* additive in the two phases. On the other hand, if the entropy and the internal energy are calculated from A in the usual way, and if the relations (3.17) are used, entropy as well as internal energy becomes additive, i.e., split each into two terms which are proportional to N_1 and N_2, respectively, and which involve variables pertaining to one phase only. This is all that is required for the thermodynamical treatment.[10]

If now with the values of entropy and energy so obtained, the work functions A_1 and A_2 for the individual phases for the same value of the temperature are formed, their sum A_1+A_2 is different from A. This is evidently due to the fact that in the thermodynamical treatment the work function is defined only for states in which the two phases are in equilibrium with each other whereas our A includes the definition of the "work function" for more general states.

V. THE DETERMINATION OF σ

The parameter σ has been introduced so far as depending on the molecular density and the temperature of the considered phase. The exact form of this dependence has still to be established.

We have defined σ as the average value of the distance between two nearest neighbors. The geometrical probability of finding the nearest neighbor to a given point at a distance between r and $r+dr$, if the average density is given by n,[11] has been determined by P. Hertz.[12] His derivation holds for random distributions, i.e., under

[10] See, e.g., M. Planck, *Treatise on Thermodynamics* (Longmans, Green and Company, London, 1927), translated by A. Ogg, third edition, Part IV, Chapter 2.

[11] In this section we understand by $n=N/V$ the average molecular density in the phase considered, not its local value.

[12] P. Hertz, Math. Ann. **67**, 387 (1909).

the assumption that the probable number of mass points in any part v of the total volume V is given simply by nv.

A generalization of Hertz's formula is required if the probable number of mass points in a small fractional volume v at the distance r from a given point still depends on r, i.e., is of the form $p_1(r)nv$. This generalization has been given by the author[13] and the result can be stated in the following form: let $p_2(r)$ define the probability that the nearest neighbor to a given point is to be found at distances between r and $r+dr$, then we will have

$$p_2(r)dr=4\pi r^2 np_1(r)\exp(-nP(r))dr, \quad (5.01)$$

where

$$P(r)=\int_0^r 4\pi\rho^2 p_1(\rho)d\rho.^{14} \quad (5.02)$$

Formula (5.01) becomes applicable in our case if we assume $p_1(r)$ to be given by Boltzmann's theorem, i.e., by

$$p_1(r)=\exp(-\varphi(r)/kT). \quad (5.03)$$

Here the constant has been determined in such a way that p_1 becomes unity for large values of r.

From the discussions which followed Debye and Hückel's theory of ionic atmospheres it is known that (5.03) represents only an approximation, as $\varphi(r)$, the potential which holds for a pair of "free molecules," should be replaced by an average value caused by the presence of other molecules.[15] In his discussion Fowler suggests that in cases of high concentrations, like ours, the distribution "may be more uniform than is indicated by Boltzmann's law . . . ." However, it seems reasonable, as a first start, to use the simple form (5.03).

Then the average value for the distance between nearest neighbors is given by

$$\bar{r}=\int_0^\infty r p_2(r)dr, \quad (5.04)$$

and this expression should be used for σ, giving its dependence on n and T.

Though (5.04) can always be evaluated by graphical methods it is difficult to give explicit formulae for any reasonable form of $\varphi(r)$. For this reason a further simplification will be introduced. Hertz[12] has shown that, in the absence of potential forces, the "mean value of r" and the "most probable value of r" almost coincide. Therefore we shall replace, in all practical applications, $\bar{r}$ by the most probable value, i.e., the value which makes $p_2(r)$ a maximum.

Hence, we consider the parameter σ of our theory as given by the relation

$$2-\varphi'(\sigma)/kT-4\pi n\sigma^3\exp(-\varphi(\sigma)/kT)=0. \quad (5.05)$$

In the limiting case $\varphi(\sigma)/kT\to 0$, (5.05) reduces, of course, to Hertz's geometrical value $\sigma=(1/2\pi n)^{\frac{1}{3}}$. In the other extreme, $\varphi(\sigma)/kT\to\infty$, σ will coincide with r_1, i.e., the value which corresponds to the minimum of $\varphi(r)$.

From (5.05) we can derive the dependence of σ on T and V by the rules of implicit differentiation. Making repeated use of (5.05) itself, we find

$$\partial\sigma/\partial V=(\sigma/V)(2-\sigma\varphi'/kT)/D, \quad (5.06)$$

and

$$\partial\sigma/\partial T=(\sigma/T)(\sigma\varphi'/kT-2\varphi/kT+\varphi\sigma\varphi'/(kT)^2)/D, \quad (5.07)$$

with

$$D=6-4\sigma\varphi'/kT+\sigma^2\varphi''/kT+(\sigma\varphi'/kT)^2. \quad (5.08)$$

It should be mentioned that the formulae (5.01) and (5.02), with n constant, hold only in the interior of the phase considered. Near its boundary the dependence of n on h must be taken into account. Then σ becomes a function of h, besides its dependence on T and the average molecular density.

VI. THE LIQUID STATE

We are now going to establish formulae for the characteristic coefficients of the liquid state, disregarding the influence of surface tension. This influence is negligible if the volume V_1 occupied by the liquid is sufficiently large. Thus, in this and the following two sections, we shall set $\omega=0$ and let N_1, V_1 coincide with N, V.

Under these assumptions our general expression for the partition function (3.01) becomes

$$Q_1=(\Theta^{\frac{1}{3}}\Pi_1 V_1)^{N_1}/N_1!, \quad (6.01)$$

where Θ and Π_1 are defined by (3.11) and (3.07).

[13] G. Jaffé, Phys. Rev. **58**, 968 (1940).
[14] See Appendix II.
[15] R. H. Fowler, *Statistical Mechanics* (Cambridge, University Press, 1936). Cf. Sections 8.4 and 8.81.

It will be noticed that (6.01) is formally very similar to the corresponding expression which is obtained by the cell method. The fundamental assumption of this method is that the partition function of a dense gas or a liquid can be expressed as a product of the partition functions of the individual members of the assembly. This state of affairs is a necessary consequence of the simplified form in which we have written the potential energy. However, our integrations were extended over the whole disposable volume, i.e., the molecules are free to move about (and even to vaporize), carrying, so to speak, their cells with them. Therefore, there is no ambiguity as to the addition of a "communal entropy": in the limiting case of low density, $\Pi_1 \to 1$, our formula reduces to the correct formula for a classically treated gas.

From (6.01) we obtain for the work function (with the usual approximation for $N_1!$)

$$-A = N_1 kT\{\ln(\Theta^{\frac{3}{2}} V_1/N_1)+1\} - U_1, \quad (6.02)$$

if the potential energy characterizing the liquid is written in the form

$$U_1 = N_1 u_1 = 2\pi(N_1^2/V_1)\psi(\sigma_1) = 2\pi(N_1^2/V_1)\int_{\sigma_1}^{\infty} \varphi(r) r^2 dr. \quad (6.03)$$

Now the equation of state becomes

$$p = N_1 kT/V_1 - \partial U_1/\partial V_1. \quad (6.04)$$

Here, and in what follows, it has to be taken into account in performing the differentiations, that σ_1 is a known function (5.05) of n_1 and T. Equation (6.04) shows clearly that the external pressure p is the sum of the "kinetic pressure $N_1 kT/V_1$" and the "static pressure $-\partial U_1/\partial V_1$." For the calculation of the latter U_1 acts as a potential. As $\partial U_1/\partial V_1$ can easily be proved to be positive for a liquid, p may be, and usually is, the small difference of two large terms.

If we call the compressibility b, or its reciprocal, the bulk coefficient B, we obtain

$$-\frac{1}{V_1}\frac{\partial p}{\partial V_1} = B = \frac{1}{b} = \frac{N_1 kT}{V_1} + V_1 \frac{\partial^2 U_1}{\partial V_1^2}. \quad (6.05)$$

The coefficient of expansion, a, becomes

$$a = \frac{1}{V_1}\frac{\partial V_1}{\partial T} = \left(N_1 k - V_1 \frac{\partial^2 U_1}{\partial V_1 \partial T}\right) \Big/ \left(N_1 kT + V_1^2 \frac{\partial^2 U_1}{\partial V_1^2}\right). \quad (6.06)$$

Furthermore, by known methods, we obtain for the entropy η,

$$\eta_{\text{liq}} = \eta_{\text{vap}} - (\partial U_1/\partial T), \quad (6.07)$$

and for the internal energy E,

$$E_{\text{liq}} = E_{\text{vap}} - T(\partial U_1/\partial T). \quad (6.08)$$

In these formulae we have split off the energy and the entropy of the monatomic vapor. This was done because the relations obtained will hold also for any molecules if the internal motions of the molecules in the liquid state remain the same as in the vapor.

Now the specific heat at constant volume becomes

$$(c_v)_l = (c_v)_v - T(\partial^2 U_1/\partial T^2). \quad (6.09)$$

Finally, if L is called the heat of vaporization per gram, we must take into account that it includes the external work. Consequently we have

$$L = -U_1 + kN_1 T, \quad (6.10)$$

if N_1 is the number of molecules per gram.

Of course, the expressions (6.04) to (6.10) can be written in a form setting into evidence the explicit dependence on $\varphi(r)$. However, the formulae become cumbersome if this is done and they become quite prohibitive if (5.06) to (5.08) are inserted.

VII. SPECIAL FORM OF THE MOLECULAR FORCES

In order to arrive at expressions which can be compared with experimental evidence we have, first, to choose a special form for $\varphi(r)$ and, then, to introduce suitable approximations.

For $\varphi(r)$ we are going to take, on account of its adaptability, the form advocated by Lennard-Jones, namely,

$$\varphi(r) = fr^{-\lambda} - gr^{-\mu}. \quad (7.01)$$

Here f and g are positive constants and the exponents λ and μ will not be restricted to integers.

They are, however, subject to the conditions

$$\lambda > \mu > 3. \tag{7.02}$$

With these assumptions $\psi(\sigma_1)$ becomes

$$\psi(\sigma_1) - f\sigma_1^{-(\lambda-3)}/(\lambda-3) = g\sigma_1^{-(\mu-3)}/(\mu-3), \tag{7.03}$$

where σ_1 is determined as the root of (5.05).

In continuing, we shall not attempt to retain the full scope of our formulae. For a first survey it seems more reasonable to establish expressions which can easily be handled, though at the cost of using somewhat rough approximations. It is easy to derive expressions which are asymptotically correct either in the case that $\varphi/kT \ll 1$ or that $\varphi/kT \gg 1$ for the significant values of r. However, the numerical calculations show that, in all studied cases, φ/kT is of the order of unity for the equilibrium distance (see Table II). Therefore, other forms of approximation have to be tried.

In simplifying our expressions, we have to distinguish between isothermal and non-isothermal changes as they require a different degree of accuracy. In all cases we shall choose some definite temperature T where the substance exists distinctly as a liquid under comparatively low pressure ($p \sim 1$ atmos.), and we shall investigate the neighborhood of this temperature-pressure region only. Larger changes of T and p (approach to the critical region) will have to be studied separately.

A. Isothermal Changes

In treating these we start from the fact that, upon our assumptions, the density of the liquid will change very little. If, then, σ_0 is the value corresponding to T, a first approximation to (5.05) will be obtained by substituting the constant value σ_0 into $\varphi(\sigma)$ and $\varphi'(\sigma)$. By this procedure we obtain

$$\sigma_1^3 = \delta/2\pi n_1, \tag{7.04}$$

where

$$\delta = (1 - \sigma_0\varphi_0'/2kT)\exp(\varphi_0/kT) \tag{7.05}$$

is treated as constant for T constant.

In the limit $\varphi/kT \to 0$, (7.04) reduces to Hertz's geometrical formula. Since, in the liquid state, φ_0 will be positive and φ_0' negative (Appendix I), δ is a number larger than 1 and indicates that the average distance of approach σ_1 is increased by the repulsive forces at distances characteristic of the liquid state. As, however, T increases, δ approaches 1 and, for gases, σ_1 coincides with the geometrical value, the intermolecular forces being ineffective.

From (7.04) we derive

$$\partial\sigma_1/\partial V_1 = \tfrac{1}{3}(\sigma_1/V_1), \tag{7.06}$$

which simplified relation is to be used in the derivation of the pressure (6.04) and the compressibility (6.05).

Using (7.01), (7.03), and (7.06), we obtain the explicit expressions for the pressure

$$p = n_1\{kT + (\delta/3)[f\sigma_1^{-\lambda}\lambda/(\lambda-3) - g\sigma_1^{-\mu}\mu/(\mu-3)]\}, \tag{7.07}$$

for the bulk coefficient

$$B = p + (n_1\delta/9)[f\sigma_1^{-\lambda}\lambda^2/(\lambda-3) - g\sigma_1^{-\mu}\mu^2/(\mu-3)], \tag{7.08}$$

and for the heat of vaporization

$$U_1 = -L + N_1kT = (n_1\delta/\rho) \times [f\sigma_1^{-\lambda}/(\lambda-3) - g\sigma_1^{-\mu}/(\mu-3)]. \tag{7.09}$$

In the last formula ρ indicates the density, and N_1 refers to a gram.

From what has been said, these equations hold for the neighborhood of the chosen standard values of T and p. For these values themselves σ_1 reduces to σ_0, as used in (7.05).

B. Non-Isothermal Changes

If the dependence of σ_1 on T is disregarded altogether, Eq. (6.06) reduces to the simple relation

$$a = n_1kb = n_1k/B, \tag{7.10}$$

and (6.09) yields

$$(c_v)_l = (c_v)_v. \tag{7.11}$$

For a better approximation we have to revert to (5.07) and (5.08). As mentioned before, the numerical calculations show that, in all cases studied, φ_0/kT is of the order of 1. Then $\sigma_0\varphi_0'/kT$ becomes of the order of λ and $\sigma_0^2\varphi_0''/kT$ of the order of λ^2 but somewhat smaller than the term involving $(\varphi_0')^2$. We have retained only the principal term. This leads to

$$\partial\sigma_1/\partial T = (\sigma_1/T)(\varphi_1/\sigma_1\varphi_1'). \tag{7.12}$$

For the neighborhood of σ_0 the ratio $\varphi_1/\sigma_1\varphi_1'$

TABLE I. Comparison of theoretical and empirical data.

Liquid	β/γ exp.	b.p. °C	$a\times10^3$ theor.	$a\times10^3$ exp.	$b\times10^{11}$ theor.	$b\times10^{11}$ exp.	$(c_p)_l$ calc. theor.	$(c_p)_l$ calc. exp.
Mercury	57	357	0.223	0.183 (300°)	0.412	0.454 (192°)	0.0261	0.0332 (260°)
Bromine	28.3	58.8	1.18	1.22	8.0	6.25 (20°)	0.096	0.107
Carbon disulfide	26.7	46.3	1.29	1.31	11.0	8.7	0.213	0.246
Acetone	22.3	56.5	1.41	1.54	13.7	11.4	0.519	0.550
Carbon tetrachloride	21.8	76.8	1.43	1.42	20.0	15.8 (70°)	0.180	0.229 (60°)
Chloroform	20.2	61.2	1.36	1.37	15.0	14.1	0.212	0.253
Ethyl ether	19.7	34.6	1.58	1.72	23.0	20.7	0.559	0.560
Benzene	19.4	80.1	1.48	1.54	19.0	16.0	0.395	0.444
Ethyl alcohol	14.0	78.4	1.45	1.36	9.0	11.0	0.75	0.75
Water	10.9	100	1.43	0.75	2.8	4.14	1.29	1.01

may be replaced by $\varphi_0/\sigma_0\varphi_0'$. It must be emphasized, however, that the above procedure, adopted for simplicity's sake, may involve a considerable numerical error as the neglected terms are not sufficiently small in all cases.

Using (7.12) we finally obtain

$$a=\{n_1k-(3\varphi_0/(T\sigma_0\varphi_0'))(B-p)\}/B, \quad (7.13)$$

and

$$(c_v)_l=(c_v)_v+(\delta\varphi_0/T)\{\varphi_0/\sigma_0\varphi_0'+2(\varphi_0/\sigma_0\varphi_0')^2-(\varphi_0/\sigma_0\varphi_0')^3(\sigma_0^2\varphi_0''/\varphi_0)\}, \quad (7.14)$$

as corrected forms of (7.10) and (7.11).

VIII. COMPARISON WITH EXPERIMENT

Our potential (7.01) contains 4 constants. These, as well as the equilibrium distance σ_0, have to be determined from experimental data. The physical constants represented by the theory comprise, for a given temperature, the 7 quantities p, ρ, a, b, L, $(c_v)_l$, and γ. Thus, in the most general case that all five unknown constants are determined, two physical coefficients can be predicted. It will be seen, however, that the theoretical constants enter into the physical coefficients in certain groups only. Hence an independent test of the theory can be made without determination of all 5 constants.

We are going to apply our formulae to 10 liquids. They are selected from the point of view that they should represent different types of liquids (normal and abnormal, polar and nonpolar, monatomic and polyatomic) and that the empirical data should be known as completely as possible. Unfortunately, there are very few liquids for which all 7 coefficients are known at one temperature.

As the heat of vaporization is generally known for the normal boiling point only we have chosen the temperature of the boiling point and $p=1$ atmos. as standard conditions for each liquid. This procedure, however, has the inconvenience that some of the other coefficients are not known for the temperature of the boiling point. It should be remembered that, here, we are treating the liquid state only. Therefore p represents the external pressure which enters into the equation of state (6.04) or (7.07). Nothing would be changed, of course, if we imagine the liquid as existing under the pressure of its own vapor at its boiling point.

We first discuss the procedure used in determining the constants. If we introduce the 3 empirical constants

$$\alpha=3(kT-p/n_1), \quad (8.01)$$

$$\beta=9(B-p)/n_1, \quad (8.02)$$

$$\gamma=L\rho/n_1-kT, \quad (8.03)$$

and the two theoretical combinations

$$\delta f\sigma_1^{-\lambda}\lambda/(\lambda-3)=x, \quad (8.04)$$

and

$$\delta g\sigma_1^{-\mu}\mu/(\mu-3)=y, \quad (8.05)$$

our three isothermal relations (7.07), (7.08), and (7.09) assume the simple form

$$-\alpha=x-y, \quad (8.06)$$

$$\beta=\lambda x-\mu y, \quad (8.07)$$

and

$$-\gamma=x/\lambda-y/\mu. \quad (8.08)$$

Thus, if either λ or μ is assumed, the second of these exponents can be calculated from

$$\mu=(\beta+\lambda\alpha)/(\lambda\gamma-\alpha),\qquad \lambda=(\beta+\mu\alpha)/(\mu\gamma-\alpha), \quad (8.09)$$

and then x and y from

$$x=(\beta+\mu\alpha)/(\lambda-\mu),\qquad y=(\beta+\lambda\alpha)/(\lambda-\mu). \quad (8.10)$$

Of course, neither λ nor μ can be assumed arbitrarily. To specify the restrictions imposed, we observe that α is, in all cases, so much smaller than β or even γ that it can be neglected in a first approximation. Then (8.09) leads to

$$\mu\lambda=\beta/\gamma. \quad (8.11)$$

Again, p is very small compared with B and the term kT in γ is only about 10 percent of the other term. Consequently the product $\mu\lambda$ is roughly given by

$$\beta/\gamma \sim 9B/L\rho \tag{8.12}$$

and λ (or μ) has to be chosen subject to (7.02) and (8.11).

With our form of the potential $\varphi(r)$ the product $\mu\lambda$ (which is a pure number depending on empirical data only) is in a certain way characteristic of a liquid. The numerical calculations show that the values of a and $(c_v)_l$ depend astonishingly little on the individual choice of λ or μ within the permitted limits (even if these limits are approached). Therefore it seems to be more reasonable to consider $\lambda\mu$, x, and y as the three combinations of constants to be determined from (8.09) and (8.10), i.e., from the knowledge of p, B, L, and ρ. For this reason we have arranged our tables in order of decreasing β/γ.

Furthermore, for pressures of the order of 1 atmos., the terms involving p in (8.01) and (8.02) are so small compared with the principal terms that they can be neglected. This we have done throughout. It amounts to neglecting the external pressure in comparison with the internal kinetic pressure, or treating the liquid as existing under zero pressure. It will be noticed that this means adopting for the liquid that state which was introduced in Section IV as zero approximation, i.e., as solution of (4.12).

As stated above, if λ or μ is chosen arbitrarily within the permitted limits, the other exponent, as well as x and y, becomes calculable. This does not involve an independent test of our theory except in as much as β/γ must be larger than 9. It will be seen from Table I that this is true, the empirical ratio β/γ changing from 57 for Hg to 10.9 for water.

However, if one of the exponents is assumed and if the other exponent and x and y are determined in the indicated way, a and $(c_v)_l$ become calculable from (7.13) and (7.14) without a more detailed knowledge of the constants. This follows from the fact that the following relations hold

$$\delta\varphi_0 = x(\lambda-3)/\lambda - y(\mu-3)/\mu = c_1, \tag{8.13}$$

$$\delta\sigma_0\varphi_0' = x(\lambda-3) - y(\mu-3) = c_2, \tag{8.14}$$

and

$$\delta\sigma_0^2\varphi_0'' = x(\lambda-3)(\lambda+1) - y(\mu-3)(\mu+1) = c_3. \tag{8.15}$$

Thus, the coefficient of expansion and the specific heat can be calculated from the knowledge of the compressibility and the heat of vaporization. This must be considered as a rather severe test of the theory.

From the program just sketched we have deviated for practical reasons. The compressibility is either not known at all or known inaccurately for the boiling point which is our standard temperature. It is, therefore, not appropriate to choose the compressibility, in addition to the heat of vaporization, as that coefficient on which to base the calculations. The coefficient of expansion is, in most cases, known more accurately for the temperature of the boiling point. For this reason we have preferred to choose, by trial and error, b arbitrarily until an adequate agreement for a was obtained.

It should be mentioned that the approximation (7.10) would yield coefficients of expansion which are about ten times too small. Thus the dependence of σ on T is essential for the explanation of thermal expansion.

As to the specific heat we have seen that, in roughest approximation, (7.11), the specific heat at constant volume should be equal in the liquid and the vapor states. Newton and Eyring[2] have pointed out that this is approximately the case for numerous liquids whereas $(c_p)_l$ and $(c_p)_v$ differ considerably.

In next approximation the difference of $(c_v)_l$ and $(c_v)_v$ should be calculable from (7.14) and this would afford a severe test of the theory as the difference is, in most cases, small compared with either value. However, neither the state of empirical knowledge, nor the approximate nature of our formula (7.14), legitimates such a procedure. We have, therefore, tested our theory in a rougher way calculating $(c_p)_l$ from the thermodynamical relation between c_p and c_v (which relation, of course, could be obtained from our statistical equations). By this procedure we obtain

$$(c_p)_l = (c_v)_l + a^2T/J\rho b, \tag{8.16}$$

where $(c_v)_l$ is to be taken from (7.14) and where the *theoretical* values of a and b have to be in-

TABLE II. Summary of theoretical constants.

Liquid	λ	μ	$f\sigma_0^{-\lambda}$ $\times 10^{13}$	$g\sigma_0^{-\mu}$ $\times 10^{13}$	φ_0/kT	δ	$\sigma_0 \times 10^8$
Mercury	11.4	6.00	2.61	1.81	0.93	30.23	5.0
Bromine	6.0	4.22	1.365	0.809	1.23	21.5	6.7
Carbon disulfide	7.0	3.49	0.715	0.185	1.21	20,2	6.9
Acetone	6.0	3.56	0.874	0.284	1.30	20.9	7.5
Carbon tetrachloride	5.3	3.80	1.228	0.608	1.29	19.45	8.1
Chloroform	5.5	4.0	1.327	0.746	1.27	20.4	7.7
Ethyl ether	5.5	3.78	1.010	0.472	1.28	19.16	8.1
Benzene	5.3	3.62	1.067	0.435	1.31	19.4	7.9
Ethyl alcohol	5.0	3.82	1.526	0.831	1.44	23.8	7.3
Water	5.0	3.65	1.357	0.615	1.45	23.0	4.8

serted. In this calculation it is assumed that the specific heat of the internal motion of the molecules is the same in the two states.

The results of our calculations are given in Table I. The empirical data refer to the boiling point (b.p.) except where stated differently. It should be remembered that the evaluations are based on the knowledge of the heat of vaporization so that this quantity is given without deviation by the theoretical formula (7.09) with the constants as determined.

It can be stated that, with water the only exception, the agreement is satisfactory. Evidently there are deviations of a systematic nature. If the constants are determined as we have done, i.e., making the agreement of L exact and that of a satisfactory, the compressibility comes out too large and $(c_p)_l$ too small for most of the liquids. This may be due to the fact that our formulae (7.06) and (7.12) are comparatively rough approximations.[16] In that case the agreement could be improved by using the correct but inconvenient formulae (5.06) to (5.08). Furthermore, for the polyatomic molecules the assumption that the internal degrees of freedom are unchanged in the liquid may be at default. However, we do not wish to stress these arguments as it seems to us that the agreement is about as good as can be expected considering the fact that the simple potential (7.01) correlates the behavior of liquids which are as widely different as mercury and ethyl alcohol.

Our theory, of course, includes the dependence of all coefficients on temperature. It is easy to show that the variability is qualitatively in the required direction, L decreasing with rising temperature, b and a increasing with rising temperature, the former more strongly, the latter weakly with a possibility of a change of sign. These conditions will have to be investigated separately, presumably in connection with a more elaborate choice of the potential.

So far, besides the exponents λ and μ, only the combinations x and y have been used. However, the knowledge of the number δ is involved implicitly. Inserting the known constants c_1 and c_2 [(8.13) and (8.14)] into the definition of δ, (7.05), we obtain a transcendental equation for δ, namely,

$$\delta = (1 - c_2/2\delta) \exp (c_1/\delta). \qquad (8.17)$$

From this δ can be easily determined by graphical or numerical methods. Finally, δ being known, we can obtain the equilibrium distance σ_0 equating it with σ_1 in (7.04).

The values of the constants which result from our calculations are summarized in Table II. We have not tabulated the coefficients f and g but rather $f\sigma_0^{-\lambda}$ and $g\sigma_0^{-\mu}$. The reason for this procedure is that the values of f and g depend very strongly on the values of the exponents λ and μ which are somewhat arbitrary within the permitted limits (see above, p. 474). The "energy terms" $f\sigma_0^{-\lambda}$ and $g\sigma_0^{-\mu}$ change very much less and their difference gives immediately the potential energy of two molecules at the average distance of nearest neighbors.

An estimate of this potential energy is best made by comparing it with kT. Therefore a column for φ_0/kT has been added. It will be seen that this ratio is of the order of unity, showing a fairly regular increase as β/γ decreases.

In the last column the equilibrium value σ_0 (for the b.p.) is given. In all cases σ_0 is of the anticipated order of several A. However, it seems that the obtained values are somewhat large. Hertz's geometrical formula would make σ_0 about 2.7 to 3.1 times smaller. The true values may be in between, probably nearer our values. The fact that σ_0 appears too large is evidently due to the fact that the probability (5.03) exaggerates the inhomogeneities of the microscopic distribution, as suggested by Fowler.

The fact that the simple potential coordinates the facts in a satisfactory way for liquids of widely different nature should not be taken as a proof of its correctness but rather of its adapta-

[16] In this connection it might be mentioned that the neglected terms are of greatest importance in the case of water.

bility. Except, perhaps, in the case of the monatomic Hg where the theoretical value 6 could be assigned to μ, the potential (7.01) can represent, at best, a very rough approximation to real conditions. This is best illustrated by the fact that liquids with no or negligible dipole character, such as CCl_4 and C_6H_6, show up in our table between dipole neighbors without noticeable discontinuity.

Further independent tests of the theory can be derived from the study of the vapor pressure law and of the surface tension. This will be done in the second part of the paper.

APPENDIX I

It has to be proved that the conditional Eq. (4.12) has a root $n_1=n_{10}$ for sufficiently low values of T. It will be useful if we introduce the volume V_1 as independent variable, instead of n_1, keeping N_1 constant. Then (4.12) takes the form

$$N_1kT=V_1\partial U_1/\partial V_1, \tag{a}$$

where

$$U_1=n_1u_1=2\pi(N_1^2/V_1)\psi(\sigma_1). \tag{b}$$

With the specific assumptions regarding $\varphi(r)$ made in Section II the function $\psi(\sigma_1)$ defined by (2.12) will have the same general character as $\varphi(r)$ possessing one zero for finite values of σ_1, say at $\sigma_1=r_0<r_1$, and its minimum at $\sigma_1=r_1$.

Preliminarily we are going to assume that, for any given value of T, the parameter σ_1 increases in a monotonic way with V_1. If, then, we introduce V_1 as independent variable $\psi(V_1)$ will have its only finite zero at V_{10} and its only (negative) minimum at V_{11}. Here V_{10} and V_{11} are the values of V_1 corresponding to $\sigma_1=r_0$ and $\sigma_1=r_1$, respectively. Consequently U_1, as defined by (b), will have its only (negative) minimum at a value $V_1=V_1^*$ with $V_{10}<V_1^*<V_{11}$.

Finally the function $\phi(V_1)=V_1\partial U_1/\partial V_1$ will have its only finite zero at $V_1=V_1^*$ and will change from negative to positive values there. Furthermore, it will approach zero asymptotically for $V_1\to\infty$. Consequently the curve $\phi(V_1)$ will certainly be intersected by the horizontal N_1kT for sufficiently low values of T in at least two points. That intersection which corresponds to the lowest value of V_1 represents the state of highest density compatible with (a). As it occurs for $V_1>V_{10}$, and therefore for $\sigma_1>r_0$, $\psi(V_1)$ will be negative, as it should (to make $\Pi_2/\Pi_1>1$). Furthermore, it can be shown to make the compressibility positive (having $\partial\phi/\partial V_1>0$) and is therefore physically acceptable.

The limiting temperature above which there are no roots to (a) will be given by the maximum of $\phi(V_1)$ (or the highest maximum if there are several). Consequently the critical volume and the critical temperature are given by (a) together with

$$\partial U_1/\partial V_1+V_1\partial^2U_1/\partial V_1^2=0. \tag{c}$$

It is easy to derive from (a) and (c) the two conditions

$$N_1kT/V_1^2+\partial^2U_1/\partial V_1^2=0 \tag{d}$$

and

$$2N_1kT/V_1^3-\partial^3U_1/\partial V_1^2=0. \tag{e}$$

These are the conditions for the critical point in the usual form as they express the vanishing of $\partial p/\partial V_1$ and $\partial^2 p/\partial V_1^2$, p being given by

$$p=N_1kT/V_1-\partial U_1/\partial V_1 \tag{f}$$

[see Eq. (6.04)].

We have, so far, assumed that $\partial\sigma_1/\partial V_1$ is positive throughout, for any given value of T. It remains to be shown that, for the dependence of σ_1 on T and n_1 accepted by us, this is the case. From our Eqs. (5.06) and (5.08) it follows that $\partial\sigma_1/\partial V_1$ is certainly positive as long as φ' is negative and φ'' is positive, i.e., at least as long as σ_1 is smaller than r_2. That is sufficient to prove the existence of the zero of $\phi(V_1)$ at $V_1=V_1^*$ though it cannot be claimed that there are no further zeros for finite values of $V_1>V_1^*$.

It is not our object to investigate here which restrictions must be imposed on $\varphi(r)$ and T if $\phi(V_1)$ is to have only one zero and one maximum. Nor shall we investigate the physical nature of the other roots of (a) if there are several such roots with $\partial\phi/\partial V_1>0$. The numerical calculations of Section VIII which are based on the special form of $\varphi(r)$ adopted in Section VII show that $\partial\sigma_1/\partial V_1$ is positive for all values of σ_1, and for all relevant values of T (i.e., for values of T above the freezing point). Then $\phi(V_1)$ has one maximum only and there is only one root to (4.12).

APPENDIX II

As we have given previously[13] only the result of the generalization of Hertz's formula we shall sketch the proof here. For the details and the exact definition of the probabilities involved we refer to the paper of Hertz.[12]

Let us single out a mass point A and let us imagine two spheres of radii r and $r+dr$ described about it. If the nearest neighbor B is to be contained within the zone so defined, two conditions must be fulfilled:

1. There must really be a point in the zone. The probability for this event is, by definition, given as

$$4\pi r^2np_1(r)dr. \tag{α}$$

2. The point within the zone must be the nearest neighbor to A, i.e., the sphere of radius r must *not* contain any points. The probability for this event is given by

$$1-\int_0^r p_2(\rho)d\rho. \tag{β}$$

Thus the joint probability of the two events is given by the product of (α) and (β), and we obtain for $p_2(r)$ the integral equation

$$\left[1-\int_0^r p_2(\rho)d\rho\right]4\pi r^2np_1(r)=p_2(r). \tag{γ}$$

If we introduce the function $P(r)$ defined by (5.02) (γ) reduces to

$$\left[1-\int_0^r p_2(\rho)d\rho\right]n(dP/dr)=p_2(r). \tag{δ}$$

This equation is identical in form with the one treated by Hertz and shown by him to be solved, under the given conditions, by

$$p_2(r)=nP'\exp(-nP) \tag{ϵ}$$

as stated in the text.

Note on the Nature of the Gas Mixture in Self-Quenching Geiger-Mueller Tubes

PAUL WEISZ
Bartol Research Foundation of the Franklin Institute, Swarthmore, Pennsylvania
(Received September 12, 1942)

The effect of different quantities of the "quenching gas" on the discharge mechanism of Geiger-Mueller tubes has been investigated. The experimental results are correlated with the general picture of the discharge mechanism; a very brief and integrated preliminary account of the mechanism is given.

FROM studies on the breakdown of spark gaps, and from theoretical and experimental work on the discharge process of Geiger-Mueller tubes itself, we conclude that the intrinsic difference between self-quenching and non-self-quenching G-M (Geiger-Mueller) tubes lies in the particular nature of the action of ultraviolet photons in each case.

In the G-M tube which is not self-quenching, a great number of photons are emitted during the discharge process. These travel through the gas to the cathode wall and produce a considerable number of photoelectrons there. Part of these attach to molecules forming negative ions of relatively small mobilities. The negative ions release their electrons when reaching the strong fields in the vicinity of the wire, thus forming new discharge centers, unless the field conditions have been kept such that multiplication cannot occur until all negative ions are collected. This accounts for the fact that a high external resistance is required for the proper operation of such tubes, high enough to make the recovery time RC of the tube greater than the collecting time of the negative ions.

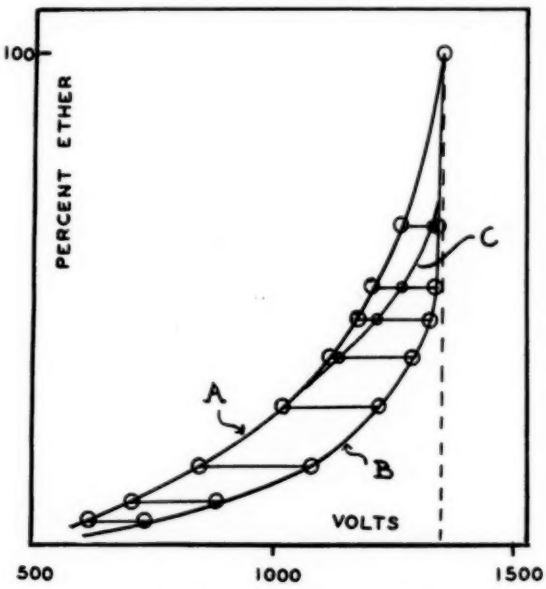

FIG. 1. The plateau region for the argon/ethyl-ether counter. The counter is $\frac{1}{2}''\times 3''$. The central wire is 0.003"; the total pressure, 6 cm of Hg.

In so-called self-quenching G-M tubes, no evidence has been found for the presence of photons at appreciable distances from the wire. It was suggested[1] that the addition of the polyatomic gas which causes the essential modification of the tube to a self-quenching one may quench the production of these photons by providing modes of energy loss other and more probable than by excitation of ultraviolet energy levels. However, experimental evidence, particularly the phenomena of perpetuation of the discharge process along the wire as studied with a "segmented" G-M tube,[2] and a finding to be reported here, seem to suggest that ultraviolet light quanta are still produced, but are quickly absorbed by the "quenching gas," probably within a distance of a few mean-free paths in the gas.

Thus it is the purpose of the quenching gas to absorb all ultraviolet quanta produced, or ultimately to make the probability of production of negative ions by way of photons and photoelectrons as nearly as possible equal to zero. Since this probability will depend on the density of the quenching gas, an investigation was made of the quenching properties as a function of the partial pressure of the quenching gas. This was accomplished by studying the width of the

[1] M. E. Rose and S. A. Korff, Phys. Rev. **59**, 850–859 (1941).
[2] W. E. Ramsey, Phys. Rev. **61**, 96–97 (1942); H. G. Stever, Phys. Rev. **59**, 765 (1941), and Phys. Rev. **61**, 38–52 (1942).

"plateau," for mixtures of argon as the "multiplication gas" and ethyl-ether as the quenching gas. The plateau is defined as that region of applied electrode potentials which lies between two limits A and B, such that beginning at the potential A all pulses are of a convenient pulse size (three volts in this case), and that the tube starts to show multiple discharges when the potential is increased beyond B, and the tube is operated with a normally small external resistance of 1 megohm. The appearance of such multiple pulses can be interpreted in the light of the above picture of the mechanism as being evidence for the production of photoelectrons, their subsequent capture and release, and thereby the repetition of the discharge process.

Figure 1 shows the results of the plateau measurements for a tube containing argon/ethyl-ether at 6-cm total pressure; the partial ether pressure is expressed in percentage of total pressure. It can be seen that for this total pressure, an ether content of about 20 to 25 percent yielded the optimum plateau. At relatively high ether contents, the pulses were no longer of equal amplitudes but showed appreciable distribution in size up to potentials indicated by curve C, although the average pulse size was still approximately 3 volts at A. In the light of the picture outlined the following explanation suggests itself: At great densities of the quenching gas the absorption of photons becomes so intense that even the propagation of the mechanism along the wire cannot always take place along its entire length. The pulse size, being proportional to the total amount of charge produced, may then be nearly proportional to the length along which each discharge is able to propagate before it fails in producing at least one more photoelectron. The pulse size may thus be subject to appreciable fluctuations.

Similar measurements concerning optimum plateau conditions were made at different total pressures, and the following data obtained:

Total pressure	Approx. % ether for opt. plateau
6 cm	20 to 25%
15 cm	7 to 10%
40 cm	approx. 3%.

It appears that the absolute pressure or density of the quenching gas alone determines the quenching characteristics regardless of what the total gas pressure may be, the partial ether pressure for optimum conditions being about 1.5 cm of mercury. It seems noteworthy that this finding seems to favor the concept of photons being *absorbed* by the presence of a sufficient amount of the quenching gas, in preference to a picture of the mechanism involving the assumption of some action by which this gas prevents the creation of quanta during the ordinary discharge process.

The Magnetic and Optical Anisotropy of Selected Microscopic Crystals and the Linear Magneto-Optical Anisotropy of Their Suspensions

WILFRIED HELLER, GERMAINE QUIMFE, AND YEOU TA
School of Chemistry, Institute of Technology, University of Minnesota, Minneapolis, Minnesota, and Laboratoire des recherches physiques, Sorbonne, Paris, France

(Received August 3, 1942)

Superposition of magnetic and orthogonal hydrodynamic orientation is used for measuring the relative magnitude of magnetic anisotropy in paramagnetic and diamagnetic, organic and inorganic, microscopic anisometric crystals, dispersed in liquids. Some magnetically biaxial crystals show a "two-step" orientation. The optical anisotropy of the crystals is determined and compared with the magnetic anisotropy. The criteria as regards the probable magnitude of magnetic double refraction and of magnetic dichroism in suspensions of the crystals are discussed. The sign and a series of complications in sign of magnetic double refraction and of magnetic dichroism in such suspensions are deduced. Magnetic double refraction and magnetic dichroism, as actually observed in dispersed systems of ultramicroscopic V_2O_5 crystals and of α-FeOOH crystals are in agreement with the deductions. Provided their size is ultramicroscopic, α-FeOOH crystals are able to orient themselves either parallel or perpendicular to the lines of force, depending on their size, axial ratio, and magnetic anisotropy, and depending on temperature. The resulting magneto-optical complications in suspensions of the crystals, as observed, are briefly reviewed. A competition between morphic and intrinsic magnetic anisotropy is made responsible for the phenomenon of switching orientation. The colloidal phenomenon of "thixotropy" and the optical effect of "morphic conservative" dichroism are used for detecting the switching of orientation from perpendicular to the lines of forces at low temperature, to parallel above 25°C.

THE magneto-optical properties exhibited by suspensions of microscopic or ultramicroscopic (colloidal) crystals are sometimes complicated though generally less than their electro-optical properties. An unequivocal interpretation has been possible only in a few instances.[1] The basic difficulty has been, as in the case of electro-optical properties, that too many variables were involved and the authors have not taken time to test theoretically or experimentally the influence of the variables. The result is a maze of possible interpretations beside the one accidentally preferred in a given case. The number of possible interpretations is considerably reduced if one is informed of the direction of magnetic orientation of the crystals and of their basic optical properties. This paper deals with the investigation of these specific questions, with respect to a few selected crystals of microscopic size. The magneto-optical properties of suspensions of these crystals are briefly discussed on the basis of the results. The crystals used are described in Table I. They were acicular, partly lathlike, with the exception of the disklike anthracene crystals.

[1] See review in W. Heller, "Propriétés magnétooptiques des solutions colloïdales," monograph 806 in *Actualités scientifiques et industrielles* (Hermann and Company, Paris, 1939).

I. DIRECTION OF MAGNETIC ORIENTATION AND MAGNETIC ANISOTROPY

(a) Method

The magnetic anisotropy of crystals is usually determined on macroscopic specimens and by using the torsion method.[2] Many substances that give crystallographically well-defined ultramicroscopic or microscopic crystals cannot be obtained in faultless macroscopic specimens. One was therefore confronted with the necessity of devising a new method. Our new method, at present applicable to microscopic anisometric

TABLE I. Orientation of the longest crystal axis with respect to the lines of force. *r*: rhombic; *t*: tetragonal; *m*: monoclinic; ?: unknown; *: the torque due to anisometric shape is opposite to the torque due to intrinsic magnetic anisotropy.

*I: diamagnetic; ||: (1) quinone (*m*); (2) hydroquinone (*t*); (3) *p*-nitrosoguajacole (?)
II: diamagnetic; ⊥: (4) alizarine (*r*); (5) indigotine (*r*); (6) tartrazine (*r*); (7) saccharine (*r*); (8) anthracene (*m*)
III: paramagnetic; ||: (9) V_2O_5 (*r*)
*IV: paramagnetic; ⊥: (10) α-FeOOH (*r*)

The orthorhombic α-FeOOH crystals are uniaxial (negative) above 6100A.

[2] See, e.g., D. Bhagavantam, Ind. J. Phys. **4**, 1 (1929); the magnetic anisotropy of a considerable number of crystals has been investigated recently by S. Banerjee, Zeits. f. Krist. **100**, 4, 316 (1938).

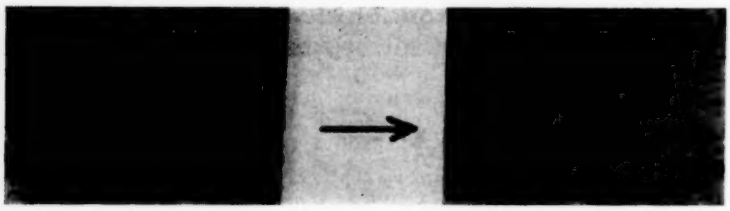

FIG. 1. Unoriented (left) and magnetically oriented (right) sedimentation of microscopic quinone crystals. (Arrow: direction of applied field.)

crystals, but possibly applicable also to ultramicroscopic crystals, is based on the superposition of magnetic and orthogonal hydrodynamic orientation of crystals floating in a liquid. Barring complications due to the anisometric shape of the crystals (see below), the relative, and possibly also the absolute, magnitude of magnetic anisotropy can then be determined by taking advantage of the fact that magnetic orientation is given up in favor of hydrodynamic orientation at critically high rates of flow, $\sim v_0$,[3] if H is constant, and at critically low field strengths $\sim H_0$ if v is constant. The higher the magnetic anisotropy, the higher is $\sim v_0$ and the lower is $\sim H_0$.

Crystals *1*, *4*, *5*, *8* (Table I) were prepared by sublimation in vacuum, crystals *3*, *6*, *7* by crystallization from solution; α-FeOOH crystals were obtained by grinding a macroscopic specimen under distilled water. V_2O_5 crystals of microscopic size had developed in a colloidal solution aged for more than 10 years. Each kind of crystals was investigated in those of the following media in which it was practically insoluble: water, a 5 percent aqueous solution of $MnSO_4$, ethyl alcohol, nitro-benzene, glycerol, glycerol-water mixtures, glycerol-ethyl alcohol mixtures. The maximum magnetic field strength was 22,800 gauss (tronconic poles; frontal diameter: 2 cm; pole distance: 2 cm). By test with a new magnetometric method[4] the field was found to be perfectly homogeneous within a radius of at least 5 mm. In order not to disturb this homogeneity, a microscope was constructed entirely of brass, by Yeou Ta, which had a stage only 1.5 cm wide. A small amount of the dilute dispersed system was poured into a small trough which was then placed on the stage and at the center of the field. Horizontal flow, either parallel or perpendicular to the horizontal direction of the lines of force, was produced by means of a tiny capillary tube. A small amount of dispersed system was squeezed out of or sucked into it.

[3] The sign $\sim$ shall signify that ranges are meant.

[4] W. Heller and J. Rabinovitch, Comptes rendus **207**, 1088 (1938).

(b) Results

In absence of flow, all crystals oriented themselves in a field of 20,000 gauss, but only a few, such as indigotine, at less than 1000 gauss. The direction of the longest crystal's axis was always strictly parallel or perpendicular to the lines of force. Table I gives the direction. It was the same in all media. Figure 1 shows quinone crystals after sedimentation in zero field (left) and after sedimentation under the influence of 22,000 gauss (right).

Some crystals oriented themselves in two steps. Upon establishment of the field, they rotated first around one axis and then, after a distinct delay, around another perpendicular axis. The phenomenon, in order to occur, required an appropriate accidental initial position of the crystal at the moment when the field was established. It was most pronounced and very striking for indigotine crystals. One concludes that biaxial crystals which show a two step orientation, have a susceptibility χ_β which is distinctly different from both χ_γ and χ_α.

Orientation by flow was superimposed after magnetic orientation had been established. The direction of flow was perpendicular to the direction of magnetic orientation of the longest crystal's axis. The values $\sim v_0$ and $\sim H_0$ were found to vary within large limits. The resistance of magnetic orientation towards the hydrodynamic torque increased in the following sequence: (1) saccharine; (2) *p*-nitroso-guajacole; V_2O_5;

hydroquinone; tartrazine; (3) anthracene; α-FeOOH; (4) indigotine; quinone; alizarine. The method would have to be put onto a more quantitative basis in order to distinguish between the crystals arranged within one group. Saccharin crystals abandoned magnetic orientation at 20,000 gauss upon the slightest movement of the liquid; alizarine crystals maintained, at the same field strength, magnetic orientation not only in rapid laminary flow, but also in turbulent flow. During laminary flow, alizarine crystals directed their longest axis strictly perpendicular to the direction of flow, which was parallel to the lines of force. In zero field, however, these crystals, like all other crystals, oriented themselves very readily by flow.[5]

Strong differences in the facility of magnetic orientation showed up also in the ability of settled crystals to overcome adhesion and friction on the lower glass walls. Alizarine crystals overcame them readily, the crystals in group 2 and 3 required tapping on the glass walls. In some instances surface orientation was abandoned in favor of magnetic orientation. This was observed on droplets which were brought onto a glass slide. Alizarine crystals, accidentally oriented in the boundary glass-droplet-air, tangentially to this boundary, became oriented radially wherever the direction of the lines of force was tangential to this boundary. Radially oriented crystals remained firmly attached to the boundary, however, and they returned into tangential orientation at the instant when the field was removed.

(c) Conclusions

An orientation in the homogeneous field can be due to a permanent moment, to an anisotropy of the induced moment, or to anisometry of the crystals. All organic crystals investigated have paired electrons so that there is no permanent moment. Neither do the two inorganic crystals seem to have a permanent moment. "Morphic" orientation requires a strong difference in the susceptibilities of medium and particles. It is therefore *a priori* unlikely, excepting α-FeOOH (mean χ: $\geqslant 39\times10^{-6}$). Nevertheless, the possibility is considered in Table I. The orientation observed is for all crystals of series I and IV opposite to that expected if it were due to morphic orientation. The orientation in series II and III is that expected for morphic orientation. Because of its weak resistance towards the hydrodynamic torque, it is not impossible that the orientation of saccharin was morphic though the weak difference in the susceptibilities ($\chi_{\text{liquid}}-\bar{\chi}_{\text{crystals}}$) is an argument against it. This difference was practically the same in all cases excepting α-FeOOH. The sequence found above with regard to the resistance of magnetic orientation towards the hydrodynamic torque can therefore be regarded as the sequence in the magnitude of the induced magnetic anisotropy.[6] However, α-FeOOH crystals may have a higher magnetic anisotropy than expressed in the sequence, because of the comparatively stronger and opposite morphic torque.

II. INTRINSIC AND MORPHIC OPTICAL ANISOTROPY

The optical anisotropy of several of the crystals is already qualitatively known. Nevertheless, all crystals were investigated between 5000 and 6000A with a polarizing microscope and a set of light filters. The results are abstracted in Table II. The italicized crystals exhibited a dichroism that had the same sign as the double refraction. Those crystals not italicized were not dichroitic.

Effects of "morphic" optical anisotropy appear if acicular crystals are lined up parallel to each other, as they are (at least statistically) upon orientation in the magnetic field. Intrinsic and "morphic" double refraction have the same sign for all crystals of group A in Table II. Their signs are opposite for all crystals of group B. All dichroisms have the same sign in group A.

TABLE II. The direction of the maximum refractive index, n_γ, with respect to the longest axis of the crystals. Italicized crystals show dichroism; k_γ is always parallel n_γ; 5000–6000A.

A: n_γ is parallel:	*V_2O_5; α-FeOOH; quinone; p-nitroso-guajacole;* hydroquinone; saccharine
B: n_γ is perpendicular:	*alizarine; indigotine; tartrazine*

[5] Suspensions and colloidal solutions of these crystals and of the other crystals of group 4 can therefore be expected to show a pronounced increase in viscosity under the influence of a magnetic field. Only the analogous effect in the electric field [e.g., Y. Björnståhl and O. Snellmann, Kolloid Zeits. **78**, 259 (1937)] is definitely known.

[6] The magnetic anisotropy of anthracene had been investigated before (reference 2).

The situation is more complicated in group B (see discussion below).

III. COMPARISON BETWEEN INTRINSIC MAGNETIC AND INTRINSIC OPTICAL ANISOTROPY

In seven out of the nine acicular crystals, the direction of maximum induced magnetic moment and the direction of maximum refractive index are parallel to each other (or possibly at small angles). For α-FeOOH they are orthogonal (also for saccharin, if orientation was due to intrinsic anisotropy). Bhagavantam[2] found such cases before, and he discussed them. One might add to his discussion that it is not surprising that orthogonal directions are found. The direction of the maximum refractive index depends on the optical wave-length; it changes within the region of selective absorption. The two directions may therefore be parallel or orthogonal in the same crystal, depending on the spectral region considered.

IV. REMARKS ON THE MAGNETO-OPTICAL ANISOTROPY OF CRYSTAL SUSPENSIONS

The results emphasize the often overlooked fact that the probable magnitude of magneto-optical effects in suspensions cannot be anticipated on the basis of the mean susceptibility of the dispersed phase. The only criteria are, first, the magnitude of magnetic anisotropy and the magnitude of optical anisotropy of the crystals and, second, their size and shape and concentration and the viscosity of the medium. Quinone, for example, is very weakly diamagnetic[7] (mean χ: -0.39×10^{-6}). Nevertheless, strong magneto-optical effects should be expected in its dispersed systems. Inversely, dispersed systems of strongly paramagnetic crystals cannot always be expected to exhibit strong magneto-optical effects.[8] This is exemplified by the behavior of FeOCl crystals. Colloidal solutions of these crystals exhibited no, or fairly weak, magneto-optical effects which followed the law $n_{\parallel}-n_{\perp}=C\times H^2$ (C: Cotton-Mouton constant) up to the highest field strengths used ($\sim$30,000 Gauss).[9] The latter phenomenon which is unusual for coarse colloidal particles, suggested a very weak magnetic anisotropy. Microscopic specimens[10] showed a well-pronounced optical anisotropy, but the crystals failed completely to orient themselves when floating in glycerol. Their magnetic anisotropy seems therefore to be very weak. On the other hand, the same crystals appeared to be most strongly paramagnetic; when brought into an inhomogeneous field the dry crystal powder rushed violently towards the region of maximum field strength; one is reminded very strongly of the behavior of ferromagnetic substances.

Table III gives a deductive survey of the linear magneto-optical effects to be observed, in suspensions of these crystals, in the direction of propagation of the light beam.[11] Saccharin is

TABLE III. Theoretical linear magneto-optical effects in suspensions of microscopic crystals. Wave-length: 5000–6000A, except in last horizontal column; *: the torques due to intrinsic magnetic anisotropy and to morphic magnetic anisotropy are of opposite sign. The sign of the optical effects is given under the assumption that the intrinsic magnetic anisotropy predominates.

	Double refraction		Dichroism			
			Consumptive		Conservative	
	Intrinsic	Morphic	Intrinsic	Morphic	Intrinsic	Morphic
V_2O_5	+	+	+	+	+	+
*quinone	+	+	+	+	+	+
*p-nitrosoguajacole	+	+	+	+	+	+
*hydroquinone	+	+	None	None	+	+
*α-FeOOH	−	−	−	−	−	−
alizarine, indigotine, tartrazine, benzopurpurine	+	−	+	−	+	−
benzopurpurine below 4500A	−	−	+	−	−	−

[7] P. Pascal, Comptes rendus **152**, 862, 1010 (1911); Ann. Chim. Phys. **25**, 289 (1912).

[8] Suspensions of ferromagnetic crystals, however, can always be expected to exhibit magneto-optical effects. Even cubical crystals receive a torque in the homogeneous field, as shown by P. Weiss on the example of magnetite [J. de Phys. **5**, 435 (1896)]. For theoretical aspects see L. W. McKeehan, Phys. Rev. **43**, 913 (1933). Suspensions of microscopic and colloidal magnetite crystals exhibit a pronounced magnetic double refraction and a strong magnetic dichroism (W. Heller, Kolloid Beih. **39**, 1 (1933)). Both effects were interpreted as morphic effects. More recently, the magnetic dichroism of magnetite suspensions has been "rediscovered" and more extensively studied [C. W. Heaps, Phys. Rev. **57**, 528 (1940); W. C. Elmore, Phys. Rev. **60**, 593 (1941); H. Mueller and M. Shamos, Phys. Rev. **61**, 631 (1942)].

[9] W. Heller and H. Zocher, Zeits. f. physik. Chemie **166**, 365 (1933).

[10] These crystals were kindly given to us by Dr. St. Goldsztaub (Laboratoire des recherches minéralogiques, Sorbonne, Paris) who prepared them and identified them by x-ray analysis.

[11] There are several types of dichroism. Dichroism may be due to actual absorption of light within the crystals ("consumptive" dichroism). Like double refraction, consumptive dichroism may be due to intrinsic anisotropy or to anisometry ("intrinsic consumptive" and "morphic consumptive" dichroism). A "conservative" dichroism is

omitted since no pronounced effects can be expected. Benzopurpurine (acicular crystals) has been added since both the direction of magnetic orientation[12] and the dispersion of intrinsic double refraction[13] are known. (This substance has historic interest in colloid optics.) The complications that may arise in some of the suspensions are: (a) competition between intrinsic magnetic anisotropy and morphic anisotropy as regards the orientation and, implicitly, as regards the sign of the optical effects; (b) competition between intrinsic and morphic double refraction; competition between intrinsic and morphic dichroism; (c) change of the sign of double refraction with the wave-length. Heterodispersion in suspensions may complicate the experimental expression of these complications.[1]

The magneto-optical properties of suspensions and of colloidal solutions containing V_2O_5 crystals,[14] α-FeOOH crystals,[15] and tartrazine crystals[16] have already been investigated. It is of interest to compare the results actually obtained in the two former cases with those to be expected from Table III.

(a) Colloidal Dispersions of V_2O_5 Crystals

V_2O_5 sols should exhibit very simple magneto-optical properties. Very simple properties had been found. Double refraction and dichroism are always positive for any field strength, no matter what the (colloidal) size, axial ratio, and concentration of the crystals. Neither aggregations of the colloidal crystals nor a change in temperature affects the sign of the effects. Magneto-optical tests on suspensions of microscopic crystals are not available.

(b) Colloidal Dispersions of α-FeOOH Crystals

Since the fundamental investigations by Cotton and Mouton,[17] iron oxide sols had been the prototype of complicated magneto-optical properties. Most of them seem now to have been cleared up.[15] A part of the complications was found magneto-optically to be probably due to a variable and possibly heterogeneous chemical and crystallographical nature of the crystals contained in these sols.[15] These magneto-optical deductions have been confirmed by x-ray investigations of all sols involved.[18] Iron oxide sols may contain crystals of α-FeOOH, β-FeOOH, α-Fe_2O_3, FeOCl. By the use of uncommon methods of preparation, still other crystals can be obtained. By appropriate methods, sols can be obtained which contain only, and at temperatures below 50°C invariably, α-FeOOH.[15,18] Notwithstanding their simple constitution, such sols exhibit quite complicated magneto-optical properties. Freshly prepared sols give a positive double refraction and a positive dichroism. As the crystals grow by "aging" of the sols, the effects become negative. Monodisperse sols become therefore at a certain age temporarily isotropic. The smaller the particles were initially, the sooner occurs the inversion. This leads at intermediate age to a change of positive effects into negative effects with rising field strength, if small and large crystals are present at the same time. Negative effects can be inverted into positive effects by forcing the crystals to form aggregates of strongly anisometric shape and of comparatively weak structural anisotropy. Rising temperature also leads to an inversion of negative effects into positive effects. This inversion is reversible. By contrast, hydrodynamic double refraction and hydrodynamic dichroism are always positive,[15] whatever the sign of the magneto-optical effects. This and other observations lead to the conclusion that no optical changes of the crystals themselves are involved, but that the α-FeOOH crystals and their aggregates may orient themselves either parallel or perpendicular to the lines of force. In order to understand the existence of two opposite tendencies of orienta-

---

the result of anisotropic light diffraction. It may be due to anisometry ("morphic conservative" dichroism) or to intrinsic double refraction ("intrinsic conservative" dichroism). Completely opaque crystals may exhibit conservative dichroism. Consumptive dichroism and both double refractions, on the other hand, are effects of transmitted light. Opaque, microscopic crystals exhibit predominantly therefore a dichroism, whereas double refraction is weak by comparison.

[12] H. Zocher, Zeits. f. physik. Chemie **98**, 322 (1921).

[13] H. Zocher and F. C. Jacoby, Kolloid Beih. **24**, 365 (1927).

[14] W. Heller and H. Zocher, Zeits. f. physik. Chemie **164**, 55 (1933).

[15] W. Heller, as quoted under reference 8. For a concise review of these investigations see W. Schütz, *Handbuch der Experimentalphysik* **16/1**, p. 316–318.

[16] W. Heller and A. Piekara, to be published shortly.

[17] A. Cotton and H. Mouton, Ann. de Chim. et Phys. (8) **11**, 145 (1907).

[18] W. Heller, O. Kratky, and H. Nowotny, preliminary communication in Comptes rendus **202**, 1171 (1936).

tion, one assumed that one torque is due to an anisotropy of the induced magnetic moment, and the other is due to the anisometric shape. This concept required the further assumption that the maximum induced moment is perpendicular to the longest dimension of the anisometric crystals. On this basis, the whole complex of phenomena, those enumerated above as well as many others, could be explained satisfactorily. Positive effects were regarded as a consequence of magnetically predominating morphic anisotropy (parallel orientation); negative effects were considered as a consequence of predominating intrinsic magnetic anisotropy (perpendicular orientation).

It became desirable to find some direct proof, first for the assumption of two orthogonal torques and, second, for the concept of a change in the direction of orientation. The results reported under Section I are proving now that the former assumption was justified. Attempts to test the second assumption by using microscopic specimens failed. The crystals maintained a perpendicular orientation within the entire investigated range of 18°–50°C. However, a second attempt with colloidal crystals was successful. The respective experiments were carried out by Miss Quimfe and one of us.[19] A new optical method was used[20] and advantage was taken of the phenomenon of "thixotropy."[21] A thixotropic "gel" was used which, according to x-ray evidence,[22] contained exclusively α-FeOOH crystals of an average size of 1000A. By volume, 2.45 percent of the dispersed system consisted of crystals (102.2 g FeOOH per liter), the rest consisted of an aqueous solution of magneto-optically inactive electrolytes. The gel could, by gentle shaking, easily be liquefied into a readily fluid "sol." Upon subsequent rest, it took a little less than 15 minutes, at 15°C, until the crystals had lost again their freedom of rotation and translation. At 45°C, it took a little less than 5 minutes. (This applies only to setting in the magnetic field.) Figures 2 and 3 give the optical results (numerically valid for the above, directly used concentration, and for a layer of 1 cm. The layer actually used was 0.37 mm; the wavelength was 6200A). The curves A in Fig. 2 show the absorption coefficients $k_{\parallel}$ and $k_{\perp}$ after exposure of the sample to a magnetic field of 11,000 gauss, as observed at various temperatures if the crystals possessed their maximum

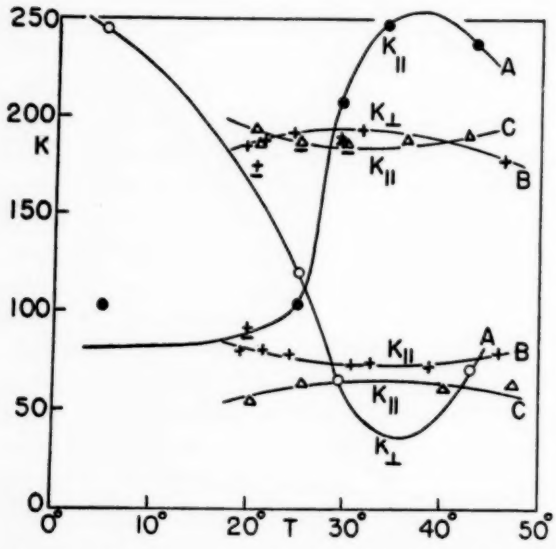

FIG. 2. The thermic variation of the absorption coefficients $k_{\parallel}$ and $k_{\perp}$ in suspensions of statistically (A) and statically (B, C) oriented ultramicroscopic α-FeOOH crystals. Curves A: Magnetic orientation at various temperatures while the crystals have a maximum freedom of rotation. Curves B: Magnetic orientation at 16.9°C, maintained until the crystals had lost their freedom of rotation. Subsequent variation of temperature in the permanently anisotropic system (not underlined points: ascending temperature; underlined points: subsequently descending temperature). Curves C: Magnetic orientation at ~45°C, maintained until the crystals had lost their freedom of rotation. Subsequent variation of temperature in the permanently anisotropic system (not underlined and underlined points: like in B).

Note: The lower curve C should be identified by $K_{\perp}$ rather than by $K_{\parallel}$.

[19] W. Heller and G. Quimfe, communicated in preliminary form, Comptes rendus **206**, 64 (1938).

[20] W. Heller and G. Quimfe, Phys. Rev. **61**, 382 (1942). A detailed description will be given elsewhere.

[21] A gel is called "thixotropic" if by mechanical action it can be transformed into a definitely fluid dispersed system and if it sets again spontaneously within a certain time after the mechanical action has ceased. A certain minimum concentration of dispersed phase (which may be smaller than one percent by weight) and appropriate physicochemical conditions are prerequisites of thixotropy. Colloidchemically, the phenomenon is defined as an isothermal and reversible sol-gel transformation. Physically, it is defined as an isothermal and reversible, partial or total immobilization of the dispersed particles, under the influence of forces acting between the particles. This immobilization, at fairly large equilibrium distances [E. A. Hauser, Kolloid Zeits. **48**, 57 (1929); W. Heller and G. Quimfe, Comptes rendus **205**, 857, 1394 (1937)], can temporarily be abolished by shear (e.g., by shaking). For a comprehensive review of the colloid-chemical aspect of thixotropy see H. Freundlich, *Thixotropy, Actualités scientifiques et industrielles*, monograph 267 (Hermann and Company, Paris, 1935).

[22] We are indebted to Dr. H. Nowotny for carrying out the x-ray analysis.

freedom of (damped) translation and rotation at the moment when the sample was exposed to the orienting influence of the field. The dichroism (curve *A* of Fig. 3) which, at 6200A, is exclusively conservative and predominantly morphic, changes from positive to negative, as higher and higher temperatures of exposure are chosen. (The maximum near 35°C is the consequence of the decrease in statistical orientation with increasing temperature. The negative temperature coefficient of the "pure" positive magneto-optical effects in α-FeOOH sols is 3 percent.)[15] In the curves *B* of Figs. 2 and 3, the same sample is considered. This time, it remained exposed to the magnetic field at 16.9°C until the crystals had become completely immobilized (determined optically). A subsequent variation of temperature did not lead to any qualitative change in dichroism of the permanently and negatively dichroitic gel. (The gel then polarized natural light very strongly. Its "polaroid" quality is quantitatively defined by the curves *B* in Fig.2.) The curves *C* in Figs. 2 and 3 were obtained after the same sample had been "liquefied" again. This time, the sample was exposed to the field at ~45°C until the crystals became immobilized. Thereupon, the temperature was varied again. The permanent dichroism is this time positive and it is again qualitatively independent of temperature. (The antisymmetrical character of the curves *B* of Fig. 2 when compared to curves *C* of the same figure is remarkable; the cause of the slight quantitative variations of $k_{\parallel}$ and $k_{\perp}$ with temperature, in these curves, is not quite clear as yet.)[23] In a final experiment we followed, on the same sample, the procedure which had led to the curves *A* in Fig. 2 and we obtained again the results shown in those curves. These results appear to offer a definite proof for the ability of colloidal α-FeOOH crystals to change their direction of orientation towards the magnetic field, from perpendicular at low temperature into parallel at higher temperatures (decrease in magnetic anisotropy).

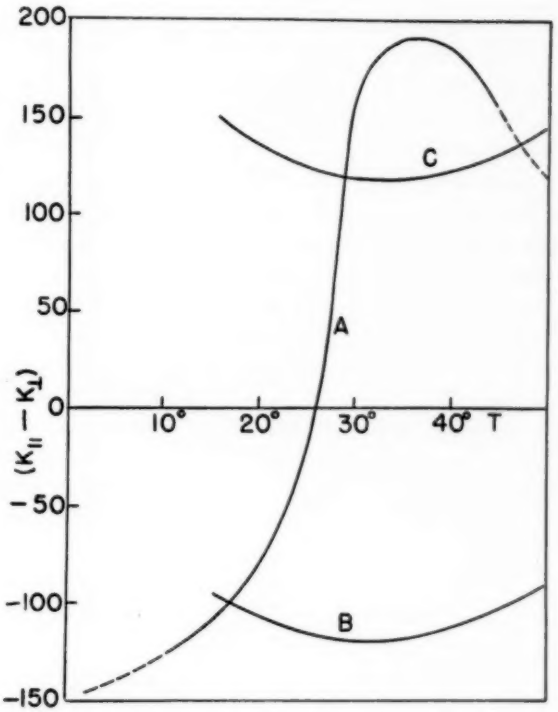

FIG. 3. The variation, with temperature, of the transitory (*A*) and permanent (*B*, *C*) morphic conservative magnetic dichroism in suspensions of ultramicroscopic α-FeOOH crystals; as deduced from Fig. 2, *A*, *B*, *C*.

It is a matter of speculation as to why the phenomenon of variable orientation can occur for crystals of colloidal size, but apparently not for crystals of microscopic size. (It might be of course that the latter also change their orientation, but at a considerably higher temperature.) One could assume that the magnetic anisotropy of α-FeOOH crystals decreases with size, within the region of ultramicroscopic dimensions. It is logical to assume that the lattice energy, and consequently the lattice spacing, are different from the normal state in crystals so small as to contain only a few lattice plans. Offhand one would expect an increase in crystal spacing and an increase in entropy as the crystal size decreases. Such a concept is contrary to the calculations of Lennard Jones,[24] but it is supported by experimental results of Finch and co-workers.[25] It is also supported by the fairly old result, ob-

[23] According to Gaubert [Goldsztaub, Thesis (Paris, 1934), p. 27] the intrinsic double refraction of α-FeOOH crystals decreases very strongly with increasing temperature. In addition to this effect, a reversible thermic change in the anisotropic structure of the gel might be involved. The simultaneous presence of these two thermic effects could account for the maxima (minima) observed.

[24] J. E. Lennard-Jones, Zeits. f. Krist. **75**, 215 (1930).

[25] G. J. Finch and S. Fordham, Proc. Phys. Soc. **48**, 85 (1936); G. J. Finch and H. Wilman, Proc. Roy. Soc. **A155**, 345 (1936). The lattice of alkali halide crystals was found to expand by as much as 0.6 percent if the size decreased to amicronic dimensions.

tained by Meissner,[26] that the melting point of crystals decreases with their thickness once they are thinner than $\sim 0.8\mu$. Finally, it has been observed,[27] that the magnetic susceptibility of hematite (a mineralogical species of α-FeOOH) decreases by more than one order of magnitude if the crystal diameter is reduced from 500μ to less than 10μ. A decrease in the mean susceptibility would certainly affect the magnetic anisotropy also. However, it is wise not to insist too much on this last argument, since there is a considerable controversy going on as to whether such variations in susceptibility with particle size are actually intrinsic effects or effects of adsorption and surface contaminations.

[26] G. Tamann, Zeits. f. anorg. u. allgem. Chemie **110**, 166 (1920); F. Meissner; *ibid.*, **110**, 169 (1920). These authors explain their observation as an effect of surface energy. The concept of differences in crystal spacing is more recent.

[27] R. Chevalier and S. Mathieu, Comptes rendus **204**, 854 (1937).

ACKNOWLEDGMENT

The experiments described in this paper and in others to follow have been carried out in the Laboratoire des recherches physiques à la Sorbonne, Paris, France. One of us (W. H.) recalls in gratitude the generosity of Professor Aimé Cotton, Head of the Department and President of the French Academy of Science, who made it possible to organize and to carry out a research project on colloid physical phenomena. The Faculté des Sciences of the Sorbonne are equally thanked for allocation of the annual receipts from the Vautier fund.

NOVEMBER 1 AND 15, 1942 PHYSICAL REVIEW VOLUME 62

The Magnetic Structure of Iron Crystals

W. C. ELMORE
Department of Physics, Swarthmore College, Swarthmore, Pennsylvania

(Received September 17, 1942)

A number of powder patterns found on demagnetized strain-free crystals of silicon-iron of known orientation are illustrated and discussed. The specimens were cut from strips of transformer steel in which fairly large crystals had been grown by the strain-anneal method. Smooth undamaged surfaces were prepared by electrolytic polishing. A magnetic field of only 10 oersteds applied normal to the specimens was sufficient to produce patterns; the intensity of the stray fields must thus be of this order of magnitude. On account of the large demagnetization factor (4π) of the specimens, the patterns are characteristic of the demagnetized state. All evidence points to a layer magnetization with alternate layers oppositely magnetized. The thickness of the layers in different specimens ranged from 10 to 50 microns. Superposed on this primary layer magnetization was a finer secondary structure, presumably localized near the crystal surface, and attributable to dendrite-like regions of reversed magnetization which reduce the magnetic energy associated with the surface stray fields.

PREVIOUS investigations of the ferromagnetic powder patterns of iron or silicon-iron crystals have failed to give a clear notion of the magnetic domain structure of these crystals. L. W. McKeehan and the writer[1,2] once studied in some detail the maze-like patterns found on mechanically polished silicon-iron crystals magnetized normal to their surface, but succeeding experiments[3] showed that the metallographic polishing used to prepare smooth surfaces played an important part in determining the scale and the geometrical form of the patterns. It is unlikely that these patterns furnish any clue to the primary domain structure of undamaged crystals. A number of patterns on iron specimens magnetized parallel to their surface have been

[1] L. W. McKeehan and W. C. Elmore, Phys. Rev. **46**, 226 (1934).

[2] W. C. Elmore and L. W. McKeehan, Trans. A. I. M. E. **120**, 236 (1936).

[3] K. J. Sixtus, Phys. Rev. **51**, 870 (1937); W. C. Elmore, Phys. Rev. **51**, 982 (1937).

published by various authors,[4] but no one has yet attempted a detailed interpretation of the patterns in terms of local domain magnetization. To obtain more reliable information concerning the magnetic structure of demagnetized crystals it appears necessary to examine patterns on annealed specimens which have smooth surfaces free from polishing damage. Since suitable surfaces can now be prepared by the method of electrolytic polishing,[5] a further study of the colloid patterns on silicon-iron crystals has been undertaken.

APPARATUS, SPECIMENS, AND FERROMAGNETIC COLLOID

The microscope-magnet assembly used for producing and observing patterns is illustrated in Fig. 1. A flat specimen placed upon the large soft iron pole piece can be uniformly magnetized normal to its surface. The magnet carrying the specimen rests on a specially built microscope stage which can be moved in a horizontal plane by a pantograph arm. The arm magnifies the motion of the stage about thirty times and with it one can draw an outline of grain boundaries and record for future reference the position of areas photographed. Photomicrographs of patterns are taken on 35-mm film (Micropan or Microcopy) and subsequently enlarged to a standard magnification. Illumination is furnished by a Pointolite lamp together with a green filter.

In the present investigation the specimens were cut with a fine jeweler's saw from 14-mil silicon iron strip (about 3.5 percent Si) containing large crystals grown by the strain anneal method. Each specimen included several crystals which averaged about 5 mm in diameter and extended through the strip. Surfaces smooth enough for the purposes of the experiment were prepared by first cleaning (etching) the specimens with dilute nitric acid and then electrolytically polishing them in an orthophosphoric acid bath by the method which has been described elsewhere.[5] No mechanical grinding or polishing was used at any stage in the process.

The orientation of individual crystals was determined by the method of etch reflections.

[4] For a brief review with references, see F. Bitter, *Introduction to Ferromagnetism* (McGraw-Hill, 1937), pp. 55 to 66. Also, see reference 3.

[5] W. C. Elmore, J. App. Phys. **10**, 724 (1939).

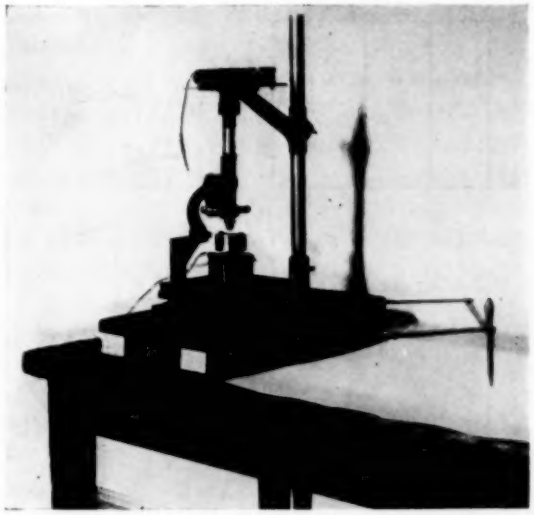

FIG. 1. Apparatus used for observing and photographing patterns.

Beautifully etched surfaces were obtained by temporarily removing the specimens from the electrolytic polishing bath prior to the completion of polishing. Usually angular coordinates for three {100} flashes were measured. When these were plotted on a stereographic projection the angles between pairs of points ordinarily differed from 90° by less than 1°. A slight tendency was noticed for the plane normals to lie too near the surface normal. A number of faint flashes were always observed, corresponding to other simple planes of high atom density. With a little practice there was no uncertainty in identifying the bright {100} flashes.

The technique of making patterns has been covered in previous papers so that only a few new observations will be recorded here. All the patterns to be described were formed with colloidal magnetite protected by soap.[6] It was noticed that the soap in the colloid formed a film on the specimen, helping to protect it from rust, and to prevent the colloid particles from adhering to its surface. This protective action made it unnecessary to coat the surface with a thin film of lacquer or grease as was done in earlier investigations. It has been found that colloidal magnetite oxidizes on standing; in a few weeks it gradually changes its color from dark red (almost black) to a lighter red and

[6] W. C. Elmore, Phys. Rev. **54**, 1092 (1938).

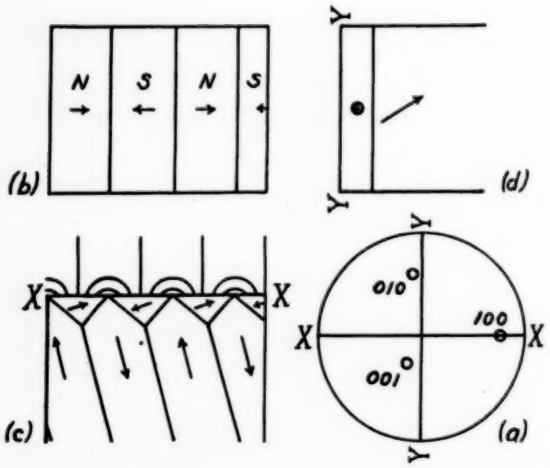

FIG. 2. Diagram illustrating one possible arrangement of magnetization at surface of crystal whose orientation is given by the stereographic projection (a). In (b), (c), and (d) are diagrams of magnetization at surface, and at representative sections $X-X$ and $Y-Y$ whose orientations are indicated in (a). The form of stray field to be expected from this structure is indicated above the $X-X$ section.

becomes less magnetic. Although the magnetic properties of the colloid can be partially restored by adding a small amount of photographic reducing agent, such as hydrochinon, together with a little alkali, patterns can be formed more readily with a freshly prepared colloid.

RESULTS AND DISCUSSION

Patterns were observed on a dozen or more crystals of known orientation. In general an applied normal field of only 10 oersteds was required to develop a pattern, although the pattern gained somewhat in sharpness when the field was moderately increased. On raising the field to 100 oersteds little or no further change was noticed. Therefore, the intensity of the surface stray fields must be of the order of magnitude of only 10 oersteds,[7] an important bit of information in deciding what sort of magnetic structure is responsible for the patterns. Thus the block structure once proposed[1] to account for the maze patterns on mechanically polished silicon-iron crystals need not be considered since it would result in much too intense stray fields. Before examining the new patterns in detail, let us consider in a general way what sort of magnetic structure an iron crystal may be expected to possess.

[7] W. C. Elmore, Phys. Rev. **58**, 640 (1940).

In an earlier paper devoted to patterns on cobalt[8] a review was made of the various factors which contribute to the formation of ferromagnetic domains.[9] For minimum energy a ferromagnetic crystal tends to be magnetized uniformly throughout its volume (minimum exchange interaction energy), to be magnetized only in certain directions (minimum magnetic anisotropy energy), and in the absence of an applied field to be magnetized so that there are no internal or superficial magnetic poles (minimum magnetic energy). The domain structure of a particular crystal represents a compromise state of magnetization, one which is consistent with minimum total energy insofar as energy losses accompanying its previous magnetic history permit. In unmagnetized ferromagnetic crystals free from strains (other than those of magnetostrictive origin) one expects to find the domain magnetization occurring principally in layers parallel to a direction of easy magnetization with adjacent layers ordinarily having opposite magnetization. Thus the layer magnetization in unstrained iron crystals will be parallel to $\langle 100 \rangle$ axes.

The nature of the boundaries between ferromagnetic domains was discussed theoretically first by Bloch[10] and more recently by other authors.[11] At the so-called 180° boundaries separating oppositely magnetized layers minimum energy results when the electron spins responsible for ferromagnetism do not reverse their direction abruptly, but take one hundred or more atom spacings for the transition. In the transition region the magnetization vector is supposed to turn about the boundary normal, thereby making $\nabla \cdot \mathbf{I} = 0$. Hence there is no contribution to the boundary energy of purely magnetic origin. In iron one ordinarily expects the 180° boundaries to be parallel to $\{100\}$ planes, since in the transition layer the changing direction of magnetization will then least offend the forces of magnetic anisotropy.[12]

[8] W. C. Elmore, Phys. Rev. **53**, 757 (1938).
[9] For a recent discussion, see W. F. Brown, Jr., J. App. Phys. **11**, 160 (1940).
[10] F. Bloch, Zeits. f. Physik **74**, 295 (1932).
[11] L. Landau and E. Lifshitz, Physik. Zeits. Sowjetunion **8**, 153 (1935); R. Becker and W. Doring, *Ferromagnetismus* (Springer, 1939), p. 187.
[12] This conclusion appears obvious on viewing a model of the magnetic anisotropy surface of iron. Reference 4, p. 195.

Next let us consider the boundary between two regions each magnetized parallel to a different ⟨100⟩ axis. This 90° boundary may be expected to occur only if there result no internal magnetic poles. A simple analysis shows that the boundary must therefore occur on a plane having a zone axis of form ⟨110⟩. As with the 180° boundaries, the magnetization can again change its direction through the 90° boundary so that $\nabla \cdot \mathbf{I} = 0$. To prove this, resolve the magnetization into two components, one normal and the other parallel to the boundary. The normal component does not depend on position; the other component can reverse its direction by turning about the boundary normal, so that neither component contributes to $\nabla \cdot \mathbf{I}$. Hence the energy of the 90° boundary need not contain a contribution of magnetic origin. However, widespread magnetostrictive stresses will always be set up by such a boundary, very likely making the boundary energy per unit area somewhat greater than that of the 180° variety where magnetostrictive stresses will be of minor importance since they must be primarily localized in the boundary itself. Hence it is not unreasonable that, in well-annealed iron crystals, the total area of 90° boundaries will be small, and that a 90° boundary on a {100} plane will occur but rarely. The energy per unit area of domain boundaries in iron crystals is not known accurately, but it is probably of the order of a few ergs per cm².

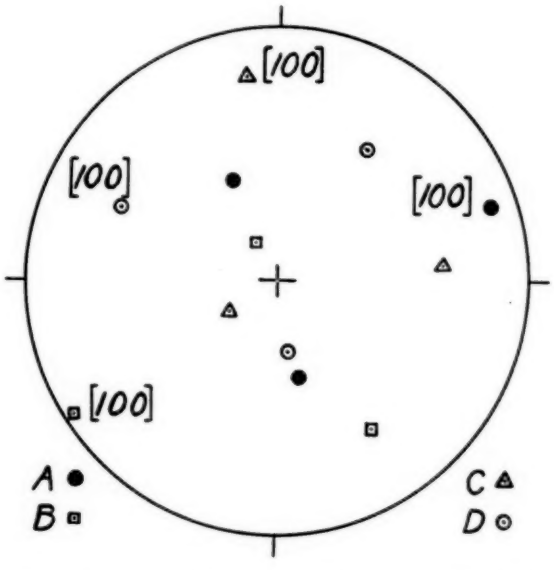

FIG. 3. Stereographic projection of the ⟨100⟩ axes of crystals A, B, C, and D. The north pole of the projection coincides with the surface normals, and the azimuth agrees with that of the various patterns illustrated in the text. The symbol [100] for each crystal has been assigned to the axis least inclined to the surface; symbols for the other two axes may be supplied by reference to the right-hand rule.

According to the previous discussion one expects an unstrained (ideal) iron crystal to possess for the greater part of its magnetic structure a layer magnetization, with boundaries

FIG. 4. Pattern on crystal A near grain boundary; normal applied field of 22 oersteds. Magnification 100×.

separating oppositely magnetized layers on {100} planes, and with the layer magnetization parallel to one of the three ⟨100⟩ axes of the crystal. At a crystal surface which contains no direction of easy magnetization the layer structure will necessarily be modified in some way in order to avoid a large surface energy of magnetic origin. One possible modification of the layer structure is indicated in Fig. 2, where (a) gives the orientation of the crystal, (b) the magnetization at the surface, (c) and (d) the magnetization at representative sections $X-X$ and $Y-Y$ whose orientations are indicated in (a). For minimum energy the magnetization in the surface domains of triangular section will occupy a direction in between the ⟨100⟩ direction least inclined to the surface and the projection of the latter direction in the surface. The surface, therefore, will be covered with bands of north and south poles, giving the sort of stray field indicated above the $X-X$ section. Most of the lines of induction form closed circuits within the crystal.

A second possible modification of the simple layer structure which will minimize surface stray fields is suggested by the magnetic structure of cobalt. An analysis of colloid patterns on cobalt

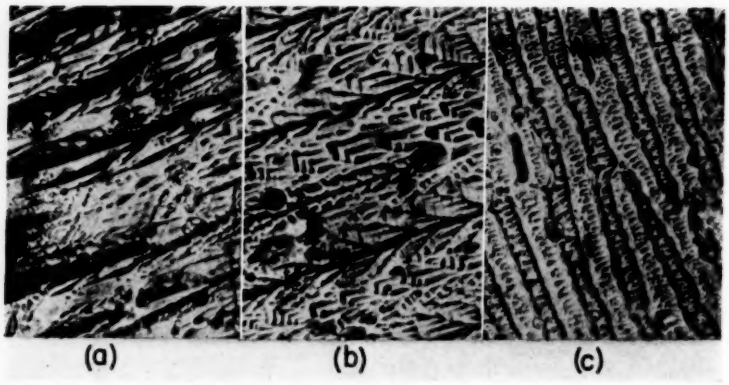

FIG. 5. Patterns on crystal A; normal applied field of 55 oersteds. The patterns (a) and (b) illustrate the development of a fine structure attributed to dendrite-like domains of reversed magnetization localized near the surface; (c) illustrates a second type of pattern found on crystal A. Magnification 100×.

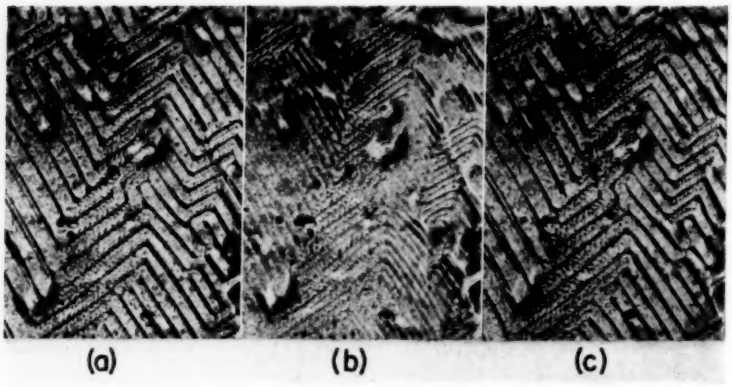

FIG. 6. Patterns on crystal B; (a) normal field of 95 oersteds; (b) no applied field; (c) same as (a) with direction of field reversed. Magnification 100×.

indicates that at surfaces considerably inclined to the hexagonal axis (the one direction of easy magnetization) there always occur dendrite-like regions of reversed magnetization extending a short distance into the primary layer magnetization. This surface fine structure evidently decreases the energy of magnetic origin at the cost of increasing, to a lesser extent, the energy tied up in the domain boundaries near the crystal surface. It is therefore reasonable to expect that the magnetic dendrites will occur whenever the magnitude of the surface stray field tends to exceed the value required for the formation of new nuclei of reversed magnetization, ordinarily a matter of a few oersteds. The dendrites constitute a fine structure superposed on the primary layer structure.

From the many patterns observed on different crystals it has been necessary to select for

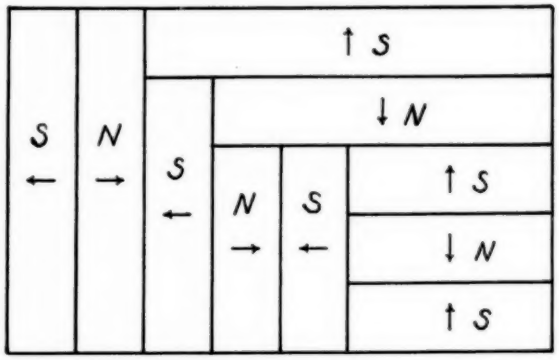

FIG. 7. Diagram of portion of crystal surface, suggesting arrangement of layer magnetization of Fig. 2 which will account for corners and other features in a maze pattern.

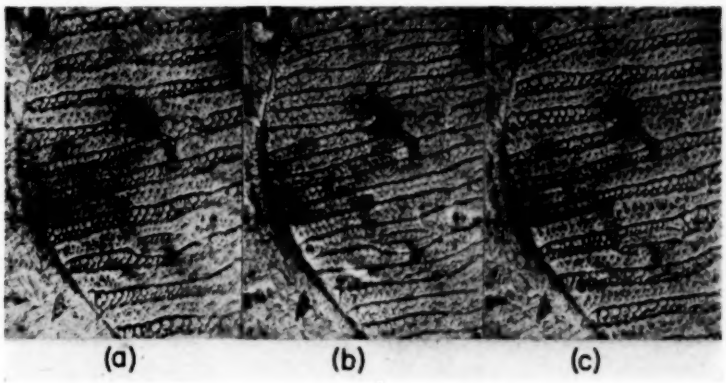

FIG. 8. Patterns on crystal C; (a), (b), and (c) as in Fig. 6. Magnification 100×.

reproduction only a few typical cases. These patterns, which occurred on four crystals designated by A, B, C, and D, show the variety in form which the magnetic structure can take. In addition some of the patterns reproduced here possess individual features which have been very helpful in deciding what arrangement of magnetization is responsible for a particular type of pattern. A stereographic projection, Fig. 3, shows the orientation of the ⟨100⟩ axes of the four crystals.

Let us first consider the pattern on crystal A, since this crystal has but one direction of easy magnetization, the [100] axis, approximately parallel to its surface. In Fig. 4 is shown the pattern near a grain boundary, produced by a normal field of 22 oersteds. This pattern, together with other patterns found with reversed field and with no field, is very similar to that found on prism planes of cobalt crystals. Hence there is little doubt that here we have a layer magnetization occurring in the [100] direction. Presumably the layers extend through to the opposite face of the crystal. The occurrence of the large magnetic dendrites at the grain boundary is especially to be noted and compared with the similar behavior exhibited by the cobalt patterns at a grain boundary.[13] In Figs. 5a and 5b are illustrated the changes in the pattern on crystal A occurring at successively greater distances from the grain boundary. The predominant layer structure can still be distinguished, but now the former bands are covered with many dendrite-like regions of reversed magnetization, presumably localized near the surface. The lack of fine structure near the grain boundary suggests that either strain, or a slight curvature of the surface (caused by the depression of the grain boundary by etching and by electrolytic polishing) has reduced the magnitude of the stray field by making the underlying magnetization more nearly parallel to the surface. The stray field in the vicinity of the grain boundary is thus too weak to initiate the fine structure. The pattern on crystal A differed from patterns on other crystals in that it completely changed its character near the diametrically opposite grain boundary. The pattern found there is illustrated in Fig. 5c. Although the heavy colloid deposits now run perpendicular to the [100] direction, the magnetic dendrites continue to be parallel to this direction. The evidence suggests that here we have a structure of the sort illustrated in Fig. 2, i.e., the primary layer magnetization occurs in either the [010] or in the [001] direction, with the principal domain boundaries on (100) planes.

In Fig. 6 are illustrated maze-like patterns found on crystal B, with no applied field, and with a positive or negative normal field of 95 oersteds. On relating the patterns to the crystal orientation the fact is noted that the fine structure occurs only with the lines perpendicular to the [010] axis (inclined about 20° to the surface) and not with the lines perpendicular to the [100] axis (inclined only a few degrees to the surface). It was further observed that the

[13] Reference 8, Fig. 4.

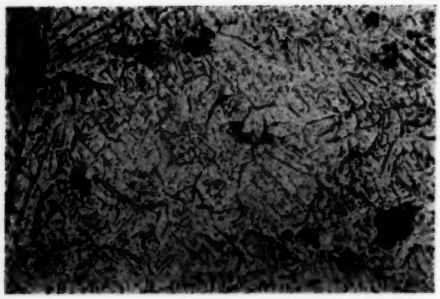

FIG. 9. Pattern on crystal D; normal applied field of 22 oersteds. Magnification 100×.

pattern did not change its scale near grain boundaries, differing in this respect from the pattern on crystal A, Fig. 4. The location of the fine structure, the orientation of the principal pattern lines, and the behavior at grain boundaries all point to the magnetic structure of Fig. 2, at least as regards sets of parallel lines in the pattern. It remains to be demonstrated how the two-layer structures, parallel to the [010] and the [100] planes, can join together to form corners and other pattern details without producing excessive local magnetic fields. The only apparent way in which this can be done is suggested in Fig. 7. Each rectangular strip in this diagram represents the top of a domain of triangular cross section, as in Fig. 2, and is covered with magnetic poles of polarity indicated by *N* or *S*. A careful study of the colloid distribution in the three patterns of Fig. 6 tends to confirm this sort of arrangement. The narrowness of the pattern lines may be attributed to a slight non-uniformity in the distribution of surface poles on each domain of triangular cross section.

The similarity between the present patterns and the finer scaled maze patterns characteristic of mechanically polished crystals suggests that the two must have a similar explanation. Since the structure responsible for the earlier maze patterns is closely related to the damage left from polishing, it is reasonable to conclude that the fine-scaled layer magnetization (layers about 2 microns thick) is localized near the surface and that it gives way to a coarser layer magnetization within the crystal. Indeed evidence for such a structure was reported when the maze patterns were first described.[1] Kennard has already proposed[14] that a layer magnetization similar to Fig. 2 is responsible for the sets of parallel lines in maze patterns, but he attributes the surface stray fields to the "surface tension" of domain boundaries, rather than to the inclination of the direction of easy magnetization with respect to the surface, the view here adopted. It seems likely that the surface energy (tension) of the boundaries is too small to play an important part in producing surface stray fields.

Let us consider the patterns shown in Fig. 8, found near a grain boundary on crystal C. It is evident that the distribution of the colloid with no applied field, and with applied normal fields, the orientation of the bands, and the behavior of the pattern at the grain boundary all point again to the domain structure of Fig. 2, with boundaries between layers occurring on (100) planes. The bands, except for local imperfections, were observed to extend all the way across the crystal and to be covered everywhere with fine structure indicating the presence of local magnetic dendrites. It is interesting to compare the fine structure of Figs. 5c, 8, and 6 with one another, and to relate them to the angles between the surface and the ⟨100⟩ axes concerned. The three angles are, respectively, 6°, 12°, and 20° and the three patterns suggest, reasonably enough, that the dendrites point with increasing angles into the crystal surface.

Many of the patterns on other crystals were similar to those which have been discussed, indicating that layer magnetization, accompanied by a finer-scaled surface structure, is of common occurrence. The pattern of crystal D, Fig. 9, however, shows that the magnetic structure may be much more complicated in a crystal whose surface approaches the orientation of a {111} plane. The structure in Fig. 9 is very fine scaled and at first sight appears to bear no relation to the orientation of the crystal. Close inspection, however, reveals local groups of parallel lines whose orientation is for the most part along the traces of {100} planes in the surface. Although these lines suggest local regions of layer magnetization, it is likely that

[14] E. H. Kennard, Phys. Rev. **55**, 312 (1938).

the pattern fails to reveal the nature of the domains lying deep in the crystal.

The scale of the various magnetic structures herein described deserves special mention. On the assumption that the interpretation of the patterns is substantially correct, then the thickness of the layer domains ranges from ten to fifty microns, varying from crystal to crystal, but remaining fairly uniform over considerable areas of one crystal. The structure of crystal D, of course, constitutes an exception. Ideally the scale of a magnetic structure is set when the energy associated with domain boundaries just equals that associated with the external surface of the crystal, since the former varies inversely and the latter directly with a length characterizing the structure.[8,9] On account of the complexity of the magnetization in the surface domains, it appears impossible to make any accurate estimates of the energies involved. The variation in layer thickness for different crystals in the same specimen may be attributed partly to differences in crystal orientation, and partly to the effect of previous magnetic history. The relative importance of these two factors has not yet been looked into.

There are still to be investigated many interesting points regarding colloid patterns on iron crystals. It should be possible to follow in detail changes in magnetic structure accompanying the magnetization process, and to correlate abrupt structural changes with Barkhausen noise. The particular form taken by the magnetic structure is undoubtedly related to the previous thermal and magnetic history, grain size, the existence of strains, the hysteresis properties, initial permeability, etc., of the specimen. Definite information regarding these matters should lead to a better understanding of many aspects of ferromagnetism.

Letters to the Editor

PROMPT publication of brief reports of important discoveries in physics may be secured by addressing them to this department. The closing date for this department is the third of the month. Because of the late closing date for the section no proof can be shown to authors. The Board of Editors does not hold itself responsible for the opinions expressed by the correspondents. Communications should not in general exceed 600 words in length.

A Simplified Electron Microscope

C. H. BACHMAN AND SIMON RAMO
Electronics Laboratory, General Electric Company, Schenectady, New York
October 31, 1942

AN electron microscope has been constructed to test a number of new methods of obtaining photographs. The aim has been to obtain in as simple a manner as possible both as regards operation and construction a resolving power in the range of the greatest present usefulness of electron microscopy (say ten times better than light microscopy), and to operate in a voltage range sufficient to obtain this resolution for the usual thin specimens. The instrument is a combined electron and light microscope and utilizes unipotential electrostatic electron lenses. Such a general scheme of design has proved to possess, as expected, the following desirable characteristics:

(1) The electrons are accelerated and focused by a single, crudely regulated voltage.

(2) The unipotential lenses can readily be used in a multiple-stage magnifying system of compact construction so that the chamber to be evacuated becomes very small.

FIG. 1. Photograph of replica from specimen of carbonyl iron.

(3) A short electron path results from the use of a multiple lens electron-optical system in combination with a stage of light-optical magnification. This small cathode to fluorescent screen distance and the medium resolving power make it possible to align the entire electron-optical system permanently.

(4) The chamber can be re-evacuated to operating conditions within a few minutes after insertion of a new specimen. This and the external photographic technique which a final light-optics stage facilitates, eliminate the need for specimen and photographic film insertion locks.

(5) The over-all weight and dimensions, if proper advantage is taken of the above conditions, are such that it is feasible to design a portable instrument.

This approach to the electron microscope problem requires that one obtain fluorescent screen images capable of enlargement by light-optical means. Images on screens which have been prepared and used in this instrument are believed to be capable of 10–20-diameters enlargement. With the reduced electronic magnification (for a given final magnification), the fluorescent screen images are exceedingly bright for a given current density at the specimen. The apparent brightness of the image for visual observation remains nearly constant as the magnification in the light-optics stage is increased since the N.A. of the light lens increases in nearly the same proportion. The photographic exposure time is several times higher than for the conventional electron-on-film recording, usually being one-half minute or more.

Figure 1 is of a replica taken from a metallographic specimen of carbonyl iron.

A more detailed description of the design and development of this instrument will be published shortly in the *Journal of Applied Physics*.

Note on Induced Color in Diamonds

J. M. CORK
University of Michigan, Ann Arbor, Michigan
November 2, 1942

IN a previous letter entitled "Induced Color in Crystals by Deuteron Bombardment"[1] the transformation in color (from amber to green) effected in diamonds was described as a body change. This conclusion resulted from the fact that light coming from the gem has suffered many internal reflections and hence has always passed through the green region. It has now been shown that the change in color does not extend throughout the body of the crystal.

Two identical amber tinted crystals, each of 2.8 karat and of distorted dodecahedral form and each with a flat basal surface of several square millimeters were available for irradiation. These gems were arranged with their basal planes in contact and mounted with one stone imbedded in wax so that all but the plane surface was covered, while the other was exposed to the deuteron bombardment. The upper stone was nicely transformed to green, while the under one was in no way discolored. This indicates that the alteration in color probably is produced only as deep as the penetration of the energetic deuterons.

[1] J. M. Cork, Phys. Rev. **62**, 80 (1942).

New Methods for Preparing Surface Replicas For Microscopic Observation

VINCENT J. SCHAEFER
General Electric Company, Schenectady, New York
October 26, 1942

RECENTLY a method was described[1] for studying surfaces in the electron microscope by the direct replica method. The technique, briefly, consists in flowing over the surface a dilute solution of a resin dissolved in a suitable solvent. With the evaporation of the solvent, a very thin film coats the specimen. The coated specimen is then immersed in water, the replica film peeled from it, brought to the water surface, and mounted in the usual way for study in the microscope.

In a number of instances, especially with certain types of metallographic specimens which form corrosion products upon contact with water, it is desirable to remove the surface replica without immersion in water. Three new methods for removing replicas have recently been devised in this laboratory which overcome these corrosion problems and simplify the stripping process.

FIG. 1. Electron micrograph of replica of oil quenched 1.1 carbon steel surface.

One of these termed the "warm method" consists of the following procedure. After the thin replica film is formed on the specimen a 20 percent solution of gelatin dissolved in warm water is applied to the surface (about 0.5 drops per cm^2). The water is evaporated from the gelatin by a stream of warm dry air. Upon drying, the gelatin film often cracks off the surface spontaneously or may be split off by inserting a razor edge under one side. As the gelatin leaves the surface it takes with it the replica film. This

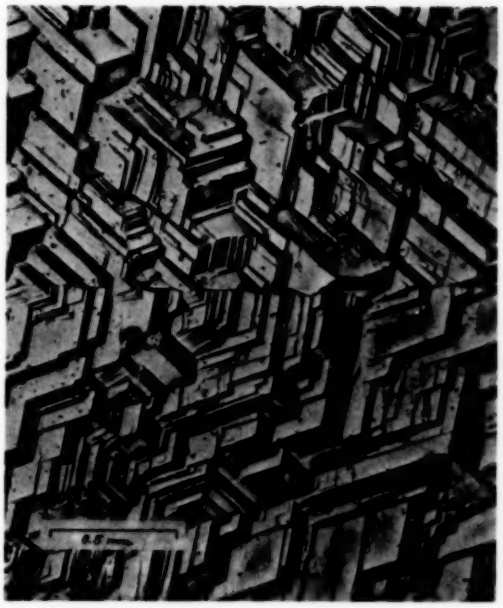

FIG. 2. Photomicrograph of replica of etched quartz surface at crystal boundary.

double film is then placed gelatin side down in a shallow tray, washed with several changes of warm water until the gelatin dissolves, leaving the replica floating on the surface ready for mounting.

Figure 1 is an electron micrograph of a polyvinyl formal replica removed by this method from a Nital etched specimen of oil quenched 1.1 percent carbon steel.

A second procedure termed the "cold method" may be preferred for some specimens. Again with polyvinyl formal resin as replica material the dry film is covered with a dilute 0.5 percent solution of gelatin (or other surface active protein) dissolved in distilled water. A lens of protein solution several mm thick should be applied and the specimen placed on the freezing coils of a refrigerator. As soon as the lens is frozen the lower part of the specimen is placed in a shallow tray containing liquid air and left there until the frozen protein solution in contact with the replica cracks off at the resin-metal interface due to the unequal contraction of the cooling materials. The lens, now having the replica film as part of it, is lifted from the specimen, placed on a piece of filter paper, and warmed to room temperature. The replica is then floated on a water surface and mounted in the usual manner.

A third procedure is mentioned here because it has been found to be very useful for preparing high contrast photomicrographs of the structure of surfaces by the replica method in which specimens ranging all the way from etched quartz crystals to scored metal surfaces, soft leaf mining worms to flower petals are used. The best results with this third method are obtained with thicker replica films since the distance between the high and low spots of the type of specimens described is often a micron or more. After the replica film is formed by flowing a one to

ten percent solution of a suitable resin over the specimen the solvent is evaporated. A strip of transparent scotch tape is pressed into optical contact with the coated specimen and then pulled away from it. When this is done the replica adheres to the scotch tape. This may be fastened to a sheet of glass for study under the light microscope, the Cellophane surface serving as a cover glass. Figure 2 is a photomicrograph of such a replica obtained from an etched quartz crystal showing the contact between a primary and a penetration crystal.

Acknowledgments are due to Miss Ethel Thompson, who prepared many of the replicas and the electron micrograph shown in Fig. 1 and to Miss Margaret Murphy, who prepared the metallographic specimens used in developing the warm and cold methods described.

[1] V. J. Schaefer and D. Harker, J. App. Phys. **13**, 427 (1942).